An Interactive Energy System with Grid, Heating and Transportation Systems

Diaz de Cerio Mendaza, Iker

Publication date:
2014

Document Version
Publisher's PDF, also known as Version of record

An Interactive Energy System with Grid, Heating and Transportation Systems

by

Iker Diaz de Cerio Mendaza

A Dissertation Submitted to
the Faculty of Engineering and Science at Aalborg University
in Partial Fulfillment for the Degree of
Doctor of Philosophy in Electrical Engineering

August 2014
Aalborg, Denmark

Aalborg University
Department of Energy Technology
Pontoppidanstræde 101
Aalborg East, DK-9220
Denmark
Phone: +45 99 40 92 40
Fax: +45 98 15 14 11
http://www.et.aau.dk

Printed in Denmark by Uniprint
First Edition (August 2014)

ISBN:978-87-92846-42-6

Public Defence of PhD Dissertation

Thesis Title:

An Interactive Energy System with Grid, Heating and Transportation Systems

Ph.D. Defendant:

Iker Diaz de Cerio Mendaza

Supervisor:

Assoc. Prof. Birgitte Bak-Jensen

Co-supervisor:

Prof. Zhe Chen

Assessment Committee:

Assoc. Prof. Florin Iov (Chairman)

Department of Energy Technology
Aalborg University
Pontoppidanstræde 101
9220 Aalborg, Denmark

Prof. W.L. Kling

Department of Electrical Engineering
Eindhoven University of Technology
5612 AZ Eindhoven, The Netherlands

Prof. Göran Andersson

Power Systems Laboratory
ETH Zürich, ETL G 26
Physikstrasse 3
8092 Zürich, Switzerland

Defence Date and Place:

Tuesday, October 7, 2014
Pontoppidanstræde 101, Room 23, Aalborg University

Copyright Statements

To my parents, sister and girlfriend
for their love and support

Preface

This thesis is written according to the project DSF 09-067255 entitled *Development a Secure, Economic and Environmentally Friendly Modern Power Systems* supported by the Danish Council for Strategic Research, Aalborg University, Energinet.dk, HEF Net A/S, Dong Energy, Alstom, kk-electronic, Risø-DTU and Huazhuong University of Science and Technology (HUST). I specially acknowledge the institutions mentioned above for both the financial support and the technical assessment provided during each of the quarterly meetings. Additionally, I would like also to make a proper recognition to the Department of Energy Technology at Aalborg University and Otto Mønsteds Fond for supporting me financially in the participation of conferences and the study abroad.

This research work was performed under the supervision of Assoc. Prof. Birgitte Bak-Jensen (main supervisor) and Prof. Zhe Chen from the Department of Energy Technology. I would like to express my deepest gratitude to both for giving me the opportunity of doing this research and for their patience, exceptional guidance and kindness during my fellowship period. Furthermore, their technical and personal support has been an essential ingredient to accomplish it. I would like also to thank all the industrial partners and in particular, Per Lund (Energinet.dk), Allan Jensen (HEF Net A/S), Brian Kirby (Alstom) and Poul Tørgersen (kk-electronic) for the interesting and fruitful discussions during the quarterly meetings which have indeed influenced notoriously my work. In this context, Allan Jensen needs to be doubly considered due to the key information provided about the network and the user consumption without which it this work would not be possible. Without resting a bit of importance, Prof. Claus Leth-Bak and John K. Pedersen have to be also acknowledged for their guidance and helpful comments.

I would like also to express my appreciation to some of my closest collaborators Alberto Pigazo from the Department of Electronics and Computers at University of Cantabria, Spain, and Ireneusz Grzegorz Szczesny, Jayakrishnan R. Pillai and Konstantinos Kouzelis from the Department of Energy Technology at Aalborg University. All of them have showed an incredible interest and professionalism in our common research activities. I would like to take also the opportunity to thank Dr. Miguel Ortega-Vazquez from the Department of Electrical Engineering at the University of Washington,

Seattle, for giving me the invaluable opportunity of collaborating with him during the last phase of my thesis. In the same way to Prof. Daniel Kirschen making it possible for me to be part of the REAL Lab during the time I was collaborating with Dr. Ortega-Vazquez.

I also appreciate very much the technical discussion I have had with my project colleges, Chengxi Liu, Zakir Hussain Rather, Pietro Raboni, S. Mostafa F. Astaneh and Jiakun Fang and the rest of the fellows in the Department of Energy Technology at Aalborg University.

Finally, but not least, I would like to deeply thank my parents, sister, girlfriend and rest of my family members for the unconditional love, patience and support that I have received during the time I was working on my PhD studies. You will always be in my thoughts.

Iker Diaz de Cerio Mendaza

August 1, 2014
Aalborg Øst, Denmark

Abstract

The environmental consciousness and the fact of achieving greater energy independency have led many countries to apply important changes in their energy systems. The intensive renewable energy growth of the last decades represents the most notorious example at this moment. However, this is not only occurring with power generation purposes, there is an interest on extending this tendency to other strategic systems like the heating, gas and transportation. This implies that at least an important part of these systems will have to be electrified. From a power system perspective, this means that it will have to undergo a significant load increase in the future.

Due to its nature, most of this load is expected to be accommodated at the power distribution level. This implies a need for finding new alternatives to operate and control the medium and low voltage networks. Considering the technical and economic aspects of these networks, an active demand response represents a promising solution. This research work is based on the opportunity of interacting the electrical power system and the heating, gas and transportation systems to ensure a correct and efficient operation of the distribution systems.

The aim of this work is to introduce new modelling approaches, methods of analysis and control strategies to represent the active loads and the power distribution systems in the future. Unlike for large transmission systems, in distribution systems a more detailed modelling from each network element is required. The models developed in this thesis include different features (thermal, mechanical, chemical...) which are not normally considered in the traditional power system modelling. In this sense, they are intended to serve as a reference for the new researchers starting in the field. Moreover, the grid studies and the demand response strategies introduced are intended to be beneficial for distribution system operators (DSO) in the planning and development of the future distribution networks.

The following thesis covers four main areas; modelling of active loads and residential user requirements, flexibility definition and quantification, stochastic impact assessment of LV networks and control of the demand response in LV networks.

In a first stage, different residential and non-residential loads are modelled with system analysis purposes. The active loads considered can be categorized as: thermostatic

loads (electric water heaters and heat pumps), loads for hydrogen generation (alkaline electrolyzers) and load for electric mobility (plug-in and vehicle-to-grid concepts). Many of these are considered domestic loads and they fulfill certain need to the household they belong. Depending on the user requirements, these may perform a different power consumption patterns. In this context, the thermal comfort or mobility needs from Danish users are statistically analyzed. The outcome is used to generate random profiles that define the different thermal and mobility requirements from the users of a network.

The flexibility expected from users holding these loads, despite of being constantly mentioned, is usually not properly defined and even rarer quantified. Therefore, it represents another significant factor to be assessed. In this work, a methodology to probabilistically quantify the potential flexibility from residential users is introduced. The approach is based on non-flexible consumer clustering and subsequent statistical analysis and the comparison with the power consumption pattern of flexible consumers. The strong relationship of certain loads flexibility and the season of the year are clearly highlighted.

Demand response, especially from residential users, is lately acquiring lots of attention due to the advantages that it introduces in regards the power system regulation. However, depending on the load penetration and location, distribution grids may be leaded to serious congestion problems. In this situation, not only the security and reliability of these networks are in danger, the flexibility offered by the active loads may also be limited. It is then decisive, to understand what is the hosting capability of this networks and their vulnerable points. In this stage of the thesis, a methodology for stochastically evaluating the impact caused by thermostatic and plug-in electric vehicle loads in low voltage grids is introduced. Even though the actual systems seem to be over-designed, sometimes their hosting capability may be poor for the integration levels expected.

Finally, in the last stage of this research work the control of the demand response in LV networks is tackled. The hierarchical structure presented aims to control the operation of heat pumps and plug-in electric vehicles to satisfy technical and commercial aspects of LV grids. This strategy allows system operators to perform their energy commitments, taking advantage of the flexible demand, while ensuring the security and reliability of the LV network each moment of the day. A proper demand response strategy makes possible to obtain economic benefits from the balancing service provision while decongesting the LV network in critical moments.

Dansk Resumé

Øget miljøbevidsthed og en højere grad af energi-uafhængighed har ledt mange lande til at indlede større ændringer i deres energisystemer. Den enorme vækst af vedvarende energi gennem de sidste årtier repræsenterer denne kendsgerning. Dette sker dog ikke kun med det formål at producere elektricitet, idet der også er en interesse for at udvide denne tendens til andre strategiske systemer som varme-, gas- og transportsystemerne. Dette indikerer, at en stor og vigtig del af disse systemer vil blive elektrificeret. Hvad elnettet angår, vil det forårsage en betydelig belastningsforøgelse i fremtiden.

Denne forøgelse forventes at blive tilpasset på el-distributions niveau, hvilket forudsætter et behov for nye alternativer til at håndtere og styre mellem- og lavspændingsnettet. Tages de økonomiske og tekniske aspekter af disse net i betragtning, vil et fleksibelt elforbrug repræsentere en lovende løsning. Dette forskningsarbejde tager afsæt i mulighederne for interaktion mellem det elektriske energisystem og varme-, gas- og transportsystemerne, for at opnå sikker og effektiv drift af distributionssystemet.

Hensigten med arbejdet er at introducere nye modeller, analysemetoder samt styringsstrategier for fremtidens fleksible elforbrug og fremtidens el-distributionsnet. I modsætning til større transmissions-systemer, er en mere detaljeret modellering fra hvert netværkselement påkrævet, når det gælder distributionssystemer. Modellerne udviklet i denne afhandling inkluderer forskellige funktioner (termiske, mekaniske, kemiske...), som normalt ikke er taget i betragtning i den traditionelle elsystemsmodellering. Intentionen er at modellerne skal fungere som reference for nye forskere på området. Ydermere forventes analyserne på elnettet og de introducerede strategier for det fleksible elforbrug, at være til nytte for distributionsselskaberne (DSO) i planlægningen og udviklingen af det fremtidige distributionsnet.

Afhandlingen dækker fire hovedområder: Modellering af det fleksible elforbrug og forbrugerkrav, fleksibilitetsdefinition og kvantificering, stokastisk undersøgelse af påvirkningerne på lavspændingsnettet samt styring af det fleksible elforbrug i lavspændingsnettet.

I første fase er forskellige belastninger for boliger og andre lagringssystemer modellerede i system-analyse øjemed. Det fleksible elforbrug, der er taget i betragtning, kan kategoriseres som: Termiske belastninger (elektriske vandvarmere og varmepumper),

belastninger til brintudvikling (alkalisk elektrolysator) og belastning til elektrisk mobilitet (opladning af elbiler samt anvendelse af el-biler som energilager med mulighed for afladning til nettet). Mange af disse er tiltænkt lokale behov, og de imødekommer visse behov i husholdningerne. Afhængigt af forbrugerkravet, vil disse haveforskellige forbrugsmønstre. I denne kontekst er den termiske komfort samt kørselsbehovet for de danske forbrugere statistisk analyseret. Resultatet er benyttet til at skabe tilfældige profiler, der definerer el-forbrugernes forskellige termiske og mobile behov.

Den forventede fleksibilitet fra disse forbrugere, er – udover at være nævnt hyppigt – som regel ikke defineret og endnu sjældnere kvantificeret. Derfor repræsenterer dette en vigtig faktor som bør vurderes. I dette forskningsarbejde introduceres en metode til probabilistisk at kvantificere den potentielle fleksibilitet hos disse forbrugere. Tilgangen er baseret på, efter at have lavet en statistisk analyse på en ikke-fleksibel forbrugsklynge, at sammenholde den med elforbrugsmønsteret for fleksible forbrugere. Der er fundet en stærk sammenhæng mellem belastningsfleksibilitet og sæson, hvilket er tydeligt fremhævet i afhandlingen.

Det fleksible elforbrug specielt fra forbrugerene, har på det seneste krævet stor opmærksomhed jævnfør de fordele det medfører hvad angår styringen og balancen i elnettet. Imidlertid vil distributionsnettet kunne risikere store overbelastningsproblemer afhængigt af belastningens størrelse og placering. I så fald vil ikke kun driftssikkerheden og pålideligheden af disse netværk være i fare, men fleksibiliteten af de aktive belastninger vil også være begrænset. Dermed vil det være af afgørende betydning at kunne fastlægge overføringskapaciteten for disse netværk og se nettenes svagheder. I denne fase af specialet introduceres en metode til stokastisk at evaluere indflydelsen af termiske belastninger og belastningen af elbiler i lavspændingsnettet. Selvom de nuværende net er overdimensionerede, kan deres egnethed i forhold til det forventede integrationsniveau være begrænset.

I den sidste fase af forskningsprojektet, er styringen af den fleksible belastning i lavspændingsnettet håndteret. Den hierarkiske struktur, som er præsenteret, har til formål at styre driften af varmepumperne og elbilerne således, at tekniske og kommercielle aspekter for lavspændingsnettet bliver tilfredsstillet. Denne strategi tillader systemoperatørerne at opfylde deres energiforsyningsforpligtigelse ved at udnytte den fleksible efterspørgsel, samtidigt med at den sikrer sikkerheden og pålideligheden af lavspændingsnettet hver dag, året rundt. Et hensigtsmæssigt fleksibelt elforbrug gør det muligt at drage økonomisk fordel for den balanceansvarlige samtidigt med, at man aflaster lavspændingsnettet i kritiske perioder.

Contents

List of Figures

List of Tables

Acronyms

AE	Alkaline Electrolyzer
AVR	Automatic Voltage Regulators
CHP	Combine Heat and Power
COP	Coefficient of Performance
DG	Distributed Generation
DHW	Domestic Hot Water
DR	Demand Response
DSM	Demand Side Management
DSO	Distribution System Operator
EB	Electric Boiler
EES	Electrical Energy Storage
EV	Electric Vehicle
EWH	Electric Water Heater
HP	Heat Pump
HPWH	Heat Pump Water Heater
HWST	Hot Water Storage Tank
ICT	Information and Telecommunication Technologies
LV	Low Voltage
MV	Medium Voltage

NLTC No-Load Tap Changer

OLTC On-Load Tap Changer

PEV Plug-in Electric Vehicle

PV Photovoltaic

P2G Power to Gas

SH Space Heating

ST Secondary Transformer

TSO Transmission System Operator

V2G Vehicle to the Grid

Part I

Report

Chapter I

Introduction

In this chapter, a short summary of the project idea, objectives and limitations are outlined. Those aspects are based on an introduction of the actual Danish system, seen both from the power system and market perspective. The "Smart Energy System" concept is also summarized here.

1.1 Background and Motivations

The environmental awareness and the importance of achieving greater levels of energy independency are leading many countries to consider renewable energy as an alternative to the fossil fuels. For those part of the European Union (EU), this fact is also motivated by the energy targets agreed between the state members. These, which are known as the "20-20-20"targets, are covered on a directive of March 2007 [1]:

- A 20% reduction in EU greenhouse gas emissions from 1990 levels.
- A 20% increase on the share of EU energy consumption produced from renewable resources.
- A 20% improvement in the EU's energy efficiency.

The outcome of this policy is already quite relevant considering the renewable energy share in the gross final consumption of the EU-28 countries in 2012. However, its actual status varies from country to country. While countries like Sweden, Estonia and Bulgaria have already accomplished their share, countries like Malta, Luxembourg and United Kingdom are still far from the defined numbers [2]. Once the discussion is moved to the generation of electricity, the 2013 European statistics show a predominant increase of wind and PV technologies within the power generating capacity installed in the EU since 2000 [3].

The Danish energy policy has always included differences in comparison with the other EU members. The motivation for modernizing its energy system and making it more environmentally friendly has historically represented Denmark in this context. Due to its long coastline, the Danish climate is characterized by consistent and strong winds. In the absence of other natural energy sources such as coal, water in high elevations or large sun radiation, the effort and dedication has focused in implementing the wind technology as basis for electrification. A good example is the revolution of the modern wind industry, given in the early 70s in Denmark [4]. This posture has been maintained and even accelerated during the past years. In March 2012, the Danish Ministry of Climate, Energy and Building reinforced the long-term goal: the 100% of the energy supply -electricity, heating, industry and transport- is to be covered by renewable energy by 2050. In accordance with this, new energy targets for 2020 are defined stepping up the ones set by previous plans [5].

- More than 35% of the final energy consumption is to be supplied by renewable energy.
- Approximately 50% of electricity consumption to be supplied by wind power.
- A reduction in the gross energy consumption of 7.6% in relation to 2010.
- A reduction in greenhouse gas emissions of 34% in relation to 1990.

To achieve those ambitious targets and phase out the fossil fuel dependency, an improvement of the energy efficiency is required. This is claimed to be obtained by electrifying the energy consumption and expanding the renewables supply. In the commitment of this task, special importance is given to the wind power, exploiting both offshore and onshore technologies, and the PV power generation. Consequently, the energy supply of an entire country will depend and rely on an intermittent, variable and unpredictable energy source in the future.

1.2 The Danish Case

In the previous section, the particularity of the Danish case is reveled. In relation to a reconversion of an energy system there is not at this point a country comparable to the Denmark. However, the realization of this plan also entails a number of challenges and difficulties that have to be addressed in the coming years.

1.2.1 Problem Description

The wind power share is one of most illustrative features indicating that this change is already happening. By the end of 2013, the wind power capacity installed in Denmark was 4772 MW [6]. As a consequence, the wind power share hit 33.2% of the total electricity consumption in the country [7]. According to the predictions of Energinet.dk

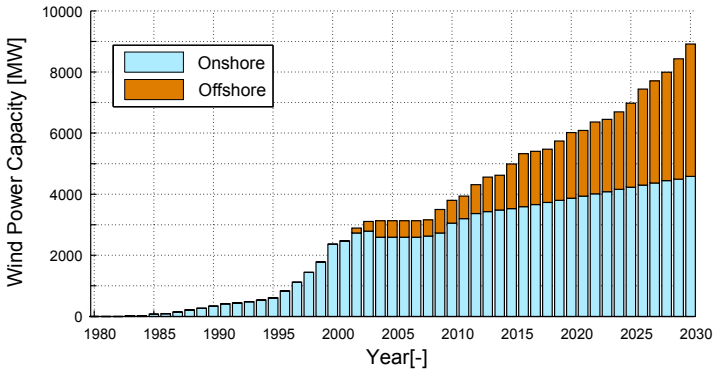

Figure 1.1: *Estimation of the Wind Power Capacity in Denmark.*

-Danish TSO-, shown in Fig. 1.1, the installed capacity will continue growing exponentially. This growth seems to be moderate in the onshore case, but significant for the offshore technology.

In line with this, the installed capacity estimated for the PV power rub 574 MW by mid 2014 [8]. Its evolution during the coming years is projected in one of the last reports published by Energinet.dk and DONG Energy [9]. Even though the development of the installed capacity may be depreciated, since the expansion rate considered in the report is the same as the one given 2012, the results shown in Fig. 1.2 indicate a linear tendency in the expected growth of this technology.

In the traditional power system, the conventional power plants were accommodating their output in order to follow changes occurring at the load side or to aid the system

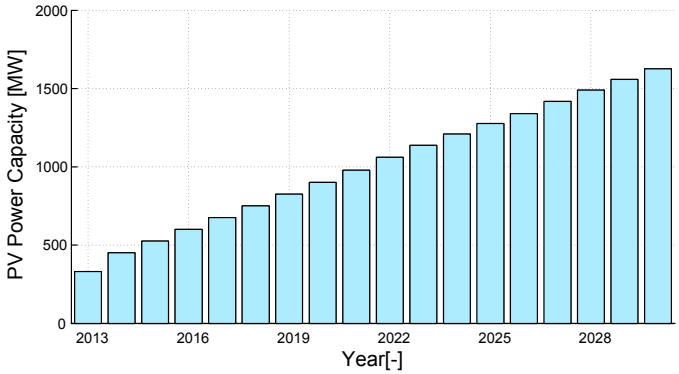

Figure 1.2: *Estimation of the PV Power Capacity in Denmark [9].*

performance. The transition from fossil-fuel based generation to a complete renewable one implies a number of challenges which need to be seriously addressed. The power production from renewable energy sources, like wind and photovoltaic, is characterized for being intermittent, variable and unpredictable. This means that their production rate depends on physical conditions which are out of any operator control capability. Therefore, this kind of generation has to be utilized whenever it is available. In these sense, large network reinforcements, higher balancing capacity and more investment resources will be required in order to maintain the balance between the generation and consumption.

Some of the existing studies have predicted the possible grade of imbalance between generation and load under the large wind integration expected in Denmark. Fig. 1.3 illustrates a comparison between the actual and 2050 scenario made by [10]. In this figure it is appreciable how the current penetration levels are acceptable to maintain the balance between supply and demand in the transmission system. This task is nowadays performed by controlling local generation i.e small CHPs and some of the central power plants and the employment of the international interconnections, especially during moments with power excess. From 2020 to 2050, the performance of this task gets more complicated due to the frequent moments of imbalance and even more challenging the magnitude of imbalance.

This context gets further aggravated due to the fact that some of the large conventional power plants are going to gradually phased out on their power generation commitment. This significantly affects a crucial part of the actual power system, the system inertia and the short circuit capacity. On the one hand, the inertia of the power system is mostly provided by the mechanical rotating masses of large generators. If part of those disappears the system inertia reduces making the power system more vulner-

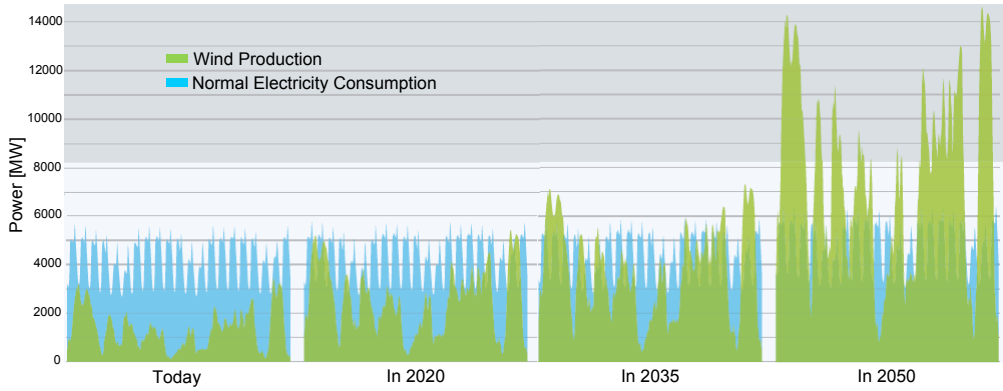

Figure 1.3: *Wind Production VS Electricity Consumption Expected in Denmark by 2050 [10].*

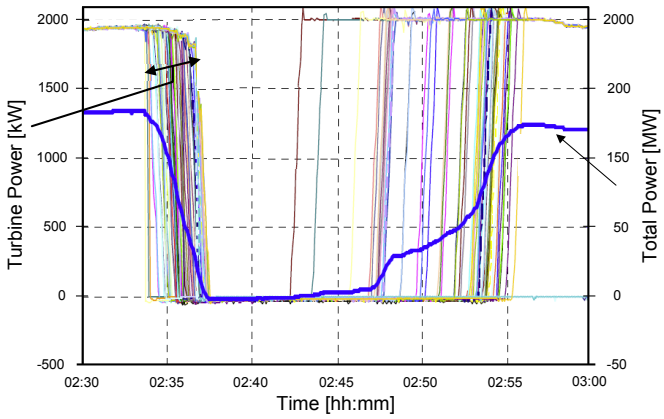

Figure 1.4: *Shutdown of the all Wind Turbines in Horns Rev [11].*

able to any incident that may occur during its operation. In this way, the loss of the synchronous generators represents a loss of the conventional power system stabilizers and with that a part of the short circuit capacity. As a consequence, all these technical aspects make the operation and control of a power system like that very challenging for any system operator.

The consequences of the Danish energy policy, are already affecting the current power system operation. In [11], the field records of an incident happened in the offshore wind farm of Horns Rev clearly illustrates what has been described. The wind farm, which is located at the west coast of Denmark, is composed of 80 Vestas V80 wind turbines of 2 MW. In January 20^{th}, 2005 a wind storm made all the wind turbines in the wind farm exceed their over-speed limit consequently pitching-out and forcing their stand still mode. In consequence, in less than 4 minutes a loss of around 140 MW happened as it is depicted in Fig. 1.4.

This loss of generation may not represent such a big deal for a large power system such as the one in United States, Russia or China. However, for a small size country like Denmark, with a relatively small power system, this kind of events might suppose a large destabilization of its normal operating conditions. Larger and more serious events are foreseen to happen with the levels of renewable energy expected in the future.

1.2.2 The Power System

The Danish power system is divided in two parts, the western part (DK1) and the eastern part (DK2). The actual generation capacity and the system load are depicted in Table 1.1. In this context, the main producers of electricity are DONG Energy with 6137 MW and Vattenfall with 1816 MW [12]. Since the early eighties, the large develop-

Table 1.1: *Generation Capacity And System Load In Denmark (2012) [12]*

Generation Technology	**Capacity (MW)**	**Peak Load (MW)**
Condensing Thermal Power	1955	
CHP, District Heating	7082	
CHP, Industry	811	7091
Hydro Power	9	
Wind Power	4163	
Total	14020	7091

ment of distributed generation has made Denmark a very singular case. Back then, its topology was characterized as a classical centralized systems, where few large steam turbines produced the electricity for the entire country. The generation capacity installed posteriorly became more and more dispersed being wind turbines and CHP plants the prevalent technologies. In Fig. 1.5, the evolution up to now and the one expected for the future is illustrated. As seen, the scenario is significantly different. In the past, the few power plants injecting at the transmission system defined predominantly the power flow. Nowadays, the large number of assets interacting with the system makes more arduous the task of defining the power flow behavior.

Furthermore, it cannot be neglected that different offshore wind farms are already under operation along the Danish coasts. The most important ones are Horns Rev part I and part II of 160 MW and 209 MW and Rødsand of 207 MW. In Fig. 1.5, the direction in which the current power system is expected to develop is also illustrated. Among the large scale offshore wind farms projected: Horns Rev part III (400 MW), Anholt (400 MW) and Kriegers Flak (600 MW). Different locations, along the Danish coasts, have also being appointed as promising sites for future offshore projects [14]. Finally, this figure also shows the conventional power plants that are already phased-out and the ones expected in the future. Some of these generation units have already been dismantled. Others instead are expected to be converted into synchronous condensers with the purpose of maintaining the system stability.

1.2.2.1 The Transmission System

In Denmark, the transmission system is basically composed by the 400, 150 and 132 kV voltage levels. The main power carriers are the 400 kV overhead lines connecting the north and south of Jutland and the 400 kV overhead line connecting the west and east of Zealand. Through these lines the power is transported to the load centers for posteriorly be distributed to the consumers exploiting the lower voltage levels. The left hand side picture of Fig. 1.6 shows the configuration of the Danish transmission system

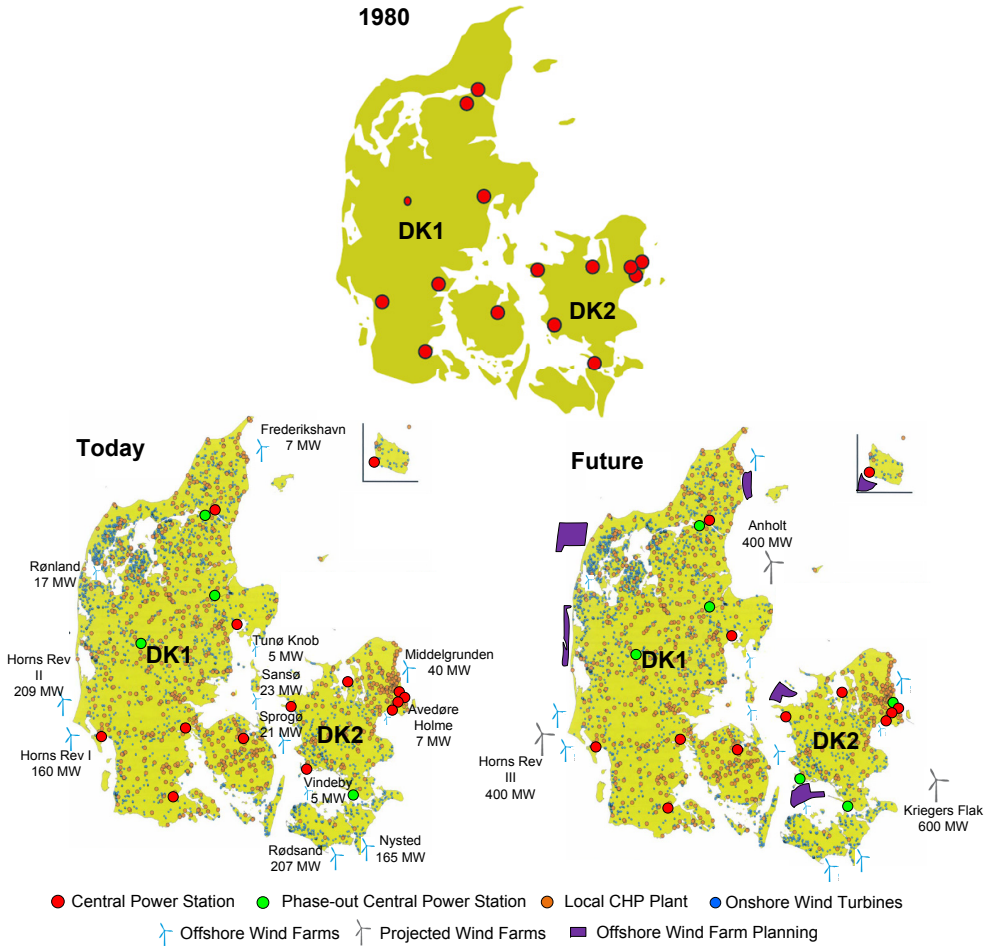

Figure 1.5: *Evolution of the Distributed Generation in Denmark [13].*

in 2013. The power interconnections with its neighboring countries are also an important feature in this system. Denmark is located geographically between the continental Europe and the Nordic countries. Therefore, the interconnection with Germany is made via an AC line of 1780 MW and via and HVDC cable of 600 MW (KONTEK). The interconnection with Sweden consist in an AC line with an export and import capacity of 1700 and 1300 MW and an HVDC cable of 740 MW (Konti-Skan). Finally, the interconnection with Norway is based on several HVDC cables with a total capacity of 1000 MW (Skagerrak). Nowadays, the Danish TSO employs these interconnections in

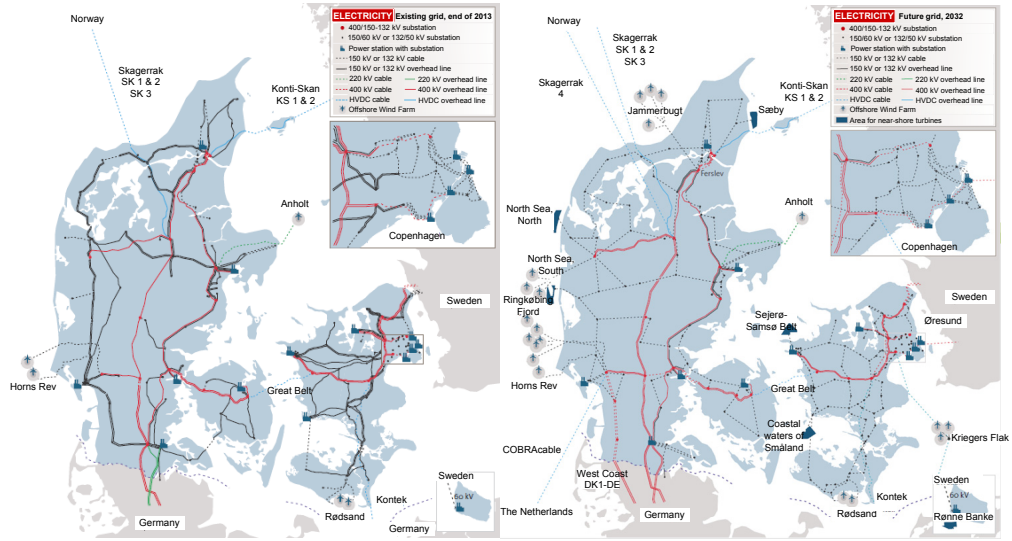

Figure 1.6: *Evolution of the Transmission System in Denmark [17].*

order to regulate the power system under different levels of wind power generation. In what the system expansion refers, the upgrade and improvement of the actual interconnections represents key aspect for Energinet.dk. Examples of this philosophy are: the new 700 MW HVDC line reinforcing the connection with Norway, the 700 MW HVDC line (COBRA) connecting Denmark and the Netherlands and the additional 400 kV line expected to be constructed in Jutland to reinforce the existing one [15], [16].

1.2.2.2 The Distribution System

The distribution systems in Denmark are basically composed of all the voltage levels existing below the 60 kV level. The most common ones are the 60, 20 and 10 kV for the MV and 0.4 kV for the LV. In 2007, there were around one hundred distribution system operators (DSO) in the whole country.Those were and are committed to distribute the electrical power within the safety and quality standards to each of the individual consumers. Fig. 1.7 shows a list of the DSOs and their operation zones back in time [18]. The classification of those falls into non-profit cooperatives, municipalities of companies with concession. Recently, many of those have started to get merged with the purpose of expanding their operation limits and business areas.

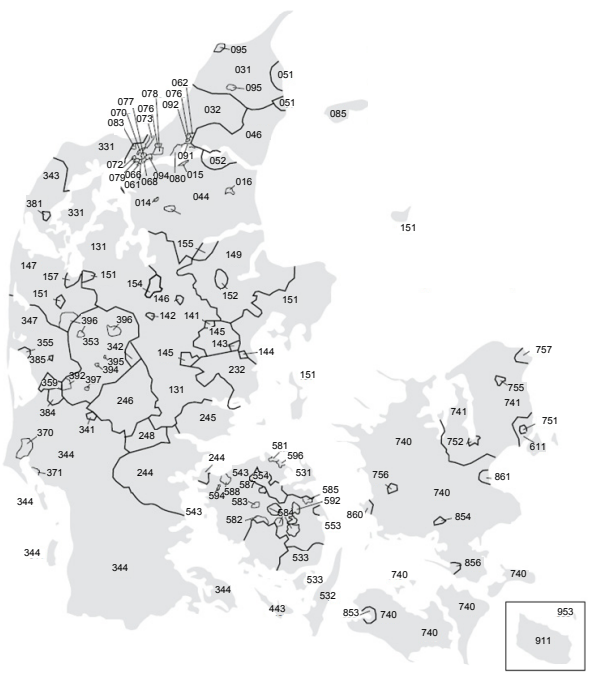

No.	Companies	2007 Transport of electricity. GWh	2007 Metering points 1000
14	Hornum	4	0.6
15	Nibe	20	2.3
16	Kongerslev	6	0.9
23	Nyfors	346	38.1
31	ENV	551	52.6
44	HEF	846	77.2
46	ESV	335	39.4
51	Frederikshavn	151	16.6
52	AKE	944	62.5
58	Sæby	55	4.6
68	Bejstrup	1	0.1
70	Fjerritslev	22	2.4
72	Gøttrup	2	0.2
73	Hjortdal	4	0.6
75	Aabybro	18	0.2
77	Skræm	1	0.1
78	Skovsgaard	22	0.8
79	Øslev-Døstrup	1	0.1
80	Øland	2	0.3
81	Mønstrup	1	0.1
82	Knøsgaard	2	0.3
83	Klim	3	0.3
84	Aars	33	3.7
85	Læsø	13	2.5
91	Gjøl Syd	4	0.5
92	Fristrup	0	0.0
95	Hirtshals	19	2.5
96	Tårs	6	1.1
131	Energi Midt	1501	147
141	Hammel	53	3.5
142	Kjellerup	35	2.6
143	Brabrand	87	8.7
144	Viby	104	11.2
145	GE	287	23.1
146	Bjerringbro	101	2.3
149	ELRO	567	50.7
151	NRGi	1725	152.8
152	Energi Randers	254	32.7
154	Viborg	177	19.4
155	Energi Hobro	126	6.8
232	Østjysk Energi	491	56.1
244	TRE-FOR	1738	130.7
245	Energi Horsens	715	53.3
246	MES	235	15.9
248	VOS	52	5.1
331	Thy-Mors	403	28.2
341	GEV	71	4.7
342	Ikast	92	8.1
343	Thy Højspændingsværk	126	14.8
344	Syd Energi	3445	262.1
347	NOE	465	29.2

No.	Companies	2007 Transport of electricity. GWh	2007 Metering points 1000
348	RAH	372	26.3
351	Vestforsyning	269	18.3
353	EnergiMidt Vest	526	43.5
255	Ringkøbing	32	2.7
357	Struer	79	6.1
359	Skjern	95	4.5
370	Aal *)	13	1.8
371	Hjerting	15	3.0
381	Hurup	26	1.9
384	Tarm *)	26	2.3
385	Videbæk	48	2.3
392	Borris *)	9	0.5
394	Kibæk	12	1.3
395	Studsgaard *)	1	0.2
396	Sunds	22	2.2
397	Sdr. Felding *)	17	0.8
398	Vildbjerg	39	2.0
443	Ærø	32	5.3
531	Ravdex	204	15.5
532	LEF	81	12.1
533	SEF	243	32.7
543	Energi Fyn	977	84.1
552	Faaborg	114	14.3
553	Nyborg	114	9.3
554	Odense	640	74.0
581	Bårdese	5	1.4
582	Nørre-Broby *)	8	0.8
583	Verninge *)	3	0.4
584	Midtfyn	64	6.0
585	Ullerslev *)	10	1.4
587	Pårup	10	2.3
588	Brenderup *)	10	1.7
592	Rolfsted	17	1.1
594	Ejby	15	1.2
596	Hasmark-Egense	6	1.7
611	DONG, City	2920	359.6
740	SEAS-NVE	3669	354.5
741	DONG, Nord	5479	549.7
751	DONG, Frederiksberg	359	60.3
752	Roskilde	169	22.4
755	Hillerød	133	13.5
756	SK-EL	132	16.1
757	Helsingør	122	17.9
853	Nakskov	107	9.0
854	NKE	124	17.0
856	Vordingborg	48	5.4
860	Korsør	68	9.4
861	Køge	95	8.0
911	Ølstykraft	244	28.0
953	Cristiansø *)	1	0.1

Figure 1.7: *Distribution System Operators in Denmark (2007) [18].*

1.2.2.3 The Heating System

The heating system is another characteristic part of the Danish energy system. In 1903, the first CHP plant was built to treat the waste in a more environmentally friendly way. Since then, the local heating management developed into a district heating technology which nowadays supplies entire urban areas. Indeed, the space heating and water heating of more than 60% of the Danish households are supplied with district heating today [19]. According to the Danish Energy Agency, in 2012, 73% of the thermal power was produced by the existing 670 centralized and decentralizes CHP plants [20]. Fig. 1.8 illustrates the location of the main technologies used in Denmark for heating supply. The district heating is mostly concentrated in the major cities and large urban cores as it is described. In those, the district heating network consists of a number of distribution networks interconnected by a transmission grid. The transmission networks are normally operated up to 125 °C and 25 bar and distribution networks up to 95 °C and between 6 and 10 bar pressure. The longest district heating network, approximately 50 km long, is located in the Copenhagen area and supplies annually 35 PJ of thermal energy.

However, this technology may not represent the most cost-effective solution for sup-

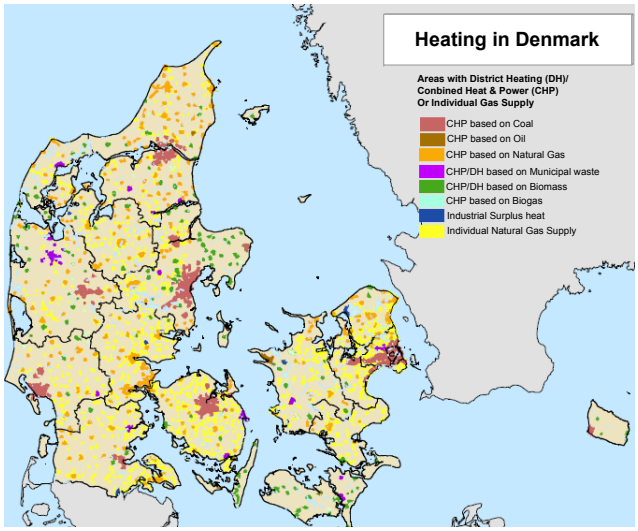

Figure 1.8: *Location of the Heating Technologies in Denmark.*

plying heat to remote areas where the density of population is low. Logically, individual heating and small CHPs are the predominant technologies employed in those places. In rural areas specially, the oil and gas burners and the electric heating are mostly utilized as the heating source.

In the future, the modernization of the heating system will pass by the utilization of more efficient and environmentally friendly heating technologies. This implies the use of large and small EBs and HPs both at district heating and domestic level. Moreover, the current CHP plants will be reconverted in order to accommodate biomass and biofuels that makes their combustion more eco-friendly. Finally, the thermal storage present on the district heating networks and large heat storage tanks are intended to be exploited with the purpose of making the heating system more flexible.

1.2.2.4 The Gas System

Besides the transmission system, Energinet.dk is also responsible for the operation, control and expansion of the natural gas system in Denmark. According to the last publications, since 2006, Denmark has slightly decreased its annual consumption of natural gas. The average consumption, before and during 2006, was around the 4 billion Nm^3 and in 2012 around 3.2 billion Nm^3. 2010 got out of this trend, due to the fact that it was a cold year therefore increasing the consumption from central power station.

The major part of the natural gas transported thought the Danish gas transmission system comes physically from the North Sea. This is partially distributed within the

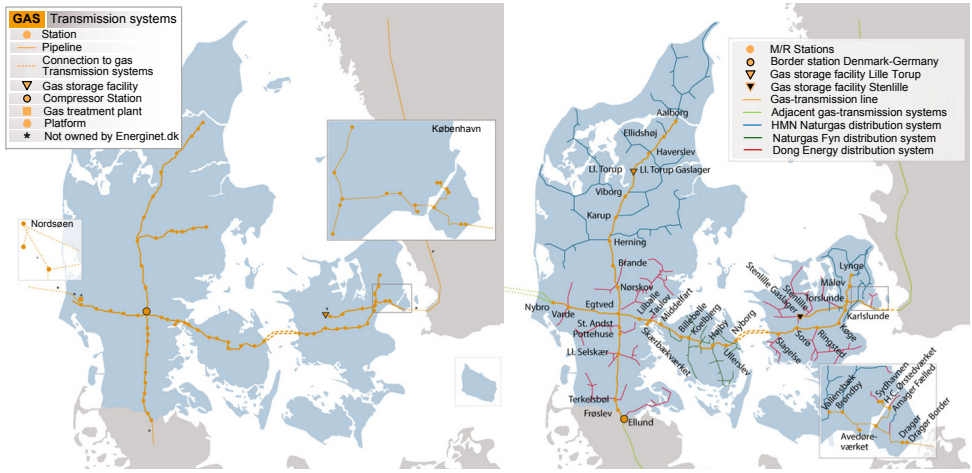

Figure 1.9: *Natural Gas Transmission and Distribution Systems in Denmark [21], [22].*

country for supplying its own demand and partially exported to neighboring countries via the Tyra, NOGAT and Syd Arne pipelines. Approximately 16% of the natural-gas production in 2012 was exported to the Netherlands, whereas 18% to Sweden and 13% to Germany. According to Energinet.dk, Fig. 1.9 shows the transportation, distribution and interconnection infrastructure of natural gas in Denmark. Table 1.2 summarizes the capacities of the main elements composing this infrastructure [23].

In accordance with the estimations made by the Danish Energy Agency, the gas supplies from the North Sea are expected to decay between 2018 and 2042, being more likely to be exhausted in 2040. The total natural gas consumption is also foreseen to decrease from the 3.5 billion Nm^3/year (151 PJ) in 2013 to 2.8 billion Nm^3/year (118 PJ) in 2022. However, the consumption of the so called renewable gases or fuels will take over the reduction expected in natural gas supply. Among the alternatives, biogas and hydrogen are two seriously considered renewable fuels. According to the previous institution, the biogas production will grow from 0.17 billion Nm^3/year (6.6 PJ) in 2013 to approximately 0.51 billion Nm^3/year (20 PJ) in 2022 [24].

However, to achieve the objective of a 100 % renewable energy system by 2050, several alternatives and technologies need to be taken into account. Generating hydrogen with renewable energy and injecting it into the current natural gas system is one of them. Hydrogen is a very volatile gas that when it reacts with oxygen gets highly flammable. In consequence, it is important to know the impact produced in the equipment (process, storage and measuring) of the current infrastructure. In this sense, Energinet.dk in collaboration Danish Gas Technology Centre, GreenHydrogen.dk and DONG Energy have carried out a research project to investigate the possibilities of mixing hydrogen in

Table 1.2: *Natural Gas Entry-Exit Transmission Capacity [23]*

Millon Nm^3/day		**Capacity**	**Max. Flow**		
			2010/2011	**2011/2012**	**2012/2013**
Nybro	Entry	32[2]	23	19	14.1
Lille Torup*	Withdrawal	8	7	7	6
Stenlille Gas*	Withdrawal	12	10	11	9.3
Exit Zone Denmark	Exit	26	22	22	19.5
Ellund	Entry/Exit	4.7/8.3	4/8.5	4/7.6	5.2/2.2
Dagør Exit	Exit	9[2]	8	7	7.7

* Storage Facility

[1] Swedish system not designed for this capacity, it is limited to 6 million Nm^3/day

[2] Capacity at the receiving terminal, the supplies are constrained to 26 million Nm^3/day

different concentrations -up to 20%- with the natural gas currently transported through the gas networks. The test system selected is established between the decommissioned stations, Helle M/R and Agerbæk M/R. The outcome of this investigation is intended to show if the hydrogen damages the actual infrastructure and in which way it does it. In consequence, Energinet.dk should learn how the gas system reacts and the way that it needs to be maintained for ensuring a reliable green gas system in the future [25].

1.2.2.5 The Transport System

Denmark has a well-developed and modern transportation system. According to the figures presented by the Ministry of transport in 2011, there exists 74.171 km of road network, 2667 km of rail network, 113 seaports and 23 airports. Considering the types of transport -road, rail, sea and air- the total energy consumed by the road transport is by far the highest one at national level. In 2010, this energy consumption reached 160.6 PJ. In the same line, the road transport is responsible for a considerable part of the contaminant emissions. Based on the previous statistics, around 2.16 million private vehicles, 14.496 busses and coaches and 148.766 motorcycles were part of this system in 2010 [26].

A fossil-fuel based transportation system is not compatible with the sustainable development that Denmark has planned for its entire energy system. In this context, a system transformation is planned to be given gradually towards the electrification of the country mobility. Seing the battery charging infrastructure developed and distributed recently along the country, the first steps of this conversion are appreciable. Two companies have developed the mayor part of this infrastructure, Clever and Better Place. The fast and conventional charging stations are already established in the thirty biggest

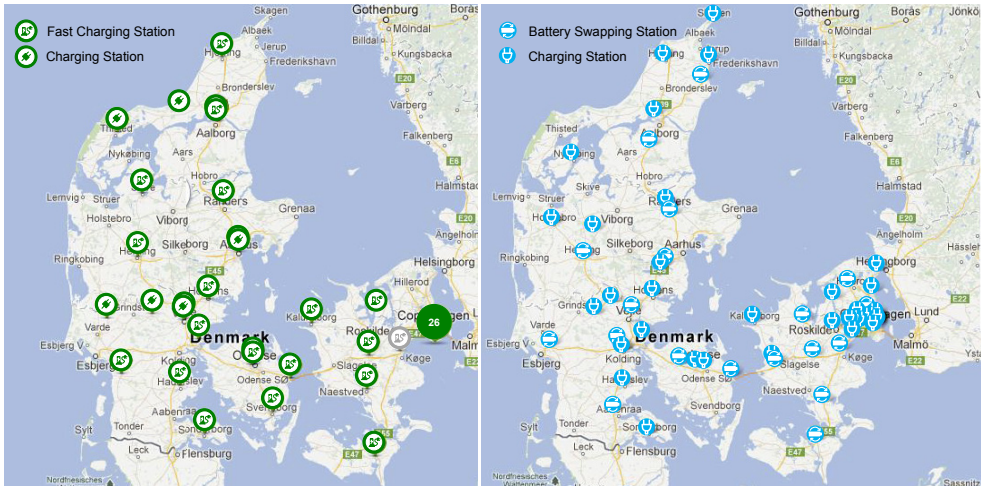

Figure 1.10: *EV Infrastructure in Denmark [27].*

cities in Denmark. The charging points are located is places where there is agglomeration of people such as top attractions, amusement parks, shopping centers or hotels. The charging takes between 20-30 minutes and several hours depending on if fast or the conventional charging is considered [27]. The location of the existing battery swapping stations was decided based on accessibility, location/zoning, visibility, security, property price, property size and shape, neighborhood. Fig. 1.10 illustrates the location of the battery swapping and charging stations existing in Denmark in 2012. Notice that the mayor part of the battery swapping and fast charging stations were distributed along the main motorways E20 and E45 which go from the north of Jutland to Copenhagen. Most of the stations have 4 battery chargers and a capacity for swapping 12 batteries per hour. The average swapping time is from 3 to 4 minutes.

From a user perspective, the system conversion is expected to be encouraged by the tax exemptions applied to the new EVs. As matter of comparison, the taxation applied nowadays in any vehicle acquisition is up to 180 % of the vehicle value. This hinders to some Danish consumers having access to an own private vehicle.

1.2.2.6 The Nordic Power Market

As a part of the named Scandinavian countries, Denmark trades and exchanges its power in the NordPool Spot. This is owned by the Nordic and Baltic TSOs and is regulated by the Norwegian Water Resources and Energy Directorate (NVE). In this platform three mayor markets are operated; the day a-head (Elspot) and the intra-day (Elbas) markets in the Nordic and Baltic Regions and N2EX market in United Kingdom. Currently,

370 companies from 20 countries trade and compete among the different markets. The energy volume traded at the NordPool Spot hit 432 TWh in 2012, where 334 TWh were in Elspot and 3.2 TWh in Elbas [28].

Nowadays, 80% of the power consumption from the Nordic countries is traded at Elspot. The prices for each hour of the following day are calculated based on the expected supply, demand and the transmission capacity. The auction starts at 8 a.m every day. Buyers and sellers are allowed to enter, modify and remove their bids until 12 a.m that is when the market closes. Based on the aspects mentioned before, from 12 a.m to 1 p.m, the market prices are calculated. Finally, from 1 p.m to 3 p.m all trades are invoiced and sent to the buyers and sellers. Elbas or the intra-day market is a continuous market where the trading happens until the hour before the power is delivered. The numbers given before clearly represent the big difference in the energy amount traded at Elbas in comparison with Elspot. That is because this platform is used to compensate the imbalances originated during the day of operation which differ from what it was defined at the Elspot. Every day the TSOs publish their power transmission capacity to Elbas. Based on this, the different parties make their offers on how much they want to buy or sell. The trading is then set according to the first-come first-served rule. This means that if transmission capacity is available, parties from neighboring countries can participate in the trade too.

In case imbalances still remain an additional platform, called the regulation power market (RPM), is employed. Unlike with the other two, this market is operated by the TSOs in each country. The RPM is utilized to trade up and down regulating power. Its aim is to anticipate excessive use of automatic reserves and to restore their availability.

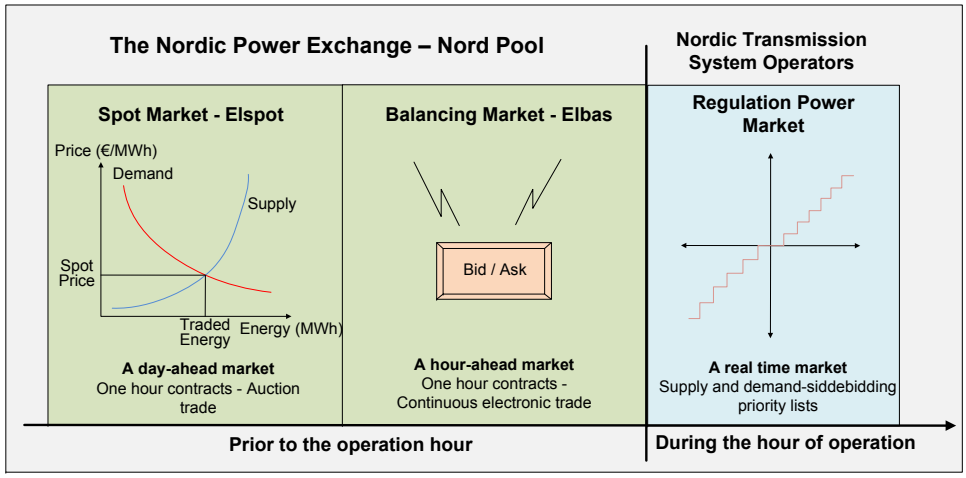

Figure 1.11: *The Nordic Power Exchange Market [29].*

In the RPM all bids can be submitted, adjusted, or removed until 45 minutes before the operation hour. These are collected and sorted in a list with increasing prices for up-regulation and decreasing prices for down-regulation. Depending on the potential congestions in the system, the TSO activates the cheapest regulating power.

Fig. 1.11 graphically represents the interaction among the different trading platforms within a time line.

1.3 The "Smart Energy System"

According to what it is described in the previous sections, a conceptual and technological re-structuration of the Danish energy system is planned to happen in the coming years. Therefore, each of the subsystems composing it (power, gas, heating and transport), are going to be affected in one way or another. Since renewable energy stands for the main power source in the future, especially wind and PV power, large and intensive instabilities are expected to be given in the power system. In order to cope with the challenges of a 100% renewable energy based power system, Energinet.dk has appointed four strategic areas [30]. As Fig. 1.12 depicts, they are summarized as:

– Expansion and upgrade of the existing network and the interconnections with the

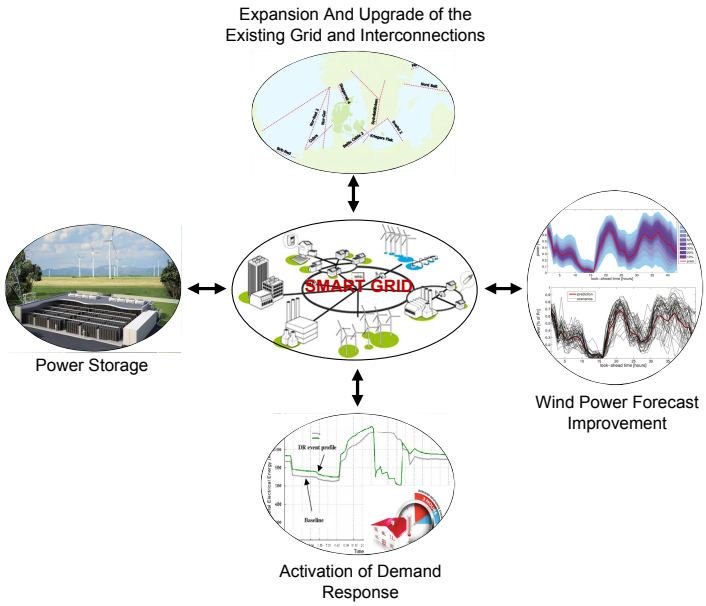

Figure 1.12: *Strategic Areas for Energinet.dk.*

neighboring countries.

- Design and development of advance techniques for wind power forecast.
- Deployment and implementation of large power storages exploiting technologies like, compress air, batteries and the gas system.
- Exploit the flexibility from active loads by the activation of the DR.

All these aspects are considered from the future smart grid perspective. To maintain the system stable, the TSO in lack of the traditional generation adjustment will have to rely more and more on the wind power forecast. Based on this forecast, the operation strategy will be decided and planned accordingly. Then, the smart infrastructure, the power interconnections and the different storage technologies distributed across the country will be utilized as system regulators.

However, such a scenario is only imaginable with an infinite power exchange capability of the interconnected systems. This situation is improbable, especially considering that the neighboring countries may in the future have the same ambitious targets regarding renewable energy as Denmark. Under these circumstances, the Danish TSO would find impossible to balance the system since its similes face the same problems and needs at the same moment.

It is in this case when the DR acquires real sense. According to the Nordic power market, this is a voluntary and temporary adjustment of electricity demand as a response to a price signal or a reliability-based action [31]. An active DR allows a local power management decreasing the international dependency on this matter. Taking that into consideration, the authorities and institutions agree that the Danish solution passes by the integration and combination of the different energy systems in what is called the "Smart Energy System" [10]. This concept relies in the close interaction of systems with different natures and requirements in order to have a global equilibrium. In this context, the power system represents the backbone of the whole energy system and its link with the rest of the systems is represented by the DR. In other words, the employment of controllable loads will transform the electrical energy in other energy vectors. Fig. 1.13 summarizes the way that the power system is expected to be linked with the gas, heating and transportation systems. The excess of renewable generation in the power system is distributed within the heating system, via the demand of small and large scale EB and HP, within the gas system, via the demand of large electrolyzers, and within the transport system via the demand of EVs. In the same way, when there is lack of generation, the stored hydrogen can be converted into power via fuel cells and the discharging from EVs can be encouraged.

For a feasible implementation of this concept, an important grade of electrification is required from the other systems. Energinet.dk, estimates that approximately 80.000 HPs are installed nowadays in Denmark expecting 420.000 more by 2030 [32]. In the same way, its previsions regarding electric vehicles (EV) rub 1.1 million units [33]. As a consequence, the electrical power system is foreseen to undergo a considerable load

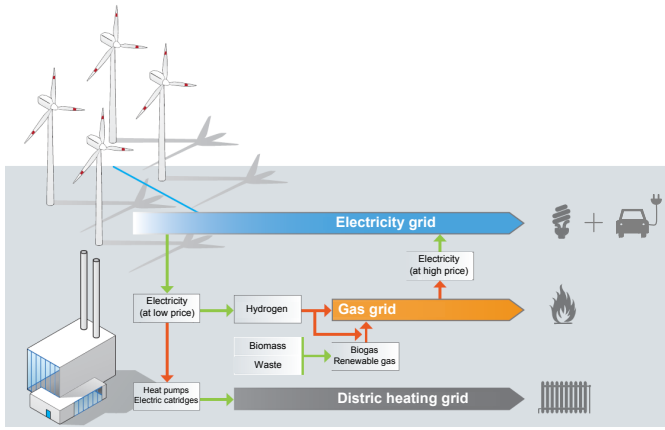

Figure 1.13: *The "Smart Energy System" [10].*

growth in the coming years. In Fig. 1.14 an estimation made by the Danish Ministry of Climate, Energy and Building regarding the electricity consumption expected due to this electrification phenomenon is illustrated. From 2015 to 2035, the industry and services (I&S) and the district heating (DH) seem to be the sectors that will require the highest amount of energy individually. But it can neither be neglected that a significant percentage of the total energy required will be demanded by electric vehicles (EV) and individual heating systems (IH). The individual heating systems refers to electric water heaters and HPs outside the areas of collective district heating and natural gas supply. The continuous development of the EV infrastructure, the tax exemptions applied to

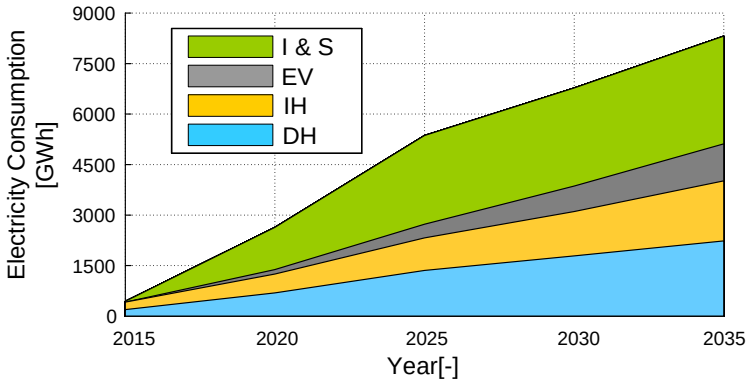

Figure 1.14: *Growth of the Electricity Consumption Foreseen by 2035 [10].*

the new EVs and the stimulation plans for replacing the old fashion heating systems are the best example that this is already happening in Denmark.

Although this affects every power system level, the nature of the expected loads points out the power distribution systems especially. From a DSO perspective this represents a challenge and an opportunity at the same time. One of the most concerning issues for them is how to accommodate large numbers of highly rated loads in networks that were not designed with that purpose. In [34], a study made in several 0.4 kV radials determined that the electricity consumption expected in Denmark by 2025, would extensively overload a large percentage of the actual LV networks. Therefore, the consequences are already well known; large voltage deviations, phase unbalances, overloading of the current infrastructure. On the other hand, understanding the flexible character of these loads, the advantages of the DR can be exploited.

1.4 Project Goals, Objectives and Methodology

This PhD project represents one of the working tasks of a global project called "Development of a Secure, Economic and Environmentally-friendly Modern Power Systems", where it is intended to provide different technical and economical solutions for renewable energy based power systems. This PhD project aims *to assess the feasibility of the interaction between the power system and the gas, heating and transportation systems and the impact that this causes in the power grid.* Based on the energy system designed by the Danish authorities, EWH, HP and PEV systems and large scale electrolyzers will gradually be accommodated in the current system. Taking these into consideration, this work addresses the following topics focusing on the distribution systems and in particular on the LV ones.

- First, to investigate the single load behavior and the user requirements.
- Second, to define and quantify the flexibility that active loads are able to provide.
- Third, to examine the hosting capability of the current LV systems with the purpose of finding the nature and location of potential bottlenecks.
- Finally, to propose new alternatives for controlling the DR in LV networks with high penetration of active loads.

The software platforms employed to carry this research through are Matlab/Simulink in what load and consumer modelling concerns and DIgSILENT PowerFactory for all the tasks related with the active loads and LV network simulation. The methodology utilized is summarized in the following steps:

- The single load behavior and the variables affecting its power consumption pattern are comprehended by independently modelling each of the loads. This permits a better understanding of aspects like, the relation between the thermal

power demand of a household and the electrical power consumption from the thermostatic loads. Furthermore, the direct relation between the driving pattern of a user and the power demand of the domestic battery charger located at home is also appreciated.

- The statistical analysis made on the thermal and mobility requirements from Danish residential users highlights the seasonal influence on the electrical demand from thermostatic loads. Moreover, different profiles representing the daily behavior of users in possession of these loads are generated. These are essential for the definition of their power consumption pattern during the time domain simulations.
- A comparison between non-flexible consumers and flexible consumers is made based on measurement campaign data obtained from the DSO. These makes possible to define and quantify the potential flexibility that certain loads may be able to offer in the future. The limitations to provide flexibility from thermostatic loads during the winter and summer seasons is to be highlighted.
- Depending on the location where new loads are accommodated the LV network behaves differently in terms of power flow. An steady state analysis is used to investigate the current capacity and hosting capability of LV grids when submitted to different load penetrations. Moreover, the nature and location of possible constrains are intended to be underlined.
- Finally, through time domain simulations, the future dynamic behavior of LV grids is intended to be represented. Depending on the load penetration, high congested periods, which may last for few hours, may constrain the power transfer capability of these networks.

1.5 Technical Limitations

The need for simplifying the problem implies sometimes to consider some limitations on the investigation. In this case:

- The active load models, which are based on commercial data-sheet from manufactures, are selected three-phase connection. The reason is the simplification of the network analysis from a single-phase unbalance to a three-phase balance problem. The single-phase is a common connection in LV networks and the unbalances between phases may represent an important challenge in some particular networks. Especially in those where a single consumers or a group of them located in remote areas are supplied with a single phase connection. In Denmark instead, the three-phase is a common connection in residential areas. The power carrier is normally connected thought a 35 A fuse to the household cable box [35].

Therefore, since this research work in based on the Danish case this simplification does not represent a significant constraint for the potential findings.

- The common load of each consumer is unique and is represented by the data obtained from a measurement campaign of the DSO. In the time domain simulation, this is illustrated by one-hour based consumption profiles. Since the power consumption is averaged within this time interval the sudden peaks characteristic of this kind off systems are eliminated. The synchronization of several peaks is one of the mayor concerns for DSOs since it may lead to continuous melting of the system protection.
- The plurality in device and storage capacity is not contemplated within the modelled residential consumers. Among the users with HP systems, 300 and 500 l HWSTs are distributed in equal proportion. The same battery size is considered among the users with PEV systems. In the reality, the user should select the size and capacity of the system according to their thermal and mobility requirements. Different individuals have different necessities.
- The system penetration of PV or another type of distributed generation is not contemplated in this case. Even though, nowadays it may not be many of those in the test systems considered, they may significantly appear in the future.
- The power quality issues originated by an active control of flexible loads are not considered in this case. Especially with thermostatic loads, a frequent and synchronized activation of these units may result in unacceptable variations of the voltage.
- Even though the ICT represents the backbone of such a smart system, their influence is not considered in this study. In fact, the data process and exchange capability and the size of the data-storage are aspects which will definitely affect the performance of any control implemented in the power distribution network.

1.6 Thesis Outline and Publications

This thesis is composed of two major parts, **Part I – Report** and **Part II – Publications**. The first part is an introduction, a state of the art, the load modelling and a finally summary of the research reflected in the publications. This part of the report is structured in several chapters, as follows:

- **Chapter 1** introduces the Danish case and sets the project scope. It also defines and describes the methodologies used together with its limitations. Moreover, this chapter provides a guideline on how this thesis can to be utilized.
- **Chapter 2** summarizes the state of the art and lists the most relevant literature which has influenced the work reflected in this thesis. It especially focuses on

areas like modelling of active loads, impact assessment of LV network and different strategies utilized for solving technical constrains in LV networks.

- **Chapter 3** provides a detailed description of the mathematical models developed in order to represent the flexible loads considered in this work. Each model is validated with different simulations and the results are discussed with the purpose of understanding their behavior better.
- **Chapter 4** introduces statistical analysis made on thermal and driving requirements from Danish residential users. Additionally, this chapter summarizes the methodology employed to generate profiles which realistically represent the habits from residential users concerning these two aspects.
- **Chapter 5** summarizes the methodology employed in order to define and quantify the potential flexibility from residential loads. This approach is validated considering the case of a heat pump where its potential flexibility is deducted from its power consumption pattern.
- **Chapter 6** briefly describes the approach utilized to analyze the impact caused in LV grids by the upcoming HP and PEV loads. It also illustrates a way to probabilistically identify possible vulnerable points in this system when it is submitted to various levels of load penetration.
- **Chapter 7** addresses an important subject of this thesis, namely the control of the DR in LV networks. The work developed in previous chapters serves to comprehend the natural behavior of the loads, the users and the network. Based on this, the chapter introduces a hierarchical structure proposed for controlling HP and PEV loads in the LV grid according to different technical and commercial aspects.
- **Chapter 8** is the concluding chapter of this thesis. A part from the project conclusions and contributions some guidelines for future work are also provided here. Furthermore, the chapter underlines the main achievement and contributions of this thesis.

In the second part of the thesis, **Part II – Publications**, the main outcome of this research project is presented with a list of manuscripts. This collection includes the following peer-reviewed journal papers (accepted, under review or to be submitted) and conference contributions:

Conference Papers

C1. **Diaz de Cerio Mendaza, I.**; Bak-Jensen, B.; Zhe Chen, "Alkaline electrolyzer and V2G system DIgSILENT models for demand response analysis in future distribution networks," *PowerTech (POWERTECH), 2013 IEEE Grenoble* , vol., no., pp.1,8, 16-20 June 2013

C2. **Diaz de Cerio Mendaza, I**; Pigazo, A; Bak-Jensen, B.; Zhe Chen, "Generation of domestic hot water, space heating and driving pattern profiles for integration analysis of active loads in low voltage grids," *Innovative Smart Grid Technologies Europe (ISGT EUROPE), 2013 4th IEEE/PES* , vol., no., pp.1,5, 6-9 Oct. 2013.

C3. Bjerregaard, P.T.; Grzegorz Szczesny, I.; **Diaz de Cerio Mendaza, I.**; Pillai, J.R., "Intelligent control of flexible loads for improving low voltage grids utilization," *Innovative Smart Grid Technologies Europe (ISGT EUROPE), 2013 4th IEEE/PES* , vol., no., pp.1,5, 6-9 Oct. 2013

C4. Kouzelis, K.; **Diaz de Cerio Mendaza, I**; Bak-Jensen, B., "Probabilistic Quantification of Potentially Flexible Residential Demand" *in Proc. of Power and Energy Society General Meeting (PES)*, 2014 IEEE, accepted, July 2014.

C5. **Diaz de Cerio Mendaza, I.**; Bak-Jensen, B.; Zhe Chen; Jensen, A., "Stochastic Impact Assessment of the Heating and Transportation Systems Electrification on LV grids" *in Proc. of Innovative Smart Grid Technologies Europe (ISGT EUROPE), 2014 5th IEEE/PES* , accepted, Oct. 2014.

Journal Papers

J1. **Diaz de Cerio Mendaza, I.**; Grzegorz Szczesny, I.; Pillai, J. R. ; Bak-Jensen, B., "Flexible Demand Control to Enhance the Dynamic Operation of Low Voltage Networks", *Smart Grid, IEEE Transactions on* , vol.6, no.2, pp.705,715, March 2015.

J2. **Diaz de Cerio Mendaza, I.**; Grzegorz Szczesny, I.; Pillai, J. R. ; Bak-Jensen, B., "Active Control of Demand Response in Low Voltage Grids for Technical and Commercial Aggregation Services" *IEEE Trans. on Smart Grids*, under review, 2015.

Since the papers listed above contain the mayor part of the technical description and the results of this thesis, it is important to define their relationship with the report chapters. This is shown in Table 1.3

Table 1.3: *Relationship between Chapters in the Report and Publications*

Chapter in the Report	1	2	3	4	5	6	7	8
Publication	-	-	C1	C2	C4	C5	C3, J1, J2	-

Chapter II

State of the Art

In this chapter, a summary of the most relevant literature for this research work is presented. The biography utilized tacked a large spectrum of topics, from the active load modelling till the different strategies utilized for solving technical constrains in LV networks. Additionally, the approaches employed to asses the impact originated by the integration of flexible demand are also discussed.

2.1 Introduction

The availability and the capacity of energy storage is an important aspect in the control and operation of renewable energy based power systems. Fig. 2.1 gives an overview of the main storage technologies available or under development nowadays. In the previous chapter has pointed out, the Danish solution to achieve a 100 % carbon free energy

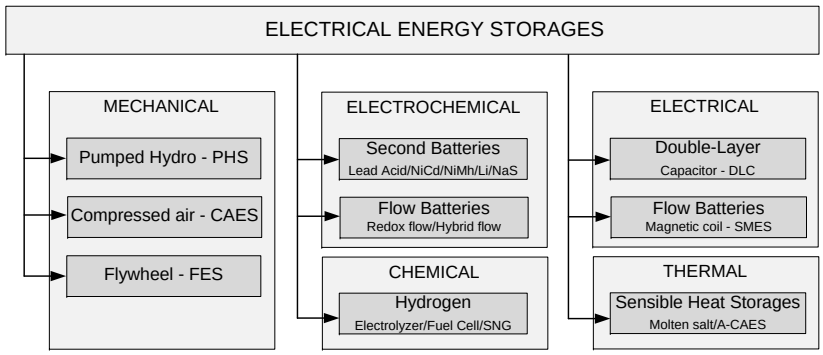

Figure 2.1: *Types of Electrical Energy Storage [36]*

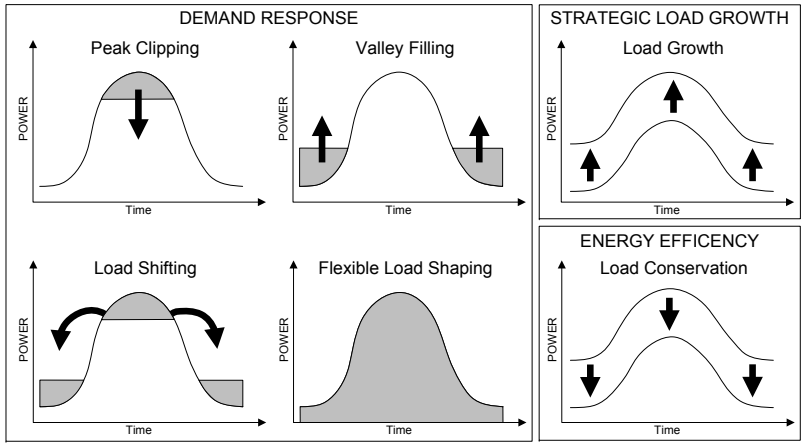

Figure 2.2: *Categorization of the DSM [39]*

system passes for interacting the power system and the gas, heating and transportation systems. Therefore, the conversion of electrical energy into other energy vectors makes accessible and available new storage possibilities which will indeed be needed in the future. Based on the design and configuration of IDAs Climate Plan for 2050 [37], the thermal, electrochemical and chemical systems seem to be the storage solutions that match appropriately with the Danish case. In this context, the DSM and in particular the DR represents the physical interconnection between those and the power system.

According to [38], *"DSM encompasses the entire range of management functions associated with directing demand-side activities, including program planning, evaluation, implementation, and monitoring"*. This is normally categorized depending on the load shape objective that is sought [39]. Fig. 2.2 illustrates that those are normally divided as, demand response, strategic load growth and energy efficiency. The strategic load growth and the energy efficiency refer to the increase or decrease of the load with the purpose of achieving an efficient performance of the system in the long-run [40]. According to the U.S Federal Energy Regulatory Commission, DR is defined as *"the changes in electricity usage by end-use consumers from their normal consumption pattern in response to changes in the price of electricity over time, or to incentive payments designed to induce lower electricity use at times of high wholesale market prices or when system reliability is jeopardized"* [41]. Among the load shapes pursued by a DR strategy, peak clipping, valley filling, load shifting and flexible load shaping are the most common ones. Furthermore, according what it is stated in chapter 1, small scale thermostatic loads (EWH and HPWH) and PEVs are expected to be connected at the LV level while large scale EWH, HPs for district heating purposes and P2G systems at the MV level.

The demand side participation is not an innovative technology in what the power

system regulation concerns. After World War I, large EB were introduced in Canada in order to utilize the surplus of hydroelectric power [42]. However, it was during the late 70s early 80s when it became rather interesting in aspects such as the energy conservation and the load management. This was mainly encouraged by the rise in the cost of electricity and the competition from alternative energy sources [43], [44]. In the last years, this interest has significantly grown due to the advantages that DR introduces in terms of renewable energy integration. A practical demonstration carried out in [45] illustrates the potential from Danish CHP plants and the local district heating in the provision of power regulation services. The test unit under study, located in Ringkøbing, is composed by a gas engine and gas turbine of 4.7 MW_{el} and 5.9 MW_{th} each, an electric boiler of 11 MW_{el} and a gas boiler of 40 MW_{th}. The system is additionally composed by 250.07 MWh of heat storage and a heat demand of 85000 MWh. Under high wind power generation conditions, the price of the regulating power market may became negative for several hours. During those hours it is clearly illustrated how the plant, with the employment of EB, actively responds to the need for increasing the system demand. In this sense, it benefits from the fact that it generates and stores heat in cheap electricity periods while aiding the system regulation.

Inspired by the smart grid debate, the DR at residential level is frequently appointed as a potential source of flexibility for renewable energy based power systems. The heating is one of the promising sectors which are intended to be exploited with those matters. By default, buildings and households have large thermal capacities. From a thermal point of view, their time constant is quite significant comparing with the electrical dynamics. This fact makes the thermal and electrical demand to be practically detached. Therefore, it is possible to move power consumption from the heating systems in time without compromising the comfort of household residents [46].

In this context, the flexible demand from domestic EWH and HP systems is particularly underlined. In [47] and [48], it is claimed that an active participation from HP systems can reduce the operation cost and the CO_2 emissions in power systems with high level of wind power share. In the same way, [49] and [50] show that the frequency fluctuations, characteristic of renewable energy based power systems, are possible to be suppressed with the synchronized response of numbers of these appliances. In [51] is demonstrated that with proper control it is possible to reduce the storage capacity required from more expensive systems for the compensation of the power fluctuations.

EWHs are also commonly used as a source of flexibility with various purposes. The thermostat set-point control of aggregated EWH was utilized in [52] to demonstrate the economic benefit for user participating in DR programs and the provision of balancing reserve for utilities. The direct control approach is exploited in [53] to make EWH follow power regulation signals. By the participation in the power regulation market, the load-serving entities are able to recover the investments made in the telecommunication infrastructure to communicate with the assets. The reduction of the amount of PV power curtailment, due to network stress conditions, and the provision of load

frequency reserves are mentioned in [54] as the advantages of controllable aggregation of EWH. Furthermore, reductions of the infeed prediction error of wind generators are claimed in [55], when allowing a large cluster of those participating in the active power regulation.

The road transport is another sector which may represent a source of flexibility in the future. In this sense, the active control of EV charging seems to be also in the core of the DR discussion. Even though, their storage availability may be bounded depending on the participation context, it is possible to shift their charging operation as well as vary their charging rate [56]. The opportunities introduced by the collective response from PEVs, especially in the provision of load frequency services, is emphasized in [57–60]. By controlling the charging of those, the system operator could benefit from lower system frequency deviations and an increase of the available regulation capacity. The reduction of the system generation costs is underlined in [61]. Indeed, displacing the charging operation to valley hours is possible to avoid system overloading while reducing the power generation cost. As with the EWHs, the charging flexibility offered by PEVs is also possible to be employed in order to compensate the power forecast errors from renewables and in consequence the cost those implies [62], [63].

In line with this, the application of V2G concept launches new alternatives in the regulation of the power system. Although, some reticence exists from some scientific sectors, due to the degradation that this implies for the EV battery [64], it represents an emerging technology for battery storage applications. This technology is presented in [65–69] as an interesting solution to contribute in the future power system stabilization. In cases where the system frequency fluctuates due to high renewable energy share, a coordinated response from number of EVs performing as V2G allows to compensate the frequency deviations. Moreover, it is stated that a faster and more stable frequency control and up and down regulation is possible when comparing with the conventional generation units. Additionally, their synchronized response shows potential in other areas like the voltage support and the peak shaving in distribution systems [70], [71].

Other promising sectors, such as the generation of alternative and renewable fuels, are also expected to offer flexibility. This is the case of the hydrogen generation and the active response from electrolyzer loads. Even though, their research, development and implementation is not widely extended yet, more than for stand-alone or autonomous systems, they are considered important for the regulation of future power systems. This fact is appreciable with the increase of demonstration projects developed within the last years in Europe, which aim to demonstrate the capability from hydrogen storage systems to integrate more renewable energy [72]. Although as it has mentioned before, its employment is still mostly limited to small scale applications, the obtained results may be potentially implementable into large scale cases.

In stand-alone systems, i.e inhabited places with good wind condition but without connectable grid, the option of having a load with fast dynamics, such as an electrolyser, is very attractive for energy harvesting purposes. In [73–75] it is demonstrated how this

load is able to follow the dynamics of wind and PV power generation providing at the same time storage capacity for the excess of energy. Another example of the synergy between renewable energy production and hydrogen is given in remote or islanded communities where an autonomous energy system is needed. The technical advantages of using electrolyzers to balance the renewable generation, which normally represents the base generation in such a systems, is underlined in [76–80]. Furthermore, the storage capability of this energy vector allows a larger penetration of renewables and in consequence a mayor utilization of these sources. The minimization of the grid impact produced by large scale renewable energy plants is also investigated recently [81–85]. Here, the feasibility and effectiveness of using large size electrolyzers connected at the point of common coupling of a single generator or power plant to smooth the power injected to the network is demonstrated. Moreover, the provision of medium to long-term energy balancing services is also one of the mentioned advantages of such a system. Finally, in [86] it is evidenced that the strategic location of grid connected electrolysers in the transmission system reduces the total system load and improves the voltages of operation. According to [87] and [88], the total construction and operation cost of future expansions on the transmission system could be reduce with their implementation facilitating at the same time larger accommodation of wind power in the system.

Up to this point, the potential from different load technologies to provide DR services at a higher system level are described. However, it cannot be neglected that most of these loads are expected to be integrated into the distribution levels of a power system. This means that it is important to assess the opportunities and limitations that those introduce at the local level. This research work is oriented in this direction, therefore the next subsections introduce the most influential literature used to carry this out. The aspects covered in the selected literature are; modelling of flexible loads, their technical and economic impact in the distribution networks and the control alternatives for the correction of the network constrains.

2.2 Modelling of Active Loads

The load representation in large and complex power system studies is traditionally simplified and aggregated depending on the aim of the analysis. Once the analysis gets out of this context and moves towards small and local systems these methods become less able to represent the natural characteristics of the load. This is the case of LV distribution grids, where depending on the load and its independent behaviour the network responds differently. In consequence, there is a need to capture this singularity when they are modelled. So, to represent their electrical behaviour, i.e power consumption pattern, additional and interdisciplinary aspects needs to be taken into account.

It is true that a wide spectrum of potentially flexible loads exits, especially at residential level. However, for this work the most relevant ones based on the prognostics made by the Danish authorities have been selected. Therefore, the load models devel-

oped and used for the system analysis are EWHs, HP, PEV systems and electrolyzers. Then, the literature survey and the posterior analysis will be focused on those.

2.2.1 Electric Water Heater

Via a water immersed resistor/electrode the EWH uses electric energy as heat source to heat water stored in a tank. As a thermostatic load, the modelling of its power consumption normally implies the consideration of thermal aspects. The range of mathematical models available in the literature vary in complexity and detail but in most of the cases the physical equations governing the system are based in the first law of thermodynamics -a simple energy balance-.

With a simple classification, those could be divided into one, two and multi node/layer models and models for aggregation purposes. The one, two and multi node/layer models intend to reflect, with more or less detail, the evolution of certain state variables (temperature, energy, etc) in the storage tank. So, in the one node/layer, the temperature of the water inside the tank is assumed uniform, meaning that it is equal at any point of the cylinder. Therefore, as it is shown in [52] and [89–91], the heat transfer is modelled as a first order differential equation. This is a very common simplification adopted in relatively small size tanks. Nevertheless, for large size tanks an especially if a precise understanding of the link between the thermal and the electrical demand is required this kind of model may present limitations.

In reality, the temperature of the water stored in the tank varies at different depths due to the change in water's density with its temperature. This thermal phenomenon is called water stratification. With the two node/layer model what is intended is to give a solution, in a more simplistic way, to the limitations of the previous model. Two water compartments are defined inside the storage tank, the upper one with an uniform temperature close to the setting and the lower one also uniform but close to the inlet water conditions. Again, an energy balance made in each compartment represents the state variable dynamics. As depicted in [92] and [93] the height of the hot water influences its temperature dynamics too. The multi node/layer model tries to simulate more precisely the temperature distribution in the tank. Therefore, the storage device is divided in n sections where in each of them a first order differential equation is solved. Each of these n equations will also reflect the heat interaction existing between different sections. Depending on the precision required to simulate this phenomenon the number of section will be more or less [94], [95].

The aggregated behaviour of a EWH population is commonly modelled by selecting the one node/layer model with a stochastic method [54], [96]. Others instead are more oriented to the definition of a group of appliance states within a time frame [97], [98].

Table 2.1: *Heat Pump Models Available in the Literature*

Technology	Reference	Window
Ground to Water	[46], [99], [100], [101], [102], [103], [104] and [105]	2007-2012
Air to Water	[49], [106], [107], [108], [109] and [110]	2011-2013
Air to Air	[111], [112] and [113]	2011-2014

2.2.2 Heat Pump System

The HP is a combination of different electro and thermo-mechanical elements defining a thermo-dynamical cycle. It aims to transfer thermal energy from one source at lower/higher temperature to another location at higher/lower temperature depending on the working mode, i.e. heating or cooling. They are normally classified based on the heat source and the kind of system used to supply the thermal demand. As it is assumable their modelling is expected to be different depending on the combination of these two aspects. As a simple reference, Table 2.1 summarizes some of the typical models published recently.

All these models aim to represent the electrical consumption pattern of the HP load under a specific thermal demand of the user. This underlines the importance of combining the electrical and thermal aspects in the modelling process of these loads. Indeed, when looking into the composition those models two parts are clearly differentiable, the HP and the sink system.

Since for representing the load pattern detailed thermal models would imply high computational costs. This problem is commonly simplified with the employment of the COP expression representative of these systems. The COP is defined as the ratio of heating or cooling power provided by the HP in respect to the electrical power consumed. When the unit is activated, the heat supply is normally deducted from this expression. Now, the discussion centres in how to define this expression, since there are various approaches to consider. On the one hand, there are cases, among them [114–116], which consider the COP invariable or constant. In reality, the COP value significantly depends on source and sinks conditions. From an aggregated perspective, this may not be very important. However, in cases where the singular behaviour of different units is to be captured this could introduce some limitations, especially because the COP may vary significantly during the unit operation time [117]. On the other hand, others use a polynomial expression to represent the COP as a function of the source and the sink conditions [118–120]. Nevertheless, this approach implies to have a more detailed modelling of the sink system to be able to calculate the variables for the COP expression.

The sinks which are normally considered in HP system models are; floor heating and HWST. The first one is normally simplified to a single-zone model where the heat dynamics are normally defined by a set of ordinary differential equations [121–123]. As

Table 2.2: *Electrolyzer Models Available in the Literature*

Technology	Reference	Window
Alkaline	[126], [127], [128], [129], [130], [131], [132] and [133]	1998-2012
PEM	[134], [135], [136], [137] and [138]	2011-2013
SO	[139] and [140]	2011

with the EWH case, the HWST is commonly represented by the n node/layer models. Depending on the level of precision required, the sectionalisation of the tank will be higher or lower. The one node/layer is commonly used by many researcher due to its simplistic implementation [49]. However, it cannot be neglected that depending on the heat demand supplied -DHW and SH- the size of the storage may increase reasonably. In consequence, larger tanks will be more exposed to the stratification phenomenon which implies its precise modelling in these cases [124].

2.2.3 Electrolyzer System

An electrolyzer is a combination of different electro-chemical elements which allow the decomposition of an electrolyte -solution of KOH in water- into hydrogen and oxygen, by passing a direct current between two electrodes. The electrolyzers are normally classified as, alkaline, proton exchange membrane (PEM) and solid oxide (SO) [125]. The AEs, which is considered as a more mature technology in comparison with the other two, is commonly used for large scale hydrogen generation applications. There is a wide literature respect to electrolyzers modelling giving possibilities to find different approaches depending on the analysis required. Table 2.2 summarizes some of the typical electrolyzer models published in the recent years.

Regarding the modelling of AE, the work carried out by Ulleberg during the late 90s must be highlighted as one the important references in this area [126], [127]. The AE model introduced is composed by three parts, the I-U characteristic curve, the thermal model and the hydrogen production. The I-U characteristic curve, which is represented by a non-linear equation, defines the current and voltage kinetics in the system electrodes. The temperature dynamics of the electrolyzer stack are defined with an energy balance made in the thermal model. Finally, the hydrogen production part refers to the set of equations used to calculate the hydrogen amount generated. Its implementation was posteriorly assessed inside a renewable energy based stand-alone power system. Its good accuracy and suitability was demonstrated in this kind of system analysis. Based on this, researchers from [129] to [131] have applied and upgraded the model depending on their convenience. However, this is not the only approach utilised to model such a kind of system. Authors in [132] employed the von Hoerner system in order to address the power control of a wind-hydrogen system. A simplification of this last

one was introduced by [133] in order to perform dynamic simulations in a wind/fuel cell/electrolyzer/ultra-capacitor system. His implementation though may be restricted due to the consideration of constant temperature and operation point.

A commonly employed method to model the PEM electrolyzers is the so called equivalent electrical circuit. This approach, which is employed from [134] to [137], intends to represent the electrical behaviour of this system based on a typical circuit composed of a series resistance and a resistance and capacitance in parallel. Nevertheless, there are also other ways to perform this task. Authors in [138] introduce a model with similar structure as for the one presented by Ulleberg for the AE but for PEM electrolysers instead.

Due to its fast load dynamics, the solid oxide electrolysis has recently captured a lot of attention in the power regulation aspect. The problem is that the technology is still under research and development which means that it is not mature technology [141]. Some of the mathematical models available are in [139] and [140].

2.2.4 Electric Vehicle and Vehicle to the Grid

Among the scientific community, the EV seems to be highly recognised in DR applications when it is capered with other flexible loads. Although, its participation in DR can be seen either from the charging (EV) or also discharging (V2G) perspective both share a common feature, the battery storage. Indeed, the battery storage represents many times the core of the modelling process of such kind of load. As it also represents a big part of the model introduced in the chapter 3, the literature review is oriented towards this aspect. Since, the aim is to perform long-term dynamic simulations the model should be simple to implement, computationally not heavy and precise.

The battery storage models available are normally classified as mathematical, electrical or electrochemical [142]. The electrochemical models are commonly used for the design and optimization of physic-chemical aspects of batteries [143,144]. However, the detail level of precision required implies the need for sets of partial differential equations which makes their resolution complex and time consuming. The mathematical models use the empirical approach to represent the system behaviour such as capacity, runtime or efficiency. However, the accuracy of the results that they provide is sometimes limited and do not offer information about the voltage current relationship [145], [146].

In what the dynamic analysis of the power system concerns, the electrical model is one of the most used methods to represents battery storage [147–149]. This is normally defined by an electrical circuit, which is a combination of voltage sources, resistors, and capacitors. Although, as it is stated in [142] there are different ways to characterize the electrical model, the Thevenin approach is frequently employed [150–152]. The reasons, when this is compared with others, are its simplicity and precision. However, its inaccurate estimation of the battery SOC may sometimes represent a drawback depending on the field of study. Its equivalent circuit normally also contains an ideal voltage source

Table 2.3: *Characteristics of the Different Battery Technologies [153]*

Technology	Lead-Acid	Ni-Cd	Ni-MH	Li-ion	Li-Po	Nas
Efficiency (%)	70-80	60-90	50-80	70-85	70	70
E. density (Wh/kg)	20-35	40-60	60-80	100-200	200	120
P. density (W/kg)	25	140-180	220	360	250-1000	120
Cycle Life (cycles)	200-2000	500-2000	<3000	500-2000	>1200	2000
Self-Discharge	Low	Low	High	High	Medium	Medium

in series with an internal resistance and, depending on the precision of the response required, various parallel RC circuits.

The discussion now moves to deciding the appropriate technology that should be considered for EV or V2G applications. According to Table 2.3, the lithium-ion seems to be one of the promising technologies in electro-chemical storage applications. Furthermore, their high energy and power density, high efficiency and long lifetime make them very attractive for the electric mobility. According to the model profile described, it is reasonable then to select the lithium-ion technology and to represent it with a Thevenin approach. So, depending on the aspect aimed to analyse, the literature offers access to different models with this characteristics. For example, the models introduced in [154], [155] are oriented to accurately represent the dynamic behaviour of the batteries during the charging and discharging process. The circuit parameters provided in [155] are validated via experimental tests. Other models, like in [156], are much more simplified focussing on the power system analysis from an aggregated perspective of the EVs. Such an approach is more normal in load frequency control and regulation aspects of a large power systems.

2.3 Techno-economic Impact of Active Load Integration in LV grids

The conceptual and technological re-structuration foreseen in the Danish energy system reflects an important process of electrification in the gas, heating and transportation systems. Therefore, the power system is expected to undergo a considerable load growth. Mostly, due to the replacement of the old fashion and fossil fuels based technology by more new and efficient electricity driven loads. Although this affects each of the power system levels, Energinet.dk considers that the distribution system and in particular the LV networks are specially targeted due to the nature of the expected loads [157]. Moreover, in this report, thermostatic loads (EWH and HP) and PEVs are appointed as the new loads that are awaited to penetrate these systems. In this context, the assessment

and posterior definition of the impact originated by their integration becomes rather important for the DSOs. Furthermore, this should be done covering both technical and economic aspects of the LV networks.

From a technical perspective, the consequences from allowing high penetration levels of highly rated loads are already well known by the DSOs. Among them; voltage deviations, unbalances, voltage flicker, overloading of the infrastructure, etc. The analysis made in [158] ratifies that thermal bottlenecks are likely to arise with an increase HP penetration. Authors in [159] state that the simultaneous operation of customer appliances aggravated by the introduction of HPs has forced already some DSOs to reinforce part of the LV networks in Netherlands. The studies carried out in [160] demonstrate that the LV grids could reach unacceptable voltage levels even for low penetration levels. The impact of phase voltage unbalances is studied in [161] for different grades of HP load allocation. Important phase deviations are underlined in here due to the problem of having synchronized start up currents from HPs. In [162], the voltage flicker is mentioned also as one of the possible consequences of having starting inrush current of residential heat pumps. This phenomenon is especially notable in the lighting which makes customers complain to the utilities because it is perceived as a service problem.

Since the EV represents also an electrical load, the consequences of its system integration are the same as with any other. Nevertheless, a short summary is made in order to describe some relevant aspects found in the literature about their accommodation in LV systems. The study performed in [163] shows that a large portion of LV feeder cables and the secondary transformer could be significantly overloaded if an uncontrolled charging is considered for those. The influence of the charging rate in the secondary transformer aging is evaluated in [164]. Substantial lifetime reduction is claimed on this piece of the electrical infrastructure when allowing high charging rates on PEVs during peak hours. As with the HP case, extensive voltage drops are appointed in [165] and [166] in relation to the uncontrolled charging of PEVs during peak periods. Finally, the different power quality issues related to the PEV performance in these networks are addressed in [167].

Although, the effect of the load combination is not yet addressed in detail there are already some studies available in the literature. Authors in [168] claim that the impact produced by the combination of HPs and PEVs is very dependent on the distributions of those in the LV feeder. Using a stochastic procedure they conclude that the voltage violations are more likely to occur when the PEV are getting charged.

Another important aspect which DSOs should put emphasis on is looking upon the current capacity and the hosting capability of their systems. To keep track precisely on this aspects may sometimes be difficult for them due to the number of systems which are responsible for operating and controlling. In relation to this, some researchers have recently focused on providing new ideas on how such a kind of studies should be performed. A deterministic approach is utilised in [169] in order to define the maximum capability of these networks to accommodate PEVs. This approach is based on varying

the PEV penetration taking the worst case scenario as a reference. Even though this may be common practice among DSOs or utilities when performing impact studies it does not always represent the reality. Especially because for the same penetration level a load distribution may result in a safe grid performance, while for another different it may not. Therefore, the load distribution or location in the LV grid becomes a rather important factor to consider since a wrong assessment may increase substantially the investment of network reinforcement. By randomly distributing the HP load, authors in [170] investigated the hosting capability of rural and urban networks. However, since for each penetration level there is not an iterative evaluation of the network under different locations of the HP loads the study may be somehow limited.

From an economic perspective, the most distinguished aspect from a large load accommodation is always the cost for network reinforcement [171]. The economic impact originated by the integration of PEVs in LV networks is assessed in [172]. Five different aspects are considered to make the evaluation; existence of voltage control, distribution and location of PEVs, charging profile, penetration level and charging rate.

The fact of not having a voltage control implies the need for voltage reinforcement in LV networks with voltage profile issues. The cost of this may vary between 7.6-30.8 €k depending on the network. The PEV location is another major conditioning in in networks that experience voltage issues. The average economic difference between the worst and the best distribution of PEVs is estimated around 18.6 €k in a possible reinforcement process. The economic impact produced by having alternative charging profiles is much related to the penetration level. In the worst case analysed the reinforcement cost due to this aspect could reach the 59.1 €k. Finally, depending on the charging rate the network impact can be very severe requiring large reinforcement in parts of the network. Depending on the charging strategy (slow or fast), the need for network reinforcement could imply a cost up to 101.1 €k.

The economic impact could be seen also from the consumer perspective. The use of ground source HPs as a heating system for different Swedish households is studied in [173]. As it is stated, in some cases this technology can be a very cost-effective solution providing up to 58% of savings per year in comparison with other technologies. However, in other cases it can be even more expensive in comparison due to growing cost of the electricity which can increase the expected investment return time.

2.4 Control and Management of Technical Constrains in LV grids

The LV grids have been traditionally designed and constructed in order to have a secure and efficient distribution of the power demanded. The "fit and forget" approach is commonly adopted by the DSOs to minimize the costs of operation as much as possible. Most of these networks have a radial topology except in some urban areas where the

link cable boxes are utilized to feed adjacent circuits during maintenance or faults. The secondary transformers are not commonly provided with OLTC technology as with the ones in the primary substations [174].

In this way, the power transfer capability in LV network is majorly constrained by two circumstances, excessive voltage drops and overloading of the infrastructure. These two are more or less correlated depending on their characteristics and design. For example, in urban areas the load is normally more concentrated. Therefore, the network circuit is composed by line cables with short length. Since this makes the network impedance to be lower the overloading is more likely to happen before a voltage constraint. On the other hand, in rural areas the consumers are more spread out which makes that the connection distances much larger. This is reflected with longer line cables and in consequence higher network impedance. So, the voltage constraint is more likely to happen in this case than the overloading.

The violation of the voltage limit is normally a problem occurring at local points of the LV distribution systems. When the steady state voltage profile gets distorted, the traditional ways employed by DSOs to compensate these deviations are summarized as [175]:

- *NLTC transformer*: In cases where the seasonal variation of the demand distorts the voltage profile of the network, the DSOs manually change the transformer tap to adjust these deviations. The standard taps available in this kind of transformers are within $\pm$ 2.5 and $\pm$ 5%.
- *Voltage regulators*: They are essentially transformers with tap changing capability which are connected in series to compensate the voltage along a specific feeder. During heavy load conditions the controller boosts voltage the most and during light load conditions the least. Normally, there are two approaches of regulation, based on the voltage at a given point downstream and to keep the voltage within a chosen band when operating from light to full load.
- *Fixed and switched capacitors*: They are located in strategic points of the network to reduce the voltage drop along the feeder by reducing current flow to loads consuming reactive power. They supply the reactive power or current to counteract the out-phase component of current required by an inductive loads and which also originates the voltage drop [176].

These solutions have been efficiently and cost-effectively operating since its introduction. However, they also have their technical limitations, i.e. regulation capacity, stepwise control, mean lifetime, tracing difficulties, etc. With the need for greater control, coordination and automation of distributed energy resources, new voltage control methods are emerging at this level. Authors in [177] proposed the utilization of the meshed connection of LV feeders as an alternative to increase the hosting capability and in consequence minimize the impact of the integration of new loads in the LV grids. This solution, even though it may be effective, implies partial reinforcement of the network which is exactly

what the DSOs tries to avoid or at least to postpone as much as possible. In [178] and [179], an active tap changing at the secondary transformer is proposed to regulate the demand according to the grid requirements. However, this approach do not consider the local characteristic of the voltage as a constraint [180], since the transformer tap adjustment changes the operation conditions in the whole system. In [180] and [181], the EES are exploited for maintaining the voltage of the network under suitable operating conditions. Nevertheless, it well known that the cost is the biggest drawback of these solutions. Other alternatives based on power electronic applications are recently becoming quite popular. The presence of DGs, such as small scale PV and wind power, allows providing regulation in these systems by altering the injection/curtailment of active and reactive power. By doing so, authors in [182] and [183] claim that the hosting capability of these networks can be increased in order to allow a larger PV generation accommodation. Another alternative in this line are the so called smart transformers and the AVRs. The analysis made in [184] demonstrates that the employment of smart transformer provides the ability to perform better voltage regulation while supporting a higher PEV and PV penetration level. On the other hand, the low time response of the AVRs allows the LV grid to be almost immune to voltage sags or voltage swells occurring in MV system [185].

Finally, the advantages introduced by a local DR in what the system voltage regulation concerns are also underlined in many cases. Authors in [186] and [187] utilize the flexibility provided by thermostatic loads to make them operate during daytime in order to mitigate the voltage rise from the PV generation. In [188] the smart strategy employed for charging different PEVs in the LV systems allows reducing the voltage impact produced by their integration.

As it is previously mentioned the overloading of the infrastructure is another aspect constraining the power distribution in these systems. The management of this has traditionally been tackled by the DSOs with a protection scheme of the network. This scheme is generally composed by a circuit breaker located at the secondary transformer level which allows power transmission up to maximum current value. Each of the feeders are provided with a protection in each of their phases. This is normally a fuse connected at the beginning of the feeder [159]. As with the voltage control, new alternatives are recently appearing in the literature concerning the utilization of DR in order to avoid system overloading in the future. By making HP systems react to local price discrimination, authors in [111] are able to reduce significantly the overloading in the power distribution infrastructure. In [189] the thermal storage connected to a HP is employed in order to shift consumption in time and distress the LV grid. By applying an operator controlled strategy the replacement of the secondary transformer is claimed to be avoidable. The algorithm proposed in [190] coordinates the charging of PEVs based on the market price to effectively shave the peak power demand and delay the need for reinforcement.

Chapter III

Modelling of Active Loads

In this chapter, the mathematical models used to represent the different active or flexible loads are introduced. In order to cover different aspects of the analysis, some of the loads are described with a simple and/or detailed approach. Moreover, with the purpose of understanding their natural behaviour they are validated and evaluated with different dynamic simulations. Part of the results depicted in this chapter can also be found in publication C1, C3 and J1.

3.1 Introduction

In the analysis of large power systems, the load at a particular bus has traditionally been represented aggregated. Since this, it might be composed by large numbers of devices such as appliances, motors, furnaces, etc its modelling needs to be significantly simplified. Depending on the type of analysis its electrical nature is reflected differently. The static models, exponential and/or ZIP, express the load characteristics at any point on time by algebraic expressions. However, these are not sometimes able to represent certain aspects of the load, such as its variation with the time and the weather or its economic dependency. In such cases, specific dynamic models have to be developed to study their effects on the power system [191]. Once the analysis is moved towards the power distribution systems the load starts to get more disaggregated. In the LV systems, in particular, the approach used to model the load has to be seen from a different perspective due to the strong influence that each of the loads have independently in the network performance. In this sense, the representation of the individual and independent behaviour of the consumers and their mayor loads becomes rather important.

Taking this into consideration, various models are developed to represent in detail the operation from different active loads. Since, their performance depends also from non-electrical aspects the models include different features (thermal, mechanical, chemi-

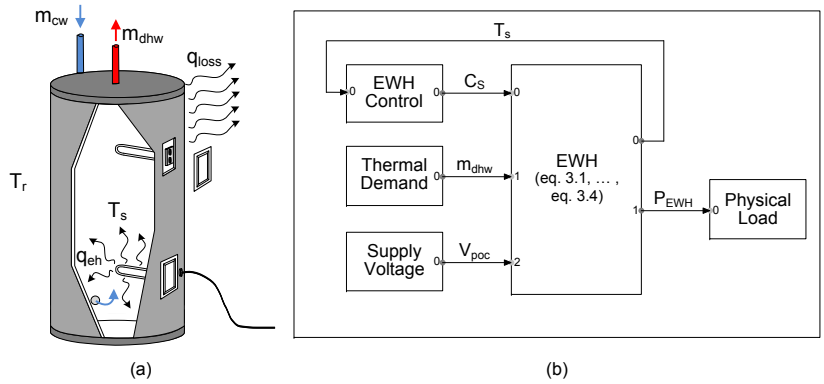

Figure 3.1: *EWH Model: (a) System Overview, (b) DIgSILENT Lay-out.*

cal. . .) in order to cover those. DIgSILENT PowerFactory, and in particular its dynamic simulation language (DSL), is the platform selected to carry out this task. Finally, the set up models are intended to serve as a reference for new researchers starting in DR area.

3.2 Electric Water Heater

Via a water immersed resistor/electrode the EWH, or EB, uses electric energy as a heat source to heat water stored in a tank. The heated water will later be used for the daily domestic activities (cleaning, cooking, washing. . .) in a household. Fig. 3.1(a) shows a simple illustration of the system and Fig. 3.1(b) its DIgSILENT lay-out. As it is depicted, the system considered is oriented to a medium size family, which may be living in a detached house or an apartment. Since, the tank size considered is relatively small the stratification effect is assumed negligible. Therefore, the one node or fully mixed tank approach is selected to model the heat transfer. The physical equations governing the system are based on the first law of thermodynamics which are described by the following differential equation [192].

$$v_t \cdot \rho \cdot Cp_w \frac{dT_s}{dt} = q_{eh} - q_{dhw} - q_{loss} \tag{3.1}$$

where v_t is the volume of the HWST, Cp_w and ρ are specific heat capacity and density of the water and T_s the water temperature in the HWST. Due to the temperature difference between the water stored and the air where the HWST is installed, a heat transfer is originated. Even though, the HWST is insulated in order to minimize this,

there is still a thermal loss (q_{loss}) which is accounted as [192]:

$$q_{loss} = UA \cdot (T_s - T_r) \tag{3.2}$$

where UA is the heat transfer coefficient and T_r is the air temperature of the room where the HWST is installed. Whenever there is a DHW request from the user, the amount of hot water drawn from the HWST is instantaneously replaced by cold water coming from the city water network. This implies that the mass flow of DHW supplied (m_{dhw}) needs to be equal to the cold water supplied to the HWST (m_{cw}). Therefore, the thermal power demanded in form of DHW (q_{dhw}) makes the one stored in HWST decrease [192].

$$q_{loss} = m_{dhw} \cdot Cp_w \cdot (T_s - T_{cw}); \qquad m_{dhw} = m_{cw} \tag{3.3}$$

where T_{cw} is the temperature of the water coming from the city network. Since, the power conversion from electrical to thermal is assumed to be given without any loss, the thermal power generated by the resistor (q_{eh}) is calculated as;

$$q_{eh} = P_{EWH} \cdot C_S; \qquad P_{EWH} = P^{rt}_{EWH} \cdot \left(\frac{V_{poc}}{V_{rt}}\right)^2 \tag{3.4}$$

where P_{EWH} is the electrical power demand of the EWH, P^{rt}_{EWH} its rated power, C_S the control signal defining the ON/OFF status of the appliance, V_{poc} the voltage at its point of connection and the V_{rt} its nominal value. From an electrical perspective, the EWH is characterized as constant impedance load [191]. This means that its power consumption is directly influenced by the voltage at what it is supplied. Based on [193], this effect is captured as it is shown in eq. 3.4.

The EWH is controlled based on a regular hysteresis or ON/OFF control. The electrical resistor turns on (C_S=1) when the T_s drops to the lower cut-off band ($\underline{T}_c$). This will keep heating the water in the HWST until the higher band ($\overline{T}_c$) is reached, that is when it turns off (C_S=0). This cycle is continuously repeated in order to keep the water temperature within the proper limits for its utilization.

3.2.1 Model Verification

The power consumption pattern from a EWH depends on aspects such as its storage size, the DHW demand from the household and the voltage level at what it is supplied.

Table 3.1: *EWH Model Features*

Parameter	v_t (l)	P^{rt}_{EWH} (kW)	UA (W/°C)	T_{cw} (°C)	T_r (°C)	V_{rt} (kV)
Value	100 - 250	2.4	1	10	10	0.4

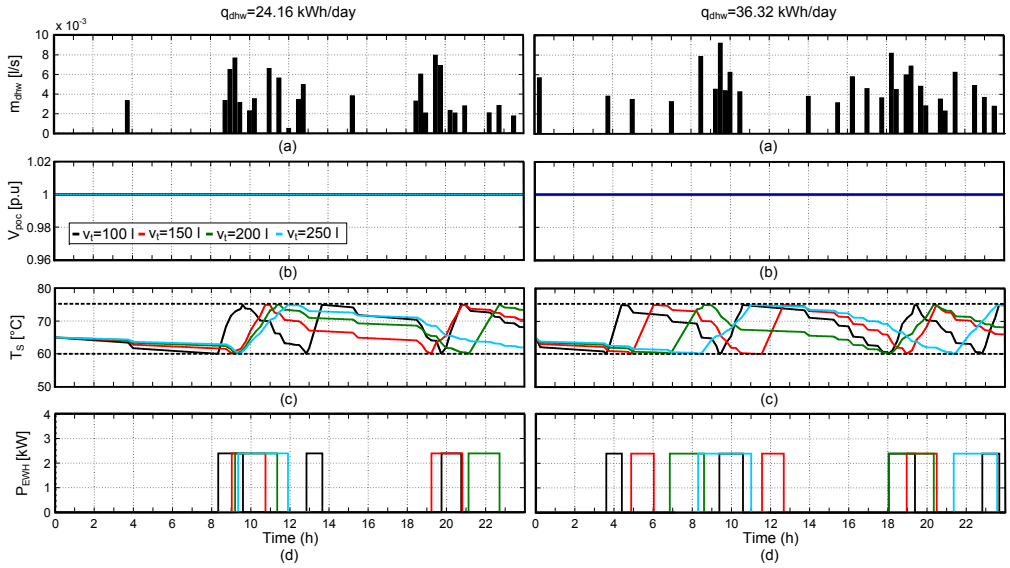

Figure 3.2: *EWH Performance with Different Storage Sizes at Constant Voltage Supply: (a) m_{dhw}, (b) V_{poc}, (c) T_s and (d) P_{EWH}.*

Table 3.1 provides the features utilized to validate the model which is introduced in the previous section. Due to sanitary reasons, the hot water inside the tank is controlled among the thermal range of 60 and 75 °C. Fig. 3.2 and Fig. 3.3 shows the results obtained in the cases designed for its validation. Subfigure (a) shows the DHW consumption profile along a day, subfigure (b) the voltage at the point of connection of the EWH, subfigure (c) the variation of T_s and subfigure (d) the active power demand of the EWH. In both of the cases designed the dynamic behaviour of the EWH is compared under two DHW drawn profiles which implied different thermal energy consumption at the end of the day.

In the first case, it is assumed that the EWH is placed in a strong location of the LV network where the voltage is invariable and equal to 1 p.u. Therefore, to study the influence of the storage size, four tank sizes are taken into account. As it is depicted in Fig. 3.2, since the storage capability from the smaller tanks is limited, the resistor switches ON more frequently to maintain the temperature within the stated limits. On the other hand, the tank with larger capacity switches ON less frequently but also remains active for a longer time. Additionally, the influence that the thermal demand has over the switching frequency of the appliance is significantly clear.

The voltage dependency is another important aspect to point out in the performance of this load. Therefore, an EWH with a storage capacity of 200 l is simulated in four

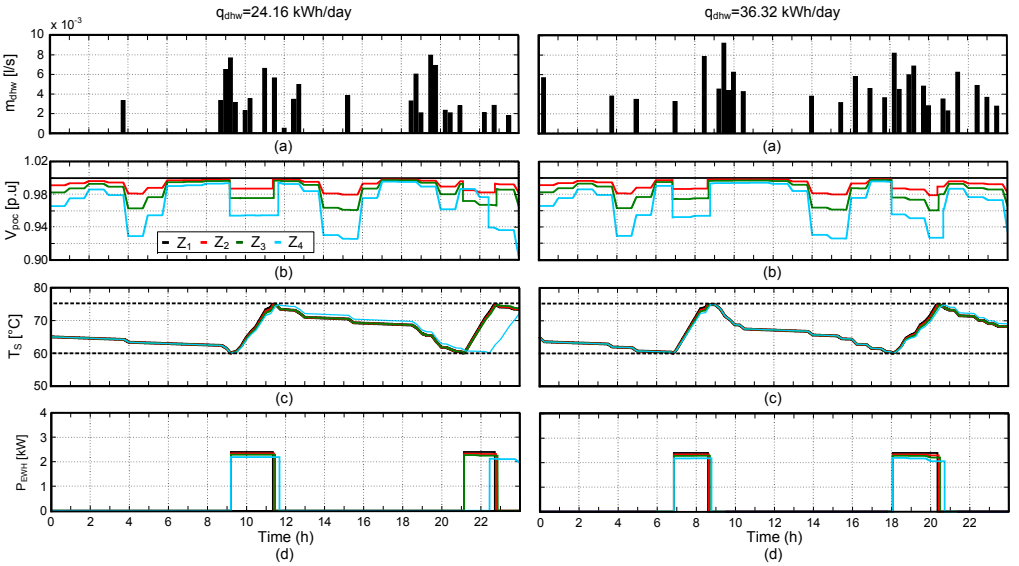

Figure 3.3: *EWH Performance with Different Network Impedances: (a) m_{dhw}, (b) V_{poc}, (c) T_s and (d) P_{EWH}.*

different locations of the LV network. To simulate the natural differences between locations distinct network impedances (Z) are considered for this second case. In Fig. 3.3 is clearly depicted how a lower voltage reduces the active power consumption of the EWH. In consequence this must remain activated for a longer time to achieve the defined thermal requirements. Furthermore, this effect may even affect indirectly the temperature dynamics of the water inside the tank consequently altering the natural consumption pattern of the device.

3.3 Heat Pump Water Heater

A HP aims to transfer thermal energy, with a high efficiency, from one source at lower/higher temperature to a sink location at higher/lower temperature depending on the working mode, i.e. heating or cooling. Therefore, by combining different elements which describe a thermo-dynamical cycle it exploits the physical properties of a volatile, evaporating and condensing fluid known as a refrigerant. This cycle in its simplest form is described as following. The gaseous working fluid enters in a heat exchanger -evaporator- at low pressure and temperature. Here it absorbs heat from the source and it starts to boil. Then, the fluid is pressurized by a compressor, which makes this circulate through the rest of the system. Now, the highly warm and pressurized

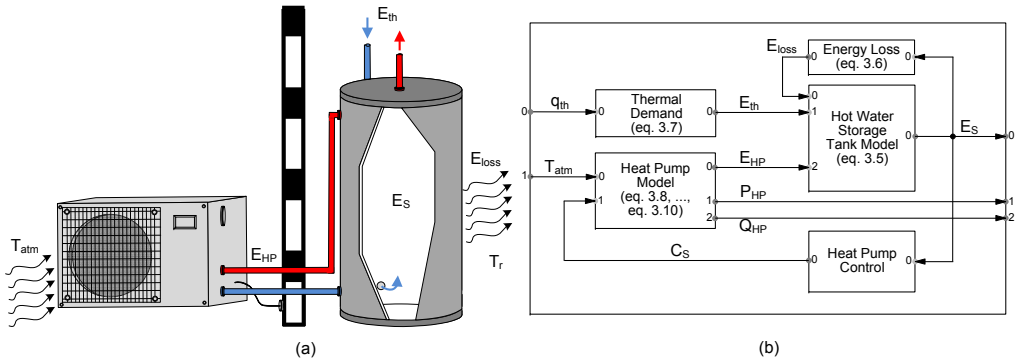

Figure 3.4: *Simple HPWH Model: (a) System Overview, (b) DIgSILENT Lay-out.*

vapour is cooled until it condenses into a high pressure, moderate temperature liquid in a heat exchanger -condenser- located at the discharge side of the compressor. The condensed refrigerant then passes through a pressure-lowering device also called expansion valve. Finally, as a simple notation the water with what the condenser is cooled is the one employed for supplying the domestic demand.

Taking into consideration the different technical and economic aspects from the existing technologies [194], the air-to-water solution interfaced by HWST represents an appropriate technology to supply the future thermal needs of residential households. With the purpose of extending the range of study of this appliance, two approaches are considered in the modelling task.

3.3.1 Simple Approach

The model described in this subsection refers to the model which is introduced in publications C3 and J1. Fig. 3.2(a) gives an overview of the variables of the simple model while Fig. 3.2(b) shows its DSL block diagram. As with the EWH, the average energy inside the tank (E_S), in per unit (p.u), is determined as:

$$E_S = \frac{E_0 + E_{HP} - E_{th} - E_{loss}}{E_{ct}} \tag{3.5}$$

where E_0 and E_{ct} are the initial energy state and the energy capacity of the HWST, in kWh. Attributable again to the temperature difference between the water stored and the air where the HWST is installed, an energy loss exists in the tank (E_{loss}) and is defined as:

$$E_{loss} = \frac{1}{3600} \cdot \int UA \cdot \left(\frac{E_S \cdot E_{ct}}{v_t \cdot Cp_w \cdot \rho \cdot k_n} - T_r \right) \cdot dt \tag{3.6}$$

where v_t is the HWST volume in liters, UA is heat transfer coefficient in W/°C, Cp_w and ρ are the specific heat capacity and the density of the water, k_n is a normalization parameter and T_r the air temperature of the room where the HWST is installed. The EWH are normally designed only to supply thermal demand in form of DHW. The case that they supply thermal demand for SH applications is rare. Unlike with those, the HP systems are frequently used to supply both forms of thermal demand. Therefore, the thermal energy consumption (E_{th}), in kWh, is calculated integrating the thermal power demand (q_{th}) of the household that is represented by the sum of the thermal power demand destined to DHW (q_{dhw}) and SH (q_{sh}).

$$E_{th} = \frac{1}{3600} \cdot \int q_{th} \cdot dt; \qquad q_{th} = q_{dhw} + q_{sh} \tag{3.7}$$

The HP unit is modelled based on the COP approach. Therefore, from the commercial data-sheet of a manufacturer [195], a polynomial interpolation is applied in order to define a COP expression as a function of the atmospheric temperature (T_{atm}).

$$COP = -1.6e^{-5} \cdot T_{atm}^3 + 0.00052 \cdot T_{atm}^2 + 0.073 \cdot T_{atm} + 3.4 \tag{3.8}$$

The HP is electrically rated at P_{HP}^{rt}=3.1 kW with a power factor of 0.98 lagging, after its compensation. Assuming that a constant speed compressor drives the unit, a soft-starter is modelled based on [161]. This should limit the starting current to two times its nominal a second after it is turned ON. Then, the thermal power produced by the HP (q_{HP}) is calculated as:

$$q_{HP} = COP \cdot P_{HP} \cdot C_S \quad where \quad P_{HP} = P_{HP}^{rt}; \quad C_S \in \{0, 1\} \tag{3.9}$$

where C_S is the control signal defining the activation of the HP according to E_S. Nevertheless, the steady state condition of q_{HP} is not instantly achieved. It takes around 15 minutes for such a system [107]. Taking that into consideration, the energy provided by the HP (E_{HP}) is then estimated as:

$$E_{HP} = \frac{1}{3600} \cdot \int q_{HP} \cdot dt \tag{3.10}$$

As with the EWHs, the HP is controlled based on a regular hysteresis control. The unit turns on (C_S=1) when the E_S drops to the lower cut-off band ($\underline{E}_C$). The HP will supply the HWST with thermal energy until the higher band ($\overline{E}_C$) is reached, that is when it will turn off (C_S=0).

3.3.1.1 Model Verification

In this case, two HWSTs are considered to validate the HP system model. Even though, the sizes of the HWSTs are different, 300 l and 500 l, the UA assumed in both is the same, 1 W/°C. Having same UA, even if the tank areas are different, means that due to

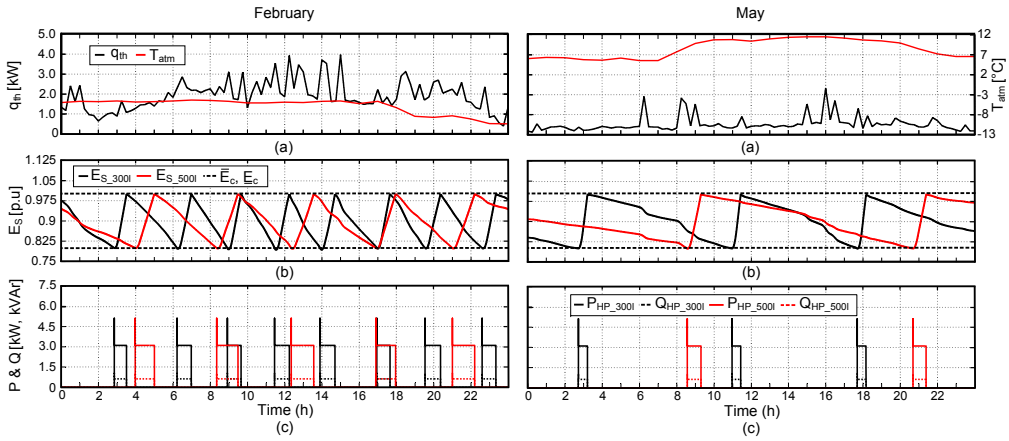

Figure 3.5: *Performance of the Simple HPWH Model: (a) q_{HP} and T_{atm}, (b) E_S, $\underline{E}_C$ and $\overline{E}_C$, (c) P_{HP} and Q_{HP}.*

different insulation characteristics the heat losses for the same temperature conditions are the same in both HWSTs. Since it is supposed that the HWSTs are installed in the household basement where the T_r considered is 10°C. The hot water inside the tank is controlled within the thermal range of 60 to 75°C. Based on [192], it can be said that this is equivalent to control the HWST within the energy range of 20.93-26.17 kWh for the 300 l tank and 34.89-43.61 kWh for the 500 l one. This limits in per unit values are $\underline{E}_C$=0.8 p.u. and $\overline{E}_C$=1 p.u.

The performance of the HP system model is compared in Fig. 3.5 under different operating conditions. In the left hand illustrations, the HP with different HWST is compared under high thermal demand conditions which may represent of a cold winter day in February. The figures on the right-hand side instead compare the same but for a typical day in May. Fig. 3.5(a) shows the T_{atm} and q_{th} of a single household within a 24 h period. Fig. 3.5(b) illustrates the evolution of E_S within this period and Fig. 3.5(c). its active and reactive power (P_{HP}, Q_{HP}) consumption. Notice once again, how for the same T_{atm} and q_{th} conditions, the HWST with lower capacity produces a more frequent activation of the HP. In the same way, the HP performance is significantly changing within different seasons. Under better atmospheric conditions and lower q_{th}, the E_S has much slower variation. As result, the HP stays OFF longer time and consequently reducing its P_{HP} and Q_{HP} consumption.

3.3.2 Detailed Approach

The electrical performance of a HP system is highly influenced by its COP. Therefore, its accurate representation makes the estimation of the power consumption pattern of

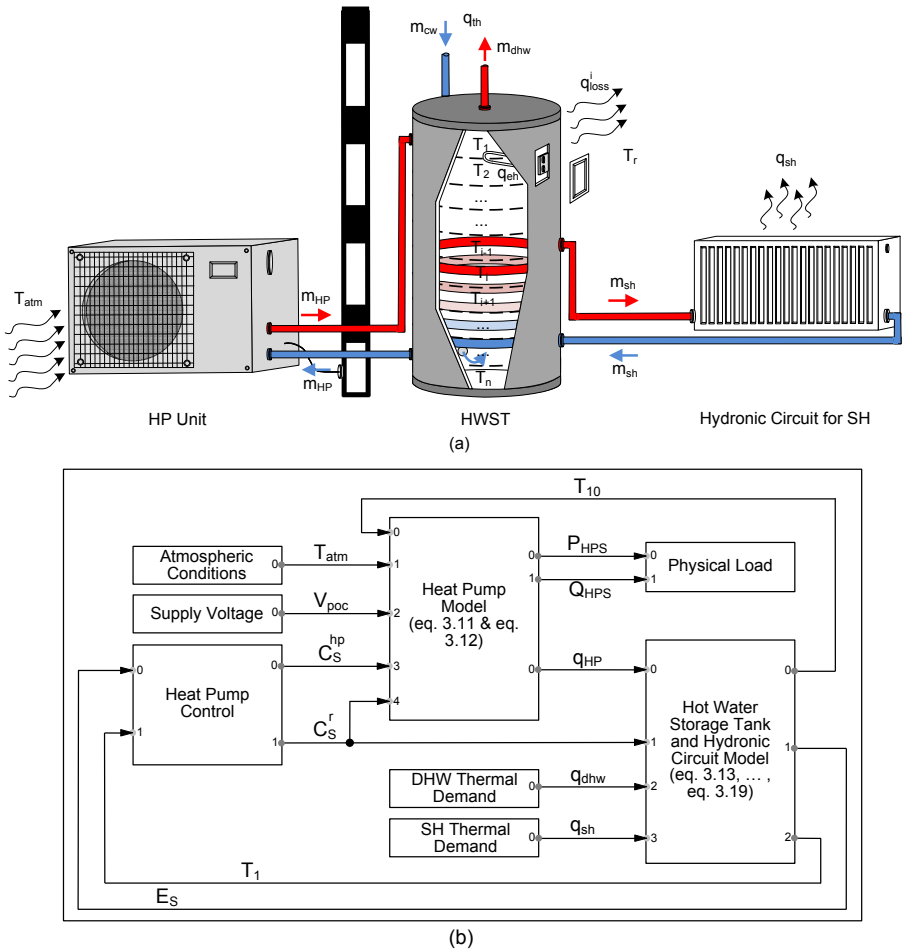

Figure 3.6: *Detailed HPWH Model: (a) System Overview, (b) DIgSILENT Lay-out.*

this load more precise. Generally, the COP depends on the source and sink conditions. Since, having a precise consideration of those is sometimes complicated its expression is commonly simplified or assumed constant. However, these assumptions may sometimes lead to improper or inaccurate representation of its electrical performance.

The aim of this model is to try to capture the physical characteristics of the HP system in order to represent its consumption pattern as good as possible. This implies the consideration of other disciplines such us heat transfer fundamentals. Taking that into consideration, Fig. 3.6(a) illustrates the system developed for this purpose. This

is composed of the HP unit, the HWST and the hydronic circuit to supply the SH demand. The HP unit is directly connected to a HWST. This means that the water from the bottom of the tank (T_n) enters in the condenser and the output water is discharged in the upper part of the tank. In the same way the hydronic circuit is linked to the HWST via a heat exchanger coil immersed in the tank. As it is comprehensible the HP unit stands for the main heat source in such a system. However, the HWST is provided with an electric resistor to aid the HP unit in adverse operating conditions where it is not able to supply the thermal demand requested itself. In Fig. 3.6(b) the DSL block diagram of the model is depicted.

The active power demand of this system (P_{HPS}), in kW, is the summation of the power consumption of the HP unit (P_{HP}) and the resistor located in the HWST (P_R). The reactive power demand, in kVAr, instead refers only to the one drawn by the motor driving the HP compressor (Q_{HPS}) [196].

$$P_{HPS} = P_{HP} + P_R; \qquad Q_{HPS} = P_{HP} \cdot \tan(\varphi); \qquad P_R = P_R^{rt} \cdot \left(\frac{V_{poc}}{V_{rt}}\right)^2 \tag{3.11}$$

where P_R^{rt} is the rated power of the resistor, V_{poc} the voltage at its point of connection and the V_{rt} its nominal value. As with the EWH load, the resistor is characterized as a constant impedance load. Hence, its power consumption is voltage dependent.

This is not the case of the HP unit. As it has been said its compressor is normally driven by a motor which characterizes this as a constant power load [191], [197]. It means that it uses the same amount of power regardless of the voltage at its POC. Furthermore, another aspect confirming this is that the newest HP models are starting to get interfaced with power electronics. This tendency is majorly justified due to the advantages that it introduces on their control and operation. What is aimed with an active control of the HP is to keep the sink temperature unalterable regardless of the source conditions. This principle relies on the adaptation of the compressor speed and in consequence the mass flow of the circulating refrigerant, to compensate any temperature variations originated in the refrigerant due to the source conditions. For example, in a cold winter day the COP decreases drastically because the refrigerant is less able to absorb heat during the evaporation process. In consequence, its temperature after the compression also decreases and so the heat transferred to the water during the condensation process. This confirms the dependency of the output temperature of the cooling water on the source conditions. Now, if the compressor speed is increased the mass flow of the refrigerant circulating through both heat exchangers is higher. Therefore, based on the heat exchange fundamentals this fact compensates the temperature decrease on the refrigerant allowing maintaining the same rate of heat supply.

However, since the compressor speed is controlled by altering the electrical torque of the motor it implies that the power demand of this load will vary according to the source and sink conditions. The representation of this important aspect would require a very detailed modelling of the thermodynamic cycle described by the HP. Developing

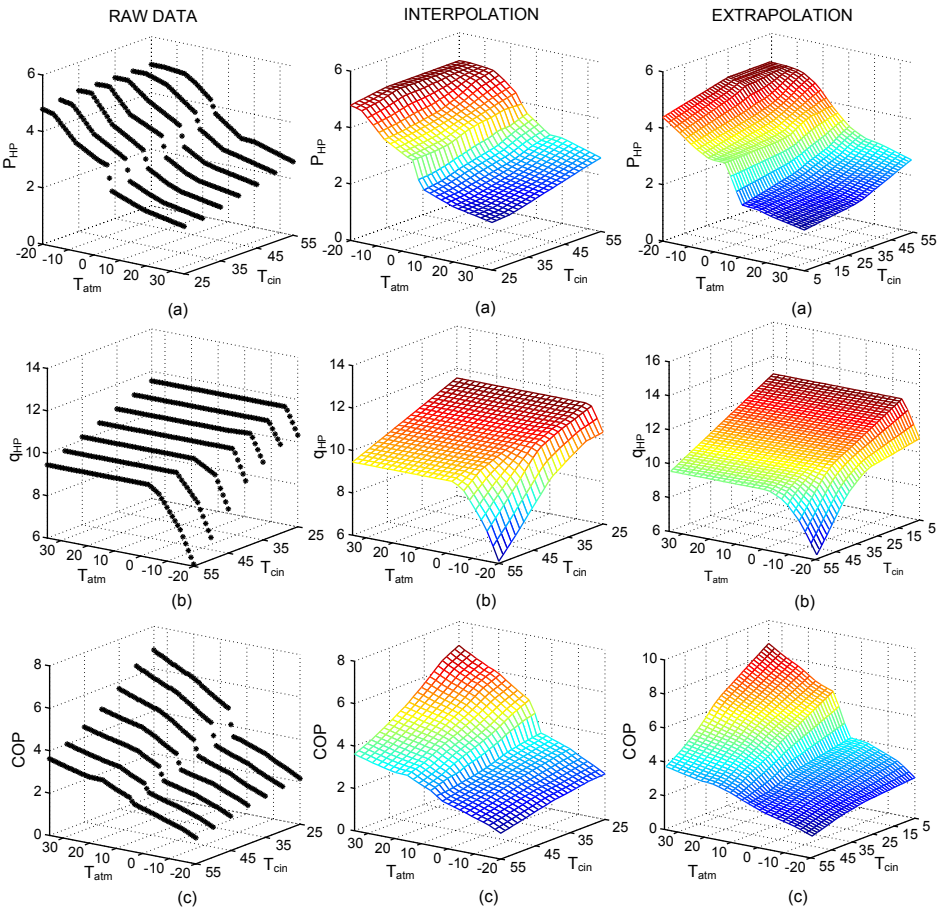

Figure 3.7: *Features of the HP Unit, (a) P_{HP}, (b) q_{HP} and (c) COP [198].*

such a model and using it to represent large number of loads would lead to a unfeasible times of simulation. Taking that into consideration, from the commercial data-sheet from a manufacturer [198], three look-up tables are developed to define the main features of this load, P_{HP}, COP and the thermal power produced (q_{HP}). So, according to what it is previously stated those should be delimited according to the source and sink temperatures as it is represented in Fig. 3.7.

$$P_{HP} = f(T_{atm}, T_{cin}); \quad q_{HP} = f(T_{atm}, T_{cin}); \quad COP = f(T_{atm}, T_{cin}); \tag{3.12}$$

It is worth to mention that based on the raw data of the data-sheet a linear interpolation and a posterior linear extrapolation was performed in order enlarge the operation range covered. Once q_{HP} is known the water temperature of the condenser output (T_{HP}) is deducted based on the equation used in [104]:

$$\frac{dT_{HP}}{dt} = \left((T_{cin} - T_{HP}) + \frac{q_{HP}}{m_{HP} \cdot Cp_w} \right) \cdot \frac{1}{\Delta t} \tag{3.13}$$

where m_{HP} is the mass flow of the water circulating in the condenser, Cp_w is the specific heat capacity of the water and Δt is the time constant of the HP thermal dynamics.

Another important part of this model is the HWST. The HP systems supplying both DHW and SH thermal demands are normally accompanied with a significant HWST. This implies that the water stratification phenomenon should not be neglected since it may have an impact on the power consumption definition. In order to represent precisely the temperature distribution in the tank a multi-node approach is utilized. So, after dividing the HWST into n sections the temperature in the node i (T_i) is deducted by solving the following differential equation [199].

$$\begin{aligned} v_i\, \rho\, Cp_w\, \frac{dT_i}{dt} &= \delta_i^{HP}\, m_{HP}\, Cp_w\, (T_{HP} - T_i) - \delta_i^{cw}\, m_{dhw}\, Cp_w\, (T_i - T_{cw}) \\ &\quad - UA_i (\, T_i - T_r) + \delta_i^{+}\, m_i\, Cp_w\, (T_{i-1} - T_i) + \delta_i^{-}\, m_i\, Cp_w\, (T_i - T_{i+1}) \\ &\quad + A_i\, \frac{\lambda_w}{z_i}\, Cp_w\, (T_{i+1} - 2\, T_i + T_{i-1}) + \delta_i^{r}\, q_i^{r} - \delta_i^{ihx}\, q_i^{ihx} \end{aligned} \tag{3.14}$$

where v_i is the volume in litres of the corresponding node, ρ is the density of the water in kg/l, UA_i is the heat transfer coefficient corresponding to the node i in W/°C, λ_i the heat conductivity of the water, 0.644 W/m°C, m_{dhw} the mass flow of DHW drawn from the HWST in kg/s, T_{cw} the temperature of the water coming from the public network, T_r the temperature of the air where the HWST is located, A_i the area of the circular layer in node i in m^2 and z_i is the height of the node in respect to the bottom part of the tank in m. δ is a parameter to define if a part of the equation is applicable to an specific node. As it is illustrated in the expression below, m_i refers to the mass flow balance in node i:

$$m_i = m_{HP} - m_{cw} \tag{3.15}$$

If m_i is positive (δ_i^{+}=1 and δ_i^{-}=0) represents that the heat transfer due to the water mixing is downwards. If m_i is negative instead (δ_i^{+}=0 and δ_i^{-}=1) means that the heat transfer is done upwards. δ_i^{HP} refers to the heat supplied by the HP so it is only applicable to the top layer, δ_i^{HP}=1 when i=1 and δ_i^{HP}=0 for the rest of the nodes. δ_i^{cw} refers to the heat transferred with the water coming from the public network. Therefore it is only applicable to the bottom node, δ_i^{cw}=1 when i=n and δ_i^{cw}=0 for the rest of the nodes. δ_i^{r} refers to the thermal power provided by the electrical resistor (q_r) so is only applicable in those nodes where this is located.

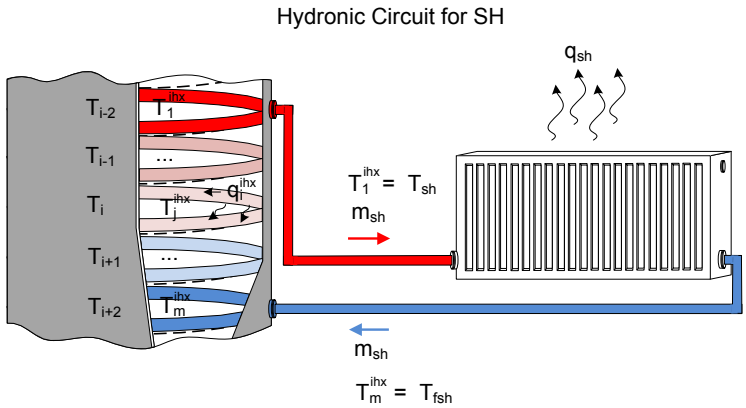

Figure 3.8: *Overview of the Hydronic Circuit for SH.*

The average energy stored in the tank (E_s) is calculated as the summation of all the average energies at the different nodes.

$$E_S = \frac{v_i \, \rho \, Cp_w \, k_n \cdot \sum_{i=1}^{n} T_i}{E_{ct}} \tag{3.16}$$

where E_ct is the energy capacity of the HWST and k_n a normalization factor.

The fluid circulating through the hydronic circuit is heated through a heat exchanger coil immersed in the HWST and cooled during the heat realise in the radiators distributed in the household. In order to simplify the problem, it is assumed that all the thermal demand required for SH purposes (q_{sh}) is aggregated in a single radiator as Fig. 3.8 shows. Therefore, the temperature of the water coming out of this radiator (T_{fsh}) is expressed as:

$$T_{fsh} = T_{sh} - \frac{q_{sh}}{m_{sh} \cdot Cp_w} \tag{3.17}$$

where m_{sh} is the mass flow of water circulating in the hydronic circuit and T_{sh} is the temperature of the water coming out from the internal heat exchanger and which is introduced in the radiator. As with the HWST, the internal coil is divided in m sections. Hence, in eq. 3.14, δ_i^{ihx} refers to the heat transferred from node i to the water running through the section j of the internal heat exchanger (q_i^{ihx}). Then, it is only applicable to those nodes where the internal heat exchanger is physically present (δ_i^{ihx}=1), not for the rest (δ_i^{ihx}=0). So, the temperature in the section j of the internal heat exchanger (T_j^{ihx}) is calculated as:

$$T_j^{ihx} = T_i - (T_{j-1}^{ihx} - T_i)\frac{UA_i^{ihx}}{m_{sh} \cdot Cp_w} \tag{3.18}$$

where UA_i^{ihx} is the heat transfer coefficient corresponding to the section of the internal heat exchanger located in the node i in W/°C. Finally, q_i^{ihx} absorbed from the water stored in the node i is calculated according to:

$$q_i^{ihx} = m_{sh} \cdot Cp_w \cdot (T_j^{ihx} - T_{j-1}^{ihx}) \tag{3.19}$$

The way of controlling this HP model is similar to the one utilized for the simple approach. Additionally, the electrical resistor is basically controlled to keep the water temperature in the upper part of the HWST above a minimum value ($\underline{T}_1$) during adverse operating conditions. The electrical resistor turns on (C_S^r=1) when T_1 drops to $\underline{T}_1$. This will heat the top layers until the maximum temperature band ($\overline{T}_1$) is reached, then it turns off (C_S^r=0).

3.3.2.1 Model Verification

Table 3.2 shows the model parameters used to validate the following approach, where h_t and r_t refers to the height and the radius of the HWST. In order to illustrate some aspects of the performance of these units, it is assumed that the thermal consumption of the household considered is relatively high. To demonstrate the high influence of the source and sink conditions in electrical consumption pattern of this loads two seasonal scenariosn are considered. Fig. 3.9 depicts the performance of the selected HP system in the mentioned scenarios, where subfigure (a) shows the thermal demand of DHW and SH in an specific household and the T_{atm}, subfigure (b) the P_{HP}, q_{HP} and COP values of the HP operation, subfigure (c) and (d) the distribution of temperatures and the E_S in the HWST and finally subfigure (e) the P_{HPS} and Q_{HPS} pattern.

As it is depicted in the left-hand figures, the adverse atmospheric conditions characteristic on the day in February lead normally the household to have a high thermal demand. If this is high enough the HP will have to operate continuously in order to

Table 3.2: *Detailed HPWH Model Features*

	Parameter	Value	Parameter	Value
HP Unit	P_{HP}^{rt} (kW)	5	$\cos(\varphi)$	0.98
HWST	v_t (l)	500	T_{cw} (°C)	9
	h_t (m)	1.475	n (-)	10
	r_t (m)	0.329	P_R^{rt} (kW)	2.4
	E_{ct} (kWh)	46.44	$\underline{E}_C$ - $\overline{E}_C$	0.6-0.8
	U (W/m^2°C)	0.9	$\underline{T}_1$ - $\overline{T}_1$	65-80
Hydronic Circuit	m (-)	6	UA^{ihx} (W/°C)	750

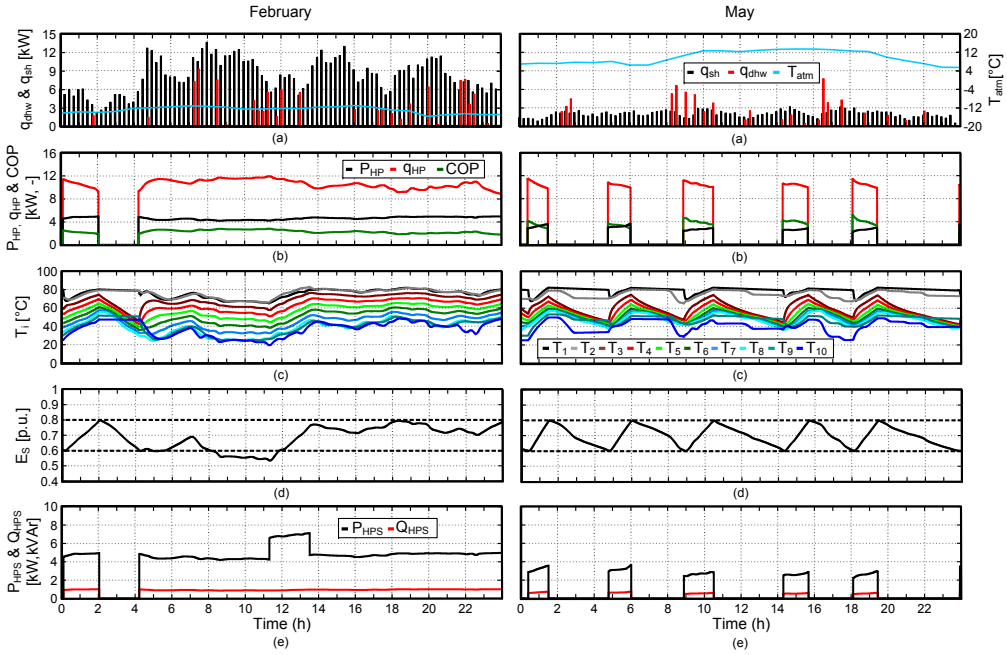

Figure 3.9: *Performance of the Detailed HPWH Model: (a) q_{sh}, q_{dhw} and T_{atm}, (b) P_{HP}, q_{HP} and COP, (c) Temperatures in the HWST, (d) E_S, $\underline{E}_C$ and $\overline{E}_C$ and (e) P_{HPS} and Q_{HPS}.*

supply the requested demand. In consequence, the potential flexibility offered by this loads may be drastically reduced during this moments. Furthermore, the combination of low atmospheric temperatures and the fact that a continuous operation of the HP unit implies the increment of the temperature of the bottom layer decreases the COP drastically. Therefore, to maintain a similar q_{HP} rate, the compressor accelerates, consequently increasing the power consumption of the unit. This fact is notable in Fig. 3.9(e) where the P_{HPS} and Q_{HPS} are not constant during the period the HP is active, but it varies according to what it is mentioned before.

In case this situation gets even more adverse it may happen that the HP unit is not able to supply the thermal demand requested, leading to an E_S decrease and a consequent drop of the tank temperature. This fact may make the temperature on the top of the HWST decrease below a certain limit, implying the need for an additional electric heating in order to ensure that the DHW is supplied within the sanitary standards. If this is happening during high congested periods of the network, the combination of both demands could aggravate this technical limitation even more.

In the right-hand figures, a regular day of May aims to illustrate the HP operation

given between seasons of the year. Similarly as with the simple approach, the favourable atmospheric conditions and a lower thermal demand of the household makes the activation of this appliance less frequent. However, the increase of COP implies that for providing a certain rate of q_{HP} the HP unit reduces its power consumption. This is especially notable if the P_{HPS} and Q_{HPS} values when the two parts of Fig. 3.9(e) are compared. In conclusion, the frequency of the HP unit activation not only varies between seasons but the power consumption rate as well.

3.4 Alkaline Electrolyzer System

An AE is the combination of different electro-mechanical elements, which allows decomposition of an electrolyte -solution of KOH in water- into hydrogen and oxygen by passing a direct current between two electrodes. The model described in this subsection refers to the model which is introduced in publication C1. In Fig. 3.10(a) a simpli-

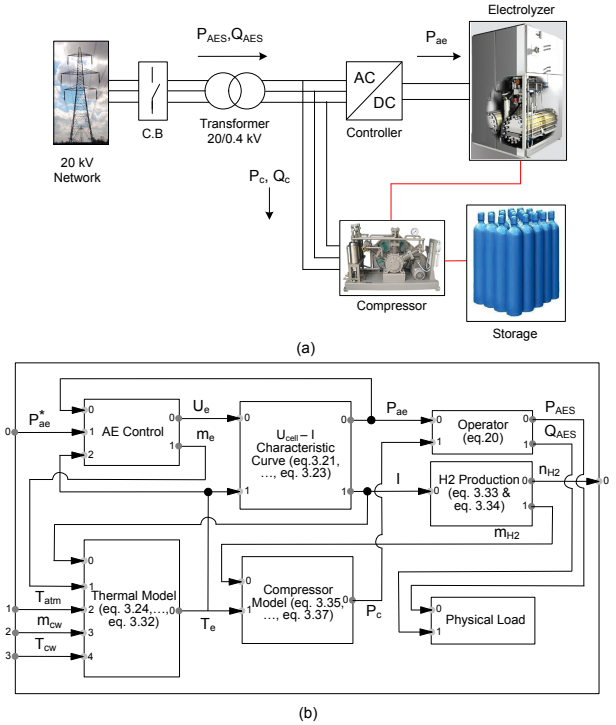

Figure 3.10: *Alkaline Electrolyzer Model: (a) Simplified Scheme of the AE Grid Connection, (b) DIgSILENT Lay-out.*

fied scheme of how this load is normally connected in the MV distribution systems is depicted. Fig. 3.10(b) shows the DSL block diagram of the AE system (AES)model developed in DigSILENT PowerFactory. At this point, it is worth to cite the work published by Ulleberg [127] since it has become an essential reference during the modelling task. The model is majorly composed of three parts, the U-I Characteristic curve, the thermal model and the hydrogen production. An additional one, the compressor, is included in this case.

In this context, the active power demand of the AES (P_{AES}) is deducted as the combination of the AE power (P_{ae}) and the compressor power (P_c) consumptions. From an electrical perspective, since the AE is essentially a controlled current process, it is characterized as a constant current load [191]. The compressor instead is a constant power load which reactive power demand (Q_{AES}) refers only to the one drawn by the motor driving it (Q_c).

$$P_{AES} = \frac{P_{ae}}{\eta_{cv}} + P_c; \qquad Q_{AES} = Q_c = P_{ae} \cdot \tan(\varphi) \tag{3.20}$$

where η_{cv} is the efficiency of the power conversion from AC to DC.

3.4.1 U-I Characteristic Curve

To represent the voltage and current kinetics in the electrodes of the AE is a complex task due to its non-linear relationship. Ulleberg proposed an expression, which was obtained based on empirical results, that includes the overvoltage dependence of the temperature resulting from the chemical reactions [127].

$$\begin{aligned} U_{cell} &= U_{rev} + \frac{r_1 + r_2\, T_e}{A_{cell}}\, I + (s_1 + s_2\, T_e + s_3\, T_e^2) \cdot log(\frac{t_1 + t_2/T_e + t_3/T_e^2}{A_{cell}}\, I + 1) \\ U_e &= n_c \cdot U_{cell} \end{aligned} \tag{3.21}$$

where U_e is the DC voltage applied at the AE terminals and n_c the number of cells connected in series, U_{cell} is the voltage correspondent to a cell and U_{rev} the reversible voltage, r_i are the parameters representing the ohmic resistance of the electrolyte (i=1,2), s_i and t_i are parameters representing the overvoltage on the electrodes (i=1...3), A_{cell} is the cell area, T_e is the electrolyte temperature and I is the DC current drawn by the AE.

The thermodynamics of the electrochemical reactions is an important aspect to be taken into account during the modelling process. The changes in enthalpy (ΔH) and entropy (ΔS) during the water splitting reaction induce changes in Gibbs energy (ΔG) and consequently in the U_{rev}. The value of these is directly influenced by the operating conditions of the AE -operating pressure and temperature- [127].

$$U_{rev} = \frac{\Delta G}{zF} = \frac{\Delta H - T_e\, \Delta S}{z\, F} \tag{3.22}$$

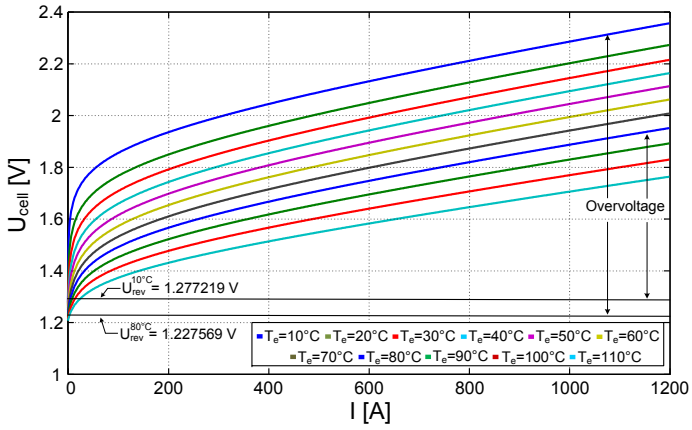

Figure 3.11: *U_{cell} - I Characteristic Curve of the AE at 7 bars.*

where z is the number of electrons transferred per reaction, $z = 2$, and F the Faraday constant, F=96485 C/mol. The changes in Gibbs energy are calculated as it is described in [192] and using the thermodynamic properties of products and reactants procured by the NIST online database. Therefore, considering the pressure of operation as 7 bars, similar to the system installed in Jülich (PHOEBUS) [126], a polynomial regression is developed in order to define U_{rev_7bar} as a function of T_e.

$$U_{rev\_7bar} = -2.483e^{-10} \cdot T_e^3 + 2.9004e^{-7} \cdot T_e^2 - 0.000733 \cdot T_e + 1.2845 \tag{3.23}$$

Based on the set of equations introduced before the curves shown in Fig. 3.11 are elaborated. As it is seen the current drawn by the AE depends on the operating T_e and the U_e which is applied to the stack terminals. Out of these curves, a two dimensional matrix is created with the purpose of determining the current drawn by the AE according to the voltage and temperature of operation.

3.4.2 Thermal Model

Due to the electrochemical reactions occurring during the hydrolysis, the temperature of the electrolyte varies. The dynamics of the temperature are represented with a thermal energy balance which is described by the following differential equation [127].

$$C_t \frac{dT_e}{dt} = q_g - q_{cw} - q_{loss} \tag{3.24}$$

where C_t is the thermal capacitance of the AE. The internal heat generation (q_g), as a consequence of the cell inefficiencies, is directly related with the P_{ae} and the efficiency

of the electrolysis process (η_e). η_e is commonly expressed as the quotient between the thermo-neutral voltage (U_{th}) and U_{cell} [127].

$$q_g = P_{ae} \cdot (1 - \eta_e) = P_{ae} \cdot (1 - \frac{U_{th}}{U_{cell}}) = n_c \cdot (U_{cell} - U_{th}) \cdot I; \quad P_{ae} = U_e \cdot I \tag{3.25}$$

$$U_{th} = \frac{\Delta H}{zF} \tag{3.26}$$

The U_{th} represents a voltage threshold of the heat release during the hydrolysis. If this value is exceeded the heat released becomes higher than the required for the water decomposition. Then, the heat accumulated in the stack increases and in consequence the electrolyte temperature. To account for this, a polynomial regression is developed once again, where U_{th} for an operating pressure of 7 bars is deducted based on T_e.

$$U_{th\_7bar} = -3.2084e^{-10} \cdot T_e^3 + 5.4591e^{-8} \cdot T_e^2 - 0.000165 \cdot T_e + 1.485 \tag{3.27}$$

The heat losses with the surroundings (q_{loss}) are expressed as the difference between the T_e and the atmospheric temperature (T_{atm}) divided by the overall thermal resistance (R_t). The thermal parameterization of [127] refers to an small scale unit. Since, it is significantly difficult to find characteristic data of real large-scale examples, C_t and R_t values are scaled up in order to achieve a coherent thermal behaviour of unit of this size.

$$q_{loss} = \frac{1}{R_t}(T_e - T_{amb}) \tag{3.28}$$

An accurate response of the AE requires a precise control of T_e. This makes the cooling system a key element of such a system. Among the different cooling methods used to get rid of the heat excess generated during the hydrolysis, circulating the electrolyte through a heat exchanger is a simple and commonly used technique. To calculate the cooling demand (q_{cw}) required by the system the number of transfer units ($\varepsilon - NTU$) method is utilized, where ε is the heat exchanger effectiveness and q_{max} the maximum theoretical cooling demand [192].

$$q_{loss} = \varepsilon \cdot q_{max}; \quad q_{max} = C_{min} \cdot \Delta T_{max} = C_{min} \cdot (T_e - T_{cw}) \tag{3.29}$$

where C_{min} is the minimum heat capacity rate and T_{cw} the temperature of the cooling water at the heat exchanger inlet. In agreement with the $\varepsilon - NTU$ methodology, ε depends on of the heat capacity ratio (C_r) and the NTU coefficient. The latest one is defined as the quotient between the overall heat transfer coefficient of the heat exchanger (UA_{hx}) and C_{min}.

$$\varepsilon = \frac{1 - e^{NTU(1-C_r)}}{C_r - e^{NTU(1-C_r)}}; \quad NTU = \frac{UA_{hx}}{C_{min}}, \quad C_r = \frac{C_{min}}{C_{max}} \tag{3.30}$$

C_{min} and the maximum heat capacity rate (C_{max}) are calculated according to the following logic:

$$C_{min} = \begin{cases} m_e \cdot Cp_e < m_{cw} \cdot Cp_{cw} & \rightarrow \quad m_e \cdot Cp_e \\ m_e \cdot Cp_e \geq m_{cw} \cdot Cp_{cw} & \rightarrow \quad m_{cw} \cdot Cp_{cw} \end{cases} \tag{3.31}$$

$$C_{max} = \begin{cases} m_e \cdot Cp_e < m_{cw} \cdot Cp_{cw} & \rightarrow \quad m_{cw} \cdot Cp_{cw} \\ m_e \cdot Cp_e \geq m_{cw} \cdot Cp_{cw} & \rightarrow \quad m_e \cdot Cp_e \end{cases} \tag{3.32}$$

where Cp_{cw} and Cp_e are the specific heat capacities of the cooling water and the electrolyte and m_{cw} and m_e the mass flow rates of the cooling water and the electrolyte.

3.4.3 Hydrogen Production

The hydrogen production rate (n_{H2} in mol/s) is directly proportional to the current drawn by the AE and the number of cells connected in series.

$$n_{H2} = \eta_F \frac{n_c\, I}{z\, F} \tag{3.33}$$

where η_F is the Faraday efficiency. The Faraday efficiency represents the difference between the actual hydrogen production and the maximum which should be achieved theoretically talking.

$$\eta_F = a_1 \exp\left(\frac{a_2 + a_3\, T_e}{I/A_{cell}} + \frac{a_4 + a_5\, T_e}{(I/A_{cell})^2}\right) \tag{3.34}$$

where a_i are the parameters defining the temperature and current dependency of the Faradays efficiency (i=1...5).

3.4.4 Compressor Model

Once the hydrogen is generated, it has to be compressed to be able to store it. Even though, it may sometimes be easily dismissed, the P_c required for the compression of the hydrogen stands for a notable part of the total system demand. In this case, P_c is calculated based on the hydrogen mass flow rate (m_{H2} in kg/s) assuming that the compression process is polytrophic (γ=1.4) and the hydrogen an ideal gas.

$$P_c = m_{H2} \cdot (w_1 + w_2) \tag{3.35}$$

The compression is considered in two stages with an intercooling in between. This is commonly done to reduce the temperature of the outlet gas at the first stage to the same as its input one. In this way, since the temperature of the inlet gas at the second stage

(T_1^i=T_2^i) is lower, the compression work required becomes also lower. This is important thing since the size of the compressor can be reduced significantly. The compression work in each of the stages (w_1, w_2) is calculated according to [200]:

$$w_1 = \frac{Cp_{H2}T_1^i}{\eta_G}\left(\left(\frac{p_x}{p_1}\right)^{\frac{\gamma-1}{\gamma}} - 1\right); \quad w_2 = \frac{Cp_{H2}T_2^i}{\eta_G}\left(\left(\frac{p_2}{p_x}\right)^{\frac{\gamma-1}{\gamma}} - 1\right) \tag{3.36}$$

where Cp_{H2} is the specific heat capacity of the hydrogen and η_G the global efficiency of the compression process. Assuming that, the input pressure and temperature conditions of the hydrogen in the first compression stage (p_1, T_1^i) are equal to the AE operating ones ($p_1 = p_e, T_1^i = T_e$) the intermediate compression pressure (p_x) is calculated as:.

$$p_x = \sqrt{p_1 \cdot p_2} \tag{3.37}$$

where p_2 is the pressure at what the hydrogen is stored.

3.4.5 Alkaline Electrolyzer Control

The performance and the load response capability from an AE depends significantly on its operating conditions. Therefore, the electrolyte temperature and the active power demand of the AE are two key variables that need to be controlled during the operation of the AE.

Regarding temperature, any pronounce variation may have an impact on the AE response when a change of its load rate is requested. According to [127], due to different mechanical, power density and voltage limitation aspects makes 80°C a convenient operating temperature for the technology considered. Therefore, to maintain the temperature at 80°C the controller acts over the mass flow of electrolyte circulating through the cooling system. In the simplified version of the AE control structure shown in Fig. 3.12 this is reflected with the PI in temperature loop. This determines the electrolyte recirculation mass flow rate needed to fulfil the refrigeration requirements and achieving the temperature conditions set by the reference.

The control of the power demand in an AE is normally realized based on a current control [201], [202]. In the simplified version considered this is assumed to be embedded in the PI placed in the power loop. This controller, which is implemented in parallel with the temperature one, acts over the DC voltage applied to the AE terminals in order to vary the current drawn and in consequence the power demand of the AE.

The large time constant as a natural characteristic of a control variable like the temperature, results in a very slow response compared with that of the power. Thus, even though a strong dependency between the power consumption and the operation temperature exists, the temperature variations are so slow that the power control dynamics are barely affected.

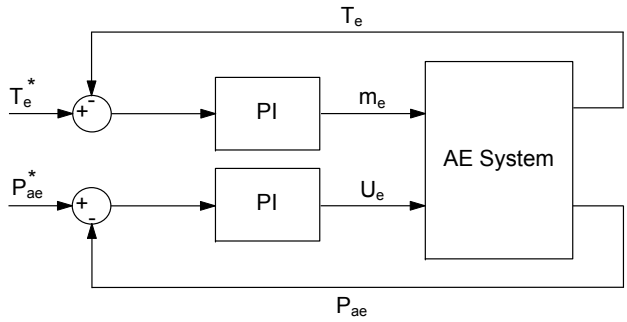

Figure 3.12: *Simplified Version of an AE control.*

3.4.6 Model Verification

In this case, the performance and load response capability of the AE are investigated under several operating conditions within a time window of a day. Table 3.3 shows the parameterization of the model utilized in order to describe the load, where $\underline{U}_e$ and $\overline{U}_e$ are the minimum and maximum operating voltages in DC and T_e^* the reference

Table 3.3: *AE System Model Features [127]*

	Parameter	Value		Parameter	Value
AE General	P_{ae}^{rt} (kW)	355	$U_{cell} - I$ **Curve**	r_1 (Ω/m^2)	7.331e^{-5}
	p_e (bar)	7		r_2 (Ω/m^2)	-1.107e^{-7}
	n_c (-)	180		s_1 (V)	1.586e^{-1}
	$\overline{U}_e$ (V)	342		s_2 (V/°C)	1.378e^{-3}
	$\underline{U}_e$ (V)	257.4		s_3 (V/°C^2)	-1.606e^{-5}
	T_e^*(°C)	80		t_1 (m^2/A)	1.599e^{-2}
Thermal Model	R_t (°C/W)	0.334		t_2 (m^2/A°C)	-1.302
	C_t (J/°C)	5.38e6		t_3 (m^2/A°C^2)	4.213e^2
	UA_{hx} (W/°C)	2100		A (m^2)	0.25
	$m_c w$ (kg/s)	1.2	**Faraday Efficiency**	a_1 (%)	99.5
Compressor	P_c^{rt} (kW)	70		a_2 (m^2/A)	-9.5788
	$cos\varphi$ (-)	0.88		a_3 (m^2/A°C)	-0.0555
	η_G (-)	0.486		a_4 (m^4/A)	1502.7083
	p_2 (bar)	150		a_5 (m^4/A°C)	-70.8005

temperature. Since, its power rating (P_{ae}^{rt}) is large in comparison with other loads in the distribution system, the AES is considered to be connected to the MV distribution network.

Two cases are taken into account for validation of the AE model. In case 1, the AE operates according to a supposed market strategy where the required response dynamics are not too pronounced. In case 2 instead, the AE is assumed connected in parallel with a wind turbine in order to balance its power output. This case is therefore characterized for requiring faster load response dynamics from the AE. Indeed, the power reference (P_{ae}^{*}) for this second scenario has been created out of the 1 minute based data of the power generation from a real wind turbine. Fig. 3.13 depicts the performance of the AE system under the mentioned scenarios, where subfigure (a) shows the power reference signal of the AE in p.u, subfigure (b) the resulting P_{ae}, P_c, and Q_c in response to the P_{ae}^{*}, subfigure (c) the DC voltage and current of the AE, subfigure (d) the electrolyte

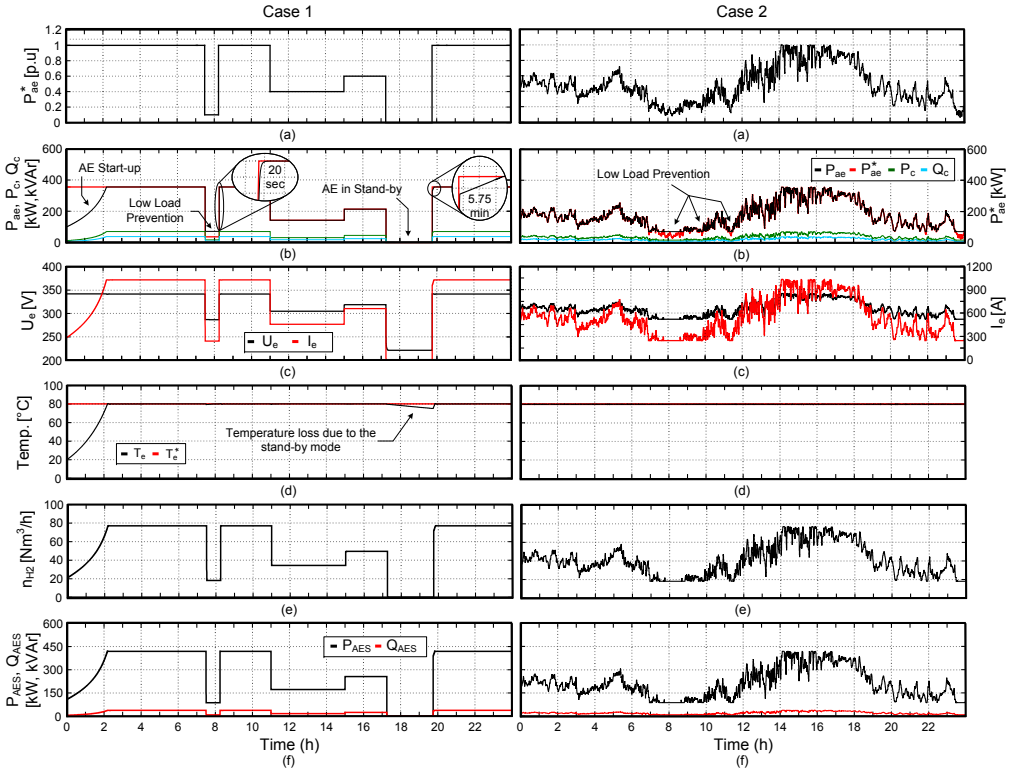

Figure 3.13: *Performance of the AE Model: (a) P_{ae}^{*} in p.u., (b) P_{ae}, P_c, Q_c and P_{ae}^{*}, (c) U_e and I_e, (d) T_e and T_e^{*}, (e) n_{H2} and (f) P_{AES} and Q_{AES}.*

temperature and its reference, subfigure (e) the hydrogen production rate and subfigure (f) the total P_{AES} and Q_{AES} of the system.

The AE are characterized for having long start-up times (from 0 to 1 p.u.), relative fast downward response capability and relative slow upward response capability. This depends very much on the size of the unit and the availability, amount and accuracy of the cooling employed [141]. In consequence, the type of regulation that this technology will be able to provide will directly depend on those aspects. This is demonstrated in the case 1, where the first appreciable thing is its long start up time, which is caused by the need of increasing the T_e. The heat generated during the electrolysis process allows the AE slowly increasing T_e in order to establish its rated power operation conditions. Around half past seven, the AE is forced to operate at 0.1 p.u of its rated power. The load response is performed almost instantaneously, in few seconds. However, the requested operation point is not precisely achieved since a limitation for when operating at low load rates exits. Operating points below 0.15-0.2 p.u. of the rated power are normally avoided since they cause degradation of the hydrogen purity. In such a situation either the AE continues operating at the defined limit or it switches into a standby mode.

Minutes after eight, the AE is requested to increase its demand from a 0.2 to 1 p.u. The response is this case is also fast but not instantaneous it takes some seconds before the steady state conditions are achieved. The time required for reaching the steady state condition depends on the point from where the AE responds to the change in the operation conditions. After 17 h, the signal received stops its power consumption and makes the AE wait for new instructions in standby mode. During the time the AE is standby mode, T_e is reduced due to the exiting heat loss with the surroundings. When, the AE is suddenly requested again for performing at its rated power its response is not fast. The reason is the need for re-heating the electrolyte up to the operating temperature since the voltage is saturated at $\overline{U}_e$=342 V. Working within a reasonable range of cell voltages, reduces the electrical power and operation costs [126]. As it is mentioned before, this aspect may represent a limitation depending on the service considered.

Looking into case 2, the strong capability of the AE in following the wind power dynamics is clearly demonstrated. This response capability is supported by the fact that AE is constantly performing within the operating conditions of temperature and pressure. Notice, in this case as well that there are moments during the day where the request demand is not satisfied due to the low load prevention.

3.5 Electric Vehicle

The EV is one of the promising solutions in the future transportation. However, it is important to understand what originated impact they can impose to the local distribution systems. To be able to do so understanding the dynamic behaviour of the EV load is required. In this case, two models are developed focusing on the representation

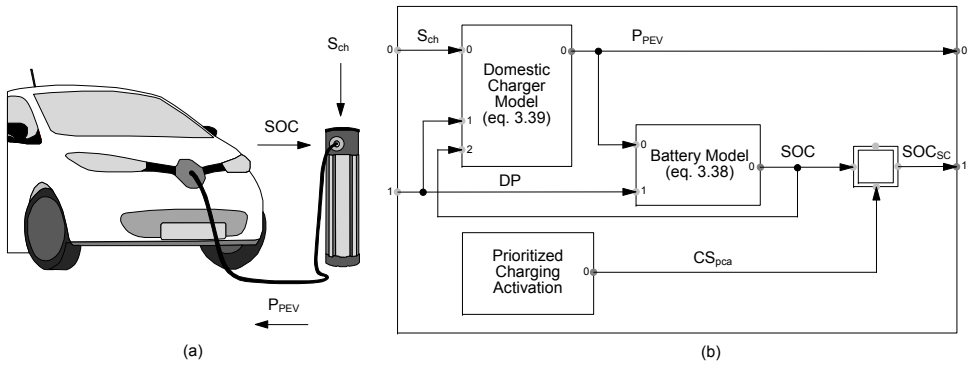

Figure 3.14: *Simple PEV System Model: (a) System Overview, (b) DIgSILENT Lay-out.*

of the steady state behaviour of a PEV connected at household level. On the one hand, the charging aspects are only described with a simple model of a PEV. On the other hand, the charging and discharging aspects are tackled with a detailed model of a PEV performing under the V2G concept.

3.5.1 Plug-in Electric Vehicle - Simple Approach

The model described in this subsection refers to the model which is introduced in publications C3 and J1. This is composed of a battery storage and a domestic charging station at the household level. Fig. 3.14 shows an overview of the system and the DSL block diagram of the model. The battery is represented by a Thevenin-based electrical model which neglects any transient effect. The relation between the terminal voltage and the open circuit voltage is assumed linear. Hence, the existing energy loss due to internal resistance of the battery is reflected as the efficiency η_b. The battery SOC, in p.u, is then calculated as:

$$SOC = SOC_0 + \frac{\frac{C_{max}}{3600} \cdot \eta_b \cdot \int P_{PEV} \cdot dt}{SOC_{max}} \tag{3.38}$$

where SOC_0 is the initial SOC in p.u and C_{max} and SOC_{max} the maximum battery capacity and the maximum SOC in kWh.

As is it previously mentioned, the PEV battery is charged through a domestic charger located at the household. The non-negligible impact that a concentration of synchronized PEV can originate in an LV network reinforces the need for controlling their charging process. Therefore, based on [203], the traditional feature of the domestic charger is additionally procured with the ability for regulating the charging rate. Therefore, the charging power (P_{PEV}) is allowed to vary from 0 to rated power of the charger (P^{rt}_{PEV}),

being calculated as:

$$P_{PEV} = \eta_c \cdot \int S_{ch} \cdot dt; \qquad 0 \leq P_{PEV} \leq P_{PEV}^{rt} \tag{3.39}$$

where η_c is the charger efficiency in p.u and S_{ch} is an external variable representing the charging capability of the PEV. Due to this existing need for controlling the charging process, S_{ch} is assumed to be calculated and dispatched by a grid supervisor.

The driving pattern (DP) performed by the PEV users during the day influences significantly the power consumption pattern from a domestic battery charger once the PEV is plugged-in at home. In this model, the DP is reflected as the home departure and arrival times and the distance driven during the considered day. The possibility for self-imposing priority in the charging process has also been contemplated in this model. This option could be adopted by a PEV user, based on his driving requirements and the fact of ignoring for being penalized. In this situation the activation signal (CS_{pca}) would be reflected in the SOC sent by the charger to the grid supervisor (SOC_{sc}).

To preserve the battery life the SOC is constantly controlled between its minimum ($\underline{SOC}$) and its maximum ($\overline{SOC}$). So, even if it is externally required, the unit control makes sure not to violate these limits.

3.5.1.1 Model Verification

The high energy density and long life time, makes the lithium-ion (Li-ion) batteries an interesting solution to be considered for electric transportation applications. Therefore, to validate the model previously introduced a 24 kWh Li-ion battery with a η_b of 0.993 is considered. Looking into the actual infrastructure, a 3-ph/400 V off-board charger represents a feasible solution for satisfying the user charging requirements [35]. Additionally, the battery charger is able to regulate the charging rate within 0 and 11 kW

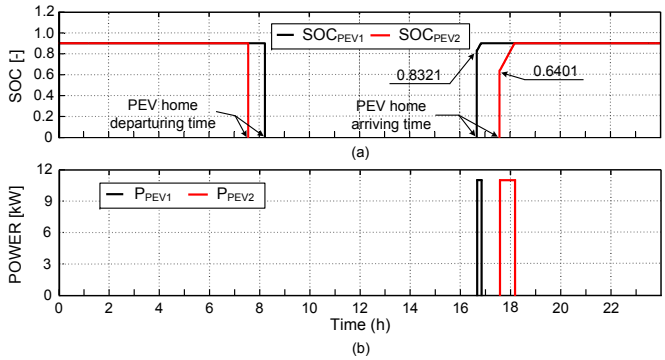

Figure 3.15: *Performance of the PEV System Model: (a) SOC and (b) P_{PEV}.*

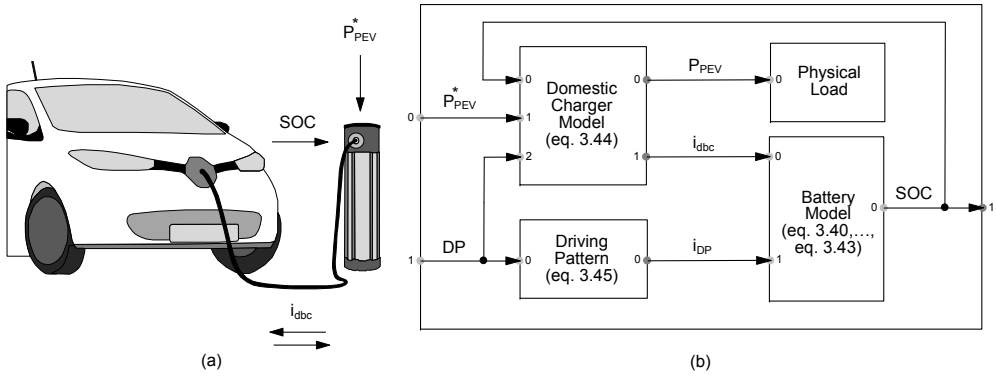

Figure 3.16: *Detailed V2G System Model: (a) System Overview, (b) DIgSILENT Lay-out.*

and its efficiency is η_c=0.98. The SOC is controlled within 0.2 and 0.9 p.u.

Fig. 3.15 illustrates the comparison between two users holding the same PEV but performing different DP. Since it is for model validation matters, in this case, the charging of the PEVs is not externally influenced. Therefore, the PEVs are allowed to charge at their rated power. Fig. 3.15(a) shows the *SOC* sensed by both battery chargers when the PEV connects at home. As it is shown in Fig. 3.15(b), the active power consumption from the chargers differs in time and quantity, demonstrating the strong relationship between the user *DP* and the impact caused in the LV grid.

3.5.2 Vehicle to the Grid - Detailed Approach

The V2G concept is defined as the ability from widespread controlled PEVs to exchange, in a bidirectional way -supplying or drawing-, electricity with the power grid in order to meet occasional needs for stabilization. The model described in this subsection refers to the model which is introduced in publication C1. Fig. 3.16(a) gives an overview of the system and Fig. 3.16(b) illustrates the block diagram of the DSL model performed in DIgSILENT. The model is developed considering that a supervisor figure decides the charging and discharging strategy from the different plugged-in PEVs in the LV grid. Therefore, this feature is in charge of setting the power reference (P^*_{PEV}) at which a specific PEV has to operate.Three parts are differentiable in this model, the battery, the domestic battery charger and the driving pattern of the user.

3.5.2.1 Battery Model

The battery in this case is modelled based on the characteristics of the li-ion cell provided in [155]. The extended Thevenin approach is used in order to calculate the DC voltage

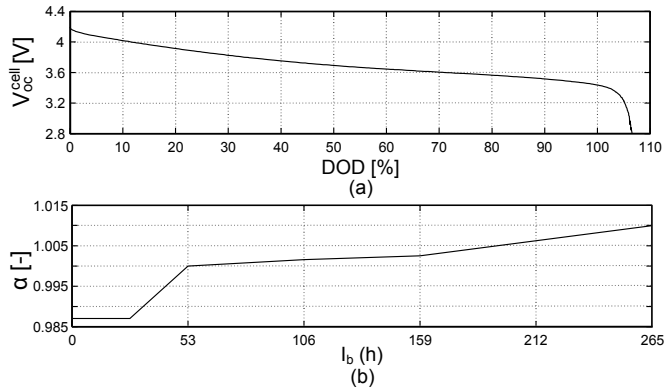

Figure 3.17: *Kokam SLPB 120216216 53Ah cell: (a) V_{oc}^{cell}, (b) α [155].*

at battery terminals (V_b). Since, any transient dynamics are once again neglected, the charging and discharging dynamics are only represented with two different internal resistors (R_{ch}, R_{dch}).

$$\begin{aligned} I_b > 0 \quad (Charge) \quad &\rightarrow \quad V_b = n_c(V_{oc}^{cell} + R_{ch}\, I_b) \\ I_b < 0 \quad (Discharge) \quad &\rightarrow \quad V_b = n_c(V_{oc}^{cell} + R_{dch}\, I_b) \end{aligned} \tag{3.40}$$

where n_c is the number of li-ion cells connected in series, V_{oc}^{cell} is the open circuit voltage of a cell. The curve depicted in Fig. 3.17(a), which is based on empirical data, provides the V_{oc}^{cell} depending on the depth of discharge (DOD) of the battery. The DC current flows through the battery (I_b) from two sources, due to the charging/discharging when the vehicle is plugged-in at home (I_{dbc}) and due to the discharge originated by the driving (I_{DP}). In consequence the power of the battery (P_b) is calculated as:

$$P_b = (V_b \cdot I_b)_{DC}; \qquad I_b = I_{dbc} + I_{DP} \tag{3.41}$$

During the charging and discharging of a battery different aspects influence this process such as the rate, temperature, etc. Since the temperature effect is assumed negligible in this case only the charging/discharging rate dependency is contemplated. This is represented by the α coefficient shown in the 3.17(b). Therefore, depending on the operating mode the SOC of the battery is calculated as:

$$\begin{aligned} I_b > 0 \quad (Charge) \quad &\rightarrow \quad SOC = \frac{1}{C_{cell} \cdot 3600} \cdot \int \frac{I_b}{\alpha} \cdot dt \\ I_b < 0 \quad (Discharge) \quad &\rightarrow \quad SOC = \frac{1}{C_{cell} \cdot 3600} \cdot \int I_b \cdot \alpha \cdot dt \end{aligned} \tag{3.42}$$

where C_{cell} is the li-ion cell capacity in Ah. In the same way, the DOD is calculated according to:

$$DOD = DOD_{max} - SOC \tag{3.43}$$

where DOD_{max} is the maximum DOD.

3.5.2.2 Domestic Battery Charger

In local distribution networks the battery-grid power exchange is highly limited by the domestic power infrastructure. The transfer capability is therefore constrained even if the battery design allows higher power rate management. As it is previously stated, the active power at what the battery is charged or discharged (P_{PEV}) is assumed to be defined by a grid supervisor which is aware of the LV grid condition.

$$\begin{aligned} Charge &\rightarrow P_{PEV} = P^{*}_{PEV} \cdot \eta_{pe} \\ Discharge &\rightarrow P_{PEV} = \frac{P^{*}_{PEV}}{\eta_{pe}} \end{aligned} \tag{3.44}$$

where η_{pe} represents the efficiency of the power conversion. In order to preserve the life of the battery, the control embedded in the charger ensures that the SOC remains always between its minimum ($\underline{SOC}$) and its maximum ($\overline{SOC}$). Additionally, with the purpose of avoiding inconveniences for the PEV user, the respond of the system is limited within the SOC range of ($\underline{SOC}_{dch}$)-($\overline{SOC}_{dch}$).

Table 3.4: *PEV-V2G System Model Features [155]*

	Parameter	**Value**		**Parameter**	**Value**
Battery	C_b (kWh)	24		Manufacturer	Kokam
	P_b^{rt} (kW)	28.27		Model	SLPB 120216216
	n_c (-)	108		Technology	Li-ion
	$\underline{SOC} - \overline{SOC}$ (-)	0.2-0.9		C_{cell} (Ah)	53
Domestic Battery Charger	P_{dbc}^{rt} (kW)	11	**Cell**	DOD_{max} (%)	106.623
	Connection	3-ph		V_{oc}^{cell} (V)	4.197 - 2.717
	V_{rt} (kV)	0.4		I_{nom} (A)	53 (1C)
	I_{max} (A)	16		R_{ch} ($m\Omega$)	1.3
	$\underline{SOC}_{dch}$ (-)	0.7		R_{dch} ($m\Omega$)	3.69

3.5.2.3 Driving Pattern

The variations of the SOC created during the periods in which the vehicle is not plugged at home are also represented in this model. The current drawn from the battery during a daily trip is deducted from the DP profile of a vehicle -in terms of speed v (km/h)- and the V_b. Based on [204], $150Wh/km$ is considered as the average energy consumption of the vehicle.

$$I_{DP} = \frac{v \cdot 150}{V_b} \tag{3.45}$$

3.5.2.4 Model Verification

Table 3.4 provides the parameterization of the different parts of the PEV-V2G model introduced and its SOC operating limits. To validate its performance, two PEVs are compared in two different driving scenarios. Fig. 3.18 depicts the results for scenarios considered, where subfigure (a) shows the DP hold by the vehicle in term of speed, subfigure (b) the received charging and discharging P^*_{PEV} reference in p.u., subfigure

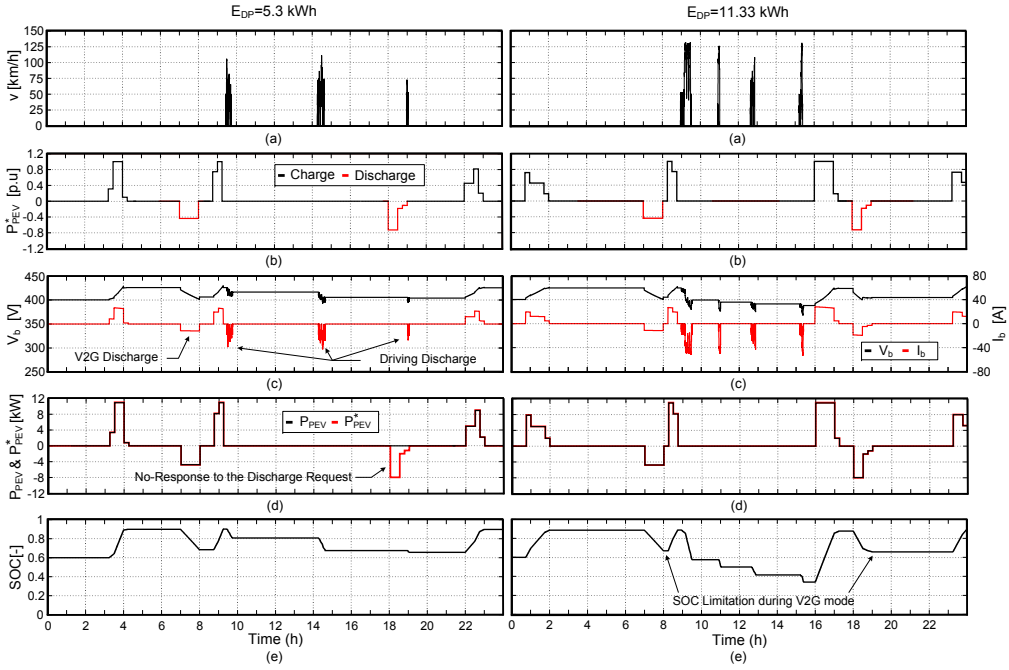

Figure 3.18: *Performance of the V2G System Model: (a) DP in terms of vehicle speed, (b) P^*_{PEV}, (c) V_b and I_b, (d) P_{PEV} and P^*_{PEV} and (e) SOC.*

(c) the voltage and current of the battery, subfigure (d) the charging/discharging power of the PEV and subfigure (e)the SOC of the battery.

The aim is to comprehend how different DP may in the future influence the charging and discharging planning for a grid supervisor. For model validation aspects, let us imagine that the figure of the supervisor plays additionally the role of an aggregator, which intends to schedule the charging and discharging of PEVs in the LV network according to a power market strategy. For example, its may be interested to charging the batteries during low price moments and discharging them during peak or high price moments. Based on this synopsis, one of the first things notable from Fig. 3.18 is that the charging/discharging strategy performed by the supervisor may significantly be influenced by the the DP performed by PEVs. This is the reason for why the charging schedule is different for the PEVs considered. However, the discharging schedule received by the PEVs, which seeks a synchronized response, is the same. Two discharging request are received coinciding with the peak moments of the day. In the right-hand case, the vehicle is plugged-in at home at its maximum SOC, therefore it is appreciable how it responds in both of them. In the left-hand case instead, the PEV responds to the one received in the early morning but for the late afternoon one it does not, because it has not arrived home yet. This aspect, which certainly adds uncertainty to the strategy of the aggregator, may limit its capability to commit the energy traded in the market. In conclusion, the DP has to be considered in the modelling of these systems and in the design of any strategy. In linewith this, notice how the discharging in this sort of purposes has been limited in order to avoid any inconvenience for the user in case the availability of vehicle is required.

Finally, remark the non-linear behaviour of the SOC originated as a consequence of the battery discharge during driving period.

3.6 Summary

This chapter introduces the mathematical models used to represent the active loads considered in this research work. The models, which cover domestic loads such as EWH, HPWH and PEV and non-domestic loads line an AES, are developed with various approaches to tackle different aspects of the analysis. Furthermore, since their performance depends also on non-electrical aspects, thermal, mechanical, chemical features are included too. The user prevalence towards the load is included since it represents an important aspect to take into account in the modelling of the domestic loads.

The simulations performed for their validation illustrate that these loads definitely have potential in what the DR concerns. However, it cannot be neglected their nature and the service that they provide to the user, since it may significantly limit the response capability that they are able to offer in the future. This is something that should be certainly considered when a DR strategy is designed either for technical or commercial purposes.

Chapter IV

Thermal Consumption and Driving Habits from Residential Users

This chapter, which summarizes the manuscript C2, aims to study the thermal consumption and driving habits from Danish residential users. This is posteriorly utilized to generate profiles which realistically represent the behavior from consumers in possession of EWH, HP or PEV loads. The intention is to use those to describe the power consumption pattern from the mentioned loads during dynamic simulations of the LV network.

4.1 Introduction

The implementation of smart grid technologies in the current power system introduces new possibilities to mobilize and activate flexibility from power consumers [205]. This represents an important aspect in the control and operation of a fully renewable based power system. This type of consumer, also known as prosumer, is distinguished for being in possession of loads with certain storage capability. This fact gives them the possibility of modifying their power consumption pattern without affecting their normal lifestyle. As it was appointed in previous chapters, EWH, HPs and PEVs are some of the loads sharing these characteristics. However, the flexibility which they are able to offer dependents very much on factors such as, the type of technology, its capacity, the strategy used to control the load, the storage existence and its capacity, the atmospheric conditions, etc. A factor, not often precisely addressed, which directly influences the operation pattern of the load is the user habits in relation to the service that the load

provides. For example, the thermal power required for either heating the home space or the DHW, is an aspect which has significant influence in the power consumption pattern of thermostatic loads. For PEVs instead, the driving pattern hold by its user is what will describe the charging performance of the vehicle when plugged-in at home.

Therefore, what this reflects is that a precise representation of the power consumption pattern of these loads implies considering those aspects. Taking this into account, this chapter summarizes the methodology employed to analyze the thermal consumption and driving habits from Danish residential users. In a first step, the data available is statically analyzed in order to develop distribution functions which capture the characteristics of the data. Based on this, the resulting functions are submitted to a random process in order to generate profiles which realistically represent the behavior from residential users in possession of these loads. Finally, the profiles are intended to be used as input data for the load models developed in previous chapters to describe their electrical performance.

4.2 Thermal Power Consumption

Regarding the thermal power demand two types of habits are considered, the SH and DHW. The SH refers to the thermal demand required for heating the habitable space of a household. The DHW instead refers to the one required for heating the water needed for carrying out the domestic activities.

4.2.1 Available Data for the Analysis

The thermal power demand data is obtained from a group of 25 single family households located in a typical Danish residential area [206]. The DHW an SH data is provided in kW and in 15 minutes intervals for a time window of a year. The annual energy consumption of the considered households varies between 4,800 to 20,000 kWh. After being averaged, this together with the ambient temperature and the wind speed is plotted in Fig.1 of publication C2. Two time horizons, a year and a week, are depicted with the purpose of showing the evolution of this demand. When looking into a year window, large seasonal variations are appreciable in the thermal power demand required for SH matters. However, the one required for DHW remains more or less stable along the year. Within a week, these variations are less pronounceable but acquire other types of dynamics. It is notable how the SH and DHW demand is significantly reduced during the night hours.

4.2.2 Methodology for the Profile Generation

Fig 3.a in paper C2 summarizes the steps which are followed in order to generate DHW and SH consumption profiles for different users. This approach basically relies on a

statistical analysis performed on the data in each time step of the time frame considered. Posteriorly, the consumption rate is randomly selected based on the result obtained. By nature the DHW demand is less continuous and more instantaneous in comparison with the SH demand. Therefore, depending on what is being considered, the data is treated slightly differently before it is statistically analyzed. On the one hand, the discontinuity of the DHW demand requires a calculation of the probability of having this type of thermal consumption. This is performed by separating the households with DHW consumption from those that do not have it for each time step. At this point, two separate features are available for the DHW case; the probability of having DHW demand and the rate of consumption in case it exists. The SH data instead does not require any pretreatment before its statistical analysis.

4.2.2.1 Statistical Analysis

No matter if the data considered refers to the SH demand or the rate of DHW consumption, the statistical analysis begins grouping data in a histogram form for each time step. Then, the data is fitted with all the possible distributions functions facilitated by the Statistics Toolbox of Matlab and the coefficients defining them are calculated with the maximum likelihood technique (MLE). These distribution functions, which are represented in their probability density function (PDF) and the cumulative density function (CDF) form, are carefully assessed looking for those that fit better the data in every time step. After that, the best distributions representing the data along the day are selected to proceed with the analysis.

Since, all the distribution functions represent the original data in a better or less good way, the intention is to find which is the best distribution function, or the less bad. In order to find this, the selected distribution functions are subjected to the Kolmogorov-Smirnov goodness test progressively increasing the grade of confidence intervals [207]. As the grade increases, the conditions for the distribution functions becomes stricter to comply. It is here, when those which do not respect the conditions are discarded remaining only the strongest one/s at the end.

However, the Kolmogorov-Smirnov goodness test is only valid to find the strongest distribution functions but it does not provide a good idea of how good the distributions fit the original data. Therefore, the graphical method called quantile-quantile (Q-Q) plot is selected for this purpose [208]. This plots the quantiles from the distribution function against the same quantiles from the original data. Depending on how good the distribution function fits the original data the two plots will overlap in a greater of lesser manner as it appreciated in the illustrations provided in publication C2. This procedure is repeated again for every time step of the selected time frame consciously assessing each plot.

Finally, the distribution function selected to represent the data in each time step will be the strongest one in the Kolmogorov-Smirnov goodness test and the one showing the best fitting in the Q-Q plot.

4.2.2.2 Profile Generation

The profile generation is a random procedure which is based on the selection of the data defined by a distribution function. The way of doing it slightly varies depending on the type of thermal demand which is considered. In the DHW case, based on the probability of having DHW consumption described anteriorly, the household with DHW consumption are assigned for each time step of the considered time frame. Then, if for a specific time step a specific household manifest its DHW demand the rating is calculated in the same way as it is done for the SH demand case.

This process is based in the Latin Hypercube sampling method. By employing the MLE coefficients of the selected distribution function, its inverse cumulative distribution function (ICDF) is portrayed. This will then be divided into equal probability segments and the limits of every segment will be mapped to their representative values of thermal power in the y-axis. Once the intervals of thermal power are obtained from the correct segmentation of the ICDF, one of them is randomly selected. From the selected interval again a random value is calculated, which will define the thermal power required for SH or DHW purposes during the specific time step of the time frame considered. This random process is repeated for every time step of the time frame considered and also for each of the n users considered.

4.3 Driving Patterns

The generation of driving profiles is focused on describing the driving behavior from PEV users living in residential areas. Therefore, it is assumed that each of the PEVs starts the first and concludes the last trip at home, independently of the number of trips performed in a daily tour. As a simple clarification, a tour is described by n trips in a day.

4.3.1 Available Data for the Analysis

The driving pattern data, which refers to the Danish case, is obtained from the work published in [209] and [210]. This is provided in a histogram form and includes information about the average distance driven in a day, the tour structure follow by the vehicles and the departure and arrival times of the first and the last trip in a day. This information is depicted in Fig.2 in publication C2. It is interesting to notice how most of the vehicles in Denmark drive less than 40 km per day. 7 to 8 a.m is the most common time frame to start the first trip of the day and 3 to 4 p.m to conclude the last one. From [210], it is derived that the tour structure which prevail in Denmark is the one composed by two trips per day, from home to place where a main activity is carried out and from there back home again (Home-Main-Home).

Since, finding any reference regarding the characterization of the Danish driving style

was quite arduous, the European project ARTEMIS is considered for this aspect [211]. The project aims to develop pollutant emission models of all kind of transport in order to estimate and quantify their pollutant emissions. However, different speed based driving cycles are available which represent the typical urban, rural and motorway trips for standard size vehicles.

4.3.2 Methodology for the Profile Generation

Fig 3.b in paper C2 summarizes the steps which are followed in order to generate driving profiles for different users.

4.3.2.1 Statistical Analysis

In the statistical analysis of the driving patterns three features are of special relevance, the distance driven by the vehicle in a day and its departure and arrival time to home. In this case, the data regarding these two features is already provided in a histogram form. This fact hinders a direct fitting of the data due to the absence of the physical data. So, a Monte Carlo procedure is applied in order to generate new data which respects the original distribution. Once the new data is created, it will be statistically analyzed for the same procedure as with the thermal consumption data. As result, the best distribution function for each case is expected to represent, i) the distance driven by the vehicle in a day, ii) its home departure time and iii) it home arrival time. These three distribution functions are posteriorly used to generate the data which defines the basic pattern of the PEVs.

4.3.2.2 Profile Generation

As with the case of the thermal power demand, the driving profile generation is characterized for its randomness. Based on the distribution function selected previously, the Latin Hypercube sampling method is utilized with the purpose of randomly defining the driving distance and the home departure and arrival times for each of the n PEVs considered. Additionally, based on the probability of a vehicle to perform certain tour structure in a day, the tour structure is randomly assigned to each of the n vehicles. These four features represent the base information required to start the driving profile formation task.

Depending on the tour structure assigned to a PEV this will perform from two to four trips a day with the purpose of completing a main or secondary activity. The time expend by the user carrying those out is what differences both activities. This means that a main activity will always require more time than a secondary one. Therefore, based on the assigned distance driven in a day, the distance driven in each of the m trips is randomly calculated respecting the linear dependency between trips.

The driving style is quite particular and very different from driver to driver which

makes it difficult to represent it precisely. In lack of any other source of information, the European project ARTEMIS is considered in order to reflect this aspect. This project offers various driving cycles categorized as urban, rural and motorway for different classes of vehicles. Depending on the area where a vehicle is located and the distance driven in the trip, its driving cycle can be represented by one or a combination of those. Thereupon, for each of the m trips an ARTEMIS driving cycle is randomly assigned and made it rigorously fit to the distance of the trip.

The driving profile formation task must be characterized by its randomness but also respecting the tour structures defined at the beginning. So, once the driving cycles for each of the m trips in a daily tour are fitted, it is time to integrate them into the time frame when the vehicle is out of home. Again, this is performed randomly but respecting that the time required to perform a main activity should be longer the one required for performing a secondary one.

Finally, this procedure is repeated for each of the n driving profiles required in order to represent the driving behavior of the n PEVs.

4.4 Observations and Discussion

The validation of the introduced methodologies is carried out assessing a single case for each of the habits that is to be represented. In all of them, the number of users considered is eighty and the time step and horizon are 15 minutes and one day. For the SH demand case, the histogram representation of the original data shows how during early morning and late evening the data seem to be more concentrated which indicates that the heating systems are normally set in stand-by mode during the night hours. During the day, the data seem to be more spread reflecting the diversity of the users in what the SH demand concerns. The differences between users are normally associated to the grade of the isolation of the household and the way the user perceive the comfort. The statistical analysis underlined that "generalized extreme value" is the distribution function which fits better this data. Finally, it is appreciable how the profiles resulted from the random procedure follow the pattern defined by the original data, evidencing an increment of the SH demand right when the inhabitants start the day.

For the case of the DHW demand, it is appreciable how the probability of having this sort of consumption is higher in during the first and late hours of the day. Indeed it coincides with the periods of the day when there is more activity at home. In what the fitting of the rate of DHW consumption concerns, the "normal" distribution function is appointed in this case. Therefore, by implementing these two features into the profile formation procedure, it is perceptible how while maintaining the randomness the resulted profiles keep the sporadic and instantaneous characteristics of this way of thermal demand.

Lastly, the driving profiles resulting from the implementation of this approach maintain the probability distributions defined which makes them suitable for representing

the driving behavior from users in possession of a PEV. In the illustration different examples are given from the different tour structures considered.

4.5 Summary

This chapter discusses the importance of considering the thermal consumption and driving habits of residential users in the modelling process of thermostatic and PEV loads. This is especially relevant seeing how this aspects influence the performance of the load in respect to the LV network. Taking this into consideration, this chapter tackles the need of having a simple technique to generate profiles which realistically represent the behavior from residential consumers.

In a first stage of the chapter, two methodologies used to generate thermal consumption and driving profiles are introduced. Both approaches consist of first a statistical analysis of the original data and a posterior random process of the profile formation. In the second stage, those are validated with a series of cases. It is demonstrated how the profiles created in those cases respect the pattern defined by the original data. This makes them suitable for being employed in the representation of the electrical consumption pattern of thermostatic and PEV load models.

In the analysis of local distribution networks, this will provide a better understanding about the impact of moving from fossil fuels dependent to more electrified heating and transportation systems.

Chapter V

Potential Flexibility in Residential Demand

The flexibility term and its meaning when referring to the residential demand are defined in this chapter. Additionally, this summarizes the methodology proposed in publication C4 to probabilistically quantify the potential flexibility from flexible residential consumers. Even though, the approach is implementable to different types of appliances the case of a HP is utilized for its validation.

5.1 Introduction

Together with the smart grid concept new alternatives, in what the balancing of renewable energy based power system concerns, are arising. One of them, specially appointed for the Danish case, is the mobilization and activation of flexible residential demand. This flexibility is represented by those consumers that are able to shift their power consumption in time or alter it without inducing major changes in their lifestyle. Therefore, it is available from those in possession of loads that allow modifying their normal operating pattern. Thermostatic loads such as EWHs and HPs together with PEVs are referred as sources of flexibility at the residential level. However, it is important to differentiate between the flexibility that these loads are able to offer and what they are able to provide due to tertiary reasons (network congestions, comfort limitations, continuous operation of the load, etc.). Taking these into consideration, the response of those should be encouraged in order to aid a power system either at local or global level.

Despite of being in constant allusion, the flexibility term is usually not properly defined and even rarer quantified. In particular, different consumers have different power

requirements and consumption behaviors, leading those to hold different grades of flexibility. This is especially relevant in a future context where the flexibility is expected to become a product to be traded in flexibility markets [205]. The aim of such a platform is to aid for example a utility seeking for system demand reduction to avoid overloading or even the TSO which requires new ways for balancing the power system.

This chapter summarizes the methodology proposed in publication C4 to identify and quantify the potentially flexible demand at the residential level. This approach is based on a clustering of non-flexible consumers followed by a statistical analysis and a pattern comparison. In the case selected for its validation, the power consumption pattern of a residential consumer holding a HP and a PV panel is compared to a 3D probability distribution. This curve is created from a set of non-flexible consumers, by exploiting the similarity -in terms of energy consumption and power pattern- to the flexible consumer. In this perspective, the additional real measurements -for capturing the flexibility- could be replaced by a probabilistic virtual measurement. Hence, an advantage of its implementation is the diminution of the measurement data at the household level.

5.2 Proposed Methodology

One of the first things that need to be clarified is the differences between a potential flexible demand and the physically and implementable flexible demand. Potential flexibility is defined as the aggregated demand from all the loads which are described as flexible. In order to precisely determinate it any dispersed generation should be subtracted from this amount. However, the resulting demand might be acknowledged as flexible or not depending on the specific situation. The approach designed to identify the potentially flexible demand is based on comparison between a flexible consumer and other non-flexible consumers with similar characteristics. This procedure, which is summarized in the first figure of publication C4, is composed of three phases; customer clustering, statistical analysis and pattern comparison.

Before starting with the procedure, it is necessary to identify which are consumers having flexible loads and/or dispersed generation and which ones do not. This is done in order to divide the consumers into flexible and non-flexible consumers. Later, the non-flexible consumers will be selected and submitted to a clustering process composed of a pre-clustering and a two stage clustering process. The aim is to define the non-flexible consumers that share consumption similarities with the flexible consumer.

The pre-clustering and the successive clustering stages are based on the iterative implementation of the k-means algorithm and the DBI index [212], [213]. The k-means clustering, which aims to assign the n data-points into k clusters, was selected due to its simplicity and low computational requirements. If extra information about this algorithm is required a more extensive description is developed in the publication C4. A disadvantage using the k-means is that it does not provide explicit information about

what is the optimal number of clusters. Since, this aspect hinders any decision on that regard the DBI index is implemented to evaluate the validity of the k-means clustering. Again, if more detailed explanation of the DBI index calculation is required this is available in publication C4.

The combination of the above mentioned algorithms, named in the manuscript as the "Combined k-means & DBI (CKMDBI)", requires first the election of a maximum number of clusters. This number is subjectively decided, nonetheless it should be a realistic number which serves practical purposes for a utility. Secondly, the k-means algorithm is applied for k = 2 and the DBI is utilized to assess the validity of the clusters constructed. This procedure is iteratively performed until the maximum number of clusters is reached. The lowest DBI value shows the optimum number of clusters for the corresponding dataset. Thirdly, the k-means clustering is once again applied with k being equal to the aforementioned lowest DBI value.

Once it is introduced how the optimal number of clusters is selected for each stage, it is time to describe each of these stages. Since, only residential demand is of interest, a pre-clustering stage in terms of aggregated energy consumption is performed in order to exclude any industrial and/or large commercial consumer. For the aggregation of the energy consumption a time interval should be decided, i.e. month, here the patterns to be clustered are daily averaged along with the flexible consumer under study.

After excluding the outlier consumers, a two-stage clustering of the remaining ones is performed. First, the remaining consumers are again clustered with respect to their aggregated energy consumption for the same time interval considered in the pre-clustering stage. Secondly, these clusters are sub-clustered with respect to the average daily consumption pattern of the same time interval. To be able to do so, the patterns are first normalized by their daily maximum value. Once all the clusters are defined, the flexible consumer under study is assigned to the cluster with shortest Euclidean distance to his/her. This is done primarily in terms of energy consumption and subsequently according to the normalized demand pattern. Nevertheless, the flexible consumer's demand should first be filtered before its classification. Since the consumer has additional flexible loads and/or generation, these should be excluded prior to the class assignment.

The result is a number of N non-flexible consumers that for the chosen time interval - i.e. month- show similar aggregated energy consumption and consumption pattern as the flexible consumer once its demand has been filtered. Based on this classification, a comparison between them can be performed for subsequent time intervals, i.e other months. However, there may be consumers which are not represented by this classification in the new time intervals. Therefore, a validity test of the base classification is required for those intervals. The idea is to repeat the CKMDBI algorithm in the new intervals keeping track of how many of the N consumers remain in one class. Thus consumers, who initially belonged to the N consumers and additionally belong to classes having a large proportion of these N consumers in subsequent intervals (e.g. months), are kept and aggregated. This will result into a new M non-flexible consumer group

($M < N$), the rest are discarded.

Before comparing the flexible consumer and the M non-flexible consumers a statistical analysis of the non-flexible consumers is required. Therefore, based on the subinterval -i.e. day- selected for the comparison, a number of preselected probability distribution functions (PDF) are selected in order to fit the M consumers' data in each time step of the subinterval. Among those, the best four are chosen -at each time point- in terms of being within the predefined confidence bounds (CB) of the empirical cumulative distribution function (ECDF) form. The rest are discarded. These four distributions are then subjected to a Quantile-Quantile plot (Q-Q plot) assessment in order to define which ones fit best the data in each time step.

Lastly, after acquiring all of the best fitted PDFs for each time spot, a 3D probability distribution is readily available to compare the M consumers and the flexible consumer.

5.3 Available Data for the Analysis

For the validation of this methodology hourly power consumption data, in kilowatt hour (kWh), was provided by a regional utility for the year of 2012. The data refers to 223 consumers which are primarily supplied by a 20 kV radial feeder in the area of Støvring in Denmark. Eleven 20/0.4 kV transformers represent the power supply for the low voltage networks that distribute the electrical energy among the consumers. No existence of HP, PV or EV installations among the consumers was also reported by the utility. The consumers are classified by the utility as residential, agricultural, commercial and industrial. Fig. 5.1 illustrates the aggregated power transfer by the radial feeder during the mentioned year. The changes occurring during weekends, holydays or even seasons are well differentiated in this figure.

Additionally, similar data was also obtained for a residential consumer located in a neighboring feeder. The only difference in comparison with the rest is that this consumer had a HP in operation all year long and a PV panel from the 15^{th} of August.

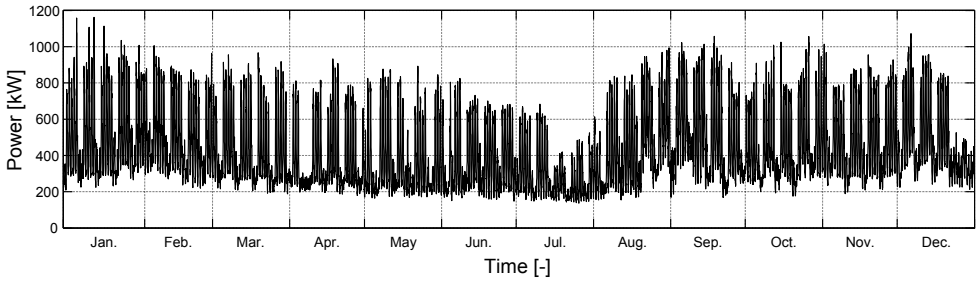

Figure 5.1: *Aggregated Power Consumption Data During 2012.*

5.4 Practical Implementation

In a first stage, the available data is filtered in order to get rid of those consumers for which the demand is disrupted or badly measured. After this process, 166 non-flexible consumers and the flexible consumer were accounted as meaningful to implement the introduced approach, Furthermore, only the data referred to weekdays was considered and due to aggregation matters the time interval selected was one month.

The possession of the HP is what it makes the flexible consumer to be considered as flexible. Therefore, subtracting the "bias" of the HP operation from the average demand profile is one of the first things to be tackled for the flexible consumer. As February is the coldest month in Denmark, it can be easily concluded that the HP will be operating most of the time. Thus, it affects more the magnitude of the average demand profile -for that month- than the shape of it. Under this assumption, every day of February was split in 6 four-hour intervals. For each interval the minimum value was found and the minimum values for equivalent intervals throughout the month were averaged. In this context, it is supposed that the averaged minimum values for the 6 four-hour intervals will most likely represent the baseload and the HP operation on average for that month.

Since, it is assumed that the baseload remains constant throughout the year, to estimate its value the same technique was also applied for the hottest month in the year. In this case, July was considered due to the fact that its consumption pattern is barely influenced since the presence of the HP is low and the PV is not installed yet. The estimation of the baseload was 158,18 Watt. Consequently, the HP plus baseload values were subtracted from the average curve of the flexible consumer in February. The baseload, as estimated in July, was posteriorly re-added again. Finally, the average February curve of the flexible consumer was available for its classification.

In the next step, as Fig. 5.2 shows, the 166 non-flexible consumers are submitted to the different clustering stages. After the pre-clustering stage, the clusters containing industrial or large commercial consumers -7 in total- were easily identified and removed as redundant information. The remaining 159 consumers were then clustered based on their aggregated energy consumption in February. 4 clusters resulted from the conducted energy clustering. The flexible consumer was classified in one of those 4 classes and consequently that particular class was sub-clustered in terms of normalized curve shape. Finally, 89 consumers were selected as the reference group of the flexible consumer in the month of February. So, these consumers represented the group considered for the posterior statistical analysis.

For subsequent months, the validity test explained in the previous section was performed in order to guarantee that these 89 consumers behave in the same manner as in the base month. For example, in May only 75 out of the 89 consumers had similar aggregated energy consumption and only 70 out of these 75 had a similar demand shape. In consequence, 70 consumers were only considered in the statistical analysis for the case of May. After this analysis several probability distributions were selected for fitting the

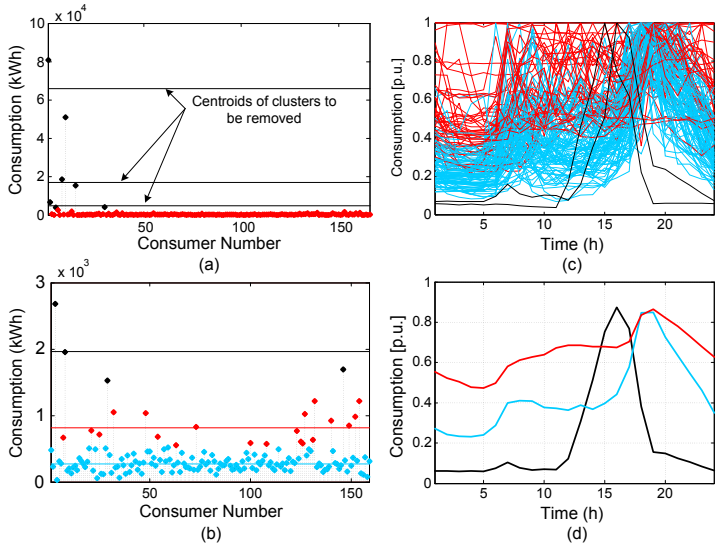

Figure 5.2: *Consumer Clustering Example for February: (a) Pre-clustering, (b) Energy clustering, (c) Normalized curve clustering, (d) Centroids of the normalized curve clustering.*

data and eventually creating the 3D probability distribution for a day. This distribution was used for quantifying the potential flexibility of the flexible consumer.

5.5 Observations and Discussion

The result of this method is a 3D probability distribution, which represents the non-flexible demand of a consumer who is similar to the flexible consumer under study. The boundaries of the 3D probability distribution are defined by areas of probability (AP). These areas denote that the load consumption of a non-flexible consumer will lie in this range with certain probability. Therefore, when the power curve of the flexible consumer and the 3D probability distribution are overlapped, whenever it is exceeded from an specific AP could be considered as potentially flexible demand.

To validate the proposed method three typical days are considered in publication C4; a typical cold winter day in February, a spring day in May and a hot summer day in July. By a simple comparison of the results, it is appreciable how different the potential flexibility obtained in the different cases and for the different APs is. In the case of February, the HP is dominating the power consumption of the flexible user at all times since it is in constant operation. Even though, the values for its potential flexibility are

the highest ones, it is hard to shift any demand on the time horizon. In conclusion, any flexibility is hardly to be available on this day.

In the case of May, which represents the transition between extreme seasons, the household thermal demand is not that high anymore but is still adequate to make the HP operate several times within the day. In such a scenario, flexibility could be offered by valley filling. July represents the opposite case of February, due to the limited thermal need required by the household at this time of the year the HP barely operates, which implies a lack of flexibility even for a low AP.

It can be concluded that the potential flexibility is more likely to be offered as flexibility in months belonging to transitional periods between summer and winter.

5.6 Summary

This chapter addresses one of the important aspects in the control and operation of future power systems, the mobilization and activation of flexible demand. Among the different types of demand, the residential one is committed to play an important role in this matter. However, when referring to this time of demand the flexibility is usually not properly defined and even rarer quantified.

In a first place, this chapter summarizes the methodology proposed in order to identify and quantify the potential flexibility of residential consumers. This is based on a comparison between a flexible consumer and other non-flexible consumers with similar characteristics. First, clustering of non-flexible customers is performed with the subsequent assignation of the flexible consumer to one of the resulting classes. Then, a 3D probability distribution of non-flexible demand is created for several days and the flexible consumer is compared to it.

In a second place, the methodology is validated using the hourly power consumption data provided by a regional utility. It is demonstrated that when the average curve of the flexible consumer and the 3D probability distribution of the non-flexible consumers are overlapped, the potential flexibility can be perceived by defining different areas of probability.

Chapter VI

Impact of Future Energy Systems Electrification

This chapter addresses the challenges faced by future LV networks due to the electrification of energy sectors such as the heating and the transportation. Besides, it summarizes the methodology proposed in publication C5 to define and evaluate the impact originated by the penetration of HP and PEV loads in LV distribution systems. Furthermore, it is of interest to quantify the LV distribution system hosting capability and to determine how and where might be potentially located their technical constrains in the future.

6.1 Introduction

The conceptual and technological restructuration of national energy systems is happening in many countries nowadays. In Denmark, this is already reflected in the increased wind and photovoltaic (PV) power penetration, the continuous development of the electric vehicle infrastructure and the stimulation plans for replacing old fashion heating systems by more efficient and environmentally friendly ones. All this examples have one thing in common, the interaction of new loads and/or generators with the power system. From a demand perspective, the power system is expected to undergo a significant load growth due to the electrification of systems such as the heating and the transportation.

Although, this phenomenon is foreseen to affect each level of the power system, the distribution systems seem to be especially targeted. The reason is the nature of the expected loads which makes the local LV networks more accessible from an integration perspective. For a DSO, this context imposes important challenges in respect to the conventional management of the LV grids. Particularly, since it is committed to accommodate an increasing number of loads in networks that were not designed for them.

Furthermore, considering the high power rating of loads such as HPs and PEVs, the performance of this commitment gets even more complex. For this reason, it is important for the DSO to realize an exhaustive evaluation of how different levels of load penetration may affect the LV grid operation. The technical consequences of increasing the load in these networks are by this time well known; voltage deviations, unbalances, overloading of the infrastructure, etc. However, in which way and where they are going to be potentially located is uncertain. It is true that most of the LV networks have a radial configuration which weakest point has traditionally been represented by furthest bus from the secondary transformer. But with the accommodation of a new load or local generation this may not be the case anymore. In this context, the behavior of the LV grid will depend on the specific network characteristics and especially on how the new load is distributed in the network.

This chapter summarizes the methodology proposed in publication C5 to evaluate the impact caused by the combination of HPs and PEVs in residential LV networks. Furthermore, it aims to quantify their hosting capability and to determine the nature and location of the potential technical constrains. The approach is based on a Monte Carlo model which uses the traditional Newton-Raphson power flow for defining the grid condition. For the same load penetration level multiple power flow calculations are performed randomly altering the location of the HP and PEV loads in the grid. By doing so, a more realistic conception of the potential system bottlenecks is obtained when comparing with deterministic procedures. Moreover, this approach probabilistically identifies the vulnerable components of the infrastructure that obviously should be under consideration of the operator.

6.2 Proposed Methodology

A common practice among DSOs or utilities when performing impact studies has traditionally been to consider a worst case scenario as a reference. However, this case which is commonly deterministic may not always represent the reality. This leads to an unnecessary over-dimension of the infrastructure and in consequence to a substantial increase on the network investment.

The methodology proposed to evaluate the impact caused by HPs and PEVs in LV networks is based on a Monte Carlo (MC) model which uses the traditional Newton-Raphson power flow for defining the grid condition. The starting point is defined by the model of the LV network to be analyzed. Each of the n users (n_u), which are represented by the existing household load (HL), are then provided with two extra loads -HP and PEV- which will be randomly activated and deactivated depending on the case considered. The distribution of the new load across a LV network is clearly not deterministic. Therefore, the aim is to respect the stochastic nature of the load distribution. For that reason, the approach is structured in two stages, the network assessment and the statistical analysis of the obtained results. In the first one, a network assessment

algorithm (NAA) has been designed to evaluate the network response according to the penetration level and the distribution of the load considered. In the second stage, the results are processed and statistically analyzed with the purpose of identifying which are potential constrains and the most vulnerable elements of the system.

6.2.1 Network Assessment Algorithm

Fig. 6.1 depicts the core frame of the NAA. This is first composed of a random process, which sets the number of study cases for a given load penetration, and based on these a posterior MC model for defining the grid condition.

As input, the NAA requires defining the penetration level of HP and PEV loads and the number of load distribution cases (n_{it}) that will be considered for the MC model. After defining and initializing the system variables, two matrices D_{HP} and D_{PEV} of n_{it} x n_u size are created in order to store which users have installed HP and/or PEV loads for a given case and which ones not. Then, for the penetration level defined and the n_{it}, the correspondent HP and PEV loads are randomly assigned among the users. Something which is important to clarify is that the probability for a specific user to hold a HP or PEV load is considered the same for all of them.

After it is certified that the number of loads assigned in every case corresponds with the penetration level defined at the beginning, the matrices for storing the results are created. As it is mentioned before, this approach focuses on defining the actual grid

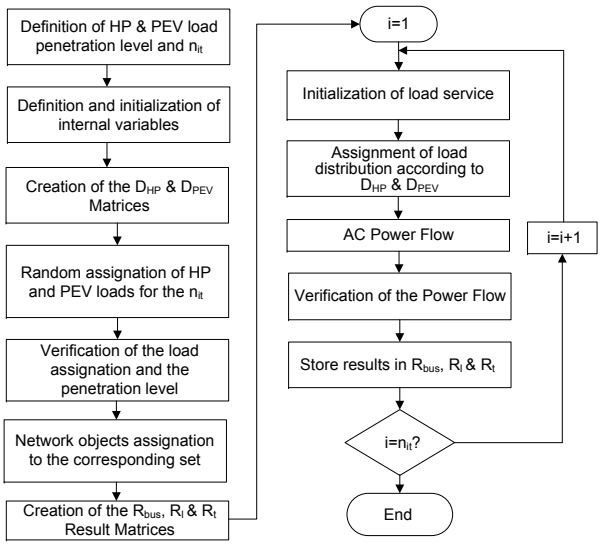

Figure 6.1: *Flow-chart describing the NAA.*

capacity, its hosting capability and the nature and location of the technical constrains. Therefore, the matrices R_{bus}, R_l, R_t will store the following results: i) voltage on the buses -cable box (CB) or point of connection (POC)- in per unit (n_{it} x n_{bus}), ii) loading of the cable (n_{it} x n_l), iii) loading of the secondary transformer (n_{it} x n_t).

After this initialization, the MC model takes over in order to begin with the network evaluation phase. For each of the n_{it}, the starting point will be resetting any previous calculations and ensuring that all the HL loads are on service -activated- while all the HP and PEV loads are off service –deactivated-. Once this is satisfied, the activation of the HP and PEV loads will be done according to the sequence imposed by D_{HP} and D_{PEV}. After, determining the case scenario for the given iteration the power flow calculation is performed in order to define what the network condition is. Then, the elements of the network are accessed individually in order to gather the data of interest for this study. Finally, the data is stored in the corresponding result matrix and the procedure is iteratively respited until i=n_{it}.

6.2.2 Statistical Analysis of the Results

Since, the previous procedure is characterized for its randomness it is required to make a probabilistic interpretation of the results obtained. Before that, it is necessary to identify three important features which represent the worst operating point of the network among the cases considered. On the one hand, the minimum voltage in the grid (V_{min}), which ensures that all the CB and POC at the LV grid are supplied with a voltage equal or higher to this value. On the other hand, the maximum line and transformer loading determine the worst condition of the most affected part of the infrastructure. After this, the obtained results are statistically analysed in order to find the probability from each CB and POC to be one supplied with V_{min}. Similarly, it is done for each of the lines in order to determine its probability of being the most loaded one. The corrective reinforcement measures of a DSO should be decided based on this analysis.

6.3 Test Network and Study Cases

The data available for the validation of this approach refers to a LV network located in a Danish rural area. Through a 315 kVA 20/0.4 kV transformer and a seven string radial network, 137 private users are supplied with electricity. Since, the zone is distinguished for not having any district heating service accessible it represents a good test system to determine the impact produced by HPs and PEVs under different penetration levels. Furthermore, the consumers belong to the same MV radial feeder introduced in the previous chapter, so hourly power consumption data is also available for them.

For being able to determine the technical limits of this LV grid, a base case is considered in order to have a reference. This stands for the moment of maximum load in the whole year, which happens at 18:00 in a Friday of January. Consequently,

the different existing HL loads which represent the actual consumption of the users are assigned with its corresponding value for that specific time. A more detailed description of how the different static loads are modelled is available in the referred publication. Then, the network response is assessed under different penetration levels. With the purpose of having reasonable times of simulation, the n_{it} selected for the MC model is 10000.

It is also of interest to evaluate how potential reconfigurations in the given network might affect its hosting capability towards these loads. In line with this, three cases have been designed:

- *Case 0 - Original Network Configuration*: The network, as it is today, but subjected to different HP and PEV penetration levels.
- *Case 1- Minor Reconfiguration*: Based on the results obtained in case 0, an additional transformer is placed in parallel with the existing one and the most loaded string is divided in two less loaded ones.
- *Case 2 - Large Reconfiguration*: Based on the results obtained in case 1, the rating of the transformers is upgraded and three additional lines are installed in order to improve the voltage profile of the weakest points of the network.

Finally, the technical operating limits are established according to the standard EN 50160 for medium voltage (MV) and LV grids. This standard states that the RMS voltage should remain between the ±10% of the nominal voltage of the network.

6.4 Observations and Discussion

From the study carried out in the test system considered, it is deducible that the hosting capability of the actual LV grids might be very limited for the load penetration levels foreseen for the future. For the case investigated, the voltage represents the mayor technical constraint in the accommodation task of HP and PEV loads. The network, as it is today, can barely handle more than 25% of the consumers in possession of a HP before the voltage limit stipulated by the EN 50160 is violated. Considering, only PEVs, it is interesting to see how only 5% of the costumers in possesion of one could make the network operate under non-acceptable points. Although, the voltage represents the principal constraint notice that the maximum loading limits of the secondary transformer and the most loaded line are not far from the maximum penetration levels defined by the voltage constraint. This is a trace which reflects the good equilibrium of network topology and its proper design and implementation.

In Table II of the referred publication, the results from the statistical analysis for each network configuration case considered are summarized. This table shows the network elements -CB and line- with highest probability to become the most vulnerable elements on this infrastructure. For the base case -case 0-, it seems realistic that for any

HP penetration level the elements with highest probability to be the most vulnerable ones are the furthest bus from the secondary transformer and the cable representing the beginning of the most loaded string. However, when HP and PEV loads are combined together the probability of the furthest bus to be supplied with the minimum voltage might significantly decrease. The reason is the higher rating of the PEV loads that makes their presence more notorious in comparison with the HP load. In consequence, it cannot be dismissed the fact that certain load distributions might make the network react in a non-expected manner. Parts which are currently considered strong might in a future be hardly exposed to technical constrains while elements that have traditionally been considered as the technical boundaries, i.e furthest node, might become less vulnerable.

Based on the low hosting capability of this test system, a small re-configuration -case 1- was performed in order to have a better and more uniform distribution of network loading. The obtained results show that its hosting capability, towards the HPs, is improved. Now, up to 50% of costumers having HPs could be integrated without violating any of the technical constrains. However, as soon as a small percentage of PEVs is taken into account the voltage drastically collapses. The loading of the most loaded line and the secondary transformers instead has improved significantly. Nevertheless, it is not by far achieved the load penetration levels expected for Denmark. Looking into the probability again, in this case the string number 2 seems to be the most affected one when only HPs are considered. Once the PEVs and HPs are combined, the strong presence of PEVs not only makes the probability of the most vulnerable element decrease again but also changes the element targeted. This aspect might be influenced by the reconfiguration of the network since a better distribution of the load makes the identification of the vulnerable points more difficult.

Since the hosting capability of this test system is still not enough for achieving the expected levels case 2 is designed. The obtained results illustrate that the efforts for improving the voltage profile in order to allow higher HP and PEV load accommodation, makes instead the main power carrier of string 3 very vulnerable to this decision. This fact underlines the complexity of employing a meshed design as a solution to allow higher load penetration levels in LV systems. Furthermore, as higher is the grade of mesh as more difficult becomes the estimation of the vulnerable points of the network.

6.5 Summary

This chapter discusses the challenges faced by DSOs due to the electrification of energy sectors such as the heating and the transportation and its impact in LV networks. First, it summarizes the methodology proposed in publication C5 to define and evaluate the impact originated by the HP and PEV loads in those systems. This approach is based on a Monte Carlo (MC) model which uses the traditional Newton-Raphson power flow for defining the grid condition. The aim is to quantify their hosting capability and to

determine the nature and location of the potential constrains that may appear in the future.

Second, it describes the test system and the cases designed for validating the proposed methodology. Third, the obtained results highlight that it cannot be dismissed the fact that certain load distributions might make the network react in a non-expected manner in the future. Parts which are currently considered strong might in a future be hardly exposed to technical constrains while elements that have traditionally been considered as the technical boundaries might become less vulnerable. Furthermore, if the reinforcement of the network implies meshing it, this effect may get even more pronounced making the identification of its vulnerable parts more difficult.

Chapter VII

Demand Response Control in Low Voltage Networks

This chapter addresses the employment of the DR in local distribution systems as an alternative for materializing different technical and commercial services. Furthermore, it summarizes the hierarchical supervisory DR mechanism, proposed in publications C3, J1 and J2, i) to enhance the dynamic operation of LV grids and ii) to aggregate the response of flexible loads with the purpose of fulfilling the energy committed in platforms such as the RPM. At the same time, the control features which are representative for each of the layers are also described together with the technique employed to forecast the up and down regulation capability of the LV network.

7.1 Introduction

The restructuration of the Danish energy system stands out two major challenges. On the one hand, a 100% renewable based power system requires new solutions for the power balance. On the other hand, the electrification of systems such as the heating and transportation is expected to congest the power transfer capability from many networks. As it is reflected in previous chapters, this last aspect is particularly relevant in local distribution networks.

Among others, the violation of the voltage limits is a serious problem to be faced in the future. The LV systems have traditionally designed and constructed in order to ensure a secure and efficient distribution of the power demand. In those cases where the seasonal variation of the demand distorts the voltage profile of the network, no-load tap changer (NLTC) transformers are utilized in order to manually adjust these deviations. Other commonly employed alternatives are the placement of voltage regulators

and shunt capacitors in specific point of the network [175], [176]. With the need for greater control, coordination and automation of distributed energy resources (DER), new control methods are emerging at this level. This is the case of the on-load tap changers (OLTC) employment at the secondary transformer (ST). Others instead are based on power electronic applications such as the injection/curtailment of active and reactive power from DER, smart transformers and active voltage regulators [184], [185]. According to the [214], the high R/X ratio of LV cables implies that the amount of reactive power required for voltage support might be high comparing with an active control of the power demand. Furthermore, the injection of reactive power might increase significantly the grid loses in those feeders where this approach is implemented.

There is no doubt that all this technology is going to be necessary to safely operate, under a reasonable growth of the demand, the actual LV systems. However, looking into the load penetrations foreseen by the Danish authorities it might happen that only those mentioned above might not be sufficient. In this context, real-time control of the DR introduces relevant opportunities to negotiate different aspects of these systems operation.

This chapter summarizes the hierarchical supervisory DR mechanism proposed in publications C3, J1 and J2. This approach, which connects the ST, feeder and consumer level control, aims to enhance the dynamic operation and interoperability of the LV networks while serving as a platform to aggregate flexible demand in response to the provision of commercial services. Considering the non-negligible R/X ratio of LV cables, the proposed strategy acts over the active power consumption of loads such as HP and PEV systems to undertake the mentioned goals. This approach has to be contextualized within the technical and commercial structure described in the *iPower SPIR* research platform [215]. This structure aims to activate and coordinate flexibility of local assets through the commercial stakeholders in order to provide system services.

7.2 Hierarchical Control of Demand Response

A hierarchical arrangement of the distribution system supervision makes it possible to identify, evaluate and tackle the technical constraints in the LV network in singular manner. This is especially relevant when the voltage drop is the key factor representing the grid constraint. Since, the voltage limit violation is normally a local problem it requires local solutions as well. Moreover, since the intermediate layers have the capacity to decide over the controlled assets, less communication infrastructure is required when compared to a fully coordinated control system. Fig. 7.1 gives an overview of the different layers constituting the hierarchical structure proposed. This could be an interesting solution for a DSO playing also the role of an aggregator (DSO-A) looking for solutions to enhance the dynamic operation of its networks and/or willing to use DR for participating in the power market. This structure is basically composed by three layers, the unit control (UC) -load level-, the subsystem control (SSC) -feeder level- and

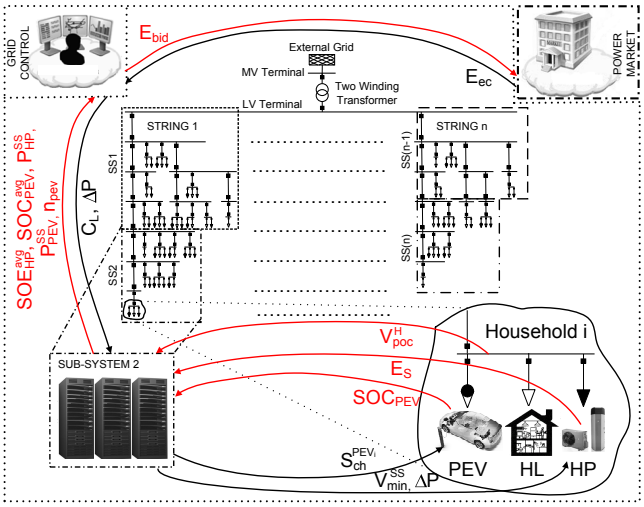

Figure 7.1: *Hierarchical Control of DR in the LV Grid.*

the distribution grid control (DGC) -grid level-. Since, the LV network is divided in different SSs a bidirectional flow of information exists between the different layers. The DGC, which stands for the main supervisor block, has a direct communication with all the SS in order to have a good overview of the LV grid condition. Furthermore, it monitors the average energy stored in the LV system and forecasts the network flexibility, in terms of up and down regulation. Based on this, it is responsible for deciding the energy bids that will be sent to the power market. The SSC instead is responsible for monitoring a group of households and in case they have HPs and/or PEVs operate them according to its needs. Finally, the flexible loads report permanently their energy status to the SS that they belong. This structure intends to respect the following aspects: i) power quality in accordance with the standard EN 50160, ii) to dismiss the user discrimination, treating them equally no matter the point of connection (POC) they are connected and iii) to satisfy the energy commitments acquired by the DGC with the power market. The obligations from each of the layers are described in the subsections below.

7.2.1 Unit Control

It refers to the embedded control of the appliance which maintains the stored energy within the stated limits. For the HP case, it also represents the strategy to adapt their operation depending on the technical constrains and demand aggregation requests. In this context, the PEVs show an advantage in respect to the HPs. Besides of being able

to control them ON/OFF, it is possible to vary their charging rate while they are ON. The HP technology considered instead either operates at the rated power or it has to be turned OFF.

7.2.1.1 Heat Pump Control Modes

As it is described in chapter 3 the HP system, as a thermostatic load, is controlled based on a regular hysteresis control. When the average energy stored in the HWST (E_S) drops below the cut-off band ($\underline{E}_c$) the HP turns ON to recoup the thermal energy loss. It will remain ON up to when the E_S reaches the upper band ($\bar{E}_c$). This stands for the passive way of controlling such a load. Nevertheless, their flexible nature allows having an active control on them. Taking that into consideration, the normal operation mode (NOM) of HP operation is provided with two extra operation modes, named as the voltage emergency mode (VEM) and demand aggregation mode (DAM). These modes are briefly introduced in the following subsections since they are extensively described in publication J1 and J2. The criteria employed for switching from one mode to another is:

$$\begin{aligned} &V_{min} \geq V_r \;\; \& \;\; k_v > k_l \;\; \& \;\; \Delta P = 0 \rightarrow NOM \\ &V_{min} \geq V_r \;\; \& \;\; k_v > k_l \;\; \& \;\; \Delta P \neq 0 \rightarrow DAM \\ &V_{min} < V_r \rightarrow VEM \end{aligned} \tag{7.1}$$

where V_{min} is the minimum voltage of operation, in this case in the SS where the HP belongs, V_r is the pre-defined limit for V_{min}, k_v and k_l are internal variables of the HP controller and ΔP is a power deficiency signal in kW. ΔP, which is explained in the DGC subsection, represents the difference between the power measured at the ST level and power rate according to the energy committed. ΔP is calculated by the DGC and is delivered to the HP systems via the corresponding SSs.

Voltage Emergency Mode

A voltage violation occurs when V_{min} becomes lower than V_r. The V_r limit is either set by regulation or by the practical experience of the DSO. Therefore, from the instant when the violation occurs until it is cleared a voltage violation region is determined. This region is where the HP system should adapt its operation in order not to aggravate more this technical constraint. The HP senses any violation based on the V_{min} received by the SS. So, when a severe violation occurs, the $\underline{E}_c$ is extended 20% in respect to the normal operation mode (NOM) settings. As a result, E_s is allowed to drop to lower energy levels making the HP remain OFF for a longer time. Considering that the activation of the load is delayed, the aggravation of this technical constraint is avoided without practically affecting the user comfort. In case further explanation is required regarding how, what and when a voltage violation is considered severe enough and/or about its mathematical formulation, this is developed in publication J1.

Demand Aggregation Mode

The aim of the DAM is to provide the HP the ability to respond when the demand aggregation need exists. This should be realized causing the minimum discomfort for the user. Therefore, as for the VEM, the HP operation is accommodated by altering the $\underline{E}_c$ and $\overline{E}_c$ bands as soon as the ΔP signal is received. The alteration of these bands is performed according to the following logic:

$$\begin{aligned} -\alpha \geq \Delta P \geq \alpha \ &\rightarrow \ \underline{E}_c = \underline{E}_c^{no}, \ \ \overline{E}_c = \overline{E}_c^{no} \\ -\alpha > \Delta P > \alpha \ &\rightarrow \ \underline{E}_c = \underline{E}_c^{da}, \ \ \overline{E}_c = \overline{E}_c^{da} \end{aligned} \tag{7.2}$$

where $\pm\alpha$ is the bandwidth defined to make the HP uninfluenced by ΔP. The reason to contemplate $\pm\alpha$ is the inexistent capability of HPs to regulate their power consumption and therefore to precisely track the ΔP without compromising the user comfort. $\underline{E}_c^{no}$ and $\overline{E}_c^{no}$ are the maximum and minimum energy bands, in p.u, for the NOM and $\underline{E}_c^{da}$ and $\overline{E}_c^{da}$ are the same but for the DAM. For further description of how $\underline{E}_c^{da}$ and $\overline{E}_c^{da}$ are dynamically altered refer to publication J2.

A demonstration of how these three modes cooperate together, to make the HP adapt to the given conditions, is illustrated in Fig. 7.2. Fig. 7.2a shows the ΔP signal received by the HP system. Fig. 7.2b shows the V_{min} profile during the time frame considered. According to the EN 50160 standard, the voltage at each point of the MV and LV systems should not vary further than $\pm$10%. However, based on practical experiences from DSOs a more conservative value is selected for this case, $\pm$6% (Vr=0.94 p.u.). During the first half hour $V_{min} > V_r$ and ΔP is equal to zero, therefore the HP system runs in NOM. In this context, $\underline{E}_c$ and $\overline{E}_c$ conserve the original settings. At hour t, ΔP becomes distinct to 0. Therefore, the HP controller switches to DAM to respond to the demand aggregation request. Notice how ΔP has a positive sign at the beginning. This means that the power consumption measured at the ST level is higher than the one defined by the energy commitment. In this context, the need for decreasing the aggregated demand of the LV grid makes the HP controller adjust $\overline{E}_c$ to trigger the advance disconnection of the appliance. As it is depicted in Fig. 7.2c.

Past $t + 1/2$ hour, even though ΔP remains still active, the HP controller switches to VEM due to a voltage violation. In consequence, the broadening of $\underline{E}_c$ allows E_S to drop to lower energy levels delaying its activation and in consequence avoiding the aggravation of this constraint. Past $2t + 1/2$ hour, the voltage gets restored and since ΔP is still active the HP controller switch from the VEM back to the DAM. Finally, as Fig. 7.2e depicts, the HP consumption of active and reactive power (P_{HP}, Q_{HP}) is successfully adapted to fulfil both technical and commercial requirements.

7.2.1.2 Plug-in Electric Vehicle Control

As it is described in chapter 3, the ability of the domestic charger to regulate the charging rate between 0 and its rated power (P_{PEV}^{rt}) is considered in this case. Therefore, the

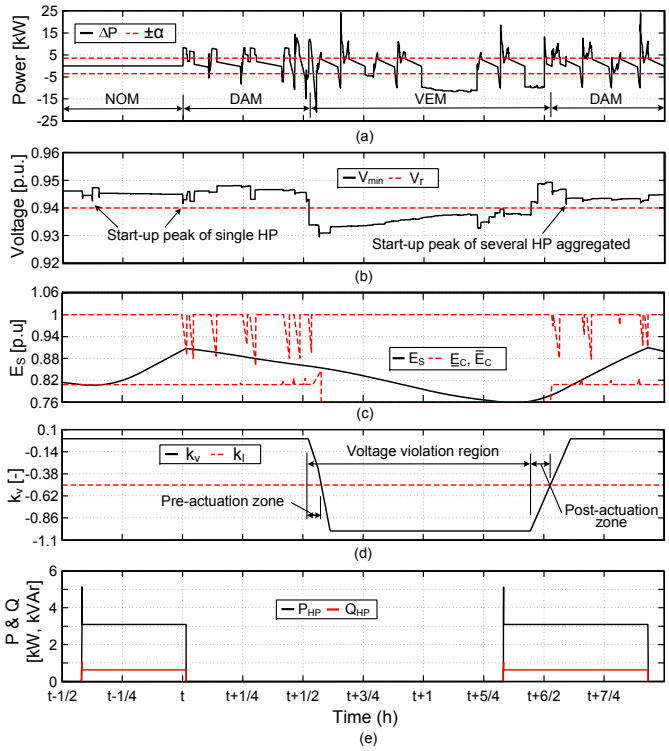

Figure 7.2: *HP control modes: (a) ΔP, (b) V_{min} and V_r, (c) k_v and k_l, (d) E_S, $\underline{E}_c$ and $\overline{E}_c$, (e) P_{HP} and Q_{HP} pattern.*

power drawn by the vehicle battery (P_{PEV}) is calculated as:

$$P_{PEV} = \eta_c \cdot \int S_{ch} \cdot dt; \quad 0 \leq P_{PEV} \leq P_{PEV}^{rt} \tag{7.3}$$

where η_c is the charger efficiency. S_{ch} represents the charging capability imposed to an specific PEV in a SS. Therefore, according to a criterion explained in the next section, the SSC coordinates the charging process of the PEVs under its domain. Finally, the UC is only responsible for ensuring that the SOC remains within the predefined limits.

7.2.2 Subsystem Control

It is defined as the layer of the control structure which is placed at the distribution feeder level. It monitors a number of households (n_h) and according to its needs it acts

over the HPs and PEVs under its domain. Since its main obligations are extensively described in J1, a summary of those is given here:

- *Measurement collection and processing*: Among them, voltage at the POC of each household (V_{poc}^{H}), the SOC of each plugged-in vehicle (SOC_{PEV}) and the E_S on each HP system.
- *Calculation of the minimum voltage in the SS (V_{min}^{SS}).* V_{min}^{SS} is afterwards dispatched to every HP system to make them shift to VEM when a violation occurs.
- *Prioritize plugged-in PEVs - Calculation and Dispatch of S_{ch}*: The SSC is constantly monitoring the available PEVs in the controlled area and their SOC too. Based on their SOC, it sorts them in an ascending manner. Then, PEVs with lower SOC are prioritized in terms of charging capacity with respect to the ones with higher SOC. This is done by assigning different amplitude values to the S_{ch} variables dispatched to the plugged-in PEVs. The S_{ch} variable received by a specific PEV (S_{ch}^{PEVi}) is calculated as:

$$S_{ch}^{PEV_i} = C_L \cdot A_p(i) \cdot x + (x-1);\ x \in [0,1];\ i = 1...n_{pev} \tag{7.4}$$

where n_{pev} is the number of available PEVs in the SS, A_p is the vector holding the different charging amplitudes and x is the binary variable defining if any voltage violation exists in the SS. When a voltage violation occurs x is equal to 0 making all PEVs reduce their charging rate in the same way and at the same time. So, the PEV with lowest SOC is assigned with the highest value of A_p making its S_{ch} the

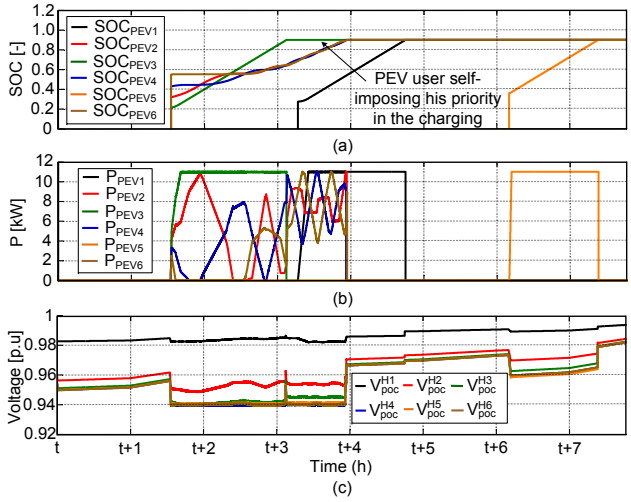

Figure 7.3: *SSC Performance: (a) SOC, (b) P_{PEVi} and (c) V_{poc}^{H}.*

highest too. C_L is the limitation variable received from the DGC to influence the charging process of the PEVs as it will be explained in the next section.
Fig. 7.3 shows an example of how the SSC operates regarding the coordination of the PEVs under its domain. For this time, let us imagine that a specific SSC, in charge of a feeble part of a LV grid, is not influenced by the DGC ($C_L = 1$). As it has been stated the SSC is constantly aware of the number of PEVs connected in the SS and their SOC. Fig. 7.3a shows the SOC of the PEVs when they arrive home. Between the hours $t+1$ and $t+2$ four PEVs arrive and plug-in at the same moment but in different locations and with different SOCs. Fig. 7.3b shows the charging rate of each PEV. PEV number 3 and 2 have the lowest SOC, so they are prioritized over 4 and 6. This is reflected for those PEVs in a higher A_p, S_{ch} and therefore charging rate. As they charge faster, at some point their SOC become higher than the rest, causing a shift on the sorting list. This is not the case for PEV3, because due to its driving requirements it self-imposes its priority over the rest. From the SSC perspective, this vehicle will hold the first position in the list until it is fully charged. Few minutes past t+3 the battery of PEV3 becomes full which allows the rest of PEVs to be charged at higher capacity. Later on, PEV1 arrives with a low SOC and plugs-in. As soon as the SSC senses it, the vehicle gets the first position in the sorting list. This makes the PEV1 to charge at the maximum capacity but subjected to the allowable grid conditions. As a consequence, the rest of the PEVs charging are forced to decrease. Between $t+6$ and $t+7$ hours, PEV5 arrives and plugs-in. Since the rest of the PEVs, connected in the SS, are already charged PEV5 is allowed to charge at maximum capacity. As result, the PEV charging is made in the fairest manner maintaining each of the V_{poc}^{H} is above V_r -see Fig. 7.3.c-.

- *Delivery of n_{pev} to the DGC*
- *Communication of ΔP to the HPs*: ΔP is used by the DGC in order to encourage a response from HPs under the need of materializing an energy commitment. This is done by delivering ΔP to the HPs in the LV grid via the different SSs.
- *Calculation and delivery to the DGC the average state of energy (SOE_{HP}^{avg}), average state of charge (SOC_{PEV}^{avg}) and total power consumption from HPs (P_{HP}^{SS}) and PEVs (P_{PEV}^{SS}) in the SS.*

7.2.3 Distribution Grid Control

Placed at the ST level, the DGC represents the central component of the hierarchical structure. It is responsible for monitoring and controlling the different SS in the LV grid. Depending on the condition of the LV grid and the set up forecast the DGC influences the operation of the HP and PEV loads via the C_L and ΔP signals delivered to each SS. Two of the tasks it focusses on are:

Equalization of the state of energy between the different SS

The purpose is to achieve an energy equilibrium among the different SS in the network in order to avoid the synchronization of the loads during high congestion periods. In practice, the DGC divides the total power transfer capability of the LV grid among the n SSs (n_{ss}) according to their average SOE ($SOE_{SS\#i}$) and the network condition. The $SOE_{SS\#i}$ of a SS is calculated based on its SOE_{HP}^{avg} and SOC_{PEV}^{avg}:

$$SOE_{SS\#i} = \left(\frac{n_{hp} \cdot SOE_{HP}^{avg} + n_{pev} \cdot SOC_{PEV}^{avg}}{n_{hp} + n_{pev}} \right)_i ; \quad i = 1...n_{ss} \tag{7.5}$$

where n_{hp} is the number of HP systems in the SS. So, when the maximum power transfer capability of the network is reached the only way to increase the power consumption capability of the SS with the lowest SOE is reducing the consumption capability from the rest. As the PEVs offer a more precise controllability, the regulation of this consumption capability is realized acting over their charging rate via the C_L variable.

Forecast of Flexibility and Participation in Regulation Market

In the Scandinavian context, NordPool Spot is the platform where most of the electricity is nowadays traded. This is performed via the two existing markets, the day-head (Elspot) and the intra-day (Elbas). To adjust the power imbalances originated after scheduling in the above markets, the TSOs employs an additional platform called the regulation power market (RPM). This is utilised to trade the up and down regulating power –normally referred to the generation side- with the purpose of anticipating excessive use of automatic reserves and to restoring their availability. In the Danish context, all bids can be submitted, adjusted, or removed in the RPM until 45 minutes before the operation hour. Then, these are collected and sorted in a list with increasing prices for up-regulation and decreasing prices for down-regulation. Depending on the potential congestions in the system, the TSO will activate the cheapest regulating power.

Although, the RPM represents an attractive trading environment for the demand side, the truth is that it is not active nowadays. In consequence, it is forced to pay the cost of the originated imbalances. Taking this into account, the RPM is considered an interesting environment to commerce the potential services that a hierarchical structure with these characteristics is able to offer in the future.

The provision of such a service requires an accurate performance of the participating technology. So, the stochastic nature of the residential demand makes forecasting of the system flexibility an important aspect for the DSO-A willing to utilise the aggregated response of residential loads in the RPM. The up and down regulation capability of a LV grid is normally represented by its maximum and minimum limits of aggregated power demand. Consequently, based on the energy stored in HP and PEV loads in the LV system a simple method is utilized to forecast, on an hourly basis, these limits. The

forecast made for a given hour defines the upper and lower flexibility bands ($\underline{FB}, \overline{FB}$), in kW, during the next hour. These two are in every case calculated according to:

$$\overline{FB} = \frac{k_{up}}{3600} \cdot (\bar{E}^{Tot}_{PEV} + \bar{E}^{Tot}_{HP} + \left[E^{Tot}_{HP}\right]_{\Delta t} + [E_{HL}]_{1h})$$
$$\underline{FB} = \frac{k_{down}}{3600} \cdot \left[E^{Tot}_{HP}\right]_{\Delta t} + [E_{HL}]_{1h} \tag{7.6}$$

where k_{up} and k_{down} are coefficients of precaution in order to make the forecast of the upper and lower bands more or less conservative. $\bar{E}^{Tot}_{PEV}$ is the maximum energy consumption from PEVs, in kWh, that could be requested during the forecasted hour. $\bar{E}^{Tot}_{HP}$ is the maximum energy consumption from HPs, in kWh, that could be requested during the forecasted hour. $\left[E^{Tot}_{HP}\right]_{\Delta t}$ is calculated based on historical records and it represents the average energy consumption from the HPs in the LV grid during the last period of Δt hours. Finally, since the forecast is one hour ahead, it becomes important to estimate the behaviour of the household during the hour in between. Therefore, based on historical records again the average energy consumption of the household load for the mentioned period ($[E_{HL}]_{1h}$) is estimated. For a more detailed information about the formulation of these refer to the manuscript J2.

Since the market closes 45 minutes before each operation hour, the energy bid (E_{bid}) in kWh has to be submitted 5 to 10 minutes before it closes. This means that the forecast of and has to be automatically performed few minutes before that in order to have the time to build E_{bid}. After the RPM clears, if the submitted E_{bid} is accepted the energy commitment (E_{ec}) will be sent to the DSO-A. Therefore, at the exact operating hour it is required to satisfy the steady state power demand related to E_{ec} (P_{ec}). So, taking into consideration the ramp time of the aggregated power demand from HPs and PEVs, the proposed control structure activates those few minutes in advance. This is described thoroughly in the manuscript J2.

In Fig. 7.4 an example of how the DGC performs under a specific energy commitment is depicted. Fig. 7.4a shows the aggregated response of the LV system to the P_{ec} signal. Few minutes after $t-1$ hour, the DGC forecasts $\underline{FB}, \overline{FB}$ limits for the time frame t to $t+1$. Minutes before the RPM closes it submits its E_{bid} based on what it has predicted. After the RPM has cleared, the bid is accepted and an up-regulation E_{ec} is received. Few minutes before t hour the DGC, via the different SS, activates the flexible demand in order to satisfy this energy commitment. Since, the control of the HP demand is less accurate than the one for the PEVs, they are first forced to respond as it is depicted in Fig. 7.4b. As the times passes, the average SOE from all the HP system in the LV network (SOE^{Tot}_{HP}) increases meaning that their HWSTs begin to get filled, see Fig. 7.4.c. As a consequence, after same time, the aggregated HP demand decays significantly and the PEVs have to take over in order to keep the power demand at the ST (P_{st}) to P_{ec}. This causes the average SOC of all the PEV in the system (SOC^{Tot}_{HP}) to increase. It is worth to notice how after responding to a given energy commitment the flexibility forecasted for the next hours is significantly reduced. The reason is the lack of

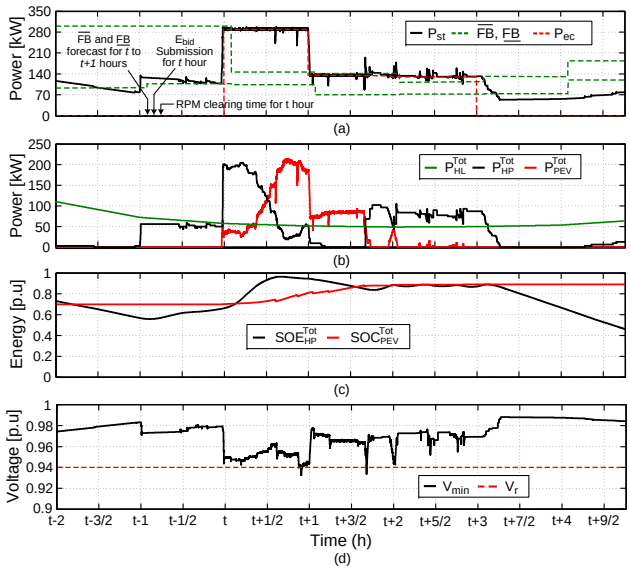

Figure 7.4: *Example of the RPM Participation: (a) P_{st}, $\underline{FB}$, $\overline{FB}$ and P_{ec}, (b) P_{HL}^{Tot}, P_{HP}^{Tot} and P_{PEV}^{Tot}, (c) SOE_{HP}^{Tot} and SOC_{PEV}^{Tot}, (d) V_{min} and V_r.*

storage capacity for the coming hours. Finally, Fig. 7.4d shows how the V_{min} of the LV network is importantly deviated due to the materialization of the energy commitment. However, the DGC keeps this successfully above its V_r limit.

7.3 Observations and Discussion

The results obtained in publications C3, J1 and J2 compare the performance of the proposed hierarchical supervisory DR structure for two days in different seasons of the year. In February, the power consumption of households in the LV network is high comparing with other months of the year. On the other hand, the low atmospheric temperatures given in winter induce those households to have a high thermal power demand too. This aspect combined with the low COP values, representative of unfavourable atmospheric conditions, forces the HP systems to operate frequently. As a result, their aggregated consumption acquires a considerable magnitude which takes up a large percentage of the power transfer capacity of this system. Furthermore, the existence of any coordination in the PEV charging process implies that the users in possession of PEVs tend to plug those as soon as they arrive home. The combination of these factors leads to a large concentration of power consumption during the peak moment of the day. As result, large and persistent voltage violations are originated during this time. In May

instead, since the thermal power demand of the household is much lower and a better atmospheric conditions makes the HPs operate less frequently. This substantially reduces their aggregated power consumption making the system capacity more available.

In publication C3 and J1, the hierarchical supervisory DR structure is oriented to avoid the system bottlenecks. Therefore, under its influence different favourable behaviours of the grid operation are achieved. First, the total HP demand is significantly reduced during the peak hours that coincide with the severest voltage deviation period. This power reduction is originated by the HPs in the SS where the voltage violation occurred, as they switch to VEM to delay their activation. Second, the PEV charging is completely avoided during this time frame and delayed to moments when the LV grid is less stressed -late evening and early morning-. Consequently, a considerable improvement of the minimum system voltage and a better load distribution along the day is obtained. In May instead, the system capacity is more available therefore HPs and PEVs are allowed to perform naturally since no violations constrains the power transfer in the LV system.

The potential benefits of using the DR mechanism for the RPM participation are assessed in publication J2. Here, it is demonstrated how a proper commercial strategy makes several things possible. First, shifting the flexible demand to off-peak hours allows DSO-A benefiting from the low market prices in those hours. Second, a reduction of the flexible demand during peak hours avoids technical congestions in the network while aiding the balancing of the system at the same time. Finally, the realization of this last aspect implies also an economical benefit due to the services provided to the system. However, in this context, there are also aspects that limit the response capability of a LV network. The most significant one is the existing technical limit which defines the maximum power transfer capability of the network. In this sense, there might be hours during the operating day that the forecasted $\underline{FB}$ and $\overline{FB}$ bands define a much higher up and down regulation capability of the LV network than what is actually possible. Since, $\underline{FB}$ and $\overline{FB}$ bands are forecasted based on the storage capability available in HPs and PEVs they do not contemplate any technical limitation. Therefore, the existence of these technical limits, in the case considered imposed by the violation of the voltage limits, will represent additional restrictions to the regulation capability that the LV systems might be able to offer in the future.

7.4 Summary

This chapter summarizes the hierarchical supervisory DR mechanism proposed in publications C3, J1 and J2 to enhance the dynamic operation and interoperability of the LV networks. Furthermore, by connecting the ST, feeder and consumer level controls it aims to serve as a platform to aggregate flexible demand in response to the provision of commercial services.

In a first place, the chapter discusses the existing methods for controlling the voltage

in LV grids. Later, it describes the proposed architecture incising in the control features of each of the layers composing it. In order to give a better understanding different examples of their individual operation performance are also illustrated.

Finally, the results obtained in the referred publications are evaluated and the benefits of such a solution are defined. It is concluded that with this alternative two major advantages can be derived. On the one hand, in congested periods the voltage levels of the LV network can be maintained within acceptable limits due to the the better distribution its aggregated demand during the day. On the other hand, by participating in the RPM the DSO-A can obtain cheaper energy providing UR in the early morning and afternoon hours and at the same time make a profit by providing DR during peak periods.

Chapter VIII

Conclusions

This chapter presents the conclusions deposed during the development of the PhD studies. Furthermore, it summarizes what are the main contributions of this scientific work. Since new potential research lines have been opened, the perspectives for future work are also described in here.

8.1 Summary

As it is described in the abstract, four areas are covered in this thesis: i) modelling of active loads and the thermal consumption and driving habits from residential users, ii) definition and quantification of residential flexible demand, iii) assessment of the impact produced in LV networks by the electrification of heating and transportation systems and iiii) the control of DR in LV grids. The first three topics represent the foundation required to understand the context of the problem. Based on them, the strategy to control the DR in LV grids has posteriorly designed and implemented. Particular attention has been paid to the activation of the flexible residential demand to undertake different technical and commercial purposes.

The modelling phase and its posterior validation have underlined several things about the loads considered. The thermal power demand of the household, which certainly varies along the year, plays an important role in the power consumption behaviour of thermostatic loads. In the case of HP systems, the COP is an additional factor influencing this pattern. Under unfavourable atmospheric conditions -high thermal demand and low COP- a frequent and sometimes even constant operation of these loads has been observed. As a consequence, a significant reduction in the flexibility that these loads are able to offer can be expected. The use of AE as a potential controllable load shows a lot of advantages for the power regulation. Even though, they present fast load dynamics some of their limitations cannot be neglected neither. Low load operation points have

to be avoided due to the degradation of the hydrogen. Moreover, after being on stand-by mode the AE might be limited to perform certain load changes due to the loss of temperature of the electrolyte. Regarding the EV load, no matter if the charging -PEV- or discharging -V2G- role is considered, their load behaviour and therefore their impact in the network depends on the DP carried out by its user along the day. All these loads show a big potential in what DR concerns. Indeed there is big optimism within the scientific community for demonstrating their capabilities. However, when performing an analysis of such a characteristics there are other aspects that have to be studied a part from the electrical ones.

Consequently, the analysis performed about the thermal consumption and driving behaviour of Danish residential users highlighted the diversity and randomness of these habits. Furthermore, the method proposed to generate profiles to realistically simulate the behaviour from users in possession of EWH, HP or PEV loads is demonstrated to be appropriate approach since it respects the pattern imposed by the original data.

Determining the flexibility from users in possession of such a loads is another key topic addressed in this thesis. Therefore, a methodology is proposed to identify and probabilistically quantify the potential flexibility from residential users. Its validation demonstrate that certain loads, such as the HP systems, are more likely to offer flexibility during months between seasons. The reason is that extreme the atmospheric temperatures and thermal consumption from the households makes these loads operate constantly or not operate at all.

The mobilization of flexible residential demand relies on the fact that large numbers of loads will be gradually accommodated in the LV systems. The impact assessment realized on a Danish LV system highlights the poor hosting capability of these systems in what the accommodation of HP and PEV loads concerns. Furthermore, it cannot be dismissed that even for low load penetration levels certain load distributions might lead the network to react in a non-expected manner. Parts which are currently considered strong might in a future be hardly exposed to technical constrains and vice-versa.

In the last stage of this research work, the control of DR in LV networks has been addressed as a potential solution for the previously mentioned challenges. As an alternative, a hierarchical supervisory mechanism is proposed to control the DR of LV networks. This solution aims i) to enhance the dynamic operation of the LV networks and ii) to serve as a platform for future operators to mobilize flexible demand in the network with commercial purposes. The results illustrate that by providing up and down regulation (UR, DR) services in the RPM, it is possible: i) to shift flexible demand to off-peak hours benefiting from the cheap energy prices characteristic of this periods, ii) to reduce the flexible demand during the peak hour benefiting from the high prices and aiding the system balance at the same time. However, it cannot be neglected that the UR and DR capability of the LV network might be significantly limited due to the existing technical constrains.

8.2 Thesis Contributions

Even though, the DR topic has captured lots of attention and the number of research publications has recently increased, the work comprised in this thesis appends several contributions:

- Detailed dynamic models of domestic and non-domestic loads developed in different software platforms.
  - Thermostatic loads (EWH and HPs).
  - An alkaline electrolyzer for large scale applications.
  - An EV load considering different approaches (PEV and V2G).

  All of those models include thermal, mechanical and chemical features which are not normally considered in the traditional way of modelling the power system.
- Different device control strategies are proposed to encourage the response from the loads considered. The design takes into consideration their specific nature and characteristics.
- A simple methodology to generate profiles which simulate the thermal and mobility requirements from users in possession of EWHs, HPs and PEVs. This approach is based on a statistical analysis of domestic hot water, space heating and driving habits from Danish residential users.
- A methodology to define and probabilistically quantify the potential flexibility from residential demand. Even though the procedure is applicable for most of the residential loads which offer flexibility, this work has focus on the HP systems and their capabilities in this matter.
- A methodology to investigate the impact generated in the LV networks by the electrification of the heating and transportation systems. The purpose of this approach is to define the current capacity and hosting capability of those in relation to the accommodation of new load. Moreover, it also underlines the nature and the location of potential bottlenecks that these systems might face in the future.
- A technical evaluation of the system capacity and dynamical performance of the LV grids is realized based on dynamic models of the active loads developed.
- A hierarchical structure for controlling the DR in LV distribution networks. In a first place, the design aims to control the operation of HP and PEV systems in order to enhance the dynamic operation of LV networks. The control strategy is implemented on real time basis in order to ensure the best performance of the whole system

- New control features are implemented in the previous structure in order to activate and aggregate the response of the flexible loads in the LV grid. Additionally, the commercial benefits of applying such a strategy are also contemplated using the RPM as a reference.

8.3 Perspectives and Future Work

This research work has addressed numerous aspects of the interaction between the power system and the gas, heating and transportation systems. However, in the development process new research lines have appeared which indeed would be interesting to be addressed in future work. Those, together with some aspects that need further analysis are summarized below.

- Even though, it might not represent an important challenge for the operation of the Danish LV networks, the unbalance scenario should be studied. Especially, to determine what is the impact originated by different load penetrations in the individual phases.
- The power quality is one of the most challenging aspects concerning the accommodation of large numbers of flexible loads in these systems. This is especially relevant for the voltage flicker which might be originated as a consequence of the start-up current synchronization of HPs.
- From a market perspective, the optimal scheduling of the flexible loads is an additional solution to avoid the reinforcement of the power infrastructure. This solution should be assessed making a technical and economical comparison with the DR control mechanism proposed in order to see what the real benefits are.
- In order to prove the feasibility of the proposed DR control mechanism, the advantages and disadvantages of its implementation should be tested in other market platforms such as the day-ahead or intraday market. also be assessed .
- The power balancing capabilities of AE have been briefly addressed in this thesis. It could be interesting to demonstrate the real potential of this technology with real system models. Particularly, in topics such as the voltage regulation of MV networks or the local power management.

Bibliography

[1] European Commission, "European 20-20-20 Targets," [Online]. Available: http://ec.europa.eu/europe2020/index_en.htm, 2013.

[2] Eurostat News, "Share of Renewable Energy up to 14.1% of Energy Consumption in the EU28 in 2012," Release 37/2014, [Online]. Available: http://epp.eurostat.ec.europa.eu, Mar. 2014.

[3] The European Wind Energy Association, "Wind in Power," Technical Report, Feb. 2014.

[4] J. Vestergaard, L. Brandstrup, and R. D. Goddard, "A brief history of the wind turbine industries in Denmark and the United States," in *Academy of international business (Southeast USA Chapter) Conference proceedings*, 2004, pp. 322–327.

[5] Danish Ministry of Climate, Energy and Building, "Accelerating Green Energy Towards 2020 - The Danish Energy Agreement of March 2012," Mar. 2012.

[6] Global Wind Energy Council, "Global Wind Statistics 2013," Technical Report, Feb. 2014.

[7] "Wind Power Share in Denmark in 2013," [Online]. Available: http://www.energinet.dk/EN/El/Nyheder/Sider/2013-var-et-rekordaar-for-dansk-vindkraft.aspx, 2013.

[8] "Photovoltaic Power Installed in Denmark by mid-2014," [Online]. Available: http://energinet.dk/DA/El/Engrosmarked/Udtraek-af-markedsdata/Sider/Statistik.aspx, 2014.

[9] Energinet.dk, "Energinet.dk's Analysis Assumptions 2013-2035," Technical Report, Apr. 2013.

[10] Danish Ministry of Climate, Energy and Building, "Smart Grid Strategy - The Intelligent Energy System of the Future," May 2013.

[11] J. R. Kristoffersen, "The horns rev wind farm and the operational experience with the wind farm main controller," *Revue E-Société Royale Belge des électriciens*, vol. 122, no. 2, p. 26, 2006.

[12] Nordic Energy Regulators (NordReg), "Nordic Market Report 2013 - Development in the Nordic Electricity Market," Technical Report Release 6/2013, Jun. 2013.

[13] Danish Energy Agency, "Distributed Generation in Denmark," [Online]. Available: http://www.ens.dk/en, 2014.

[14] Sorknæs, P.; Mæng, H.; Weiss, T.; Andersen, A.N., "Overview of the Danish Power system and RES Integration - Store Project," Technical Report, Jul. 2013.

[15] Energinet.dk, "Submarine cable to Norway - Skagerrak 4," [Online]. Available: http://energinet.dk, 2014.

[16] Energinet.dk, "Cable to the Netherlands - COBRAcable," [Online]. Available: https://www.energinet.dk, 2014.

[17] Energinet.dk, "System Plan 2013 - Energinet.dk," Technical Report, 2013.

[18] Danish Energy Association, "Danish Electricity Supply'07," Statistical Survey, Apr. 2008.

[19] Danish Energy Agency and Danish Boar of District Heating (DBDH), "District Heating – Danish and Chinese experiences," Technical Report, 2012.

[20] Danish Energy Agency, "Energy Statistics 2012," Statistical Survey, Feb. 2014.

[21] Energinet.dk, "Natural Gas Transmission System," [Online]. Available: https://www.energinet.dk/EN/GAS/, 2014.

[22] Energinet.dk, "Natural Gas Transmission and Distribution System," [Online]. Available: http://www.energinet.dk/EN/GAS/, 2014.

[23] Energinet.dk, "Exports and Consumption of Natural Gas in 2012," [Online]. Available: https://www.energinet.dk/EN/GAS/, 2014.

[24] Energinet.dk, "Natural Gas and Biogas Consumption Trends," [Online]. Available: https://https://www.energinet.dk/EN/GAS/, 2014.

[25] Energinet.dk, "Hydrogen Injection in the Natural Gas Network," [Online]. Available: https://https://www.energinet.dk/EN/GAS/, 2014.

[26] Ministry of Transport and Statistics Denmark, "Key Figures for Transport 2011," Statistical Survey, Jun. 2012.

[27] North Sea Region Electric Mobility Network, e-mobility NSR, "Danish Experiences in Setting up Charging Infrastructure for Electric Vehicles with special Focus on battery Swap Stations," Mar. 2013.

[28] NordPool Spot, "The Power of Transparency - Annual Report 2012," Technical Report, Apr. 2013.

[29] NordPool Spot, "Trade at the Nordic Sport Market (Nord Pool Spot AS)- The World's First International Spot Power Exchange," Technical Report, Apr. 2004.

[30] Energinet.dk, "Strategy Plan 2010 - Energinet.dk," Technical Report, 2010.

[31] Andersen, F.M.; Jensen, S.G.; Larsen, H.V.; Meibom, P.; Ravn, H.; Skytte, K.; Togeby, M., "Analyses of Demand Response in Denmark," Risø-R-1565(EN), Risø National Laboratory, Oct. 2006.

[32] Copenhagen Cleantech Cluster, "Denmark: A European Smart Grid Hub - Asset Mapping of Smart Grid Competencies in Denmark," Technical Report, 2011.

[33] Danish Energy Association and Energinet.dk, "Smart Grid in Denmark," Technical Report, 2010.

[34] Danskenergi and Energinet.dk, "Smart Grid in Denmark," Technical Report, 2008.

[35] J. R. Pillai, P. Thogersen, J. Moller, and B. Bak-Jensen, "Integration of electric vehicles in low voltage danish distribution grids," in *Power and Energy Society General Meeting, 2012 IEEE.* IEEE, 2012, pp. 1–8.

[36] International Electrotechnical Commission (IEC), "Electrical Energy Storage – White Paper," Technical Report, 2011.

[37] Mathiesen, B.V; Lund. H; Karlsson, K.;, "The IDA Climate Plan 2050: Technical energy system analysis, effects on fuel consumption and emissions of greenhouse gases, socio-economic consequences, commercial potentials, employment effects, and health costs," Background Report, The Danish Society of Engineers (IDA), Aug. 2009.

[38] D. G. Berkowitz and C. W. Gellings, "Glossary of Terms Related to Load Management, Parts I and II," *Power Engineering Review, IEEE*, vol. PER-5, no. 9, pp. 35–35, Sept 1985.

[39] I. Lampropoulos, W. Kling, P. Ribeiro, and J. van den Berg, "History of demand side management and classification of demand response control schemes," in *Power and Energy Society General Meeting (PES), 2013 IEEE*, July 2013, pp. 1–5.

[40] A. Chuang and C. Gellings, "Demand-side integration in a restructured electric power industry," in *CIGRE session*, 2008, pp. C6–105.

[41] V. Balijepalli, V. Pradhan, S. Khaparde, and R. M. Shereef, "Review of demand response under smart grid paradigm," in *Innovative Smart Grid Technologies - India (ISGT India), 2011 IEEE PES*, Dec 2011, pp. 236–243.

[42] M. Eaton, "Automatic Operation of Electric Boilers," *American Institute of Electrical Engineers, Transactions of the*, vol. 66, no. 1, pp. 1061–1069, Jan 1947.

[43] R. Delgado, "Demand-side management alternatives," *Proceedings of the IEEE*, vol. 73, no. 10, pp. 1471–1488, Oct 1985.

[44] D. S. Loughran and J. Kulick, "Demand-side management and energy efficiency in the United States," *The Energy Journal*, pp. 19–43, 2004.

[45] Sorknæs, P.; Mæng, H.; Weiss, T.; Andersen, A.N., "Overview of Current Status and Future Development Scenarios of the Electricity System in Denmark – Allowing Integration of Large Quantities of Wind Power," Technical Report, EMD International A/S and Helmut Schmidt University, stoRE project, Jul. 2013.

[46] T. Pedersen, P. Andersen, K. M. Nielsen, H. Starmose, and P. D. Pedersen, "Using heat pump energy storages in the power grid," in *Control Applications (CCA), 2011 IEEE International Conference on*, Sept 2011, pp. 1106–1111.

[47] M. Akmal, D. Flynn, J. Kennedy, and B. Fox, "Flexible heat load for managing wind variability in the Irish power system," in *Universities Power Engineering Conference (UPEC), 2009 Proceedings of the 44th International*, Sept 2009, pp. 1–5.

[48] G. Papaefthymiou, B. Hasche, and C. Nabe, "Potential of Heat Pumps for Demand Side Management and Wind Power Integration in the German Electricity Market," *Sustainable Energy, IEEE Transactions on*, vol. 3, no. 4, pp. 636–642, Oct 2012.

[49] T. Masuta, A. Yokoyama, and Y. Tada, "System frequency control by Heat Pump Water Heaters (HPWHs) on customer side based on statistical HPWH model in power system with a large penetration of renewable energy sources," in *Power System Technology (POWERCON), 2010 International Conference on*, Oct 2010, pp. 1–7.

[50] T. Masuta and A. Yokoyama, "Supplementary Load Frequency Control by Use of a Number of Both Electric Vehicles and Heat Pump Water Heaters," *Smart Grid, IEEE Transactions on*, vol. 3, no. 3, pp. 1253–1262, Sept 2012.

[51] S. Kawachi, J. Baba, H. Hagiwara, E. Shimoda, S. Numata, E. Masada, and T. Nitta, "Energy capacity reduction of energy storage system in microgrid by use of heat pump:

Characteristic study by use of actual machine," in *Power Electronics and Motion Control Conference (EPE/PEMC), 2010 14th International*, Sept 2010, pp. T11–52–T11–58.

[52] S. Pourmousavi, S. Patrick, and M. Nehrir, "Real-Time Demand Response Through Aggregate Electric Water Heaters for Load Shifting and Balancing Wind Generation," *Smart Grid, IEEE Transactions on*, vol. 5, no. 2, pp. 769–778, March 2014.

[53] J. Kondoh, N. Lu, and D. Hammerstrom, "An Evaluation of the Water Heater Load Potential for Providing Regulation Service," *Power Systems, IEEE Transactions on*, vol. 26, no. 3, pp. 1309–1316, Aug 2011.

[54] E. Vrettos and G. Andersson, "Combined Load Frequency Control and active distribution network management with Thermostatically Controlled Loads," in *Smart Grid Communications (SmartGridComm), 2013 IEEE International Conference on*, Oct 2013, pp. 247–252.

[55] S. Koch, F. S. Barcenas, and G. Andersson, "Using controllable thermal household appliances for wind forecast error reduction," in *IFAC Conference on Control Methodologies and Technology for Energy Efficiency*. Citeseer, 2010.

[56] F. Amoroso and G. Cappuccino, "Potentiality of variable-rate PEVs charging strategies for smart grids," in *PowerTech, 2011 IEEE Trondheim*, June 2011, pp. 1–6.

[57] M. Takagi, K. Yamaji, and H. Yamamoto, "Power system stabilization by charging power management of Plug-in Hybrid Electric Vehicles with LFC signal," in *Vehicle Power and Propulsion Conference, 2009. VPPC '09. IEEE*, Sept 2009, pp. 822–826.

[58] M. D. Galus, S. Koch, and G. Andersson, "Provision of Load Frequency Control by PHEVs, Controllable Loads, and a Cogeneration Unit," *Industrial Electronics, IEEE Transactions on*, vol. 58, no. 10, pp. 4568–4582, Oct 2011.

[59] T. Masuta and A. Yokoyama, "Supplementary Load Frequency Control by Use of a Number of Both Electric Vehicles and Heat Pump Water Heaters," *Smart Grid, IEEE Transactions on*, vol. 3, no. 3, pp. 1253–1262, Sept 2012.

[60] A. Ulbig, M. D. Galus, S. Chatzivasileiadis, and G. Andersson, "General frequency control with aggregated control reserve capacity from time-varying sources: The case of PHEVs," in *Bulk Power System Dynamics and Control (iREP) - VIII (iREP), 2010 iREP Symposium*, Aug 2010, pp. 1–14.

[61] M. Gonzalez Vaya and G. Andersson, "Centralized and decentralized approaches to smart charging of plug-in Vehicles," in *Power and Energy Society General Meeting, 2012 IEEE*, July 2012, pp. 1–8.

[62] M. Gonzalez Vaya and G. Andersson, "Integrating renewable energy forecast uncertainty in smart-charging approaches for plug-in electric vehicles," in *PowerTech (POWERTECH), 2013 IEEE Grenoble*, June 2013, pp. 1–6.

[63] M. D. Galus, R. La Fauci, and G. Andersson, "Investigating PHEV wind balancing capabilities using heuristics and model predictive control," in *Power and Energy Society General Meeting, 2010 IEEE*, July 2010, pp. 1–8.

[64] C. Zhou, K. Qian, M. Allan, and W. Zhou, "Modeling of the Cost of EV Battery Wear Due to V2G Application in Power Systems," *Energy Conversion, IEEE Transactions on*, vol. 26, no. 4, pp. 1041–1050, Dec 2011.

[65] Y. Huang, J. yong Liu, C. xin Li, and W. Gong, "Considering the Electric Vehicles in the Load Frequency Control," in *Power and Energy Engineering Conference (APPEEC), 2012 Asia-Pacific*, March 2012, pp. 1–4.

[66] J. Pillai and B. Bak-Jensen, "Integration of Vehicle-to-Grid in the Western Danish Power System," *Sustainable Energy, IEEE Transactions on*, vol. 2, no. 1, pp. 12–19, Jan 2011.

[67] J. Pillai and B. Bak-Jensen, "Vehicle-to-grid systems for frequency regulation in an Islanded Danish distribution network," in *Vehicle Power and Propulsion Conference (VPPC), 2010 IEEE*, Sept 2010, pp. 1–6.

[68] J. Pillai and B. Bak-Jensen, "Vehicle-to-Grid for islanded power system operation in Bornholm," in *Power and Energy Society General Meeting, 2010 IEEE*, July 2010, pp. 1–8.

[69] Y. Mu, J. Wu, J. Ekanayake, N. Jenkins, and H. Jia, "Primary Frequency Response From Electric Vehicles in the Great Britain Power System," *Smart Grid, IEEE Transactions on*, vol. 4, no. 2, pp. 1142–1150, June 2013.

[70] Z. Wang and S. Wang, "Grid Power Peak Shaving and Valley Filling Using Vehicle-to-Grid Systems," *Power Delivery, IEEE Transactions on*, vol. 28, no. 3, pp. 1822–1829, July 2013.

[71] M. Singh, K. Thirugnanam, S. Swami, P. Kumar, and I. Kar, "Coordination of Electric Vehicles in charging stations connected at different nodes of a distribution substation," in *India Conference (INDICON), 2012 Annual IEEE*, Dec 2012, pp. 1260–1265.

[72] L. Valverde, D. Ali, M. Abdel-Wahab, J. Guerra, and D. Hogg, "A technical evaluation of Wind-Hydrogen (WH) demonstration projects in Europe," in *Power Engineering, Energy and Electrical Drives (POWERENG), 2013 Fourth International Conference on*, May 2013, pp. 1098–1104.

[73] K. Agbossou, M. Kolhe, J. Hamelin, and T. Bose, "Performance of a stand-alone renewable energy system based on energy storage as hydrogen," *Energy Conversion, IEEE Transactions on*, vol. 19, no. 3, pp. 633–640, Sept 2004.

[74] K. Koiwa, A. Umemura, R. Takahashi, and J. Tamura, "Stand-alone hydrogen production system composed of wind generators and electrolyzer," in *Industrial Electronics Society, IECON 2013 - 39th Annual Conference of the IEEE*, Nov 2013, pp. 1873–1879.

[75] T. Maeda, H. Ito, Y. Hasegawa, Z. Zhou, and M. Ishida, "Study on control method of the stand-alone direct-coupling photovoltaic-water electrolyzer," *International Journal of Hydrogen Energy*, vol. 37, no. 6, pp. 4819–4828, 2012.

[76] I. Kyriakidis, P. Braun, and S. Chaudhary, "Effect of energy storage in increasing the penetration of RES in the remote island of Agios Efstratios," in *Power Electronics for Distributed Generation Systems (PEDG), 2012 3rd IEEE International Symposium on*, June 2012, pp. 814–819.

[77] Ø. Ulleberg, T. Nakken, and A. Ete, "The wind/hydrogen demonstration system at Utsira in Norway: Evaluation of system performance using operational data and updated hydrogen energy system modeling tools," *International Journal of Hydrogen Energy*, vol. 35, no. 5, pp. 1841–1852, 2010.

[78] Ulleberg, Ø., Mørkved, A., "Renewable Energy And Hydrogen System Concepts For Remote Communities In The West Nordic Region: The Nólsoy Case Study," Technical Report, IFE/KR/E-2008/002, IFE, Kjeller, 2008.

[79] L. Ramirez-Elizondo, G. Paap, and N. Woudstra, "The application of a fuel cell-electrolyzer arrangement as a power balancing set-up in autonomous renewable energy systems," in *Power Symposium, 2008. NAPS '08. 40th North American*, Sept 2008, pp. 1–8.

[80] G. Yu and N. Okada, "Design and Performance Evaluation of a Wind-Hydrogen Autonomous System Associated to a Rechargeable Battery," *Journal of Power and Energy Systems*, vol. 6, no. 3, pp. 353–359, 2012.

[81] R. Takahashi, H. Kinoshita, T. Murata, J. Tamura, M. Sugimasa, A. Komura, M. Futami, M. Ichinose, and K. Ide, "A cooperative control method for output power smoothing and hydrogen production by using variable speed wind generator," in *Power Electronics and Motion Control Conference, 2008. EPE-PEMC 2008. 13th*, Sept 2008, pp. 2337–2342.

[82] S. M. Muyeen, R. Takahashi, T. Murata, and J. Tamura, "Integration of hydrogen generator into wind farm interconnected HVDC system," in *PowerTech, 2009 IEEE Bucharest*, June 2009, pp. 1–7.

[83] R. Takahashi, H. Kinoshita, T. Murata, J. Tamura, M. Sugimasa, A. Komura, M. Futami, M. Ichinose, and K. Ide, "Output Power Smoothing and Hydrogen Production by Using Variable Speed Wind Generators," *Industrial Electronics, IEEE Transactions on*, vol. 57, no. 2, pp. 485–493, Feb 2010.

[84] J. Ugartemendia, X. Ostolaza, V. Moreno, J. Molina, and I. Zubia, "Wind generation stabilization of fixed speed wind turbine farms with hydrogen buffer," in *11th. Spanish-Portuguese Conference on Electrical Engineering (11CHLIE)*, 2009, pp. 1–5.

[85] D. Recalde Melo and L.-R. Chang-Chien, "Synergistic Control Between Hydrogen Storage System and Offshore Wind Farm for Grid Operation," *Sustainable Energy, IEEE Transactions on*, vol. 5, no. 1, pp. 18–27, Jan 2014.

[86] M. Kiaee, A. Cruden, D. Infield, Y. Ma, and T. Douglas, "The impact on the electrical grid of hydrogen production from alkaline electrolysers," in *Universities Power Engineering Conference (UPEC), 2010 45th International*, Aug 2010, pp. 1–6.

[87] H. Saboori, M. Mohammadi, and R. Taghe, "Composite Generation and Transmission Expansion Planning Considering the Impact of Wind Power Penetration," in *Power and Energy Engineering Conference (APPEEC), 2011 Asia-Pacific*, March 2011, pp. 1–6.

[88] M. Korpås and T. Gjengedal, "Opportunities for Hydrogen Storage in connection with Stochastic Distributed Generation," in *Probabilistic Methods Applied to Power Systems, 2006. PMAPS 2006. International Conference on*, June 2006, pp. 1–8.

[89] M. Shaad, A. Momeni, C. Diduch, M. Kaye, and L. Chang, "Parameter identification of thermal models for domestic electric water heaters in a direct load control program," in *Electrical Computer Engineering (CCECE), 2012 25th IEEE Canadian Conference on*, April 2012, pp. 1–5.

[90] A. Sepulveda, L. Paull, W. Morsi, H. Li, C. Diduch, and L. Chang, "A novel demand side management program using water heaters and particle swarm optimization," in *Electric Power and Energy Conference (EPEC), 2010 IEEE*, Aug 2010, pp. 1–5.

[91] J. Khoury, R. Mbayed, G. Salloum, and E. Monmasson, "Modeling of a hybrid domestic solar/electric water heater for hardware implementation," in *Mediterranean Electrotechnical Conference (MELECON), 2014 17th IEEE*, April 2014, pp. 560–565.

[92] R. Diao, S. Lu, M. Elizondo, E. Mayhorn, Y. Zhang, and N. Samaan, "Electric water heater modeling and control strategies for demand response," in *Power and Energy Society General Meeting, 2012 IEEE*, July 2012, pp. 1–8.

[93] J. Kondoh, N. Lu, and D. Hammerstrom, "An Evaluation of the Water Heater Load Potential for Providing Regulation Service," *Power Systems, IEEE Transactions on*, vol. 26, no. 3, pp. 1309–1316, Aug 2011.

[94] F. Sossan, A. Kosek, S. Martinenas, M. Marinelli, and H. Bindner, "Scheduling of domestic water heater power demand for maximizing PV self-consumption using model predictive control," in *Innovative Smart Grid Technologies Europe (ISGT EUROPE), 2013 4th IEEE/PES*, Oct 2013, pp. 1–5.

[95] E. Vrettos, S. Koch, and G. Andersson, "Load frequency control by aggregations of thermally stratified electric water heaters," in *Innovative Smart Grid Technologies (ISGT Europe), 2012 3rd IEEE PES International Conference and Exhibition on*, Oct 2012, pp. 1–8.

[96] P. Dolan, M. Nehrir, and V. Gerez, "Development of a Monte Carlo based aggregate model for residential electric water heater loads," *Electric Power Systems Research*, vol. 36, no. 1, pp. 29–35, 1996.

[97] N. Lu and D. Chassin, "A state queueing model of thermostatically controlled appliances," in *Power Systems Conference and Exposition, 2004. IEEE PES*, Oct 2004, pp. 59 vol.1–.

[98] N. Lu, D. Chassin, and S. Widergren, "Modeling uncertainties in aggregated thermostatically controlled loads using a state queueing model," *Power Systems, IEEE Transactions on*, vol. 20, no. 2, pp. 725–733, May 2005.

[99] F. Tahersima, J. Stoustrup, H. Rasmussen, and S. Meybodi, "Economic COP optimization of a heat pump with hierarchical model predictive control," in *Decision and Control (CDC), 2012 IEEE 51st Annual Conference on*, Dec 2012, pp. 7583–7588.

[100] F. Tahersima, J. Stoustrup, S. Meybodi, and H. Rasmussen, "Contribution of domestic heating systems to smart grid control," in *Decision and Control and European Control Conference (CDC-ECC), 2011 50th IEEE Conference on*, Dec 2011, pp. 3677–3681.

[101] Z. Yang, G. Pedersen, L. Larsen, and H. Thybo, "Modeling and Control of Indoor Climate Using a Heat Pump Based Floor Heating System," in *Industrial Electronics Society, 2007. IECON 2007. 33rd Annual Conference of the IEEE*, Nov 2007, pp. 2985–2990.

[102] P. Andersen, T. Pedersen, and K. Nielsen, "Observer based model identification of heat pumps in a smart grid," in *Control Applications (CCA), 2012 IEEE International Conference on*, Oct 2012, pp. 569–574.

[103] R. Halvgaard, N. Poulsen, H. Madsen, and J. Jorgensen, "Economic Model Predictive Control for building climate control in a Smart Grid," in *Innovative Smart Grid Technologies (ISGT), 2012 IEEE PES*, Jan 2012, pp. 1–6.

[104] C. Verhelst, F. Logist, J. Van Impe, and L. Helsen, "Study of the optimal control problem formulation for modulating air-to-water heat pumps connected to a residential floor heating system," *Energy and Buildings*, vol. 45, pp. 43–53, 2012.

[105] F. Tahersima, J. Stoustrup, and H. Rasmussen, "Optimal power consumption in a central heating system with geothermal heat pump," in *The 18th World Congress of the International Federation of Automatic Control (IFAC 2011)*, 2011.

[106] M. Brunner, S. Tenbohlen, and M. Braun, "Heat pumps as important contributors to local demand-side management," in *PowerTech (POWERTECH), 2013 IEEE Grenoble*, June 2013, pp. 1–7.

[107] T. Masuta, A. Yokoyama, and Y. Tada, "Modeling of a number of Heat Pump Water Heaters as control equipment for load frequency control in power systems," in *PowerTech, 2011 IEEE Trondheim*, June 2011, pp. 1–7.

[108] A. Mufaris and J. Baba, "Local control of heat pump water heaters for voltage control with high penetration of residential PV systems," in *Industrial and Information Systems (ICIIS), 2013 8th IEEE International Conference on*, Dec 2013, pp. 18–23.

[109] A. Mufaris, S. Kawachi, and J. Baba, "Voltage control using coordinated control of Heat Pump Water Heaters with large penetration of photovoltaic systems," in *Electric Power and Energy Conversion Systems (EPECS), 2013 3rd International Conference on*, Oct 2013, pp. 1–6.

[110] A. Mufaris and J. Baba, "Scheduled Operation of Heat Pump Water Heater for Voltage Control in Distribution System with Large Penetration of PV Systems," in *Green Technologies Conference, 2013 IEEE*, April 2013, pp. 85–92.

[111] Z. Csetvei, J. Ostergaard, and P. Nyeng, "Controlling price-responsive heat pumps for overload elimination in distribution systems," in *Innovative Smart Grid Technologies (ISGT Europe), 2011 2nd IEEE PES International Conference and Exhibition on*, Dec 2011, pp. 1–8.

[112] Nyeng, P. , "System Integration of Distributed Energy Resources – ICT, Ancillary Services, and Markets," PhD dissertation, Centre of Electric Technology, Technical University of Denmark, Feb. 2011.

[113] Y.-J. Kim, L. Norford, and J. Kirtley, "Modeling and Analysis of a Variable Speed Heat Pump for Frequency Regulation Through Direct Load Control," pp. 1–12, 2014.

[114] L. Totu, J. Leth, and R. Wisniewski, "Control for large scale demand response of thermostatic loads*," in *American Control Conference (ACC), 2013*, June 2013, pp. 5023–5028.

[115] E. Veldman, M. Gibescu, H. Slootweg, and W. Kling, "Impact of electrification of residential heating on loading of distribution networks," in *PowerTech, 2011 IEEE Trondheim*, June 2011, pp. 1–7.

[116] S. Koch, M. Zima, and G. Andersson, "Potentials and applications of coordinated groups of thermal household appliances for power system control purposes," in *Sustainable Alternative Energy (SAE), 2009 IEEE PES/IAS Conference on.* IEEE, 2009, pp. 1–8.

[117] A. Schafer, P. Baumanns, and A. Moser, "Modeling heat pumps as combined heat and power plants in energy generation planning," in *Energytech, 2012 IEEE*, May 2012, pp. 1–6.

[118] Yokoyama, R.; Okagaki, S.; Wakui, T.; Takemura, K., "Performance Analysis of a CO_2 Heat Pump Water Heating System by Numerical Simulation with a Simplified Model," in *19th International Conference on Efficiency, Cost, Optimization, Simulation and Environmental Impact of Energy Systems*, May 2012, pp. 1–6.

[119] C. Verhelst, D. Degrauwe, F. Logist, J. Van Impe, and L. Helsen, "Multi-objective optimal control of an air-to-water heat pump for residential heating," in *Building Simulation*, vol. 5, no. 3. Springer, 2012, pp. 281–291.

[120] E. Vrettos, K. Lai, F. Oldewurtel, and G. Andersson, "Predictive Control of buildings for Demand Response with dynamic day-ahead and real-time prices," in *Control Conference (ECC), 2013 European*, July 2013, pp. 2527–2534.

[121] Wimmer, R.W., "Regelung einer Wärmepumpenanlage mit Model Predictive Control," PhD Thesis, ETH Zürich, 2004.

[122] Bianchi, M.A., "Adaptive Modellbasierte Prädiktive Regelung einer Kleinw armepumpenanlage," PhD Thesis, ETH Zürich, 2006.

[123] S. Kawachi, H. Hagiwara, J. Baba, and E. Shimoda, "Thermal comfort analysis during power fluctuation compensation by use of air-conditioning system," in *Innovative Smart Grid Technologies (ISGT Europe), 2012 3rd IEEE PES International Conference and Exhibition on*, Oct 2012, pp. 1–6.

[124] R. Yokoyama, T. Wakui, J. Kamakari, and K. Takemura, "Performance analysis of a CO_2 heat pump water heating system under a daily change in a standardized demand," *Energy*, vol. 35, no. 2, pp. 718–728, 2010.

[125] A. Ursua, L. Gandia, and P. Sanchis, "Hydrogen Production From Water Electrolysis: Current Status and Future Trends," *Proceedings of the IEEE*, vol. 100, no. 2, pp. 410–426, Feb 2012.

[126] Ø. Ulleberg, "Modeling of advanced alkaline electrolyzers: a system simulation approach," *International Journal of Hydrogen Energy*, vol. 28, no. 1, pp. 21–33, 2003.

[127] Ø.Ulleberg, "Modeling Stand-Alone Power Systems for the Future: Optimal Design, Operation and Control of Solar-Hydrogen Energy Systems," PhD Thesis, Norwegian University of Science and Technology, 1998.

[128] N. Gyawali and Y. Ohsawa, "Integrating fuel cell/electrolyzer/ultracapacitor system into a stand-alone microhydro plant," *Energy Conversion, IEEE Transactions on*, vol. 25, no. 4, pp. 1092–1101, 2010.

[129] M. Maruf-ul Karim and M. Iqbal, "Dynamic modeling and simulation of a remote wind-diesel-hydrogen hybrid power system," in *Electric Power and Energy Conference (EPEC), 2010 IEEE*, Aug 2010, pp. 1–6.

[130] W. Jiang, Y. Wu, T. Yang, F. Y. Yu, W. Wang, and S. Hashimoto, "Identification and Power Electronic Module Design of a Solar Powered Hydrogen Electrolyzer," in *Power and Energy Engineering Conference (APPEEC), 2012 Asia-Pacific*, March 2012, pp. 1–4.

[131] T. Zhou, B. Francois, M. el Hadi Lebbal, and S. Lecoeuche, "Real-Time Emulation of a Hydrogen-Production Process for Assessment of an Active Wind-Energy Conversion System," *Industrial Electronics, IEEE Transactions on*, vol. 56, no. 3, pp. 737–746, March 2009.

[132] H. De Battista, R. J. Mantz, and F. Garelli, "Power conditioning for a wind-hydrogen energy system," *Journal of Power Sources*, vol. 155, no. 2, pp. 478–486, 2006.

[133] O. Onar, M. Uzunoglu, and M. Alam, "Dynamic modeling, design and simulation of a wind/fuel cell/ultra-capacitor-based hybrid power generation system," *Journal of Power Sources*, vol. 161, no. 1, pp. 707 – 722, 2006.

[134] C. Martinson, G. van Schoor, K. Uren, and D. Bessarabov, "Equivalent electrical circuit modelling of a Proton Exchange Membrane electrolyser based on current interruption,"

in *Industrial Technology (ICIT), 2013 IEEE International Conference on*, Feb 2013, pp. 716–721.

[135] F. da Costa Lopes and E. Watanabe, "Experimental and theoretical development of a PEM electrolyzer model applied to energy storage systems," in *Power Electronics Conference, 2009. COBEP '09. Brazilian*, Sept 2009, pp. 775–782.

[136] M. Kolhe and O. Atlam, "Empirical electrical modeling for a proton exchange membrane electrolyzer," in *Applied Superconductivity and Electromagnetic Devices (ASEMD), 2011 International Conference on*, Dec 2011, pp. 131–134.

[137] C. Martinson, G. van Schoor, K. Uren, and D. Bessarabov, "Equivalent electrical circuit modelling of a Proton Exchange Membrane electrolyser based on current interruption," in *Industrial Technology (ICIT), 2013 IEEE International Conference on*, Feb 2013, pp. 716–721.

[138] R. García-Valverde, N. Espinosa, and A. Urbina, "Simple PEM water electrolyser model and experimental validation," *international journal of hydrogen energy*, vol. 37, no. 2, pp. 1927–1938, 2012.

[139] P.-Y. Yan, C.-H. Cehng, A. Su, and S.-H. Chan, "Simulation study of hydrogen production through solid oxide electrolysis cell," in *Electrical and Control Engineering (ICECE), 2011 International Conference on*, Sept 2011, pp. 4075–4078.

[140] J. P. Stempien, Q. Sun, and S. H. Chan, "Solid Oxide Electrolyzer Cell Modeling: A Review," *Journal of Power Technologies*, vol. 93, no. 4, pp. 216–246, 2013.

[141] J.O. Jensen, V. Bandur, N.J. Bjerrum, S.H. Jensen, S. Ebbesen, M. Mogensen, N. Tophj and L.Yde, "Pre-investigation of water electrolysis," PSO-FU 2006-1-6287, project 6287 PSO, 2006.

[142] M. Chen and G. Rincon-Mora, "Accurate electrical battery model capable of predicting runtime and I-V performance," *Energy Conversion, IEEE Transactions on*, vol. 21, no. 2, pp. 504–511, June 2006.

[143] D. W. Dees, V. S. Battaglia, and A. Bélanger, "Electrochemical modeling of lithium polymer batteries," *Journal of power sources*, vol. 110, no. 2, pp. 310–320, 2002.

[144] J. Newman, K. E. Thomas, H. Hafezi, and D. R. Wheeler, "Modeling of lithium-ion batteries," *Journal of power sources*, vol. 119, pp. 838–843, 2003.

[145] P. M. Gomadam, J. W. Weidner, R. A. Dougal, and R. E. White, "Mathematical modeling of lithium-ion and nickel battery systems," *Journal of Power Sources*, vol. 110, no. 2, pp. 267–284, 2002.

[146] P. Rong and M. Pedram, "An analytical model for predicting the remaining battery capacity of lithium-ion batteries," *Very Large Scale Integration (VLSI) Systems, IEEE Transactions on*, vol. 14, no. 5, pp. 441–451, May 2006.

[147] S. Barsali and M. Ceraolo, "Dynamical models of lead-acid batteries: implementation issues," *Energy Conversion, IEEE Transactions on*, vol. 17, no. 1, pp. 16–23, 2002.

[148] S. Buller, M. Thele, R. De Doncker, and E. Karden, "Impedance-based simulation models of supercapacitors and Li-ion batteries for power electronic applications," in *Industry Applications Conference, 2003. 38th IAS Annual Meeting. Conference Record of the*, vol. 3, Oct 2003, pp. 1596–1600 vol.3.

[149] L. Gao, S. Liu, and R. Dougal, "Dynamic lithium-ion battery model for system simulation," *Components and Packaging Technologies, IEEE Transactions on*, vol. 25, no. 3, pp. 495–505, Sep 2002.

[150] R. Kroeze and P. Krein, "Electrical battery model for use in dynamic electric vehicle simulations," in *Power Electronics Specialists Conference, 2008. PESC 2008. IEEE*, June 2008, pp. 1336–1342.

[151] O. Tremblay, L.-A. Dessaint, and A.-I. Dekkiche, "A Generic Battery Model for the Dynamic Simulation of Hybrid Electric Vehicles," in *Vehicle Power and Propulsion Conference, 2007. VPPC 2007. IEEE*, Sept 2007, pp. 284–289.

[152] M. Einhorn, V. Conte, C. Kral, J. Fleig, and R. Permann, "Parameterization of an electrical battery model for dynamic system simulation in electric vehicles," in *Vehicle Power and Propulsion Conference (VPPC), 2010 IEEE*, Sept 2010, pp. 1–7.

[153] S. Vazquez, S. Lukic, E. Galvan, L. Franquelo, and J. Carrasco, "Energy Storage Systems for Transport and Grid Applications," *Industrial Electronics, IEEE Transactions on*, vol. 57, no. 12, pp. 3881–3895, Dec 2010.

[154] F. Marra, G. Y. Yang, C. Traholt, E. Larsen, C. Rasmussen, and S. You, "Demand profile study of battery electric vehicle under different charging options," in *Power and Energy Society General Meeting, 2012 IEEE*, July 2012, pp. 1–7.

[155] J. Barreras, E. Schaltz, S. Andreasen, and T. Minko, "Datasheet-based modeling of li-ion batteries," in *Vehicle Power and Propulsion Conference (VPPC), 2012 IEEE*, Oct 2012, pp. 830–835.

[156] J. R. Pillai and B. Bak-Jensen, "Electric vehicle based battery storages for future power system regulation services," in *Nordic Wind Power Conference*, 2009.

[157] Energinet.dk, "Cell Controller Overview and Future Perspectives," Technical Report, Doc. no. 20735/12, Case 10/678, Sep. 2012.

[158] A. Navarro-Espinosa and P. Mancarella, "Probabilistic modeling and assessment of the impact of electric heat pumps on low voltage distribution networks," *Applied Energy*, vol. 127, pp. 249–266, 2014.

[159] P. Kadurek, J. Cobben, and W. Kling, "Overloading protection of future low voltage distribution networks," in *PowerTech, 2011 IEEE Trondheim*, June 2011, pp. 1–6.

[160] M. Arnold, W. Friede, and J. Myrzik, "Investigations in low voltage distribution grids with a high penetration of distributed generation and heat pumps," in *Power Engineering Conference (UPEC), 2013 48th International Universities'*, Sept 2013, pp. 1–6.

[161] M. Akmal, B. Fox, D. Morrow, and T. Littler, "Impact of high penetration of heat pumps on low voltage distribution networks," in *PowerTech, 2011 IEEE Trondheim*, June 2011, pp. 1–7.

[162] J. Fox and E. Collins, "A voltage flicker suppression device for residential air conditioners and heat pumps," in *Harmonics and Quality of Power (ICHQP), 2010 14th International Conference on*, Sept 2010, pp. 1–8.

[163] R. A. Verzijlbergh, Z. Lukszo, J. G. Slootweg, and M. D. Ilic, "The impact of controlled electric vehicle charging on residential low voltage networks," in *Networking, Sensing and Control (ICNSC), 2011 IEEE International Conference on.* IEEE, 2011, pp. 14–19.

[164] H. Turker, S. Bacha, and A. Hably, "Rule-Based Charging of Plug-in Electric Vehicles (PEVs): Impacts on the Aging Rate of Low-Voltage Transformers," *Power Delivery, IEEE Transactions on*, vol. 29, no. 3, pp. 1012–1019, June 2014.

[165] A. Masoum, S. Deilami, P. Moses, and A. Abu-Siada, "Impact of plug-in electrical vehicles on voltage profile and losses of residential system," in *Universities Power Engineering Conference (AUPEC), 2010 20th Australasian*, Dec 2010, pp. 1–6.

[166] M. A. S. Masoum, P. Moses, and K. Smedley, "Distribution transformer losses and performance in smart grids with residential Plug-In Electric Vehicles," in *Innovative Smart Grid Technologies (ISGT), 2011 IEEE PES*, Jan 2011, pp. 1–7.

[167] F. Marra, M. Jensen, R. Garcia-Valle, C. Traholt, and E. Larsen, "Power quality issues into a Danish low-voltage grid with electric vehicles," in *Electrical Power Quality and Utilisation (EPQU), 2011 11th International Conference on*, Oct 2011, pp. 1–6.

[168] Y. Li and P. Crossley, "Monte Carlo study on impact of electric vehicles and heat pumps on LV feeder voltages," in *Developments in Power System Protection (DPSP 2014), 12th IET International Conference on.* IET, 2014, pp. 1–6.

[169] P. Richardson, D. Flynn, and A. Keane, "Impact assessment of varying penetrations of electric vehicles on low voltage distribution systems," in *Power and Energy Society General Meeting, 2010 IEEE*, July 2010, pp. 1–6.

[170] P. Mancarella, C. K. Gan, and G. Strbac, "Evaluation of the impact of electric heat pumps and distributed chp on lv networks," in *PowerTech, 2011 IEEE Trondheim*, June 2011, pp. 1–7.

[171] O. van Pruissen and R. Kamphuis, "High concentration of heat pumps in suburban areas and reduction of their impact on the electricity network," in *PowerTech, 2011 IEEE Trondheim*, June 2011, pp. 1–6.

[172] Mehmedalic, J.; Rasmussen, J.; Harbo, S., "Reinforcement Costs in Low-Voltage Grids - Deliverable D4.3-B2: Grid Impact Studies of Electric Vehicles," Technical Report, Danish Energy Association, Nov. 2013.

[173] J. Campillo, F. Wallin, I. Vassileva, and E. Dahlquist, "Electricity demand impact from increased use of ground sourced heat pumps," in *Innovative Smart Grid Technologies (ISGT Europe), 2012 3rd IEEE PES International Conference and Exhibition on*, Oct 2012, pp. 1–7.

[174] L. Ochoa and P. Mancarella, "Low-carbon LV networks: Challenges for planning and operation," in *Power and Energy Society General Meeting, 2012 IEEE*, July 2012, pp. 1–2.

[175] T. Short, *Electric Power Distribution Handbook*, ser. Electric power engineering series. Taylor & Francis, 2003.

[176] T. Gönen, *Electric power distribution system engineering*, ser. McGraw-Hill Series in Electrical Engineering. McGraw-Hill, 1986.

[177] A. Navarro-Espinosa, L. F. Ochoa, and D. Randles, "Assessing the benefits of meshed operation of LV feeders with low carbon technologies," in *Innovative Smart Grid Technologies Conference (ISGT), 2014 IEEE PES*, Feb 2014, pp. 1–5.

[178] P. Kadurek, M. Sarab, J. F. G. Cobben, and W. Kling, "Assessment of demand response possibilities by means of voltage control with intelligent MV/LV distribution substation," in *Power and Energy Society General Meeting, 2012 IEEE*, July 2012, pp. 1–6.

[179] B. Bhattarai, B. Bak-Jensen, P. Mahat, and J. Pillai, "Voltage controlled dynamic demand response," in *Innovative Smart Grid Technologies Europe (ISGT EUROPE), 2013 4th IEEE/PES*, Oct 2013, pp. 1–5.

[180] F. Marra, Y. Fawzy, T. Bulo, and B. Blazic, "Energy storage options for voltage support in low-voltage grids with high penetration of photovoltaic," in *Innovative Smart Grid Technologies (ISGT Europe), 2012 3rd IEEE PES International Conference and Exhibition on*, Oct 2012, pp. 1–7.

[181] S. Qi, L. Chen, H. Li, D. Randles, G. Bryson, and J. Simpson, "Assessment of voltage control techniques for low voltage networks," in *Developments in Power System Protection (DPSP 2014), 12th IET International Conference on.* IET, 2014, pp. 1–6.

[182] E. Demirok, D. Sera, R. Teodorescu, P. Rodriguez, and U. Borup, "Evaluation of the voltage support strategies for the low voltage grid connected PV generators," in *Energy Conversion Congress and Exposition (ECCE), 2010 IEEE*, Sept 2010, pp. 710–717.

[183] T. Stetz, F. Marten, and M. Braun, "Improved Low Voltage Grid-Integration of Photovoltaic Systems in Germany," *Sustainable Energy, IEEE Transactions on*, vol. 4, no. 2, pp. 534–542, April 2013.

[184] S. Huang, J. Pillai, M. Liserre, and B. Bak-Jensen, "Improving photovoltaic and electric vehicle penetration in distribution grids with smart transformer," in *Innovative Smart Grid Technologies Europe (ISGT EUROPE), 2013 4th IEEE/PES*, Oct 2013, pp. 1–5.

[185] P. Alcaria, S. Pinto, and J. Silva, "Active voltage regulators for low voltage distribution grids: The matrix converter solution," in *Power Engineering, Energy and Electrical Drives (POWERENG), 2013 Fourth International Conference on*, May 2013, pp. 989–994.

[186] K. Inoue and Y. Iwafune, "Operation of heat pump water heaters for restriction of photovoltaic reverse power flow," in *Power System Technology (POWERCON), 2010 International Conference on*, Oct 2010, pp. 1–7.

[187] T. Kato and Y. Suzuoki, "Daytime Operation of Heat-Pump Water Heater for Mitigating Voltage Rise Due to High Penetration of Residential Photovoltaic Power Generation Systems," in *Engineering and Technology (S-CET), 2012 Spring Congress on*, May 2012, pp. 1–4.

[188] N. Leemput, F. Geth, J. Van Roy, A. Delnooz, J. Buscher, and J. Driesen, "Impact of Electric Vehicle On-Board Single-Phase Charging Strategies on a Flemish Residential Grid," *Smart Grid, IEEE Transactions on*, vol. 5, no. 4, pp. 1815–1822, July 2014.

[189] W. J. A. v. Leeuwen, M. Bongaerts, G. M. A. Vanalme, B. Asare-Bediako, and W. L. Kling, "Load Shifting by Heat Pumps using Thermal Storage," in *Universities' Power Engineering Conference (UPEC), Proceedings of 2011 46th International*, Sept 2011, pp. 1–6.

[190] N. Leemput, F. Geth, B. Claessens, J. Van Roy, R. Ponnette, and J. Driesen, "A case study of coordinated electric vehicle charging for peak shaving on a low voltage grid," in *Innovative Smart Grid Technologies (ISGT Europe), 2012 3rd IEEE PES International Conference and Exhibition on*, Oct 2012, pp. 1–7.

[191] H. Willis, *Power Distribution Planning Reference Book, Second Edition*, ser. Power Engineering (Willis). Taylor & Francis, 2004.

[192] R. Jones, J.B.; Dugan, *Engineering Thermodynamics, First Edition.* Prentice Hall, 1995.

[193] P. Kundur, N. Balu, and M. Lauby, *Power System Stability and Control*, ser. Discussion Paper Series. McGraw-Hill Education, 1994.

[194] COWI, "Stock of heat pumps for heating in all year residence in Denmark," Technical Report, Nov. 2011.

[195] Viessmann, "Vitocal Air-To-Water Heat pump Technical Guide," Technical Manual, 2009.

[196] Schillinger, D., "Variable Speed Technology Improves Power Factor, Boosts Grid Reliability," Danfoss, Apr. 2011.

[197] R. E. . Brown, *Electric Power Distribution Reliability, Second Edition.* CRC Press, 2008.

[198] Fujitsu General Limited, "Waterstage - Future Solution of Domestic Heating," Design and Technical Manual, Mar. 2010.

[199] U. Eicker, *Solar Technologies for Buildings.* Wiley, 2003.

[200] J. Larminie and A. Dicks, *Fuel Cell Systems Explained.* J. Wiley, 2003.

[201] A. Ursua, I. San Martin, and P. Sanchis, "Design of a Programmable Power Supply to study the performance of an alkaline electrolyser under different operating conditions," in *Energy Conference and Exhibition (ENERGYCON), 2012 IEEE International*, Sept 2012, pp. 259–264.

[202] T. Zhou and B. Francois, "Modeling and control design of hydrogen production process for an active hydrogen/wind hybrid power system," *International Journal of Hydrogen Energy*, vol. 34, no. 1, pp. 21–30, 2009.

[203] M. Yilmaz and P. Krein, "Review of Battery Charger Topologies, Charging Power Levels, and Infrastructure for Plug-In Electric and Hybrid Vehicles," *Power Electronics, IEEE Transactions on*, vol. 28, no. 5, pp. 2151–2169, May 2013.

[204] Q. Wu, A. Nielsen, J. Østergaard, S. T. Cha, F. Marra, Y. Chen, and C. Træholt, "Driving Pattern Analysis for Electric Vehicle (EV) Grid Integration Study," in *Innovative Smart Grid Technologies Conference Europe (ISGT Europe), 2010 IEEE PES*, Oct 2010, pp. –.

[205] Dangrid (Danish energy Association and Energinet.dk), "Smart Grid in Denmark 2.0 - Implementation of three key recommendations for the smart grid network," Technical Report, Oct. 2012.

[206] Korsgaard, A.R., "Design and Control of Household CHP Fuel Cell System," PhD Thesis, Aalborg University, 2006.

[207] F. J. Massey Jr, "The Kolmogorov-Smirnov test for goodness of fit," *Journal of the American statistical Association*, vol. 46, no. 253, pp. 68–78, 1951.

[208] O. Thas, *Comparing distributions.* Springer, 2010.

[209] Wu, Q.; Jensen, J.M.; Hansen, L.H; Bjerre, A; Nielsen, A.H and Østergaard, J., "EV Portfolio Management And Grid Impact Study," Edison Technical Report, Mar. 2012.

[210] M. Thorhauge, G. Vuk, and S. Kaplan, "Actum project: Joint activities and travel of household members," in *Proceedings from the Annual Transport Conference at Aalborg University (Department of Development & Planning, Aalborg University)*, 2012.

[211] "ARTEMIS: Assessment and reliability of transport emission models and inventory systems," [Online]. Available: http://www.inrets.fr, 2012.

[212] C. M. Bishop, *Pattern Recognition and Machine Learning (Information Science and Statistics)*. Springer-Verlag New York, Inc., 2006.

[213] D. L. Davies and D. W. Bouldin, "A Cluster Separation Measure," *Pattern Analysis and Machine Intelligence, IEEE Transactions on*, vol. PAMI-1, no. 2, pp. 224–227, April 1979.

[214] F. Marra, G. Yang, Y. Fawzy, C. Traeholt, E. Larsen, R. Garcia-Valle, and M. Jensen, "Improvement of Local Voltage in Feeders With Photovoltaic Using Electric Vehicles," *Power Systems, IEEE Transactions on*, vol. 28, no. 3, pp. 3515–3516, Aug 2013.

[215] H. Hansen, H.-H. Holm-Hansen, O. Samuelsson, L. H. Hansen, H. W. Bindner, H. Johannsson, and P. Cajar, "Coordination of system needs and provision of services," in *Electricity Distribution (CIRED 2013), 22nd International Conference and Exhibition on*, June 2013, pp. 1–4.

Part II

Publications

Conference Contributions

Publication C.1

(*Conference Contribution*)

Alkaline Electrolyzer and V2G System DIgSILENT Models for Demand Response Analysis in Future Distribution Networks

Iker Diaz de Cerio Mendaza, Birgitte Bak-Jensen, and Zhe Chen

The paper is a pre-printed version of the final paper that has been published in the *Proceedings of the PowerTech (POWERTECH), 2013 IEEE Grenoble*, vol., no., pp. 1,8, 16–20 June 2013

DOI:10.1109/PTC.2013.6652429

Alkaline Electrolyzer and V2G System DIgSILENT Models for Demand Response Analysis in Future Distribution Networks

Iker Diaz de Cerio Mendaza, *Student-Member*, *IEEE*, Birgitte Bak-Jensen, *Senior-Member*, *IEEE*, and Zhe Chen, *Senior-Member*, *IEEE*
Department of Energy Technology, Aalborg University
Pontoppidanstræde 101, 9220, Aalborg Ø, Denmark
idm@et.aau.dk

***Abstract*— Grid instabilities originated by unsteady generation, characteristic consequence of some renewable energy resources such as wind and solar power, claims for new power balance solutions in largely penetrated systems. Denmark's solid investment in these energy sources has awaked a need of rethinking about the future control and operation of the power system. A widespread idea to face these challenges is to have a flexible demand easily adjustable to the system variations. Electro-thermal loads, electric vehicles and hydrogen generation are among the most mentioned technologies capable to respond, under certain strategies, to these variations. This paper presents two DIgSILENT PowerFactory models: an alkaline electrolyzer and a vehicle to the grid system. The models were performed using DIgSILENT Simulation Language, aiming to be used for long-term distribution systems simulations. Two voltage levels were considered: 20 kV for the electrolyzer grid connection and 0.4 kV for the plug-in electric vehicle. Simulation results illustrate the simplicity and manageability of the presented models.**

***Index Terms*—Alkaline Electrolyzer, V2G system, Demand Side Management, Smart Grids, DIgSILENT PowerFactory.**

I. Introduction

Denmark has actively supported sustainable development and renewable energy integration during the last decades. Wind power has specially suffered an extraordinary growth reaching 21.3% of the total share in 2010. In March 2012, the Danish Ministry of Climate, Energy and Building accelerated the renewable energy targets set by previous energy plans. The wind power is introduced as the primary electricity supply source in 2020, expecting to cover 50% of the national electrical consumption [1].

Considering grid instabilities and power unbalances introduced by this alternative generation the management of largely penetrated power systems becomes rather defiance. On January 2005 in the Danish offshore wind farm Horns Rev 1, a storm event resulted in zero power production from the whole park in less than five minutes. A sudden power loss of about 135 MW was originated from the shutdown of the 91 wind turbines of the wind park due to exceeding over-speed limit [2].

The strong grid interconnection with neighboring countries is a well exploited tool for regulating the actual system. This provides an extra degree of actuation to the transmission system operator (TSO) which is capable to import or export energy, depending on the instantaneous need, to keep the system frequency within the permitted limits. Despite of having plans to increase this interconnection capacity in Denmark, the future power exchange capability threatens to be drastically affected if the surrounding countries follow the same ambitious targets as Denmark. For that reason, local energy management using active control of loads is becoming a popular idea to mitigate the impact from the renewables in the power system. The Danish IDA Climate Plan defines a close interaction among the future electric, heating and transportation systems, including also the electrolysis as a possible alternative for fuel generation [3].

The following paper presents two DIgSILENT PowerFactory models: an alkaline electrolyzer (AE) and a vehicle to the grid (V2G) system. The aim is to assess their power regulation potential and their impact in future distribution systems by long-term simulations.

The literature regarding their modelling is wide; being possible to find different ways and types of models depending on the analysis required. A detailed AE model was properly introduced by Ulleberg [4], [5], dividing its structure in three main parts; I-U characteristic, thermal model and the hydrogen production. Its influence was posteriorly assessed inside a renewable energy based stand-alone power system, stating its good accuracy and suitability for this kind of system analysis. Authors in [6] used the previous work to model different electrolyzers for different hybrid system applications. Battista et al. [7] employed the von Hoerner system in order to address the power control of a wind-hydrogen system. Based also in this last one, a more simplified model was introduced by Onar et al. [8] for dynamic simulations in a wind/fuel cell/electrolyzer/ultra-capacitor system. His implementation may be restricted due to the consideration of

The authors would like to thank the Danish Council for Strategic Research for providing the financial support for the project Development of a Secure, Economic and Environmentally-friendly Modern Power Systems (DSF 09-067255).

constant temperature and operation point.

Concerning the plug-in electric vehicle (PEV) storage, lithium-ion and lithium ion polymer batteries are commonly used technologies due to their long life cycle, high power and energy density characteristics. The classification made by Chen and Rincon-Mora [9] shows that the electrical battery models are the most relevant for grid studies. Detailed lithium-ion battery models were introduced by authors in [10], [11] focusing in representing accurately their dynamic behaviour during charge and discharge periods. The representative electrical parameters were obtained via experimental tests and analytically defined as a polynomial regression. Aggregated and more simplified models were used by authors in [12], [13] instead, focusing on the load frequency response in power system analysis.

The authors intend to study the interaction of these two loads in local distribution networks. The lack of information on how to implement them in an analysis tool like DIgSILENT PowerFactory, motivate to address this issue in this manuscript.

The paper is divided in the seven sections. Section I gives a short introduction about the problem statement and the state of the art. Through section II, the AE and the V2G system models are described. In section III their implementation using DIgSILENT Simulation Language (DSL) is introduced. Section IV presents the obtained simulation results. Finally Section V and VI provide the conclusions and references.

II. Unit Modelling

A. Alkaline Electrolyzer

An AE is the combination of different electro-mechanical elements, which allows the decomposition of an electrolyte -solution of KOH in water- into hydrogen and oxygen, by passing a direct current between two electrodes.

$$H_2O(l) + Electrical\ energy \rightarrow H_2(g) + \frac{1}{2}O_2(g) \quad (1)$$

It can be considered as a mature technology in comparison with proton exchange membrane (PEM) and solid oxide electrolysis (SOE), wherefore it is commonly used in large scale hydrogen production applications. A simplified grid connection topology of a large AE in a distribution network is shown in Fig.1(a).

As an essential reference in the AE modelling, the work published by Ulleberg [5], must be stated. As he introduced three sub-parts delimited AE model structure: I-U characteristic curve for an AE cell, thermal model and hydrogen production. In Fig.1(b) is also included the compressor model.

1) I-U Characteristic Curve: The following non-linear equation, proposed by Ulleberg [5], represents the current and voltage kinetics in the electrode. This expression, including the overvoltage dependence on the temperature resulting from the chemical reactions, was obtained from empirical results.

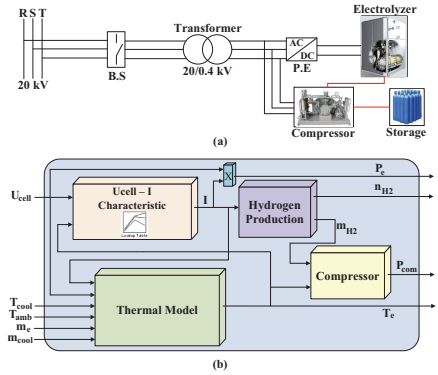

Fig. 1. Alkaline Electrolyzer: (a) Simplified grid connection lay-out and (b) Model structure.

$$U_{cell} = U_{rev} + \frac{r_1 + r_2 T_e}{A_{cell}} I + (s_1 + s_2 T_e + s_3 T_e^2) log(\frac{t_1 + t_2/T_e + t_3/T_e^2}{A_{cell}} I + 1) \quad (2)$$

$$U_e = n_c U_{cell} \quad (3)$$

where U_e is the electrolyzer voltage and n_c the number of cells, U_{cell} is the voltage of a cell and U_{rev} the reversible voltage, r_i are the parameters for ohmic resistance of electrolyte (i=1…2), s_i and t_i are parameters for overvoltage on electrodes (i=1…3), A is the cell area, T_e is the electrolyte temperature and I is the DC current drawn by the AE. The model parameters and coefficients are listed in the Table I.

For an operational pressure of 7 bars, similar as the system installed at Jülich (PHOEBUS), the curves developed from the above expression are presented in the Fig.2. Hereof a two dimensional matrix (look-up table) was created with the purpose of defining the current drawn by the AE, according to T_e and U_e applied in the stack.

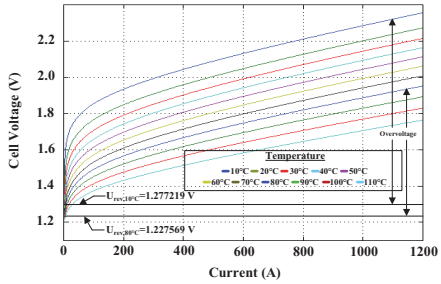

Fig. 2. I-U characteristic curve for the modelled AE cell at operating pressure of 7 bar

The thermodynamics of the electrochemical reactions is an important factor to be taken into account. The changes in enthalpy (ΔH) and entropy (ΔS) of the water splitting reaction induce changes in Gibbs energy (ΔG) and consequently in the U_{rev}. These parameters are directly affected by the working conditions of the AE (operation pressure and temperature).

$$U_{rev} = \frac{\Delta G}{zF} = \frac{\Delta H - T_e \Delta S}{zF} \tag{4}$$

where z is the number of electrons transferred per reaction (z=2) and F is the faraday constant ($\sim$96485 C/mol). The changes in Gibbs energy was calculated as described in [14], using the thermodynamic properties of products and reactants obtained from the NIST online database. Then, for the operating pressure of 7 bars, a polynomial regression was made in order to define U_{rev_7bar} as function of T_e.

$$U_{rev\_7bar} = -2.483e^{-10}T_e^3 + 2.9004e^{-7}T_e^2 - 0.000733T_e + 1.2845 \tag{5}$$

2) Thermal Model: The temperature variation of the electrolyte, during the hydrolysis, can be represented by a thermal energy balance as the following differential equation states.

$$C_t \frac{dT_e}{dt} = Q_{gen} - Q_{cool} - Q_{loss} \tag{6}$$

where C_t is the thermal capacitance of the AE. The internal heat generation (Q_{gen}) is a consequence of the cell inefficiencies and is directly related with the power consumed by the AE (P_e) and the electrolysis efficiency (η_e). This latter one can be expressed as the quotient between the thermo-neutral voltage (U_{th}) and U_{cell}.

$$Q_{gen} = P_e(1-\eta_e) = P_e(1-\frac{U_{th}}{U_{cell}}) = n_c(U_{cell}-U_{th})I \tag{7}$$

$$U_{th} = \frac{\Delta H}{zF} \tag{8}$$

The U_{th} defines a voltage threshold for the heat release in the process. If this value is exceeded the heat released becomes higher than the required for the water decomposition increasing the accumulated heat in the stack and resulting in temperature increases. Again, a polynomial regression was made to represent U_{th} as function of T_e for an operating pressure of 7 bars.

$$U_{th\_7bar} = -3.2084e^{-10}T_e^3 + 5.4591e^{-8}T_e^2 - 0.000165T_e + 1.485 \tag{9}$$

The heat released as losses (Q_{loss}) is expressed as the difference between the T_e and the ambient temperature (T_{amb}) divided by the overall thermal resistance (R_t). Based on the parameterization of [5] and the difficulties finding real characteristic data, values of R_t and C_t were scaled up to achieve a logical thermal behaviour on this unit size.

$$Q_{loss} = \frac{1}{R_t}(T_e - T_{amb}) \tag{10}$$

The cooling is a critical issue if an accurate response and control of the AE is required. Among the different cooling methods, circulating the electrolyte through a heat exchanger is a simple and commonly used technique. The cooling demand (Q_{cool}) was calculated via the number of transfer units (ε-NTU) method, where ε is the heat exchanger effectiveness and Q_{max} the maximum theoretical cooling demand.

$$Q_{loss} = \varepsilon \cdot Q_{max} \tag{11}$$

The maximum and minimum heat capacity rates (C_{min} and C_{max}), i.e. the mass flow rate (m_e and m_{cool}) by the specific heat (c_{P_e} and $c_{P_{cool}}$), are calculated according to eq.(12) and in consequence the maximum heat (Q_{max}) with eq.(13).

$$C_{min} = \begin{cases} m_e \cdot c_{p_e} & \text{if } m_e \cdot c_{p_e} < m_{cool} \cdot c_{p_{cool}} \\ m_{cool} \cdot c_{p_{cool}} & \text{if } m_e \cdot c_{p_e} \geq m_{cool} \cdot c_{p_{cool}} \end{cases}$$

$$C_{max} = \begin{cases} m_{cool} \cdot c_{p_{cool}} & \text{if } m_e \cdot c_{p_e} < m_{cool} \cdot c_{p_{cool}} \\ m_e \cdot c_{p_e} & \text{if } m_e \cdot c_{p_e} \geq m_{cool} \cdot c_{p_{cool}} \end{cases} \tag{12}$$

$$Q_{max} = C_{min}\Delta T_{max} = C_{min}(T_e - T_{cool}) \tag{13}$$

In agreement with the methodology, ε depends on of the heat capacity ratio (C_r) and NTU coefficient, being the latter one defined as the quotient of the overall heat transfer coefficient of the heat exchanger (UA_{hx}) and C_{min}.

$$\varepsilon = \frac{1 - e^{NTU(1-C_r)}}{C_r - e^{NTU(1-C_r)}};\ NTU = \frac{UA_{hx}}{C_{min}}, C_r = \frac{C_{min}}{C_{max}} \tag{14}$$

3) Hydrogen Production: The hydrogen production rate (n_{H_2} in mol/s) is directly proportional to the current drawn by the AE stack and the number of cells connected in series.

$$n_{H_2} = \eta_F \frac{n_c I}{zF} \tag{15}$$

The faraday efficiency (η_F) represents the difference between the actual hydrogen production and the maximum theoretically talking.

$$\eta_F = a_1 \exp\left(\frac{a_2 + a_3 T_e}{I/A_{cell}} + \frac{a_4 + a_5 T_e}{(I/A_{cell})^2}\right) \tag{16}$$

4) Compressor Model: The required compression power (P_{com}) in these systems is not a power demand which can be easily dismissed, since it stands for a notable part of the total system demand. Based on the hydrogen mass flow rate (m_{H_2} in kg/s), the P_{com} was modelled assuming the compression process as polytrophic (γ=1.4) and the hydrogen as ideal gas.

$$P_{com} = m_{H_2}(W_1 + W_2) \tag{17}$$

The compression was made in two stages with an intercooling, to reduce the output temperature of the gas from the first stage to the initial temperature T_e, so the compression work in each stage was [15]:

$$\begin{aligned} W_1 &= \frac{c_{p_{H_2}T_1}}{\eta_G}\left(\left(\frac{P_x}{P_1}\right)^{\gamma-1/\gamma} - 1\right) \\ W_2 &= \frac{c_{p_{H_2}T_1}}{\eta_G}\left(\left(\frac{P_2}{P_x}\right)^{\gamma-1/\gamma} - 1\right) \end{aligned} \tag{18}$$

where $c_{P_{H_2}}$ is the specific heat of the hydrogen and η_G is the global efficiency of the compression process. The input hydrogen pressure and temperature values (P_1, T_1) were assumed equal to AE operation conditions. The intermediate compression pressure (P_x) was calculated as the square root of P_1 and the storage pressure (P_2).

$$P_x = \sqrt{P_1 \cdot P_2} \tag{19}$$

The reactive power consumed by the induction motor driving the compressor was calculated considering a constant power factor of 0.88. Some of the stated assumptions taken in this model, especially the scaling up of C_t and R_t, could represent a limitation in some precise studies, requiring a deeper analysis on them. However, in this case the considered conditions seem to be realistic for the purposed pursued.

TABLE I
ALKALINE ELECTROLYZER MODEL

	Parameter	Quantity
General	Rated Power (kW)	355
	Operation Pressure (bar)	7
	N° of Cells	180
	Max. DC voltage (V)	342
	Min. DC voltage (V)	257.4
	Max. Opert. Temp. (°C)	80
Cell I-U Curve	$r_1(\Omega/m2)$	7.331e^{-5}
	$r_2(\Omega/m^2)$	-1.107e^{-7}
	$s_1(V)$	1.586e^{-1}
	$s_2(V/°C)$	1.378e^{-3}
	$s_3(V/°C^2)$	-1.606e^{-5}
	$t_1(m^2/A)$	1.599e^{-2}
	$t_2(m^2/A°C)$	-1.302
	$t_3(m^2/A°C^2)$	4.213e^2
	A (m^2)	0.25
Faraday Efficiency	$a_1(\%)$	99.5
	$a_2(m^2/A)$	-9.5788
	$a_3(m^2/A°C)$	-0.0555
	$a_4(m^4/A)$	1502.7083
	$a_5(m^4/A°C)$	-70.8005
Thermal Model	$R_t(°C/W)$	0.334
	$C_t(J/°C)$	5.38e6
	$UA_{hx}(W/°C)$	2100
	$m_{cool}(kg/s)$	1.2
Compressor	Rated Power (kW)	70
	N° of Stages	2
	η_G (-)	0.486
	P_2 (bar)	150

B. V2G System

The V2G concept is defined as the ability from widespread controlled PEV-s to exchange electricity with the power grid in a bidirectional way, supplying or drawing, in order to meet occasional need for stabilization. The modeled system focuses on representing the steady state behavior of a PEV connected at household level. The battery is capable to respond, under certain state of charge (SOC) limits, to a demand response control (DRC) signal sent from the local control center. Moreover the energy exchange during the hours that the vehicle is not connected at home was also taken in to account. Fig.4 shows the model structure with three parts easily differentiable.

1) Battery Model: The characteristics of the li-ion cell provided by [16] served as a reference for the following model, using the extended Thevenin battery approach to analyse its steady state behaviour within the low voltage grid. For that reason the transient dynamics were neglected, i.e the charge and discharge effects were represented only as a two different internal resistors ($R_{int,cha}$, $R_{int,dis}$). In that case the power (P_{batt}) and voltage (V_{batt}) of the battery were determined as the following equations state:

$$P_{batt} = (V_{batt} \cdot I_{batt})_{DC} \tag{20}$$

$$V_{batt} = \begin{cases} n_{cells}(V_{oc} + R_{int,cha} I_{batt}) & \text{if } I_{batt} > 0 \\ n_{cells}(V_{oc} + R_{int,dis} I_{batt}) & \text{if } I_{batt} < 0 \end{cases} \tag{21}$$

where n_{cells} is the number of cells connected in series, V_{oc} is the open circuit voltage of the cell (Fig.3(a)) and I_{batt} is the current running through the battery. The sources for this current are two, from a charging point at home (I_{HCP}) and from the energy exchanged in out-home hours (I_{OHEE}).

$$I_{batt} = I_{HCP} + I_{OHEE} \tag{22}$$

The α coefficient (Fig.3(b)) represents the charge/discharge (C/D) rate dependence on the battery cell capacity (C_{bc}) and V_{oc}, assuming negligible the temperature effect. Therefore, the SOC and the depth of discharge (DOD) were calculated as:

$$SOC = \frac{1}{C_{bc} \cdot 3600} \begin{cases} \int I_{batt} \alpha \cdot dx & \text{if } I_{batt} < 0 \\ \int \frac{I_{batt}}{\alpha} \cdot dx & \text{if } I_{batt} > 0 \end{cases} \tag{23}$$

$$DOD = DOD_{MAX} - SOC \tag{24}$$

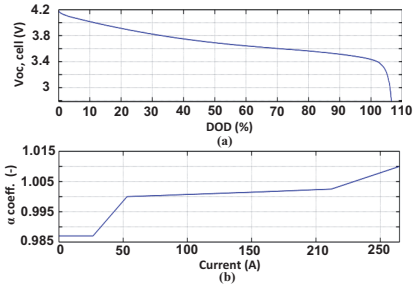

Fig. 3. Kokam SLPB 120216216 53Ah cell: (a) V_{oc} vs DOD curve (b) α coeff. vs I_{batt}.

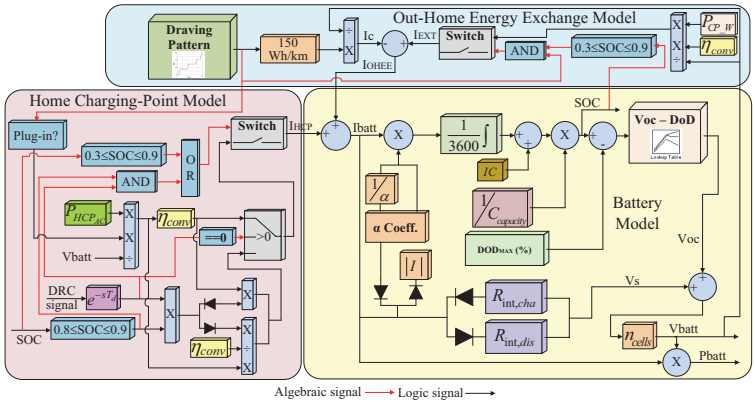

Fig. 4. V2G sytem model structure.

2) Home Charging Point Model: In local distribution networks the battery-grid-battery power exchange is highly limited by the domestic infrastructure. The V2G system capability is constrained even if the battery design allows higher power rate management. Among the different options proposed in the literature, authors found suitable the three phase connection for the Danish case and interesting for this scope.

The control of the switch, which connects and disconnects the load, is based on SOC conditions and the demand response requirements stated below. In order to avoid inconveniences for the user, the V2G system is only allowed to respond within the 80 to 90% range of the SOC. η_{conv} represents the efficiency of the AC/DC conversion and vice versa.

$$\begin{cases} C : P_{HCP} \cdot \eta_{conv} & \text{if } 0.3 > SOC > 0.9 \\ C : P_{HCP} \cdot \eta_{conv} \cdot DRC & \text{if } 0.8 > SOC > 0.9 \\ D : \dfrac{P_{HCP}}{\eta_{conv}} \cdot DRC & \text{if } 0.8 > SOC > 0.9 \end{cases} \quad (25)$$

3) Out-Home Energy Exchange Model: The SOC variations created during the periods in which the vehicle is not plugged at home were represented by the charge/discharge current I_{OHEE}. This may have different sources as well; i.e the driving energy consumption (I_c) or the plugging in external points like work place, supermarket (I_{EXT}). The current drawn from the battery during a daily trip was deducted from the vehicle driving profile -in terms of speed v (km/h)- and the V_{batt}, taking in to account an average energy consumption of 150 Wh/Km.

$$I \simeq \frac{v \cdot 150}{V_{batt}} \quad (26)$$

On the other hand, the charging mode was only taken into account for plugs in external points.

TABLE II
V2G SYSTEM MODEL

	Parameter	Quantity
Battery System	Capacity (kWh)	25
	P_{max} allowed (kW)	28.27
	N° of Cells(-)	127
	SOC Limits (-)	0.3<SOC<0.9
Cell Characteristics	Manufacturer	Kokam
	Model	SLPB 120216216
	Technology	Li-Ion
	Capacity (Ah)	53
	Voltage Range (V)	4.197-2.717
	Nom. Current (A)	53 (1C)
	$R_{int,cha}$ (mΩ)	1.3
	$Ri_{nt,dis}$ (mΩ)	3.69
Charging Station	Rated Power (kW)	11
	Grid Connection	3-phase
	AC voltage (V)	400
	AC current (A)	16
	η_{conv} (-)	0.99

III. IMPLEMENTATION

DIgSILENT PowerFactory is known as a highly sophisticated power system analysis software that allows a wide range of modelling, analysis and simulation options. The implementation work was carried out using the DSL graphical interface considering the load behaviour respect to the grid as a PQ approach. In this context the technical documentation "General Load Model", available in the software help menu, turned to be a reliable source of information.

In both models, the block definition (*.BlkDef) is the start-up point for this commitment. The algebraic and differential equations introduced in the previous section, are assigned

to each block with the purpose of representing the physical behaviour of the load. As different blocks interact within each other a "Block Diagram" element is created to set and organize these relationships. The next step is creating the common models (*.ElmDsl) out of the block diagrams and other required blocks. These are recommended to be placed inside the project grid folder, accessible from the data manager window. Another important task in this phase is the parameterization and the value assignation of the data matrix-s. Finally, with the composite model (*.ElmComp) the different DSL model sub-parts are concatenated together, closing this process down.

A. Alkaline Electrolyzer

Fig.5 intends to give an overview of what has been described before referenced to the AE case. In that graphical representation it is possible to distinguish some of the procedure phases, i.e. the I-U characteristic block definition, highlighted in orange colour. The AE Plant and Load Control are represented by block diagrams in blue and green colours respectively. On the one hand, the AE Plant comprises the I-U Characteristic, Thermal Model, H2 Production and H2 Compressor single blocks which are linked by commonly shared variables. On the other hand, the Load Control block diagram content the power and refrigeration controls. The response and performance expected from AE is dependent on its operation conditions. The operation temperature and the power consumption are essential variables that need to be precisely controlled in order to have a complete regulation capacity of the unit.

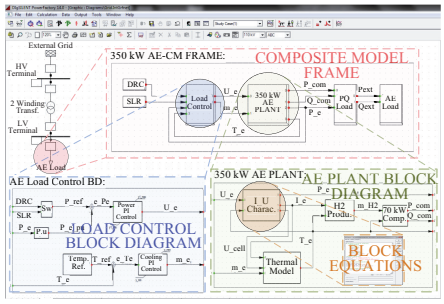

Fig. 5. AE DIgSILENT model representation.

Mechanical, power density and voltage limitation aspects induced the fact of setting the operation temperature at 80°C. The AE operation is controlled acting over two features, the power drawn from the grid and the amount of cooling provided to the unit.

Therefore, a PI determines the electrolyte recirculation mass flow rate (m_e) needed to fulfil the refrigeration requirements and achieving the temperature conditions set by the reference. An additional PI is implemented in parallel acting over the DC voltage applied in the unit terminals with the purpose of having direct control over the power consumption. The large time constant, a natural characteristic of a control variable like the temperature, results in a very slow response compared with that of the power. Thus, even existing a strong dependency between the power consumption and the operation temperature, the temperature variations are so slow that the power control dynamics are barely affected.

Finally in red colour, the composite model frame concatenates the "Load Control" and "AE Plant" block diagrams, the linking block between the DSL model and the physical load connected to the grid and both power reference input blocks. In this study, as the monitoring and control of the grid was not taken into account, the power reference signals were simply modelled as an input array using the measurement file (*.ElmFile) function of DIgSILENT PowerFactory. Again they are recommended to be placed inside the project grid folder, accessible from the data manager window.

B. V2G System

In Fig.6 the main components of the V2G system model are graphically represented. The composite model holds the common models created out of "HC Load Control", "Out-Home Energy Exchange (OEHH)" block diagrams and the "li-ion battery" single block. It also includes the block linking the DSL model and the physical load connected to the grid, the two input signal blocks and the block connecting the switching action with the physical switch in the grid. One of the two input signals provides a daily suburban driving pattern created out of the half-trips considered in [17]. The other one reproduces the DRC signal received by the unit. Both signals were also modelled as an input array. As the green colour highlights, during the "li-ion battery" common model formation the open circuit voltage and the alpha coefficient are introduced as one dimensional matrix-s. The access is through the arrow of the common model window as the picture shows. Inside, depending on the type of functions used for defining the block behaviour, the capability of writing the data will be activated or not.

Concerning the control of the V2G system, already introduced in the Home Charging Point Model section, the vehicle

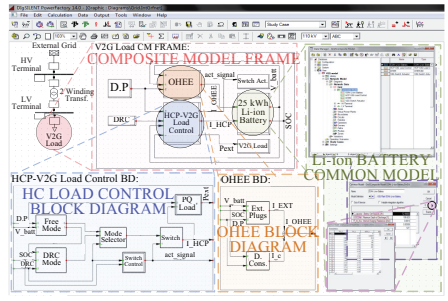

Fig. 6. V2G system DIgSILENT representation.

is assumed free to be plugged whenever the user requires, acting as a normal passive load. However, as soon as it receives a DRC signal, the unit should start acting as an active and controllable load. So as to avoid dissatisfaction and unpleasant fillings from controlled users, the response capacity is constrained to an actuation range of 10%, from 80 to 90 % of the SOC. Within this range, being the vehicle plugged in the home station; the local system control centre should be capable to charge or discharge its battery in a power spectrum limited by the domestic infrastructure capacity.

IV. Results

The performance and response capability of the modelled units were investigated under several operation conditions, within a time range of a day. The point of connection (POC) of each load acquired a special interest in the performed RMS simulations for power flow, because it represents the physical union between the load and the grid.

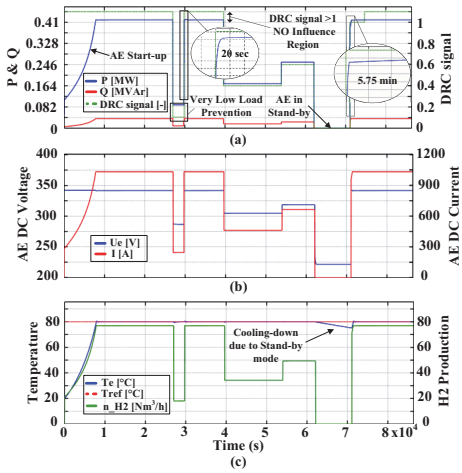

Fig. 7. AE electrolyzer simulation results: (a) P and Q consumptions messured in the POC. (b) AE voltage and current DC values. (c) AE operation temperature and H_2 production.

The AE is characterized for having long start-up times (from 0 to 100%), relatively fast downward power change dynamics and relatively slow upward power change dynamics. This is very much depending on the unit size and the accuracy, amount and availability of the cooling [18]. This may affect directly to the type of regulation that this technology can provide. Fig.7(a) shows the AE system measured active (P) and reactive power (Q) consumption at the POC. The first thing that can be noticed is the long start up time, mainly caused by the need of increasing the operation temperature. The heat generated during the electrolysis process allowed the AE slowly increasing its temperature in order to establish its rated power operation conditions. Later, a DRC signal was received forcing the AE to operate at 10% of its rated power. The down-regulation was performed very fast, in terms of seconds, but as it can be noticed the requested operation point was not possible to be achieved due to the existing limitation at low operating loads. Operating points below the 15-20% of the rated power should be avoided due to the degradation of the hydrogen purity. In this case either the AE continues operating at the stated limit or it switches into standby mode. This mode can also be forced by the DRC signal as shown later on.

In the same illustration two upward power changes are represented, one produced by the returning to the free operation mode (DRC signal>1) and the second forced by the DRC signal itself. The points from where the AE responds to the change in the operation conditions were different in each case, and so the time required for reaching the steady state condition. The reason, as Fig.7(b) shows, is the saturation of the applied DC voltage in the AE terminals, at 342V. Working within a reasonable range of cell voltages, reduces the electrical power and operation costs [4]. Therefore, after the stand-by mode period some extra time was required in order to reach the operating temperature again (Fig.7(c)).

The Li-ion battery response from the V2G model could be almost considered as instantaneous. Fig.8(a) shows the V2G system measured active power (P) consumption at the POC. For figuring out about the charging time required employing the defined connection and power level, an initial full battery charging action was simulated. A possible behaviour of the system was also assessed by the sending of several DRC signals to the home station along the day. In two of them

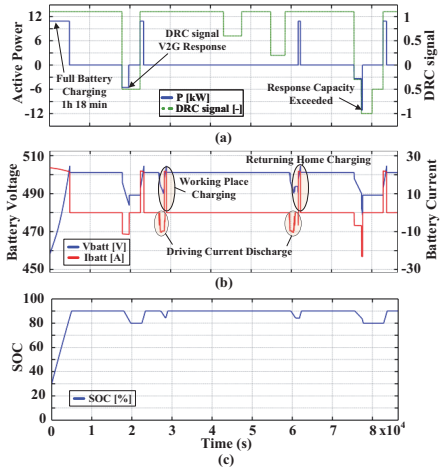

Fig. 8. V2G simulation results: (a) Active power messured in the PCC. (b) Battery voltage and current DC values. (c) State of Charge of the battery.

(early morning and late night) the vehicle was parked and plugged at home ready to respond when the signal to discharge was received. Then, the battery started to discharge the power requested by the signal, up until the permitted SOC limit (80%). As soon as it was reached its active participation was cancelled. Time after, when the load returns to the free operation mode, it tries to recover the energy supplied previously. This effect, repeated by bunches of active loads, may lead to a serious congestion problem in certain specific grids. Another two actuation requests were also received during the analysed working day, but as the vehicle was not available at home, no respond was obtained.

Fig.8(b) gives a clear view of the battery status, in terms of voltage and currents, along the day. It is possible to recognize the current drawn during the driving periods (low, due to the vehicle speed assumed), the amount current drawn by the battery when the vehicle is plugged (at working place or at home) after a trip and the battery voltage fluctuations. Fig.8(c) shows the SOC variation for the analysed case.

V. Conclusion

This paper presents two models, an alkaline electrolyzer and a V2G system, using the dynamic simulation language DSL of DIgSILENT PowerFactory. Both are expected to be useful on impact and demand response analysis of future distribution networks. In a first place, the algebraic and differential equations describing the physical behaviour of each load were introduced. In a second stage, a detailed description of their implementation on DIgSILENT PowerFactory was given. Finally long-term power flow simulations (RMS) were carried out in order to verify their simplicity and manageability.

The obtained results show that under certain control and coordination these two flexible loads have a big potential for future power regulation activities. They are able to accommodate their operation conditions to satisfy certain requirements from the operation and control of the power system. On the other hand, certain limitations on the response speed (large AE systems) and capacity (domestic V2G system case), which may affect the future demand response strategies, have also been stated.

References

[1] Accelerating Green Energy Towards 2020. The Danish Energy Agreement of March 2012. Danish Ministery of Climate, Energy and Building, Mar. 2012.

[2] J.R. Kristoffersen, "The Horns Rev Wind Farm and the Operational Experience with the Wind Farm Main Controller", Copenhagen Offshore Wind, 26-28 Oct. 2005.

[3] B. V. Mathiesen,"100% Renewable Energy Systems in Project Future Climate: the case of Denmark", *in Proc. 2009 5th Dubrovnik Conference on Sustainable Development of Energy Water and Environment Systems*. Guzovic, zvonimir Duic, Neven Ban, Marko (ed.) University of Zagreb.

[4] Ø. Ulleberg, "Modeling of advanced alkaline electrolyzers: a system simulation approach", International Journal of Hydrogen Energy. vol. 28, Issue 1, pp 21-33, 2003.

[5] Ø. Ulleberg, "Modeling Stand-Alone Power Systems for the Future: Optimal Design, Operation and Control of Solar-Hydrogen Energy Systems", PhD Thesis, Norwegian University of Science and Technology, 1998.

[6] N. Gyawali and Y. Ohsawa, "Integrating Fuel Cell/ Electrolyzer/ Ultracapacitor System Into a Stand-Alone Microhydro Plant", IEEE Transactions on Energy Conversion. vol.25, no.4, pp 1092-1101, 2010.

[7] H. De Battista, R.J. Mantz and F. Garelli, "Power conditioning for a windhydrogen energy system", Journal of Power Sources 155 (2) pp 478-486, 2006.

[8] O.C. Onar, M. Uzunoglu and M.S. Alam, "Dynamic modeling, design and simulation of a wind/fuel cell/ultracapacitor based hybrid power generation system", Journal of Power Sources, vol.161, pp 707-722, May 2006.

[9] M. Chen and G.A Rincon-Mora, "Accurate electrical battery model capable of predicting runtime and I-V performance", IEEE Transactions on Energy Conversion, vol.21, no.2, pp. 504-511, June 2006.

[10] R.C. Kroeze and P.T. Krein, "Electrical battery model for use in dynamic electric vehicle simulations", IEEE Power Electronics Specialists Conference (PESC), 2008 , vol., no., 15-19, pp.1336-1342, June 2008.

[11] M. Zheng; B. Qi and X. Du, "Dynamic model for characteristics of Li-ion battery on electric vehicle", 4th IEEE Conference on Industrial Electronics and Applications (ICIEA), 2009, vol., no., 25-27, pp.2867-2871, May 2009.

[12] K. Shimizu, T. Masuta, Y. Ota and A. Yokoyama, "Load Frequency Control in power system using Vehicle-to-Grid system considering the customer convenience of Electric Vehicles", International Conference on Power System Technology (POWERCON), 2010, vol., no., 24-28, pp.1-8, Oct. 2010.

[13] J.R. Pillai and B. Bak-Jensen, "Vehicle-to-Grid for islanded power system operation in Bornholm", IEEE Power and Energy Society General Meeting, 2010 , vol., no., 25-29 , pp.1-8, July 2010.

[14] J.B. Jones and R.E Dugan, "*Enginnering Thermodynamics*" Prentice Hall, 1995, ISBN-10: 0023613327.

[15] J. Larminie and A. Dicks, "*Fuel Cell Systems Explained*", 2nd Edition, John Wiley Sons, 2003, ISBN-10: 047084857X.

[16] J.V. Barreras, E. Schaltz, S.J. Andreasen and T. Minko, "Datasheet Modeling of Li-Ion Batteries"*in Proc. 2012 IEEE Vehicle Power and Propulsion Conf*. pp.830-835.

[17] S. Bashash, S. J. Moura, J. C. Forman, and H. K. Fathy, "Plug-in hybrid electric vehicle charge pattern optimization for energy cost and battery longevity", Journal of Power Sources, vol. 196, no. 1, pp. 541-549, Jan 2011.

[18] J.O. Jensen, V. Bandur, N.J. Bjerrum, S.H. Jensen, S. Ebbesen, M. Mogensen, N. Tophj and L.Yde, "Pre-investigation of water electrolysis, PSO-FU 2006-1-6287", project 6287 PSO, pp. 134, 2006.

Publication C.2

(*Conference Contribution*)

Generation of Domestic Hot Water, Space Heating and Driving Pattern Profiles for Integration Analysis of Active Loads in Low Voltage Grids

Iker Diaz de Cerio Mendaza, Alberto Pigazo, Birgitte Bak-Jensen, and Zhe Chen

The paper is a pre-printed version of the final paper that has been published in the *Proceedings of the Innovative Smart Grid Technologies Europe (ISGT EUROPE), 2013 4th IEEE/PES*, vol., no., pp.1,5, 6-9 Oct. 2013

DOI:10.1109/ISGTEurope.2013.6695288

Generation of Domestic Hot Water, Space Heating and Driving Pattern Profiles for Integration Analysis of Active Loads in Low Voltage Grids

Iker Diaz de Cerio Mendaza[1], *Student-Member*, *IEEE*, Alberto Pigazo[2], *Member*, *IEEE*, Birgitte Bak-Jensen[1], *Senior-Member*, *IEEE*, and Zhe Chen[1], *Senior-Member*, *IEEE*
[1]Department of Energy Technology, Aalborg University, Pontoppidanstræde 101, 9220, Aalborg Ø, Denmark
[2]Dept. of Electronics and Computers, University of Cantabria, Gamazo, 1. 39004. Santander, Cantabria, Spain
idm@et.aau.dk, alberto.pigazo@unican.es

***Abstract*—The changes in the Danish energy sector, consequence of political agreements, are expected to have direct impact in the actual power distribution systems. Large number of electric boiler, heat pumps and electric vehicles are planned and will cope large percentage of the future power consumption at household level. Despite of the well-known flexible service that this kind of loads can provide, their flexibility is highly dependent of the domestic hot water and space heating demand and the driving habits of each user. This paper presents two methodologies employed to randomly generate thermal power demand and electric vehicle driving profiles, to be used for power grid calculations. The generated thermal profiles relied on a statistical analysis made from real domestic hot water and space heating data from 25 households of a typical Danish residential area. The driving profiles instead were formed based on conclusions derived from previous analysis on Danish driving patterns and the driving cycles extracted from the European project ARTEMIS. The obtained random profiles will allow electrical networks in Denmark to be analyzed while maintaining the probability of the original data set.**

***Index Terms*—Domestic Hot Water, Space Heating, Driving Patterns, Heat Pump, Electric Vehicle, Demand Response.**

I. Introduction

The most notable characteristic from the Danish energy sector nowadays is represented by the constant increment of renewable energy. Furthermore, this tendency will be accelerated in order to achieve the energy targets established by last political agreements. In March 2012, the Danish Ministry of Climate, Energy and Building set the new guidelines to speed up the energy sector reconversion [1].

Energinet.dk, the Danish transmission system operator (TSO), has already pointed out some solutions in order to overcome the challenges related to these alternative energy sources. Among them; reinforcement and expansion of the existing power grid, upgrading and extending the power interconnection with the neighbouring countries and improving wind forecasting [2]. As a part of the whole strategy, a complementary solution is getting also attention recent years, the smart grid concept. In late 2012, Energinet.dk together with the Danish Energy Association (Dangrid) published some key recommendations for establishing the mentioned smart grid concept in Denmark [3]. In this report, large effort and attention was focused on indicating the importance of flexibility from future power consumers. This kind of users, also known as prosumers, are distinguished for holding loads with certain storage capability that allows them to modify their power consumption behaviours without affecting drastically their comfort. Thermostatic loads -electric boilers (EB) and heat pumps (HP)- and electric vehicles (EV) are mentioned as possible and feasible alternatives for the Danish case. However, the high power ratting characterizing them make their accommodation challenging for the local operator. The power consumption pattern from these active loads depends on factors like, the type of technology, their way of control, the storage capacity and the atmospheric conditions. A factor, sometimes not precisely assessed but which has crucial importance defining this pattern, is the user consumption habits.

This paper analyse the thermal and driving habits from typical Danish families. The purpose is to evaluate the impact on the power grid, once the mentioned loads are installed.

II. Available Data for the Analysis

A. Domestic Hot Water and Space Heating

The domestic hot water (DHW) and space heating (SH) data, belong to a group of 25 single family houses located in a typical Danish residential area [4]. This data was recorded in 15 minutes intervals during one year. The annual energy consumption, from the considered houses, varies between 4,800 to 20,000 kWh. Fig. 1.a and 1.b shows the SH and DHW average power consumption (q_{sh} and q_{dhw}) respect to the atmospheric temperature (T_{atm}) and the wind speed (v_{wind}). Large season differences are appreciable in the SH demand. The DHW instead remains quite stable along the year. High demand moments seem to be more attractive to be analysed, therefore the methodology will be introduced focusing on them. Wednesday was selected as example.

The authors would like to thank the Danish Council for Strategic Research for providing the financial support for the project Development of a Secure, Economic and Environmentally-friendly Modern Power Systems (DSF 09-067255).

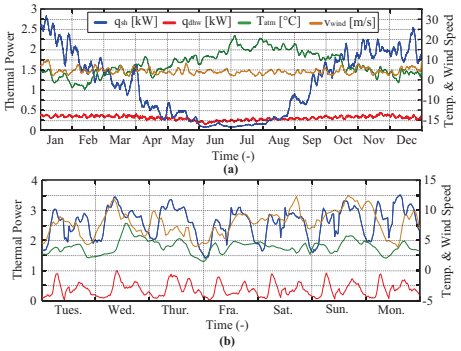

Fig. 1. Average thermal power consumption: (a) over a year, (b) In the first week of January.

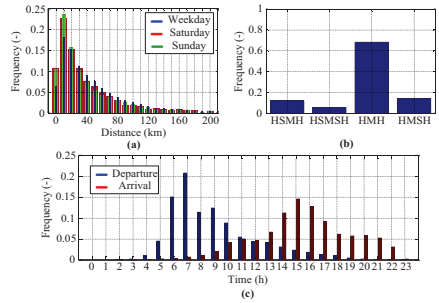

Fig. 2. Danish driving pattern: (a) Driving distance in a day, (b) Tour structure in a day, (c) Departure and arrival time of the first and the last trip in a day.

B. Driving Pattern

The work published by Qu et.al [5], as part of the EDISON project, and by Thorhauge et.al [6] served as a base reference for the driving profile generation task. Fig. 2 summarizes the most relevant information affecting this work. Fig. 2.a and 2.c, extracted from [5], shows the histogram of the total driving distance in a day and the histogram of the departure and arrival time of first and last trip in a day. The information plotted in Fig. 2.b is instead extracted from [6] and it depicts the distribution of the trips in a daily tour structure. The daily tour starts and ends at home (H) and depending on the tour type, trips with main (M) activity (work, school…) or secondary (S) activity purposes are covered in between.

An interesting fact is that a large percentage of the cars drive less than 40 km per day in Denmark. 7 to 8 a.m is the most common time frame to start the first trip of the day and 3 to 4 p.m to conclude the last one. Furthermore, the prevalent tour structure seems to be the one holding two trips per day. From home to place where a main activity is carried out and from here back home again (Home-Main-Home).

Another important source of information became the European project ARTEMIS [7]. From here, different speed based driving cycles were obtained to represent typical urban, rural and motorway trips for standard cars.

III. Methodology for Profile Generation

The data analysis and the profile generation task were carried out in Matlab/Simulink. Concretely, the Statistics Toolbox was used to analyse the SH and DHW consumption data. Since the methodology adopted for creating the SH and DHW power profiles and the driving profiles were different, they will be described separately in this manuscript.

A. Domestic Hot Water and Space Heating

The thermal demand is generally represented by the SH and DHW need from its inhabitants. The DHW consumption, by nature is less continuous and more instantaneous in comparison with the SH one, that is why the data requires to be pre-treated in advance (Fig. 3.a). First, the houses with consumption are separated from the ones without at every time step of the 96 samples on a day. Then, the probability to have consumption is calculated in each time step. Finally only the data from the houses with consumption is going to be considered for the rest of the DHW data analysis.

The statistical part begins with grouping of the data -SH or DHW from the houses with consumption- of the time step considered in a histogram. Then, the coefficients defining the distribution functions facilitated by Statistics Toolbox of Matlab, will be calculated using the maximum likelihood (MLE). As Fig. 4 shows, the result is the formation of the probability density function (PDF) and the cumulative density function (CDF) form each distribution function. This process is repeated for every time step of a day, assessing carefully which distributions fit the data better. Then the best distributions representing the data along the day are finally selected to proceed with the analysis. The intention is to find out the best, or the less bad, distribution function. Therefore, the Kolmogorov-Smirnov goodness test is applied to the anteriorly selected distributions. The distribution functions are submitted to this test, increasing progressively the grade of confidence intervals. As the grade increases the conditions for the distribution functions becomes stricter to comply. It is here when, the ones not respecting the conditions, are discarded remaining the strongest one -or ones- at the end [8]. The Kolmogorov-Smirnov goodness test is valid to find the strongest distribution functions but does not give a clear view of how good the original data is fitted. In this case the graphical method, so called quantile-quantile (Q-Q) plot, is used to find how good is the fitting [9]. As an example, Fig. 5 shows the Q-Q plot from four distribution functions defining the SH consumption at 8 a.m. This method plots the quantiles from the distribution function against the same quantiles from the original data, as the blue crosses illustrate in Fig. 5. The red line instead aims to show how the representation would be if the distribution from the original data and the distribution function would be the same. So in this sense the goodness of the fit will be characterized by how the blue crosses stick to the red line. This procedure is repeated again for every time step of

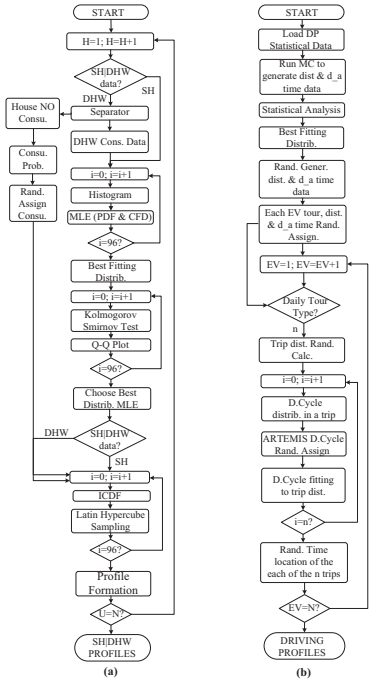

Fig. 3. Flowchart describing the methodology for the profile generation: (a) SH and DHW demand, (b) EV driving.

the day, consciously assessing each fitting. As result the best distribution function will be chosen to represent the original data along the selected day.

The next part is the random generation of the profiles which is approached differently depending on if the data is SH or DHW. The DHW requires first, to assign randomly the household with DHW consumption, on basis to the probability assessment made anteriorly. Then, if a moment of consumption occurs in a household, the amount of it is defined following the same procedure as for the SH. In both cases, this process is based in the Latin Hypercube sampling method [10]. Its main advantage, in comparison to conventional sampling methods for Monte Carlo simulations, is the reduction of the necessary runs for a simulation in order to follow randomly a distribution in an accurate and reasonably way.

Employing the MLE coefficients of the corresponding time step and for the selected distribution function, the inverse cumulative distribution function (ICDF) is portrayed. Afterward, the ICDF is divided into equal probability segments. For this specific case, authors found it convenient to divide the function into ten segments of a little bit less than 10% probability. This is because of the non-consideration of the

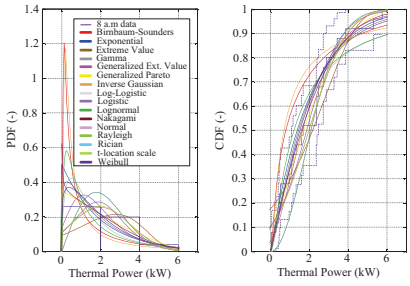

Fig. 4. PDF and CFD of the SH consumption data at 8 a.m time spot.

distribution tails, since in most cases they do not represent the data appropriately. The limits of every segment are mapped to their representative values of thermal power in the y-axis. Once the ten intervals of thermal power are obtained from the correct segmentation of the ICDF, one of them is randomly selected. From the selected interval again a random value is calculated, this will define the SH or DHW demand during that time of the day. This random process is repeated for every time step and also for each user considered. Finally, the formation of the demand profiles is achieved tracking on the set of points generated over the analyzed day.

B. Driving Pattern

The methodology introduced by the flowchart in Fig. 3.b focuses on the driving profiles from EVs which users are located in residential areas. It is assumed that each EV starts the first trip and concludes the last one at home, independently of the amount of trips made in a daily tour. In absence of the original data, the Monte Carlo method was applied to generate new data. The generated data respects the original data distribution, aim of interest in this study. Then, these data is analyzed using the same statistical tools and procedure as the one used for the thermal consumption data. The best distribution functions, for both the driving distance and the departure and arrival time, will be used to generate randomly the values of these variables for the amount of EVs considered. Fig. 6.a and 6.b shows these generated values for a fleet of 80 EVs driving in a typical weekday. The random assignation of these two variables, together with the type of tour that

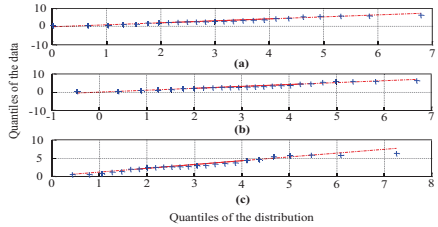

Fig. 5. qqplot-s for the distributions selected at 8 a.m: (a) Generalized extreme value, (b) Normal, (c) Weibull.

the EV performs, is also made randomly for every EV. This information establishes the base for starting the driving profile formation task.

Depending on the type of tour assigned to an EV, this will perform from two to four trips per day (n) with main or secondary purposes. So, according to this, the distance driven in each of the n trips is randomly calculated. Something to take into account is the existing linear dependency between trips. Therefore the summation of the n trips distance has to be in accordance with the total distance driven in the day. The driving style is quite particular and very different from driver to driver, making it very difficult to estimate it precisely. Authors are neither aware of specific statistical studies, centered in the Danish case and focused on: trip destinations, road frequencies, driving styles/cycles and type of vehicles that may have an impact in the way of how to build the driving profiles. In the absence of this information, the speed based driving cycles collected in the European project ARTEMIS were used to simulate the driving behaviours from the EV drivers. The project offers various driving cycles, categorized as urban, rural and motorway, for different class of vehicles. According to the area where the EV is located and the distance traveled, the driving performed during a trip can be differently categorized, even multi-combined. Thereupon the type of driving cycle is randomly distributed over the trip duration. So in accordance to this distribution the ARTEMIS driving cycle is selected and fitted rigorously to the distance previously associated to driving environment.

Once the n trips have been fitted pursuant to the distance travelled and the category of driving, is time to locate them into the out-home time frame of the EV. The driving profile formation task must be characterized by its randomness but also respecting the tour structures introduced at the beginning. Fig. 7 summarizes the logic behind the distribution of the n trips of a daily tour for an EV. Basically, it is assumed that the duration of an activity, either main or secondary, is defined by the time from when a trip ends (t_a) and starts the next one (t_d). In this sense, it is understandable that a main

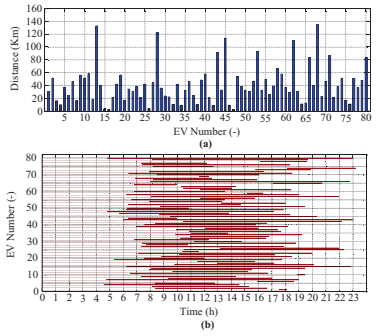

Fig. 6. Randomly generated values for 80 EV: (a) Driving distance in a day, (b) Out-home time frame.

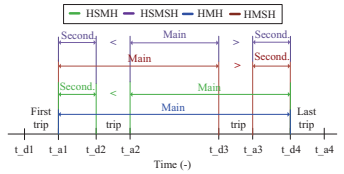

Fig. 7. Trip distribution in a daily tour structure.

activity should have a longer duration than a secondary one. So, independently of the tour structure, the random location of the trips should have that into consideration. This procedure is repeated for every EV driving profile creation.

IV. Results

The behavior from thermostatic loads under high thermal consumption conditions is normally an interesting fact to analyze in grid integration studies. If these loads are not accordingly sized for peak demand moments their normal operation might be affected. Concerning HPs, this is reflected on a continuous operation, reducing the flexibility capable to provide. Hence, the thermal part of this study was decided to be focused on a high SH and DHW consumption day, concretely the second day of January. Fig. 8 gives an overview of the main outcome for the SH demand case. Fig. 8.a shows the distribution of the original data in a histogram form. It is appreciable how during early morning and late evening the data seem to be more concentrated, which might indicate the stand-by mode of the heating systems. During the day time the data seem to be more spread reflecting the diverse need of SH thermal power from the customers. The demand differences are normally associated with the grade of the isolation of the household and the way of evaluating the comfort by each user. After the statistical analysis, it was concluded that the "generalized extreme value" was the best

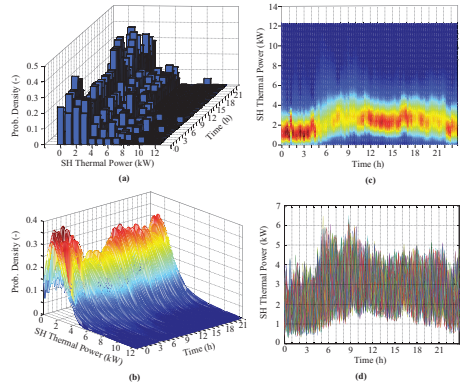

Fig. 8. SH Comsumption Results: (a) Histogram of the SH original data, (b) Data fitting by the "generalized extreme value" distribution function, (c) top view of the Fig. 8.b, (d) SH profiles for 80 households.

distribution function fitting the original data along that day. Fig. 8.b shows graphically the result of this fitting. The best way to see the daily pattern of the SH demand is to rotate Fig. 8.b and look at it from the top, as Fig. 8.c indicates. Based on this, Fig. 8.d presents the randomly generated SH profiles for a total number of 80 households. The obtained profiles follow the original data, evidencing an increment of the SH demand, from 5:30 to 7 a.m, right when the inhabitants start the day.

As it was stated before, the DHW is characterized for being more sporadic and instantaneous way of thermal consumption. Fig. 9.a shows the probability to have DHW consumption, calculated after separating the household with consumption from the ones without. Fig. 9.b shows, in a histogram form, the distribution of the original DHW data from the households with consumption. It is notable the existence of instants where the distribution of data is mainly centralized in a single bin, due to the lack of information in those instants. The statistical analysis performed on these data concluded that the "normal" distribution function was the most suitable to represent the original data. Fig. 9.c shows graphically the result from the fitting, where the lack of information is highlighted by the the pronounced peaks. In severe cases, an interpolation was required in order to smooth the curve shape giving a more realistic sense to the analysis. Finally, Fig. 9.d presents the DHW profiles generated for a total number of 80 households.

Fig. 10 indicates the most relevant results achieved for the EV driving case. Fig. 10.a shows the detailed driving profile from a specific EV holding HMH tour. In both trips a motorway and urban driving cycles can be distinguished which are given in an opposite succession. Fig. 10.b shows the driving profiles from four EV holding different tour structures. It is appreciable the tour differences between EVs, mainly represented by the number of trips and how they are performed. Finally Fig. 10.c presents the obtained driving profiles for a total number of 80 EVs. The profiles maintain the original

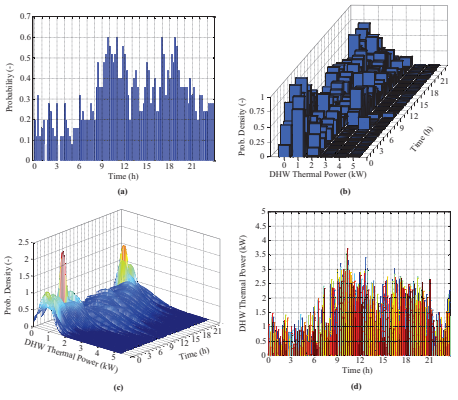

Fig. 9. DHW Comsumption Results: (a) Probability for having DHW consumption, (b) Histogram of the DHW original data, (c) Data fitting by the "normal" distribution fuction, (d) DHW profiles for 80 households.

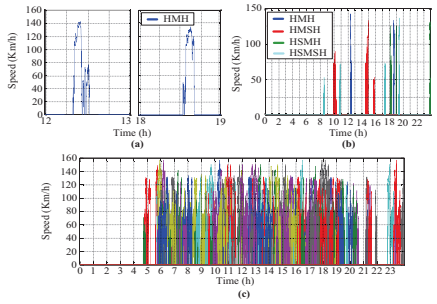

Fig. 10. EV Driving Results: (a) Detailed view of the driving profile of an EV performing HMH tour, (b) Conbination of EVs performing different tours, (c) Driving profiles for 80 EVs.

probability distributions allowing them to be used for a wider analysis of power distribution networks in the future.

V. Conclusion

This paper introduces the two methodologies employed to generate random profiles which simulate demand and behavior from domestic users. The first methodology defines thermal demand profiles relying on the statistical analysis made out of the SH and DHW data from 25 typical Danish households. The second methodology creates EV driving profiles out of the conclusions derived from the EDISON project. The resulted profiles follow the pattern established by the original data allowing to be used to define the power consumption pattern of HP and EV models. Their usage, in the analysis of local distribution networks, will provide a better understanding about the impact of moving from fossil fuels dependent to more electrified heating and transportation systems.

Acknowledgment

Authors acknowledge the Danish Meteorological Institute and the EDISON project for the technical support provided.

References

[1] Accelerating Green Energy Towards 2020. The Danish Energy Agreement of March 2012. Danish Ministery of Climate, Energy and Building, Mar. 2012.
[2] Strategy Plan 2010. Energinet.dk (online).
[3] Smart Grid in Denmark 2.0 - Implementation of three key recommendations for the smart grid network. Dangrid (Danish energy Association and Energinet.dk), Oct. 2012.
[4] Korsgaard AR. Design and Control of Household CHP Fuel Cell System. PhD thesis. Aalborg University. 2006.
[5] Wu, Q.; Jensen, J.M.; Hansen, L.H; Bjerre, A; Nielsen, A.H and Østergaard, J.; "EV Portfolio Management And Grid Impact Study" Edison Report. Mar. 2012.
[6] Thorhauge, M; Kaplan, S and Vuk, G project: Joint activities and travel of household members" in Proc. of the Annual Transport Conference at Aalborg University, 2012. Trafikdage. ISSN 1603-9696.
[7] ARTEMIS:Assessment and reliability of transport emission models and inventory systems. http://www.inrets.fr (Online).
[8] F. J. Massey, "The Kolmogorov-Smirnov test for goodness of fit," Journal of the American Statistical Association, vol. 46, 1951. pp. 68-78.
[9] O. Thas, Comparing Distributions, Springer, 2010, ISBN: 978-0-387-92709-1
[10] C. Lemieux, Monte Carlo and Quasi-Monte Carlo Sampling, Springer, 2009. ISBN 978-0-387-78165-5.

Publication C.3

(*Conference Contribution*)

Intelligent Control of Flexible Loads for Improving Low Voltage Grids Utilization

Peter Thais Bjerregaard, Ireneusz Grzegorz Szczesny, Iker Diaz de Cerio Mendaza and Jayakrishnan R. Pillai

The paper is a pre-printed version of the final paper that has been published in the *Proceedings of the Innovative Smart Grid Technologies Europe (ISGT EUROPE), 2013 4th IEEE/PES*, vol., no., pp.1,5, 6-9 Oct. 2013

DOI:10.1109/ISGTEurope.2013.6695287

Intelligent Control of Flexible Loads for Improving Low Voltage Grids Utilization

Peter Thais Bjerregaard, Ireneusz Grzegorz Szczesny, Iker Diaz de Cerio Mendaza, *Student-Member*, *IEEE*, and Jayakrishnan R.Pillai, *Member*, *IEEE*
Department of Energy Technology, Aalborg University, Pontoppidanstræde 101, 9220, Aalborg Ø, Denmark
idm@et.aau.dk

***Abstract*—Denmark has a plan to increase the amount of renewable energy in the power system in the coming decades. The wind power penetration is scheduled to increase to more than 50% by 2020. To cope with the high amount of fluctuating production, large power system reinforcements would be desirable. In order to limit the need for reinforcements the smart grid concept is getting a lot of attention. As a part of the whole concept, an active demand response is expected from end-consumer's units like heat pumps and electric vehicles. This paper looks into the challenge of controlling these units in an intelligent manner. A centralized control strategy is developed at the secondary substation level in order to maximize the grid utilization thereby reducing the need for grid reinforcements. The simulation results show that the control strategy allows heat pumps and electric vehicles to charge in a time-effective manner while respecting the grid codes.**

***Index Terms*—Heat Pump, Plug-in Electric Vehicle, Demand Response, Low Voltage Grids.**

I. Introduction

Denmark has set-up ambitious goals for becoming fossil fuel independent by 2050. The expected wind power growth, in the already largely penetrated power system, will play an important role to achieve the Danish energy goals. However, for the electrical infrastructure this represents a challenge, as according to the energy targets for 2020, 50% of the power consumption must be supplied from the wind turbines [1]. As the wind power production is dependent upon the weather conditions, solutions are needed to tackle the challenges originated in the system by the large degree of fluctuating generation. The Danish strategy is oriented to transform the actual power system to which it is commonly referred as smart grid. A part of this concept relies in what is commonly known as demand side management [2]. In the future, the end-consumer will be rewarded by planning their consumption in order to assist the power system needs. The consumers may not have direct control of their units, the controllability is handled over to an aggregator via a service contract. The service partner could bring savings to the consumer while generating its own profit by controlling these units according to a market price or a flexibility needed by the distribution and transmission system operators (DSO and TSO).

This paper presents a multi-layer control, designed to treat the end-consumers equally no matter the point of connection (POC) they are connected to. The proposed control strategy gets advantage from the flexibility offered by heat pumps (HPs) and plug-in electric vehicles (PEVs) to improve the grid utilization while ensuring the comfort needs by the users. The stakeholders of the control strategy would therefore be the DSOs and/or future aggregator's while the end-consumers will be the main beneficiaries.

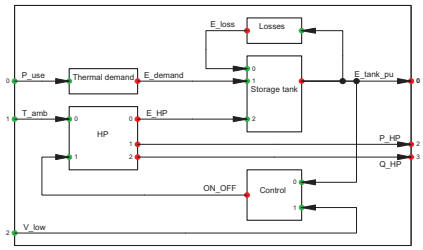

Fig. 1. HP System DIgSILENT Model lay-out.

II. Single Unit Modelling and Control

The whole system analysis was carried out in DIgSILENT PowerFactory. DIgSILENT Simulation Language (DSL) was used to perform the modelling and control of HPs and PEVs.

A. Heat Pump System

In this case, an air-to-water HP interfaced by a storage tank was considered appropriate to supply the thermal needs from a household. Fig. 1 shows the DIgSILENT model lay-out. Two sizes of hot water tank were taken into account, 300 l and 500 l assuming a heat transfer coefficient (*UA*) of 1 W/°C in both. The average energy inside the tank in per unit (E_tank_pu) was calculated based on the first law of thermodynamics:

$$E\_tank\_pu = \frac{E\_i + E\_HP - E\_demand - E\_loss}{E\_cap} \quad (1)$$

where E_i is the initial energy stored in the tank and E_cap the energy capacity of the tank. The water tank was considered energy-less at 55°C and full at 70°C, corresponding to the energy limits of 19.19-24.42kWh for the 300 l one and 31.98-40.70 kWh for the 500 l one.

The energy loss in the tank (E_loss) produced by the temperature difference between water inside and the room temperature was represented by the following equation:

$$E\_loss = \frac{1}{3600} \cdot \int UA \cdot \left(\frac{E\_tank\_pu \cdot E\_cap}{V\_t \cdot C_{p\_w} \cdot \rho \cdot k_c} - T\_r\right) \cdot dt \quad (2)$$

where T_r is the temperature of the room where the tank is installed ($\approx 10°$C), C_p_w is the specific heat capacity of the water (4.187 kJ/kg°C), V_t is the volume of the tank (l), ρ the density of the water (1 kg/l) and k_c a normalization factor.

The energy provided by the HP (E_HP) is calculated as the integral of the thermal power generated by this unit (q_SH).

$$E\_HP = \frac{1}{3600} \int q\_HP \cdot dt \tag{3}$$

The HP was assumed to be driven by an induction motor with a rated power (P_HP) of 3.1 kW and a power factor of 0.98 lagging. A soft-starter was modelled in order to limit the starting current to two times its nominal current for one second shortly after it is turned on.

$$q\_HP = COP \cdot P\_HP \tag{4}$$

The expression of coefficient of performance (COP), function of the ambient temperature (T_amb), was deducted from [3] using a linear interpolation.

$$COP = (0.078 \cdot T\_amb) + 2.791 \tag{5}$$

The thermal energy consumption (E_demand), in form of domestic hot water (DHW) and space heating (SH), was estimated integrating the thermal power demanded by the user (P_use) in kW.

$$E\_demand = \frac{1}{3600} \int P\_use \cdot dt \tag{6}$$

The control of the HP is based on regular hysteresis control. The HP turns off when the water tank energy reaches 1 p.u and turn on when the tank energy drops to 0.828 p.u (80% of the bandwidth). The HP has also embedded an voltage emergency control, which allows unit to adapt to the severe under-voltage issues that occur in the grid. If a minimum voltage drop in the grid (V_low) is severe enough, the HP control would gradually lower the upper and lower bands: In case of the lower band, this would be up to 0.785 p.u (the 20% of the bandwidth remaining) in order to ensure that the HP is able to stay off during certain time. In order to avoid excessive sensitivity of the emergency control, an adaptive delay was implemented to decide the correct time of actuation.

As soon as the voltage drop is cleared, the HP control steps instantly from 0.785 to 0.828 p.u, the start-up currents from many HPs could coincide creating an undesirable situation.

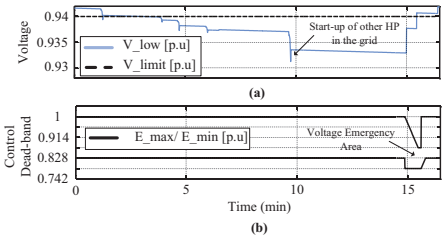

Fig. 2. HP Emergency control illustration.

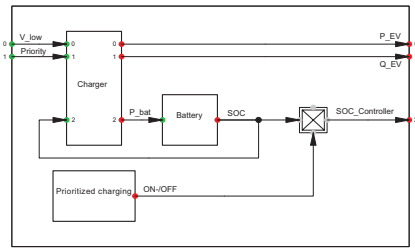

Fig. 3. PEV System DIgSILENT Model lay-out.

To avoid this effect the HP control is tuned to gradually increase the lower energy limit. Fig. 2 is an illustration of the emergency control operation.

B. Plug-in Electric Vehicle System

Fig. 3 shows the DIgSILENT Model lay-out of the PEV system. The li-ion technology and the size of 24 kWh were considered as a reasonable modeling approach, taking into account the Danish case. The battery was represented with an impedance type model, where the relation between the battery terminal voltage and state of charge (SOC) is linear [4]. Due to battery degradation reasons the SOC was constantly maintained between 0.2 and 0.9 p.u, being calculated as:

$$SOC_{pu} = SOC_i + \frac{\frac{C_{max}}{3600} \cdot \eta_b \cdot \int P\_bat \cdot dt}{SOC_{max}} \tag{7}$$

where SOC_i is the initial battery SOC in p.u, C_{max} the maximum battery capacity in kWh, η_b the battery efficiency -given 0.993 p.u- and SOC_{max} the maximum SOC in kWh.

The model also incorporates the possibility of self-imposing the priority to charge the PEV battery. This option could applied by a user, careless by the fact of being penalized, to charge his PEV on a highest priority based on his driving requirements (Prioritized charging).

Regarding the power charger located at the household level, an off-board 3-ph/400 V type represent a feasible solution for this type of analysis. Based on [4] a continuous charging capacity regulation was assumed, allowing the charging power (P_bat) variate between 0 to 11kW.

$$P\_bat = \eta_c \cdot \int S_{charge} \cdot dt, \quad 0 \leq P\_bat \leq 11\ kW \tag{8}$$

where η_c is the battery charger efficiency in p.u ($\approx$ 0.98 p.u) and the S_{charge} is an internal variable of the PEV control that depends on $Priority$ control signal and V_low signal. As it will be explained further on, both signals are sent to the PEV load by the sub-system controller. The logic behind the generation of S_{charge} variable is represented below.

$$\begin{aligned} if \quad V_{low}(t) &> V_{lim} \quad \rightarrow \quad S_{charge}(t) = priority(t) \\ else \quad V_{low}(t) &\leq V_{lim} \quad \rightarrow \quad S_{charge}(t) = -1 \end{aligned} \tag{9}$$

where V_{lim} is the minimum voltage drop allow in the entire grid in p.u. The voltage limit set by the standard EN 50160 is

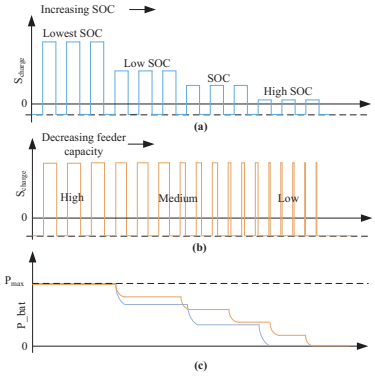

Fig. 4. (a) $Priority$ signal influence in S_{charge} variable, (b) V_low signal influence in S_{charge} variable, (c) S_{charge} variable influence in P_bat.

$\pm 10\%$. In this case, a more conservative value, of $\pm 6\%$, was selected based on practical experiences from DSOs.

Fig. 4 shows a graphical representation of S_{charge} dynamics under the influence of $Priority$ and V_low and the impact produced in P_bat as a consequence. The amplitude of the S_{charge} variable is influenced by the $Priority$ control signal, which represents a charging priority of the PEVs connected in the subsystem based on their SOC. This means, as Fig. 4.a shows, that higher the SOC of a PEV the lower will be the amplitude of the received $Priority$ signal, decreasing the P_bat capability. On the other hand, the duty cycle of S_{charge} depends on the V_low signal, which represents the feeder capacity reflected by the voltage levels. This means, as Fig. 4.b shows, that if the voltage limits violations occur frequently -becoming S_{charge} negative-, the S_{charge} duty cycle will be decreased until the PEV P_bat adapts to the constrains of the feeder. Fig .4.c illustrates the effect of both signal in P_bat.

As the rated power of the PEV charger is high, this has the ability to measure and regulate the total household electricity consumption. The PEV control was equipped with a continuous current control which operates embedded in the same voltage control concept. If the total current demand of the household (I_H) becomes higher than a rated current allowed by the installed fuses (I_{rat}) -assumed to be 35 A-, the charger reduces the charging power acting over duty cycle of S_{charge}.

$$\begin{aligned} if \quad I_H(t) \quad &< I_{rat} \quad \rightarrow \quad S_{charge}(t) = priority(t) \\ else \quad I_H(t) \quad &\geq I_{rat} \quad \rightarrow \quad S_{charge}(t) = -1 \end{aligned} \tag{10}$$

III. Local Control Strategy

The control structure is divided into three layers, as it is presented in Fig. 5. The bottom layer represents the individual control of the considered units, HPs and EVs. Assuming that in every household a smart meter is available, the voltage at the POC is measured and send it to the sub-system controller. The inter-layer holds the sub-system controllers, which act as a data-hub gathering signals and parameters from the active loads belonging to their monitoring area and actuating in consequence. The local grid control is depicted by the top-layer. The main task of this controller is to gather the average energy from every sub-system and accordingly prioritize among them.

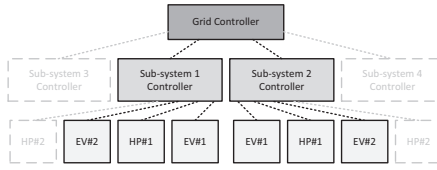

Fig. 5. System Control Overview.

A. Sub-System Control

Every sub-system controller; a) processes the gathered data, b) calculates the average energy supplied to the sub-system, in per unit (p.u), c) creates priority list of the connected EVs according to the voltage in the POC and the state of charge (SOC), d) sends the lowest voltage measured in the controlled area to all the HPs and PEVs connected to the sub-system and e) sends the ranked list of EVs and the average energy of the sub-system to the grid control.

The PEVs have an important advantage with respect to the HPs in terms of flexibility. Despite offering the possibility of controlling them ON/OFF, it is possible to vary the charging power capacity while they are ON. The considered HP technology instead does not allow this. Either the HP consumes at rated power while it is ON, or it has to be shut down. For this reason the PEVs have a greater collaboration with the sub-system controller.

The sub-system controller monitors constantly the amount of PEVs connected in the controlled area and their SOC. Then, it ranks the connected PEVs from lowest to highest SOC. Based on this, the controller generates and assigns the amplitude of the $Priority$ control signal which is send to every PEVs. This signal is constantly being adapted by the sub-system controller according to the SOC of the connected PEVs and to satisfy the voltage constrains of the monitored part of the grid. Another task carried out by sub-system control is to find out the lowest voltage among the controlled POC (V_low) and communicated to all the active loads. As it was explained in the previous sections, if the signal is lower than V_{lim}, HPs will switch to emergency mode and the duty cycle of S_{charge} variable of PEVs will be decreased.

The sub-system aims to treat the end-consumers equally no matter the point of connection (POC) they are connected and the constraints on it. This is more notable if we consider the PEVs, where the P_bat of the different PEVs track each other to ideally complete their charging in the most fair manner for everyone. Every sub-system controller is able to utilize at maximum capacity its area until a grid violation occurs.

Fig. 6 is an illustrative example of how the sub-system controller operates. Let us imagine that in a weak part of certain low voltage (LV) grid, a sub-system controls the charging operation from five PEVs. Fig. 6.a shows the SOC

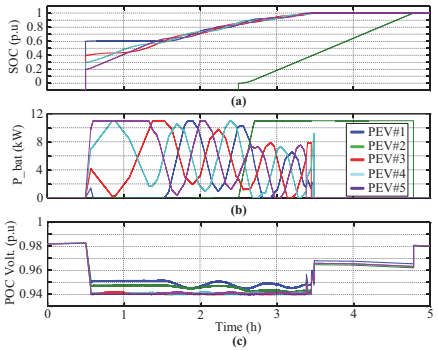

Fig. 6. Illustrative example of the Sub-System Control, (a) SOC, (b) P_bat, (c) Voltage at the POC.

of the considered PEVs when they are plugged-in at home. Before the PEVs arrive home, the SOC is represented with a negative value. At 0:30 a.m four of the PEVs arrive at the same time at different locations in the feeder and with different SOCs. The PEV number 4 and 5 have the lowest SOC, which means they have higher priority to be charged at higher P_bat than PEV 1 and 3. As they charge faster, at some point their SOC become higher than EV 3, which causes a shift on the priority list, see Fig. 6.b. At 2:30 a.m, PEV 2 connects to the grid with an empty battery. Therefore it receives the highest the priority, making the P_bat of PEV 1,3,4 and 5 decrease while the one of number 2 stays at the maximum allowed by the grid conditions. As Fig. 6.c shows, the sub-system control keeps the voltage in the different POC of the grid over the allowed limit while charging the PEVs in a fair manner.

B. Grid Control

The grid control defines which sub-systems need to be prioritized based upon the average energy stored in the HP water tanks and EV batteries. In practice it is responsible of dividing the total capacity between the sub-systems in order to equalize the charging time of the PEVs connected in the whole LV grid. By doing so, all PEVs will try to assist the grid needs when voltage violations occur, even if it is the case of other sub-system where the PEVs does not belong. HPs, due to power controllability issues stated previously, they are not suited for this way of control either. They will only switch to the emergency mode while the lowest voltage in the subsystem violates the established limit. The grid control has a higher relevance in grids with large differences between the relative strength of the feeders.

Fig. 7 illustrates the operation of the grid controller. The controller creates a list of all sub-systems connected to the grid and calculates the average energy stored (E) in the HP water tanks and PEV batteries. Based on the estimated E levels the lowest value (E_L) is found and compared it to the remaining E levels. Then the controller sends a power limitation signal C_{lim} to every Y sub-system controller to act in consequence.

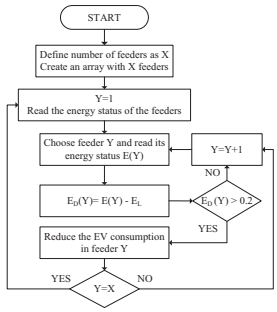

Fig. 7. Flowchart of Grid Control strategy.

C_{lim} in p.u is generated based on the linear function:

$$C_{lim}(Y) = -K_s\ (E(Y) - E_L) \tag{11}$$

The higher C_{lim} value is the more power is reduced in the Y subsystem. The slope of the function (K_s) would need to be adjusted accordingly to every type of grid.

IV. Case Study

A LV distribution grid located in typical Danish residential area was considered in this analysis. Through a 630 kVA transformer 166 private houses are supplied with electricity. The grid topology is radial, however each feeder is equipped with an additional cable that connects it with the adjacent feeder. Generally the tie points of the additional cables are out of service, except during abnormal service conditions. According to the estimated load penetration, 83 HPs and 45 EVs were randomly distributed across the LV grid. Therefore, a number of 9 sub-systems was found suitable for handling this amount of loads, being each subsystem responsible for a maximum of 12 HPs and 6 PEVs. Fig. 8, besides of showing the LV grid lay-out and the sub-systems location, shows how the units are distributed along the different feeders. It also shows the voltage drop results obtained from a load flow analysis. It is inferred that the weakest feeder is number 6, which holds a significant voltage drop of 0.93 p.u.

In order to challenge the control strategy, a winter weekday typically characterized by high thermal consumption period which demands continuous and heavy operation of the HPs.

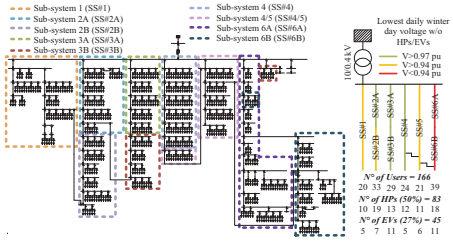

Fig. 8. Danish LV grid and sub-systems lay-out.

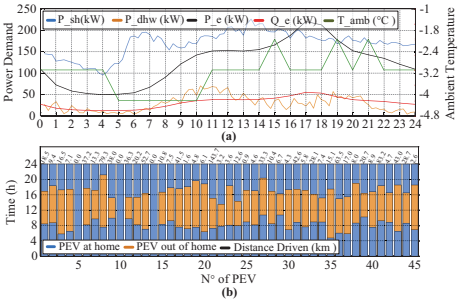

Fig. 9. Data for the case study:(a) Aggregated power demand and T_amb, (b) PEVs driving pattern.

Fig. 9.a shows the aggregated thermal power demand, in domestic how water (P_dhw) and space heating (P_sh) terms, the aggregated active and reactive power demand (P_e and Q_e) and the T_amb. The thermal power demand was generated out of [5]. Fig. 9.b shows the driving patterns created out of the statistical analysis made in [6]. The home departure/arrival time and the distance driven in the day are illustrated for every PEV considered.

V. Results

Fig. 10 shows the obtained simulation results where a comparison between an uncontrolled and controlled grid is made. Fig. 10.a and 10.b show the aggregated charging behavior from the PEVs of every sub-system (SS#) under no-control and using the proposed control strategy. It can be observed for the uncontrolled case that the vehicles tend to plug instantly, as soon as they arrive home in the late afternoon hours. Under the influence of the control strategy the PEVs tend to wait and start charging during the instants when the grid is less stressed, late evening and early morning. A better distribution of the HP power consumption is notable in Fig. 10.c in the controlled case, even if it is not as significant as for PEVs. This is consequence of the lower influence from the grid control on the HPs and the lack of flexibility that they are able to provide in high thermal demand periods.

Fig. 10.d and Fig10.e shows the MV/LV transformer loading and the voltage drop in the weakest point of the weakest sub-system -sub-system SS#6- once all the loads in the system are considered. It is notable that in a uncontrolled situation high consumption is grouped in peak demand period creating voltage drops in SS#6 that almost reach the limit imposed by EN 50160. The grid control presented the ability to be able decrease the transformer loading, between 4 p.m and 7 p.m, keeping the voltage above the reference of 0.94 p.u. The reason behind is that the grid control does not allow to charge PEVs between 4 p.m and 9 p.m because of the low voltage levels. The proposed aggregated grid control has thus presented the ability to provide an effective voltage regulation and flexible demand utilization thereby ensuring intelligent demand side management in local distribution grids.

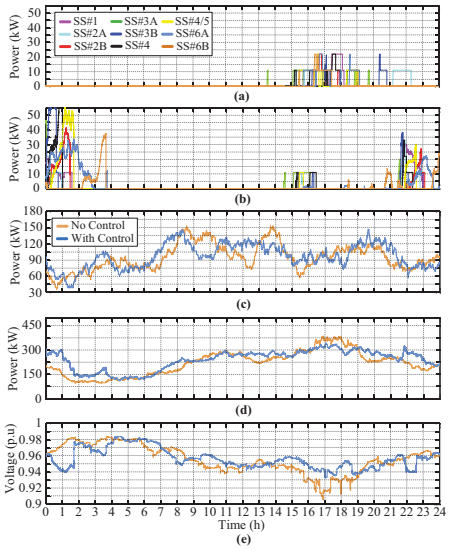

Fig. 10. LV Grid Results: (a) No controlled PEV aggregated power demand, (b) Controlled PEV aggregated power demand, (c) HP aggregated power demand loading, (d) Transformer loading, (e) Minimum grid voltage.

VI. Conclusion

The increasing penetration of HPs and PEVs in the local distribution grids is a highly challenging scenario for the utilities. In this work, a centralised grid control at the LV substation transformer is proposed to provide intelligent demand side management of HPs and EVs. The grid controller connects several sub-systems on different radials, which coordinate the operation of HPs and EVs in the local nodes to fulfill both grid and user comfort requirements. The results show that the proposed control design makes possible to utilize the flexibility offered by these units. The power consumption is shifted from highly congested periods to less loaded periods, thereby the maintaining the voltage levels within acceptable limits.

References

[1] Ministry of Climate Energy and Building. (2011, Feb.). Energistrategi 2050 - fra kul, olie og gas til groen energi. (in Danish).

[2] Dangrid (Danish energy Association and Energinet.dk). (2012, Oct.). Smart Grid in Denmark 2.0 - Implementation of three key recommendations for the smart grid network.

[3] Dansk varmepumpe industri A/S. http://www.jordvarme.dk/ [Online].

[4] M. Yilmaz, "Review of battery charger topologies, charging power levels and infrastructure for plug-in electric and hybrid vehicles,"IEEE Trans. on Power Electronics, vol. 28, pp. 2151 2169, May 2013.

[5] A. R. Korsgaard, "Design and control of household chp fuel cell system,"Ph.D. dissertation, Aalborg University, 2006.

[6] W. Qiuwei, A. H. Nielsen, J. Østergaard, T. C. Seung, F. Marra, Y. Chen, and C. Trholt, "Driving Pattern Analysis for Electric Vehicle (EV) Grid Integration Study, in *Proc. 2010 IEEE PES Innovative Smart Grid Technologies Conference Europe*.

Publication C.4

(*Conference Contribution*)

Probabilistic Quantification of Potentially Flexible Residential Demand

Konstantinos Kouzelis, Iker Diaz de Cerio Mendaza and Birgitte Bak-Jensen

The paper is a pre-printed version of the final paper that has been published in the *Proceedings of the PES General Meeting | Conference & Exposition, 2014 IEEE*, vol., no., pp.1,5, 27-31 July 2014

DOI:10.1109/PESGM.2014.6938836

Probabilistic Quantification of Potentially Flexible Residential Demand

Konstantinos Kouzelis, *Student-Member*, *IEEE*, Iker Diaz de Cerio Mendaza, *Student-Member*, *IEEE*, and Birgitte Bak-Jensen, *Senior-Member*, *IEEE*,
Department of Energy Technology, Aalborg University, Pontoppidanstræde 101, 9220, Aalborg Ø, Denmark
{kko, idm}@et.aau.dk

***Abstract*—The balancing of power systems with high penetration of renewable energy is a serious challenge to be faced in the near future. One of the possible solutions, recently capturing a lot of attention, is demand response. Demand response can only be achieved by power consumers holding loads which allow them to modify their normal power consumption pattern, namely flexible consumers. However flexibility, despite being constantly mentioned, is usually not properly defined and even rarer quantified. This manuscript introduces a methodology to identify and quantify potentially flexible demand of residential consumers. The procedure is based on non-flexible consumer clustering and subsequent statistical analysis. Consequently, the power consumption pattern of a flexible consumer is compared to a 3D probability distribution created by the previously referred methodology. The results show a strong relationship between the amount of potential flexibility and the probability of providing it. Finally, it is concluded that residential flexibility is most likely to be offered during transitions between summer and winter.**

***Index Terms*—Flexibility, Active Load, Heat Pump, Residential Demand, Demand Response.**

I. Introduction

The Danish power system is year by year experiencing a growth of the wind power penetration. The power interconnection between neighbouring countries is nowadays decently employed by the transmission system operator (TSO) for system balancing purposes. However, its future feasibility may be limited if the energy policies from the adjacent countries are as ambitious as the Danish one. Therefore, the need for alternative solutions has originated a big interest for the smart grid concept. In October 2012, Dangrid -partnership between Energinet.dk and the Danish Energy Association- released some key recommendations for implementing the smart grid in the Danish case. In this report, the importance of having active demand and particularly the flexibility, which consumers could offer in the future, was highlighted [1].

Thermostatic loads -electric boilers (EB) and heat pumps (HP)- and electric vehicles (EV) are normally appointed as possible sources of flexibility at the residential level. In this sense, residential consumers employing this type of loads should be encouraged to aid the systems needs at local or global level. In spite of the potential which these loads introduce, the comfort requirements of the users must be ensured at all times.

The flexibility term is constantly used for this matter but is not always well defined and quantified. Different power consumers have different grades of flexibility. Furthermore, consumers of the same class are subject to further grouping depending on the nature of their flexible devices. Thus, in this paper, the classification of electricity consumers is a prerequisite so as to identify which flexibility is available from which group. Several clustering techniques have been applied for consumer classification like the Kohonen self-organizing map [2], the k-means and the fuzzy k-means algorithms, hierarchical clustering and the modified follow the leader [3]. Additionally, agglomerative hierarchical clustering and adaptive vector quantization were examined in [4]. Various cluster adequacy measures including the Davies Bouldin indicator (DBI), the Dunn index, the clustering dispersion indicator, the similarity matrix indicator and others have been implemented to assess the validity of the clusters [3], [4].

In this paper, a new methodology for identifying and quantifying potentially flexible demand at the residential level is introduced. This approach is based on clustering of non-flexible consumers, subsequent statistical analysis and pattern comparison. In the tackled case, the power consumption pattern of a residential consumer holding a HP and a photovoltaic (PV) is compared to a 3D probability distribution. This is created from the non-flexible consumers, by exploiting the similarity -in terms of energy consumption and power pattern- to the flexible consumer. In this perspective, additional real measurements -for capturing the flexibility- can be replaced by a probabilistic virtual measurement. Hence, an advantage of its implementation is the diminution of the measurement data at the household level.

II. Available Data

Hourly power consumption data in kilowatt hour (kWh) for the year of 2012 were obtained for this study. The data referred to 223 consumers, primarily supplied by a 20kV radial feeder in the area of Støvring in Denmark. Particularly, eleven 20kV/400V transformers radially provide the power supply at low voltage level. Moreover, similar data for a residential consumer located in a neighbouring feeder were acquired. However, this consumer had also an installed HP, all year, and

The authors would like to thank the Danish Council for Strategic Research and the ForskEL program which provide the financial support for the "Development of a Secure, Economic and Environmentally-friendly Modern Power Systems" (DSF 09-067255) and the "TotalFlex" project respectively.

a PV operating from the 15th of August. The utility reported that no HP, PV or EV installations were present among the 223 consumers. After filtering bad measurements, 166 non-flexible consumers plus the flexible one remained.

III. Methodology

Potential flexibility is defined as the aggregated demand of all the loads which can be described as flexible in the smart grid sense. Moreover, any dispersed generation should also be subtracted from this amount. The result, depending on its pattern, might be flexible or not. In order to identify the potentially flexible demand, a flexible consumer is compared with other non-flexible consumers with similar demand patterns.

The procedure is depicted in Fig. 1.a. The first step, is to identify which consumers have flexible loads and/or dispersed generation and which ones do not. Since the targets are major residential loads/generators, this information should be readily available by a utility. Thus, the consumers are divided into flexible and non-flexible consumers. Then, the non-flexible consumers are clustered. This is a very important step as the flexible consumer will be later classified depending on this clustering. On the grounds that, only residential demand is of interest, a pre-clustering stage in terms of aggregated energy consumption is necessary, so as to exclude any industrial and/or large commercial consumers. Regarding the aggregation, a time interval should be decided (e.g. month). For this interval, the patterns to be pre-clustered are additionally daily averaged along with the flexible consumer under study. The latter will be used for the pattern clustering at a later stage. The choice of the time interval will also be discussed later.

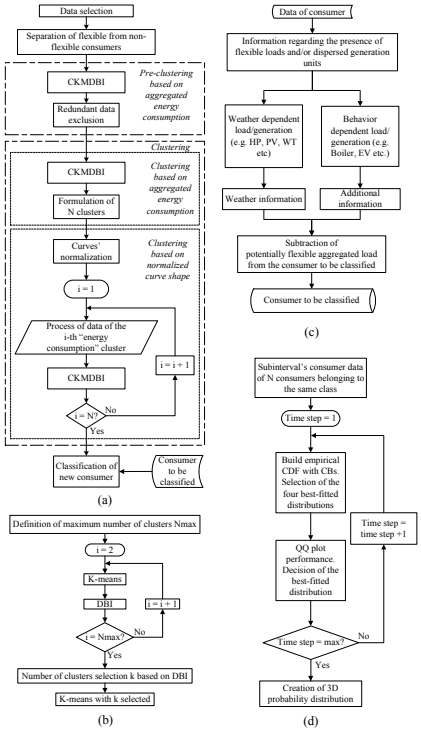

Fig. 1. Flow charts: (a) Clasiffication methodology, (b) CKMDBI algorithm, (c) Flexible consumer data processing, (d) Statistical analysis.

As far as the pre-clustering/clustering is concerned, the k-means algorithm [5] and the DBI index [6] are iteratively implemented as shown in Fig. 1.b. K-means clustering aims to partition N observations into K clusters. For doing so, the objective function to be minimized is:

$$J = \sum_{n=1}^{N} \sum_{k=1}^{K} r_{nk} |x_n - \mu_k|^2 \tag{1}$$

where N is the number of datapoints, k is the number of clusters, $r_{nk} = 0, 1$ depending on whether the n_{th} datapoint belongs to the k_{th} cluster, x_n is the n_{th} datapoint and μ_k is the center of the k_{th} cluster. K-means can be perceived as a two stage iterative optimization procedure initially minimizing J in respect to r_{nk} and subsequently in respect to μ_k.

To evaluate the validity of the k-means clustering, a cluster separation measure is needed. Thus, the DBI index is implemented. The calculation of the DBI is presented as follows:

$$DBI = \frac{1}{K} \sum_{k=1}^{K} R_k \tag{2}$$

where K is the number of clusters and R_k = maximum of R_{kj}, $k \neq j$. R_{kj} is calculated as:

$$R_{kj} = \frac{S_k + S_j}{M_{kj}} \tag{3}$$

S_k being:

$$S_k = \left\{ \frac{1}{T_k} \sum_{j=1}^{T_k} |x_j - \mu_k|^2 \right\}^{\frac{1}{2}} \tag{4}$$

where T_k is the number of observations in the k_{th} cluster, x_j is the j_{th} observation of the k_{th} cluster and μ_k is the center of the k_{th} cluster. M_{kj} is given as:

$$M_{kj} = \left\{ \sum_{i=1}^{N} |\mu_{ik} - \mu_{ij}|^2 \right\}^{\frac{1}{2}} \tag{5}$$

where μ_{ik} is the i_{th} component of the N-dimensional centroid of the cluster k.

To combine the above mentioned algorithms, a maximum number of clusters is firstly selected. This number is subjectively chosen, nonetheless it should be a realistic number which serves practical purposes for a utility [3]. Secondly, the k-means algorithm is applied for $k = 2$ and the DBI is utilized to assess the validity of the clusters constructed. This procedure is iteratively performed until the maximum number of clusters is reached. The lowest DBI value shows

the optimum number of clusters for the corresponding dataset. Thirdly, the k-means clustering is once again applied with k being equal to the aforementioned lowest DBI value. To conclude with, this algorithm will be addressed as "Combined K-means & DBI (CKMDBI)" for the rest of the paper.

Following the pre-clustering stage, a two-stage clustering of the remaining consumers is performed. In the first step, consumers are clustered with respect to their aggregated energy consumption. In the second step, these clusters are sub-clustered with respect to the average daily consumption pattern of their observations. To do so, the patterns are first normalized by their daily maximum value. Finally, all clusters are defined and the flexible consumer under study is assigned to the cluster with the shortest Euclidean distance to him/her. This is done primarily in terms of energy consumption and subsequently according to the consumers normalized demand pattern. Nevertheless, the flexible consumer's demand should first be filtered before classification. Since the consumer has additional flexible loads and/or generation, these should be excluded prior to the class assignment. For this, information regarding the presence of such devices is necessary. These devices can be characterized as weather dependent or behaviour dependent based on their operation. Although behaviour dependent devices require activity information for extracting their average signature from the average demand curve, this is not the case for the weather dependent ones. Assuming that the weather data are available, it is feasible to identify the extra demand added by these loads, once the days with prevalent dispersed generation are excluded. Accordingly, these days are excluded from the clustering process as well. This is also the reason why the time interval for aggregation should be chosen to serve the needs illustrated here. In conclusion, the refined average demand curve is approximately free of any additional loads and/or generation and hence, it can be classified as already presented. The whole process is shown in Fig. 1.c.

Having classified the N non-flexible consumers and the flexible consumer in the chosen time interval (e.g. month), a comparison between them in subsequent time intervals can take place. However, a validity test of the classification in those intervals should be performed. The idea is to repeat the process of Fig. 1.b and keep track of how many of the N consumers remain in one class. This is equivalent to assigning a probability that a consumer will not change his/her initial behaviour in future time intervals. The aim is to account only for the main behavioural trend of the N non-flexible consumers. Thus consumers, who initially belonged to the N consumers and additionally belong to classes having a large proportion of these N consumers in subsequent intervals (e.g. months), are kept and aggregated. This will result into a new M non-flexible consumer group ($M<N$), discarding the rest.

At this point, the comparison between the selected M consumers and the flexible consumer should be realized. This comparison will most likely be of interest for a subinterval (e.g. day). Assuming that the behaviour of the M consumers does not drastically change within the interval under study, the comparison can be performed in that subinterval. After choosing the subinterval of interest the methodology described in Fig. 1.d is applied. Firstly, the M consumers' data are selected and for each time step of the subinterval the empirical cumulative distribution function (ECDF) is constructed along with its confidence bounds (CB). Secondly, a number of preselected probability distribution functions (PDF) are chosen and fitted to the data. The best four distributions -at each time point- in terms of being within the predefined CBs are chosen whereas the rest are discarded. Thirdly, these distributions are subject to a Quantile-Quantile plot (QQ plot) assessment [7]. The best fitting distribution for each time step is chosen. Lastly, after acquiring all of the best fitted PDFs for each time spot, a 3D probability distribution is readily available which will serve for comparison between the M consumers and the flexible consumer.

IV. Application

The previously defined methodology was applied to the available data. Firstly, the data selection procedure accounted for 166 consumers and a flexible consumer for processing. The application was conducted only for weekdays but it can be likewise performed for weekends as well.

Next, a time interval of one month for aggregation was selected. According to Fig. 1.c, in order to subtract the "bias" of the HP operation from the average demand profile of the flexible consumer, weather data should be taken into account. As February is the coldest month of Denmark, it can be easily concluded that the HP will be operating most of the time. Thus, it affects more the magnitude of the average demand profile -for that month- than the shape of it. In compliance with this conclusion, every day of February was split in 6 four-hour intervals. For each interval the minimum value was found and the minimum values for equivalent intervals throughout the month were averaged. The assumption is that the minimum value in a 4 hour interval will most likely be a value where roughly only the HP and the baseload are operating. Hence, 6 values -one for each interval- were obtained representing the baseload and the HP operation on average for that month. Each of the 6 values was representative for the whole interval. The same idea was also applied in the hottest month, July, in order to estimate the value of the baseload itself, assuming that the baseload remains constant throughout the year. However, this time no intervals were built as the baseload was also assumed to be constant throughout the day. Additionally, the PV was not installed at that time point. The estimation of the baseload was 158,18 Watt. Consequently, the HP plus baseload values were subtracted from the average curve of the flexible consumer in February. The baseload, as estimated in July, was re-added. Finally, the average February curve of the flexible consumer was available for classification.

In the pre-clustering stage the maximum number of clusters was chosen to be 10 (the same value was chosen also for subsequent uses of the CKMDBI algorithm). However, instead of concentrating at the lowest DBI value, as done in the clustering steps, a different interpretation of the DBI was given. Since only residential consumers are of interest, the

"saturation" point of the DBI values was found and utilized. Clusters containing industrial or large commercial consumers -7 in total- were easily identified and removed as redundant information as depicted in Fig. 2.a. Consequently, the energy clustering step was conducted resulting to 4 clusters, as shown in Fig. 2.b. The flexible consumer was classified in one of those 4 classes and consequently that particular class was clustered in terms of normalized curve shape. The 3 resulting clusters along with their centroids are illustrated in Fig. 2.c and Fig. 2.d accordingly. After normalizing the flexible consumer's curve, he/she was classified in one of the 3 classes. This class consisted of 89 consumers who were the reference group of the flexible consumer in the current month. The 3D probability distribution of February days was built based on this reference group. In subsequent months, these 89 consumers were refined as explained in section II. For instance, in May -starting again from the 166 consumers and repeating the analysis of Fig. 1.a- only 75 out of the 89 consumers had similar aggregated energy consumption and only 70 out of these 75 had a similar demand shape. Thus for May days, the reference group for constructing the 3D probability distribution were these 70 consumers.

Afterwards, several probability distributions -Normal, Weibull, Generalized Extreme Value etc.- were selected for fitting the data and eventually creating the 3D probability distribution for a day. This distribution was used for quantifying the potential flexibility of the flexible consumer.

V. Results and Discussion

The result of the methodology presented above is a 3D probability distribution, which represents the non-flexible demand of a consumer who is similar to the flexible consumer under study. The boundaries of the 3D probability distribution are defined by areas of probability (AP):

$$P(a < X < b) = \int_a^b f_X(x)\,\mathrm{d}x \tag{6}$$

where *a*, *b* are ordinates, *X* is a random variable, namely the non-flexible consumption, and f_X is the PDF. By selecting different values for the ordinates *a* and *b*, a range of load consumption values is formed. The load consumption of a non-flexible consumer will lie in this range with certain probability. Furthermore, the power curve of the flexible consumer is compared with the 3D probability distribution for preselected ordinates. Whenever the curve exceeds both ordinates, the excess demand can be considered as potentially flexible demand. In this sense, when the range is altered the amount of potentially flexible demand changes inversely. It is noteworthy that, since the excess consumption is the target of analysis, $a = -\infty$. The same approach could be used for residential generation estimation purposes, with $b = \infty$ instead.

Three typical days representing the seasonal changes, along the year, were analysed in order to evaluate the impact of the HP flexibility. The obtained results are depicted in Fig. 3-5. In each one of them, subfigure (a) represents the original data of the clustered non-flexible consumers in a histogram form. Then, (b) shows the fitted PDFs along that day. Moreover,

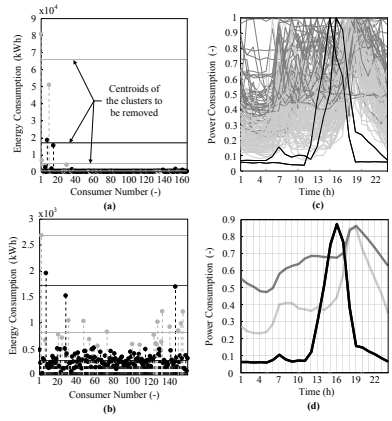

Fig. 2. (a) Pre-clustering, (b) Energy clustering, (c) Normalized curve clustering, (d) Centroids of the normalized curve clusters.

(c) is the top-view of the fitted distributions and finally (d) displays different AP with $a = -\infty$ along with the power pattern of the flexible consumer for the day of interest.

In Fig. 3 a typical cold winter day case is presented, namely February 6^{th}, 2012. Notice that most of the day, even with 99% probability, there is a considerable amount of HP operation. It is clear that the HP is dominating the power consumption of the flexible user at all times and mostly doing it at its full capacity. That is to say, that hardly any demand can be shifted on the time horizon concluding that hardly any flexibility is available on this day.

Fig. 4 depicts the case of May 9^{th}, 2012. In this month, which is a transition between extreme seasons, the household

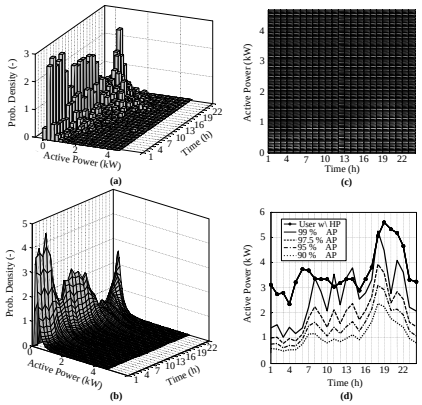

Fig. 3. February 6^{th}, 2012: (a) Data histogram, (b) 3D probability distribution, (c) 3D probability distribution top-view, (d) AP compared to flexible user.

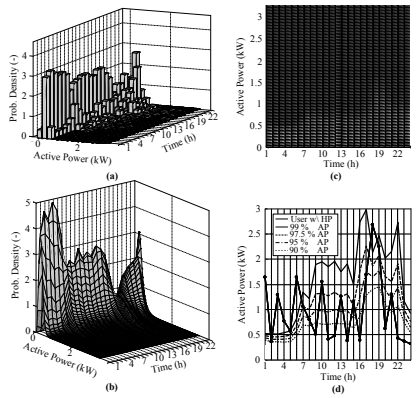

Fig. 4. May 9^{th}, 2012: (a) Data histogram, (b) 3D probability distribution, (c) 3D probability distribution top-view, (d) AP compared to flexible user.

thermal demand is not that high anymore but is still adequate to make the HP operate several times within the day. In such a scenario, flexibility could be offered by valley filling.

In Fig. 5 a typical hot summer day case is presented, July 25^{th}, 2012. Owing to the limited thermal need required by the household at this time of the year, the HP barely operates. According to the illustrated pattern of the flexible consumer the lack of flexibility is obvious, even for low AP.

Table I summarizes the most relevant results achieved. As it can be noticed, by decreasing the AP the potential HP flexibility is increased. Moreover, this potential flexibility is more likely to be offered as flexibility in months belonging to transitional periods between summer and winter. For instance on May 9^{th}, with 90% probability, 38.52% of the daily energy consumption of the flexible consumer can be considered as flexible. This information would be very valuable to a balance responsible party (BRP) when bidding on the power markets.

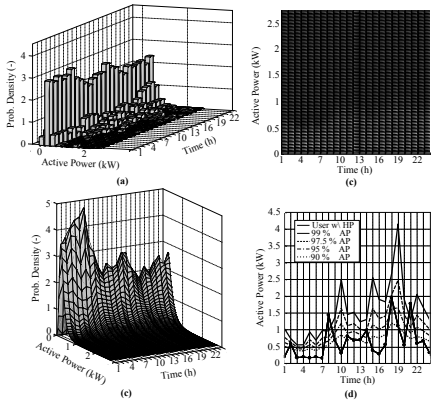

Fig. 5. July 25^{th}, 2012: (a) Data histogram, (b) 3D probability distribution, (c) 3D probability distribution top-view, (d) AP compared to flexible user.

TABLE I
POTENTIAL FLEXIBILITY RESULTS

Date	Parameter	Probability			
		99%	97.5%	95%	90%
Feb. 6^{th}, 2012	Consum. (kWh)	86.91			
	Pot. Flex. (kWh)	23.5	40.78	51.59	60.42
	Pot. Flex. / Consum. (%)	27.04	46.92	59.36	69.52
May 9^{th}, 2012	Consum. (kWh)	23.93			
	Pot. Flex. (kWh)	3.49	4.66	6.66	9.22
	Pot. Flex. / Consum. (%)	14.57	19.48	27.83	38.52
Jul. 25^{th}, 2012	Consum. (kWh)	15.48			
	Pot. Flex. (kWh)	0.95	1.37	2.24	3.33
	Pot. Flex. / Consum. (%)	6.13	8.83	14.49	21.5

Since this demand is flexible, it can be shaped as desired thus yielding considerable profit for the BRP. However, it should be understandable that although the probability is as high as 90%, there is still a 10% risk -to be taken by the BRP- that the excess load will not solely derive from a flexible load.

As can be observed, only the period from January to the middle of August was targeted. The reason is that during the rest of the months, the PV is also operating. By utilizing the presented methodology, a certain amount of residential generation can be estimated. Nevertheless, extra elaboration of the data is required which will be presented in future work.

VI. CONCLUSION

In this paper, a methodology for quantifying the potential flexibility of residential consumers in a probabilistic way was introduced. Initially, the non-flexible consumers of the grid were clustered and the flexible consumer was assigned to one of the resulting classes. Then, a 3D probability distribution of non-flexible demand was created for several days and the flexible consumer was compared to it. By defining different AP, different levels of potential flexibility could be perceived. This potential flexibility was subsequently assessed. In this respect, it was found that the demand from weather dependent flexible loads can more likely be addressed as flexible during transitions between summer and winter. This information could be very valuable to a BRP for market bidding purposes.

REFERENCES

[1] Smart Grid in Denmark 2.0 - Implementation of three key recommendations for the smart grid network. Dangrid (Danish energy Association and Energinet.dk), Oct. 2012.

[2] S. Valero, M. Ortiz, C. Senabre, A. Gabaldn, and F. Garca, "Classification, filtering and identification of electrical customer load pattern through the use of self-organizing maps," *IEEE Trans. Power Syst.*, vol. 21, no. 4, pp. 1672-1682, Nov. 2006.

[3] G. Chicco, R. Napoli, and F. Piglione, "Comparisons among clustering techniques for electricity customer classification," *IEEE Trans. Power Syst.*, vol. 21, no. 2, pp. 933-940, May 2006.

[4] G. J. Tsekouras, N. D. Hatziargyriou, and E. N. Dialynas, "Two-stage pattern recognition of load curves for classification of electricity customers," *IEEE Trans. Power Syst.*, vol. 22, no. 3, pp. 1120-1128, Aug. 2007.

[5] C. M. Bishop, Pattern Recognition and Machine Learning, Springer, 2006, pp. 424-430.

[6] D. L. Davies and D. W. Bouldin, "A cluster separation measure," *IEEE Trans. Pattern Anal. Machine Intell.*, vol. PAMI-1, no. 2, pp. 224-227, Apr. 1979.

[7] O. Thas, Comparing Distributions, Springer, 2010, ISBN: 978-0-387-92709-1.

Publication C.5

(*Conference Contribution*)

Stochastic Impact Assessment of the Heating and Transportation Systems Electrification on LV grids

Iker Diaz de Cerio Mendaza, Birgitte Bak-Jensen, Zhe Chen and Allan Jensen

The paper is a pre-printed version of the final paper that has been published in the *Proceedings of the Innovative Smart Grid Technologies Conference Europe (ISGT-Europe), 2014 IEEE PES* , vol., no., pp.1,6, 12-15 Oct. 2014

DOI:10.1109/ISGTEurope.2014.7028812

Stochastic Impact Assessment of the Heating and Transportation Systems Electrification on LV grids

Iker Diaz de Cerio Mendaza[†], *Student-Member*, *IEEE*, Birgitte Bak-Jensen[†], *Senior-Member*, *IEEE*, Zhe Chen[†], *Senior-Member*, *IEEE* and Allan Jensen[‡]
[†]Department of Energy Technology, Aalborg University, Pontoppidanstræde 101, 9220, Aalborg Ø, Denmark
[‡]HEF Net A/S, Over Bækken 6, 9220, Aalborg Ø, Denmark
idm@et.aau.dk

***Abstract*—According to the new energy policy agreements, a conceptual and technological re-structuration of the Danish energy sector is expected. One of the key points for its successful implementation is the partial electrification of the heating and transportation systems. This fact, which reflects an enormous load increase, influences already the design and planning of the future power system. Great percentage of this new load is expected to be accommodated at local distribution level. Therefore, it implies that the distribution system operator will have to handle an increasing number of highly rated loads in networks which were not designed for them. In low voltage grids especially, depending on the system penetration grade and the way they are disposed produces a completely different reaction of the network. This paper introduces a methodology for stochastically evaluating the impact caused by thermostatic and plug-in electric vehicle loads in low voltage grids. On one hand, it defines which the potential bottlenecks of the system are. On the other hand, probabilistically identifies the vulnerable components of the infrastructure that obviously should be under consideration of the operator. As a case study, a typical Danish low voltage grid is considered. The results obtained, using DIgSILENT PowerFactory, show that sometimes the hosting capability of these networks may be poor for the integration levels expected.**

***Index Terms*—Power distribution networks, heat pump, plug-in electric vehicle, system impact, smart grid.**

I. Introduction

Through the energy agreement of March 2012, the energy targets for Denmark -respect to the previous plans- were accelerated by the Danish Ministry of Climate, Energy and Building. In particular, two of them are of special interest. By 2020, 50% of the electricity consumed has to be supplied by wind power and more than 35% of the final energy consumption must proceed from renewable energy sources [1]. The outcome of this policy is already notable nowadays, i.e. the increasing wind and photovoltaic (PV) power penetration, the continuous development of the electric vehicle infrastructure and the stimulation plans for replacing old fashion heating systems by more efficient and environmentally friendly ones. From this is derived that a conceptual and technological re-structuration of the Danish energy system will be given. In such a scenario, the power system is considered to be the backbone of the whole energy system [2]. As a side-effect, this system will have to accommodate an enormous amount of load coming from the electrification of the heating and transportation systems. This loading especially targets the power distribution networks and in particular to the low voltage (LV) networks. Energinet.dk, the Danish transmission system operator (TSO), estimates that nowadays 80.000 heat pumps (HP) are approximately installed in Denmark expecting 420.000 more by 2030 [3]. In the same way, its previsions regarding electric vehicles (EV) rub 1.1 million units [2].

From a distribution system operator (DSO) perspective this context imposes important challenges in respect to the management of the LV grids. Particularly, because it is committed to handle an increasing number of loads in networks that were not designed with that purpose. Furthermore, considering the high power rating of HPs and plug-in EVs (PEV), this commitment gets even more complex. For that reason, it is important for the DSO to realize an exhaustive evaluation of how different levels of load penetration may affect the LV grid operation. The consequences of increasing the load in these networks are by this time well known; voltage deviations, unbalances, overloading of the infrastructure. Different impact assessments are available in the literature regarding the penetration of these loads in LV grids. Authors in [4] assessed the impact produced by HPs on the voltage and the thermal loading of rural and urban LV grids by randomly creating the distribution of those. In [5], authors study the phase voltage unbalances originated by different grades of HPs allocation in the considered system. A deterministic study in [6] shows that even a modest level of PEV penetration could exceed the safe operating limits of the LV grid. Similar analysis is performed in [7] but considering different charging schemes. The influence of the charging rate in the secondary transformer aging was evaluated in [8]. Substantial lifetime reduction was claimed on this piece of the electrical infrastructure when allowing high charging rates on PEVs during peak hours.

A common practice among DSOs or utilities when performing impact studies is to consider the worst case scenario as the reference. However, this case may not always represent the reality increasing as a consequence the investment of network reinforcement. For the same penetration level, a load distribution may result in a safe performance while for another

The authors would like to thank the Danish Council for Strategic Research for providing the financial support for the project Development of a Secure, Economic and Environmentally-friendly Modern Power Systems (DSF 09-067255).

different it may not. Therefore, the load distribution and/or its location in the LV grid becomes an important factor to consider while assessing the network response.

This paper introduces a methodology to evaluate the impact caused by the combination of HPs and PEVs in residential LV networks. This approach is based on a Monte Carlo (MC) model which uses the traditional Newton-Raphson power flow for defining the grid condition. For the same penetration level of load, multiple power flow calculations are performed randomly altering the location of the HP and PEV loads in the grid. By doing so, a more realistic conception of the potential system bottlenecks is obtained when comparing with deterministic procedures. Moreover, this approach probabilistically identifies the vulnerable components of the infrastructure that obviously should be under consideration of the operator.

II. Methodology

The method is structured in two stages, the network assessment and the statistical analysis of the obtained results. In the first one, a network assessment algorithm (NAA) evaluates the network response according to the penetration level and the distribution of the load considered. This algorithm randomly activates and de-activates the HP and PEV loads creating different scenarios and network behaviors. In the second stage, the results are processed and statistically analyzed to identify which are potential constrains and the most vulnerable elements of the system. Before its implementation, each of the n users (n_u) in the LV grid model which are represented by the existing household load (HL) have to be assigned with two extra physical loads representing the HP and the PEV.

A. Network Assessment Algorithm (NAA)

Fig. 1 shows the procedure utilized for obtaining the network response data. This is composed of a random process for setting the cases of study and a posterior MC model for defining the grid condition. As input, the NAA requires defining the penetration level of HP and PEV loads and the number of load distribution cases (n_{it}) that will be considered for the MC model. After defining and initializing the system variables, two matrices D_{HP} and D_{PEV} of n_{it} x n_u size are created in order to store which users have installed HP and/or PEV loads in a given case and which ones not. For the penetration level and the n_{it} defined at the beginning, the assignation of HP and PEV loads is randomly made among the users. Then, it is verified that the amount of loads assigned in each of the cases corresponds with the selected penetration level. Else an error message is displayed by the algorithm. Something which is important to clarify is that the probability for a specific user to hold a HP or PEV load is considered the same for all of them. Then, since accessing the network elements (loads, cables, buses, transformer,etc) in order makes the gathering and handling of the data an easier process, the elements are assigned in different sets depending on their type. Once this is done, the matrices to store the results of the power flow calculation are created. As this approach focuses on defining the actual grid capacity, its hosting capability and the nature and location of the technical constrains three matrices R_{bus}, R_l, R_t will store the following results: i) voltage on the buses -cable box (CB) or point of connection (POC)- in per unit (n_{it} x n_{bus}), ii) loading of the cable (n_{it} x n_l), ii) loading of the secondary transformer (n_{it} x n_t).

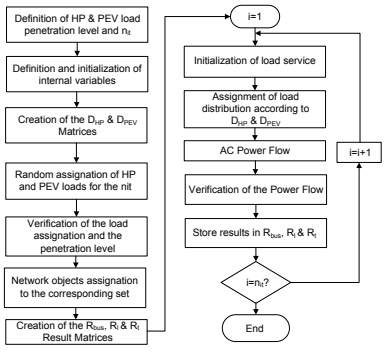

Fig. 1. Flow-chart describing the NAA.

Once this initialization phase is done, the first iteration opens the MC simulation phase. For each of the n_{it} cases, initializing the service of the load and resetting of previous calculations represents the starting point.This is basically done in order to define the same starting conditions in every cases. Therefore, it has to be ensured that all the HL loads are on service (active) while all the HP and PEV loads are off service (deactivated). If this is satisfied, the HP and PEV loads are then activated according to the sequence stipulated by D_{HP} and D_{PEV}. Once the case scenario i is successfully constructed the power flow calculation is performed in order to obtain the network response results. After verifying that the calculation it correct, each of the network elements selected are individually accessed for gathering the data of interest. This is made in an organized manner, respecting the sequence established by each of the element sets previously created. Finally, the data stored in the corresponding row of the corresponding result matrix. The row corresponds with the specific iteration of the MC simulation. This procedure will be iteratively repeated until the condition of specific iteration equal to the n_{it} is satisfied.

B. Statistical Analysis of the Results

The identification of the most vulnerable elements of the LV grid is the key to perform a good evaluation of the considered system. Since, the previous procedure is characterized for its randomness it is required to make a probabilistic interpretation of the results obtained. First, the worst operating point of the network has to be identified among the cases considered. On the one hand, this is represented by the the minimum voltage in the grid (V_{min}) since it ensures that all the CB and POC at the LV grid are supplied with a voltage equal or higher to this value. On the other hand, the maximum line and transformer

loading determines the worst operating condition of the most affected part of the infrastructure. After this is done, the set of results obtained is statistically analyzed in order to calculate the probability of each CB and POC to be supplied with V_{min}. Similarly, this is done for each of lines to determine what is its probability of being the most loaded one. The corrective measures should be decided based on this analysis.

III. Case Study

In this case, a LV distribution system located in a Danish rural area was considered. This zone is distinguished for not having any district heating service accessible. In the appendix part of this manuscript, a detailed single-line diagram of this network is available together with the line parameters in the Table III. Through a 315 kVA 20/0.4 kV transformer and a seven string radial network, 137 private users are being supplied with electricity. The customers are classified by the DSO as; residential (U_R), residential with electrical heating (U_{R+EH}), commercial (U_C), agricultural (U_A) and industrial (U_I). Since no district heating is available, the heating requirements of the users are currently satisfied with electrical heating or oil-burners. According to the Danish authorities, the old fashion heating systems from residential, agricultural and commercial users are expected to be replaced by HPs. Residential users with electrical heating instead have already their heating systems electrified. Since there is no need for replacing their heating systems this type of users were not assigned with HPs in the random process. Moreover, their electrical consumption profile have already the thermal part embedded. Regarding PEVs, any user is considered competent for hosting such a load in the future. Finally, the power demand data from the only existing industrial business reveals that its activity at this point is nonexistent. Therefore, it has not been taken into account in any additional load assignation.

The network modeling and the MC simulation were carried out in DIgSILENT PowerFactory. The NAA was written in DIgSILENT programming language (DPL) and the generated results were post-processed in Matlab. The system is assumed to be balanced and the different existing users loads and the HP and the PEV loads are modeled according to the Table I.

Fig. 2 shows the aggregated power consumption of the considered LV grid for the first week of January 2012. The highest power consumption moment ($\bar{P}_{ST}$), occurring on Friday at 18:00 h, was selected as the reference case scenario for this analysis. Therefore, the different existing user loads where

TABLE I
Load Modeling

Load	Parameter				
	Quantity	Type	Connection	P (kW)	cos φ
U_R&U_{R+EH}	122	Cte Z+Cte P	3ph-YN	data	0.95
U_C	5	Cte Z+Cte P	3ph-YN	data	0.88
U_A	9	Cte Z+Cte P	3ph-YN	data	0.93
U_I	1	Cte P	3ph-YN	data	0.90
HP	-	Cte P	3ph-YN	3	0.98
PEV	-	Cte P	3ph-YN	11	0.99

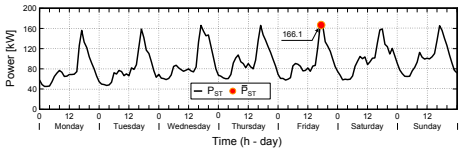

Fig. 2. Aggregated power consumption of the LV grid - January 2012.

assigned with its corresponding power consumption value at that specific time. Based on the estimations of the Danish TSO, regarding HPs and EVs, the network response was assessed for different penetration levels. With the purpose of having reasonable times of simulation, the n_{it} selected for the MC model is 10000. Moreover, this was repeated for each of the following cases:

1) Case 0 - Original Network Configuration: The network as it is today subjected to different HP and PEV penetrations.

2) Case 1-Minor Reconfiguration: Based on the results obtained in the previous case two minor changes are made in the LV grid. An additional transformer, with the same characteristics, is connected in parallel with the existing transformer. The S3C07 line is disconnected and replaced by S3CC1-1 connecting the S3CB07 cable box with the 0.4kV-T terminal.

3) Case 2-Large Reconfiguration: The changes proposed in this case are based on anterior results and the strict consideration of the physical and topological properties of the network. Therefore, four major modification are implemented. The two existing transformers are replaced by other two with similar characteristics but with a power rating of 515 kVA. In order to improve the voltage profile of the two weakest nodes, S2CB10 and S3CB14, the following lines are included: i) S2CC2-1 which connects S2CB10 with S4CB10, a strong node placed nearby, ii) S2CC2-2 connecting S2CB15 with S3CB10, for equalizing the operation of both strings and iii) S3CC2-3 connecting S3CB14 with 0.4kV-T terminal for reinforcing the furthest node of the network.

Finally, it is worth to mention that the operating limits were established according to the standard EN 50160 for medium voltage (MV) and LV grids. This standard states that the RMS voltage should remain between the $\pm 10\%$ of the nominal voltage of the network.

IV. Results and Discussion

Fig. 3 summarizes the most relevant results obtained for each of the cases. In all of them, subfigure (a) shows the lowest V_{min} for the given HP and PEV penetrations, subfigure (b) shows the loading of the most loaded line for the given HP and PEV penetrations and subfigure (c) similarly but regarding the maximum transformer/s loading. In case 0 is clearly illustrates the small hosting capability of the LV grid considered in regards the accommodation of these two loads. Notice, how with only a 25% of HP penetration the voltage limit established by the EN 50160 could be violated and overload at the same time the existing transformer. In this case, not even a 5% PEV penetration could make the LV grid

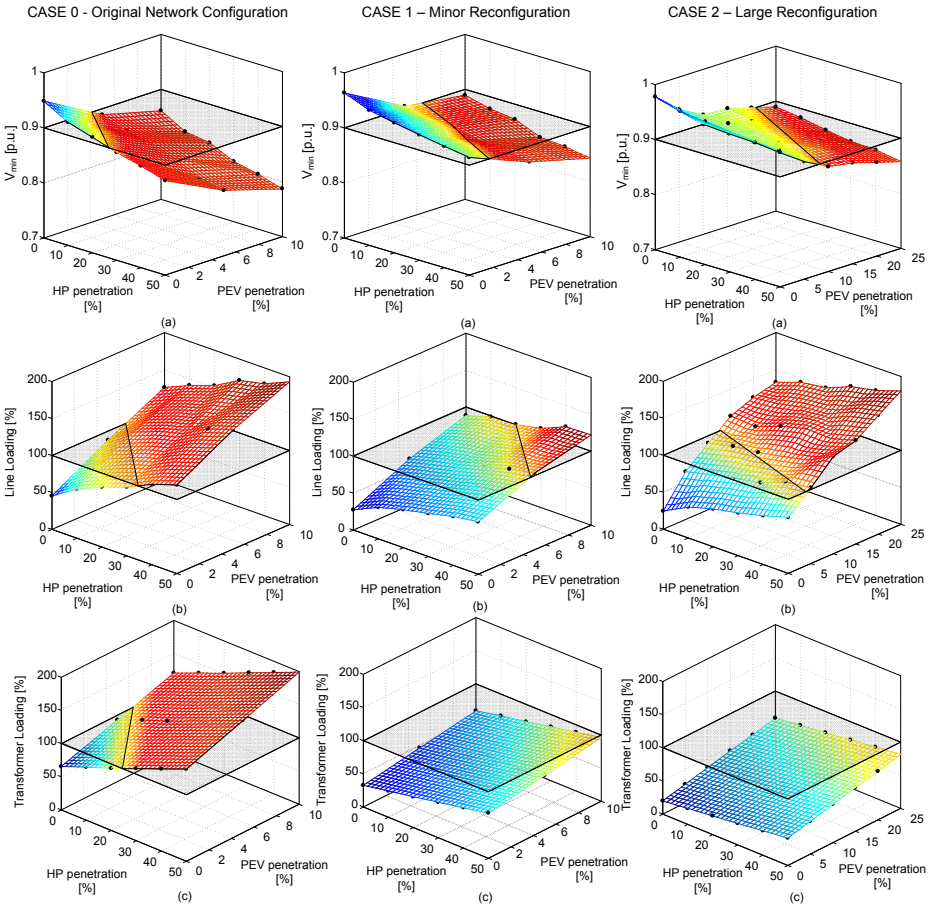

Fig. 3. Results for the different cases: (a) V_{min}, (b) Loading of the most loaded line, (c) Maximum loading of the transformer/s.

TABLE II
PROBABILITY OF THE MOST VULNERABLE ELEMENT IN THE LV GRID

	Case	**CB**				**Line**			
		10% HP		50% HP		10% HP		50% HP	
		Name	P(%)	Name	P(%)	Name	P(%)	Name	P(%)
0% PEV	0	S3CB14	99.54	S3CB14	98.9	S3C01	100	S3C01	100
10% PEV		S3CB14	60.25	S3CB14	78.59	S3C01	98.81	S3C01	99.94
0% PEV	1	S2CB10	57.56	S2CB10	42.49	S2C02	71.17	S2C02	48.58
10% PEV		S3CB14	25.46	S3CB14	24.80	S3C01	45.11	S3C01	45.47
0% PEV	2	S2CB13	34.39	S2CB14	39.54	S3C01	99.98	S3C01	99.94
10% PEV		S3CB18	22.37	S3CB18	32.50	S3C01	77.41	S3C01	98.30

perform in non-acceptable region. Based on this, the voltage and the transformer thermal loading are considered as the principal constrains of the current network. The results from the statistical analysis performed for each of the configuration cases considered are summarized in Table II. this shows the network elements, CB or line, with the highest probability for being the most vulnerable in the network. If PEVs are not considered, CB S3CB14 and line S3C01 are with a very high probability the most vulnerable elements, in terms of lowest voltage and maximum loading. This is reasonable since S3CB14 represents the furthest node from the transformer and S3C01 is the main supplier of the most loaded string. When HPs and PEVs are combined, S3C01 remains being the most vulnerable line. However, the probability of S3CB14 for being supplied with V_{min} decreases. The reason is the higher rating of the PEV loads that makes their presence more notorious in comparison with the HP load. Therefore, it cannot be dismissed the fact that certain load distributions could make the network react in a non-expected manner. Parts that are currently considered strong enough could in a future be hardly exposed while parts that have traditionally been considered as the technical boundaries may become less vulnerable.

Case 1 was designed with the purpose of making the distribution of the grid loading more uniform. From the obtained results is appreciable how the hosting capability of the LV grid is improved. The new design, in terms of voltage, accepts up to a 50% of HP penetration. However, as soon as a small percentage of PEVs appear the voltage collapses again. In comparison with case 0, the impact on the line and transformer loading is reduced. Furthermore, when only the HPs are considered, S2CB10 and S2C01 are the most vulnerable elements of the network but with a low probability. When HPs and PEVs are combined, not only the probability decreases but also the targeted element. This aspect might be influenced by reconfiguration of the network since a better distribution of the load makes the identification of the vulnerable points more difficult.

Seeing that the hosting capability of the network still may not be enough to fulfill future requirements, case 2 was considered. In terms of voltage and transformer loading, it is clear that the reconfiguration allows a higher load penetration. However, a trade-off exists. The effort of improving the voltage in some parts of the network makes string 3 quite vulnerable. In particular, the S3C01 line becomes the main bottleneck for certain HP and PEV penetration levels. Finally, it is notable again that a higher PEV presence reduces the probability of a given CB to be the most vulnerable in the network.

V. Conclusion

The expected electrification of the heating and transportation systems implies new challenges for the DSOs. Depending on how the new load is distributed in a LV grid the impact produced may be very different for same penetration level. This paper introduces a methodology for stochastically evaluating the impact caused by HPs and PEVs in these networks. The approach is based on a MC model which uses the traditional power flow for defining the grid condition. The example of Danish LV grid considered shows that the hosting capability of these networks may be poor for the integration levels expected. Moreover, from a network perspective, the high power rating of PEVs makes them more apparent than the HP loads. Therefore, grid parts that are currently considered as strong, under certain load distributions could be hardly exposed in the future.

References

[1] Accelerating Green Energy Towards 2020. The Danish Energy Agreement of March 2012. Danish Ministry of Climate, Energy and Building, Mar. 2012.

[2] Smart Grid in Denmark. Technical Report. Dangrid (Danish energy Association and Energinet.dk), 2010.

[3] Denmark: A European Smart Grid Hub Asset Mapping of Smart Grid Competencies in Denmark. Copenhagen Capacity, Copenhagen Cleantech Cluster. 2011.

[4] Mancarella, P.; Chin Kim Gan; Strbac, G., "Evaluation of the impact of electric heat pumps and distributed CHP on LV networks," PowerTech, 2011 IEEE Trondheim , vol., no., pp.1,7, 19-23 June 2011.

[5] Akmal, M.; Fox, B.; Morrow, D.J.; Littler, T., "Impact of high penetration of heat pumps on low voltage distribution networks," PowerTech, 2011 IEEE Trondheim , vol., no., pp.1,7, 19-23 June 2011.

[6] Richardson, P.; Flynn, D.; Keane, A., "Impact assessment of varying penetrations of electric vehicles on low voltage distribution systems," Power and Energy Society General Meeting, 2010 IEEE , vol., no., pp.1,6, 25-29 July 2010.

[7] Masoum, A.S.; Deilami, S.; Moses, P.S.; Abu-Siada, A., "Impact of plug-in electrical vehicles on voltage profile and losses of residential system," Universities Power Engineering Conference (AUPEC), 2010 20th Australasian , vol., no., pp.1,6, 5-8 Dec. 2010

[8] Turker, H.; Bacha, S.; Hably, A., -Based Charging of Plug-in Electric Vehicles (PEVs): Impacts on the Aging Rate of Low-Voltage Transformers," Power Delivery, IEEE Transactions on , vol.29, no.3, pp.1012,1019, June 2014

Appendix

TABLE III
Line parameters for the LV grid

Name	Parameter		Name	Parameter	
	R $[\Omega/km]$	X $[\Omega/km]$		R $[\Omega/km]$	X $[\Omega/km]$
S3C01,S3C02,S3C03,S3C04,S3C05,S3C06,S3C07,S3C11,S3CC1-1,S3CC2-3	0.208	0.052	S3C26	0.32	0.07
S3C08,S3C09,S3C10,S3C20,S3C21,S3C22,S2CC2-2	0.32	0.054	#1	1.91	0.094
S3C15,S3C16,S3C17,S3C18,S3C19,S3C23	0.641	0.058	#2	1.83	0.097
S1C08,S1C09,S1C10,S1C11,S2C15,S2C16,S2C17,S3C24,S3C25	0.641	0.072	#3, #4	3.08	0.101
S1C01,S1C02,S1C03,S1C04,S1C05,S1C06,S1C07,S1C12,S2C01,S2C02,S2C03,			#5	0.641	0.072
S2C04,S2C05,S2C06,S2C07,S2C08,S2C09,S2C10,S2C11,S2C12,S2C13,S2C14,	0.208	0.068	#6	1.2	0.075
S2C18,S3C12,S3C13,S3C14,S4C01,S4C02,S5C01,S6C01,#8,S7C01,S2CC2-1			#7	0.32	0.07

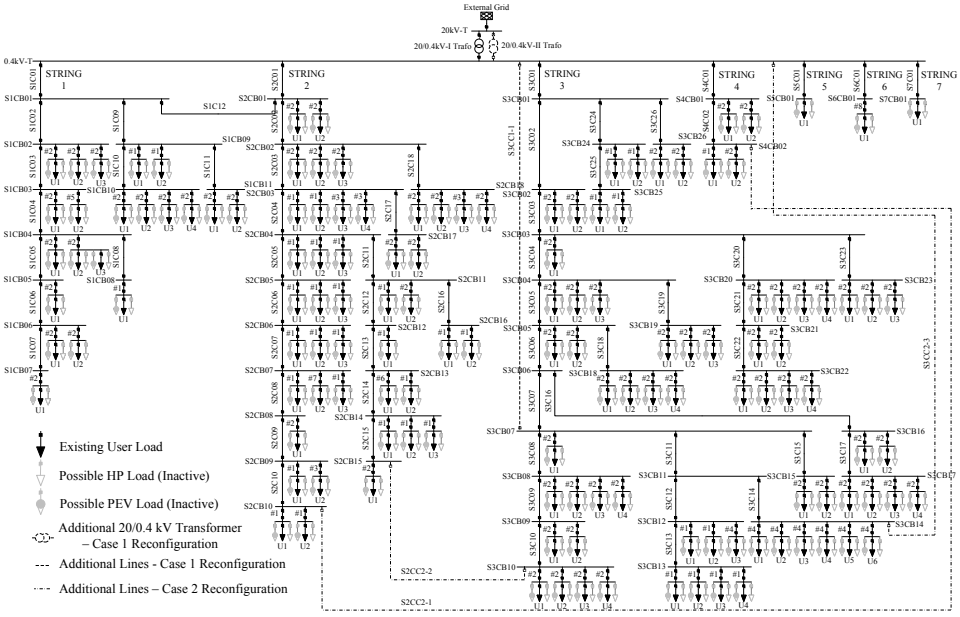

Fig. 4. 196 Bus 0.4 kV LV grid.

Journal Papers

Publication J.1

(*Journal Paper*)

Flexible Demand Control to Enhance the Dynamic Operation of Low Voltage Networks

Iker Diaz de Cerio Mendaza, Ireneusz Grzegorz Szczesny, Jayakrishnan R. Pillai and Birgitte Bak-Jensen

The paper is a pre-printed version of the final paper that has been published in the IEEE Transactions on Smart Grid , vol.6, no.2, pp.705,715, March 2015

DOI:10.1109/TSG.2014.2375894

Flexible Demand Control to Enhance the Dynamic Operation of Low Voltage Networks

Iker Diaz de Cerio Mendaza, *Student-Member*, *IEEE*, Ireneusz Grzegorz Szczesny, Jayakrishnan R. Pillai, *Member*, *IEEE*, and Birgitte Bak-Jensen, *Senior-Member*, *IEEE*

***Abstract*—Moving towards a carbon free energy system has become an objective for many countries nowadays. Among other changes, the electrification of strategic sectors such as heating and transportation is inevitable. As a consequence, the current power system load will substantially increase. In this context, the nature of the expected loads (heat pumps, plug-in electric vehicles, etc.) makes the low voltage networks specially targeted. A promising solution to overcome the challenges resulting from their grid integration, is demand response. This paper introduces a hierarchical structure for controlling the demand response of a low voltage grid. This is designed to; i) maximize the grid utilization, thereby reducing the need for reinforcement, ii) accommodate the maximum number of flexible loads and iii) satisfy the power and comfort requirements from each of the consumers in the network. The validation of the proposed concept is made using a model of a low voltage network currently operative in Denmark. The results show that by using the proposed strategy a considerable improvement of the minimum system voltage and a better load distribution is obtained.**

***Index Terms*—Demand response, low voltage networks, hierarchical control, heat pump, plug-in electric vehicles.**

I. Introduction

THE environmental awareness and initiatives to achieve a greater energy independence has driven many countries to encourage changes in their energy system. Increasing the total share of renewable energy is a well-known result of these energy policies. However, this is not only limited to the power system, heating and transportation sectors are starting to be included too. A clear example is Denmark, where the Danish Energy Agreement of March 2012 established a clear direction for the energy strategy [1]. Here, wind and photovoltaic technologies are presented as the main power sources of the future. In the same way, a "smart energy system" is proposed as a solution to handle the unpredictable and variable aspects of a 100% renewable energy based system [2]. This concept relies on the close interaction between the power, heating and transportation systems. In order this to be realizable, an electrification of the heating and the transportation systems is required. As a consequence, the power system is expected to undergo a considerable load growth in the future. Although this affects every power system level, the nature of the expected loads -heat pumps (HP), plug-in electric vehicles (PEV), etc.- makes the low voltage (LV) level more vulnerable. The distribution system operator (DSO) is then committed to handle an increasing number of high rated loads in networks which were not designed for them. A study made on several 0.4 kV radials determined that the electricity consumption expected in Denmark by 2025 would extensively overload a large percentage of the actual LV networks [3]. However, considering also the flexible character of these loads, demand response (DR) represents a potential solution to face these challenges. An effective DR is able to ensure an efficient, reliable and secure operation of the LV grid while reducing the need for reinforcement.

Lately, different DR approaches have pursued the power distribution improvement of the future LV networks. Authors in [4], [5] employ an on-load tap changer (OLTC) at the secondary transformer to regulate the demand according to the grid requirements. Since the tap adjustment changes the operating conditions in the whole LV system, these approaches do not consider the local characteristics of the voltage [6]. In [7], the electrical energy storage (EES) is exploited for maintaining the LV network under suitable operating conditions. However, it is well known that the cost is the biggest drawback of these solutions. An optimal scheduling of DR is considered in [8], [9] to maximize the energy and the benefits of the consumers while minimizing the network congestion. The papers [10]–[13] propose different hierarchical control structures to command the active loads operation. The flexibility provided by the slow thermal dynamics in smart buildings is exploited in [10] using a model predictive control. In [11], a LV grid controller with distributed intelligence defines the electric vehicle charging schedule based on the grid constrains and existing PV generation. A similar control structure, as the one presented in this study but with a completely different approach, is presented in [12], [13] for controlling the PEV charging. The concept is based on the optimization of "PEV managers" to avoid undesirable effects in the network. This feature schedules the behaviors of the PEVs according to its objectives. Since these procedures are based on the pre-scheduling of the DR, stochastic behaviors occurring within the considered time steps are not taken into account.

Different appliances are potentially controllable at household level, among them; thermostatic loads -electric water heaters, air conditioner and HPs-, washing and drying devices and electric mobility mediums -electric vehicles-. An interesting synopsis about those is made in [14], highlighting which are their strengths and weaknesses. In this work, the loads are categorized in three groups based on their operational characteristics; interruptible and deferrable, non-interruptible and deferrable and non-interruptible and non-deferrable. Taking into consideration the prognostics made by the Danish authorities regarding HPs and PEVs and the fact that they

The authors are with the Energy Technology Department, Aalborg University, Pontoppidanstræde 101, 9220, Aalborg Ø, Denmark (e-mail: idm@et.auu.dk, iszczesny11@gmail.com, jrp@et.auu.dk, bbj@et.auu.dk).

are also considered important sources of flexibility, they are selected as the controllable loads in this study.

The uncertain behaviour of the consumer demand can sometimes lead to improper levels of network operation, which may not be covered by an optimal DR scheduling [15]. Therefore, ensuring the correct performance of the LV grid in real-time is essential. A distributed control at the distribution grid could be a cheaper and more localized solution. As a base framework of such control, each consumer adapts to possible grid (voltage) regulation for their own point of connection (POC). This is especially relevant in periods of high congestion, where consumer located at the weakest points of the network may feel discriminated. Moreover, the lack of coordination and supervision in the existing grid could be inadequate to ensure complete reliability of LV network. To take into account these shortcomings, the present work aims to elaborate a hierarchical supervisory DR mechanism, connecting transformer substation, feeder and consumer level control, to enhance the dynamic operation and interoperability of the LV networks. Therefore, a special interest is put into; i) maximize the grid utilization, thereby reducing the need for reinforcement, ii) accommodate the maximum number of flexible loads, like HP and PEV loads, in the LV grid within the operating thresholds and iii) satisfy the end-consumer equally no matter the POC they are connected to. This control approach has to be understood from a supervisory perspective of the secondary distribution network. Due to the non-negligible R/X ratio of this kind of networks [16], the proposed strategy acts over the active power consumption of the mentioned loads to maintain the voltage within the admissible limits. The major contributions of this paper are:

- Detailed dynamic models of the HP and PEV systems, openly designed to be used in different kind of analysis. Moreover, each model performance is validated under different operating conditions.
- A smart and adaptive PEV charging strategy. The PEV charging capacity varies, in a flexible manner, according to the available grid capacity and energy requirements from the different PEV users.
- Advantages of applying the proposed control strategy are demonstrated for a local LV grid currently operative in Denmark. Its benefits are simulated and proven in different scenarios.

As it was mentioned previously, the voltage limit violation is mostly a local problem at the LV systems. In radial topologies, the network impedance is higher as longer the POC is from the service transformer. Therefore, end of the feeders represent normally the most vulnerable part to under-voltages. Traditionally, the LV systems were singularly designed and constructed in order to ensure a secure and efficient distribution of the power demand. In cases where the seasonal variation of the demand distorts the voltage profile of the network, it is common to find no-load tap changer (NLTC) transformers in order to manually adjust these deviations. Other alternatives are the use of voltage regulators and shunt capacitors [17]. These solutions have been efficiently and cost-effectively operating since its introduction. However, they also have technical limitations i.e. regulation capacity, stepwise control, mean life time, tracing difficulties, etc. With the need for greater control, coordination and automation of distributed energy resources (DER), new voltage control methods are emerging at this level. The usage of OLTC was previously discussed and also the repercussion that this entails. Other arising alternatives based on power electronic applications are; injection/curtailment of active and reactive power from DER, smart transformers (ST) and active voltage regulators (AVR) [18]. Nevertheless, some of these solutions are in their early development stage. There is no doubt that all these technologies are necessary to safely operate the actual systems under a reasonable growth of the demand. But, if a large electrification of the heating and transportation systems is expected, like in Denmark, other possibilities should also be taken into account. Accordingly, real-time control of the DR introduces relevant opportunities to negotiate the voltage regulation issues in the distribution network.

The rest of the paper is structured so that the reader is progressively led through the introduced control strategy, starting from the basic component modelling till the implementation of the control mechanism into the test system. Section II describes the modelling and the device control of the selected active loads. Section III describes each layer of the hierarchical structure, responsible for commanding HPs and PEVs in the LV grid. Section IV presents the LV system model and the case studies used to validate the proposed concept. In Section V, the results are presented together with a corresponding discussion. Finally, section VI provides the conclusion and the summary of the work. This paper is also organized so that it serves as a reference for future work.

II. Active Loads: Modelling and Control

The system modelling, control and analysis is performed in DIgSILENT PowerFactory. So, the dynamic load models are developed in the DIgSILENT Simulation Language (DSL).

A. Heat Pump System

Considering different technical and economic aspects [19], the air-to-water HP interfaced by a hot water storage tank (HWST) represents an appropriate technology to supply the future thermal needs of residential households.

1) Model Implementation: Fig. 1 shows the DSL block diagram of the HP system model. The average energy inside the tank (E_S), in per unit (p.u), is determined based on the first law of thermodynamics.

$$E_S = \frac{E_0 + E_{HP} - E_{th} - E_{loss}}{E_{ct}} \tag{1}$$

where E_0 and E_{ct} are the initial energy and the energy capacity of the HWST, in kWh. Attributable to the temperature difference between the water stored and the air where the HWST is installed, a heat transfer is originated. This heat transfer creates an energy loss in the tank (E_{loss}) defined by:

$$E_{loss} = \frac{1}{3600} \cdot \int UA \cdot (\frac{E_S \cdot E_{ct}}{V_T \cdot Cp_{H2O} \cdot \rho \cdot k_n} - T_r) \cdot dt \tag{2}$$

where V_T is the tank volume in liters, UA is the heat transfer coefficient in W/°C, Cp_{H2O} and ρ are the specific heat

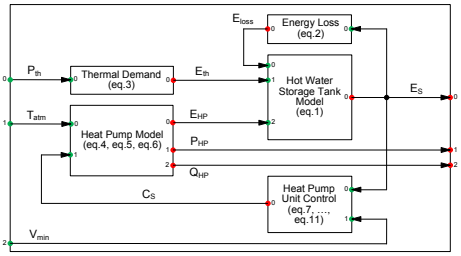

Fig. 1. DIgSILENT model lay-out of the HP System.

capacity and the density of the water, k_n is a normalization parameter and T_r the air temperature of the room where the HWST is installed. The thermal energy consumption (E_{th}), in kWh, is calculated integrating the thermal power demand of the household (P_{th}). This demand normally reflects the need for space heating (SH) and the domestic hot water (DHW).

$$E_{th} = \frac{1}{3600} \cdot \int P_{th} \cdot dt \tag{3}$$

The HP unit model is based on the commercial data-sheet of a manufacturer [20]. Applying a polynomial interpolation, an expression of the coefficient of performance (COP) as a function of the atmospheric temperature (T_{atm}) was deducted.

$$COP = -1.6e^{-5}T_{atm}^3 + 0.00052T_{atm}^2 + 0.073T_{atm} + 3.4 \tag{4}$$

The HP is electrically rated at 3.1 kW with a power factor of 0.98 lagging, after its compensation. Assuming that a constant speed compressor drives the unit, a soft-starter is modelled [21]. This should limit the starting current to two times its nominal for a second after it is turned on. The control signal C_S defines the activation of the HP according to E_S. The thermal power produced by the HP (q_{HP}) is calculated as:

$$q_{HP} = COP \cdot P_{HP} \cdot C_S \quad where\ C_S \in \{0, 1\} \tag{5}$$

Nevertheless, the steady state condition of q_{HP} is not instantly achieved. Due to its thermal dynamics, a time constant of around 15 minutes exists [22]. The energy provided by the HP (E_{HP}) is then estimated as:

$$E_{HP} = \frac{1}{3600} \cdot \int q_{HP} \cdot dt \tag{6}$$

As most of the thermostatic loads, the HP is controlled based on a regular hysteresis control. The HP turns on (C_S=1) when the E_S drops at the lower cut-off band ($\underline{E}_C$). The HP will supply the HWST with thermal energy until the higher band ($\bar{E}_C$) is reached, then it will turn off (C_S=0). In comparison with other household appliances, the HP system represents a large load, having a more notable impact in the LV network. In large numbers, they may induce serious voltage drops and overloading issues in the LV system. Therefore, a need for controlling their operation arises. However, under high or very low P_{th} conditions, this HP technology becomes hard to be directly controlled. For example, with the purpose of avoiding bottlenecks in the distribution grid, an aggressive control could turn ON and OFF the HP in a frequent manner. This could cause a reduction of the average E_{HP} due to the existing time constant of q_{HP}. Therefore, other alternatives should be considered in the control design of these units. Taking that into consideration, the HP is provided with an extra operation mode, named as the voltage emergency mode (VEM). The criteria selected to switch from the normal operation mode (NOM) to VEM and viceversa is:

$$\begin{aligned} &V_{min} \geq V_r\ \&\ k_v > k_l \rightarrow NOM \\ &V_{min} < V_r \rightarrow VEM \end{aligned} \tag{7}$$

where V_{min} is the minimum operation voltage in p.u, V_r is a pre-defined voltage limit for V_{min}, k_v and k_l are internal variables for the VEM. V_{min} is received from a subsystem (SS) control, as it is explained in section III.b.

a) Voltage Emergency Mode: A voltage violation occurs when V_{min} becomes lower than V_r. The V_r limit is either set by regulation or by the practical experience of the DSO. In this sense, from the instant when the violation occurs until it is cleared, a voltage violation region is determined. In this region the HP should self-adapt avoiding the aggravation of this technical constraint. Therefore, when the HP controller considers a voltage violation severe enough, the $\underline{E}_C$ is broadened 20% with respect to the NOM settings. As a consequence, the HPs that were supposed to switch ON in this region remain OFF delaying their activation. The question now is how, what and when a voltage violation is considered severe enough. When a violation is occurring ($V_{min} < V_r$) the HP controller senses the situation based on the logic:

$$\begin{aligned} &k_v > k_l \rightarrow \underline{E}_C = \underline{E}_C^{no}, \bar{E}_C = \bar{E}_C^{no} \\ &k_v < k_l \rightarrow \underline{E}_C = \underline{E}_C^{no}, \bar{E}_C = \underline{E}_C^{no} - (\bar{E}_C^{no} - \underline{E}_C^{no}) \cdot 0.2 \end{aligned} \tag{8}$$

where k_v is the factor representing the severity of the voltage violation, k_l is its reference value, $\bar{E}_C^{no}$ and $\underline{E}_C^{no}$ are the maximum and minimum energy bands of the NOM, in p.u. In order to determine the optimal moment to make the HP react, the k_l parameter should be carefully set by the system operator. As the grid condition differs at the beginning and the end of the voltage violation region, the control should also act differently. Therefore, a pre and post actuation zones are established.

The pre-actuation zone delimits the moment when voltage violation occurs and when the HP control considers that the violation is severe enough to consequently react. In this zone, the severity of the voltage violation should be reflected in the evolution of the k_v factor. The larger the difference ($V_{min} - V_r$), the greater and faster the variation of k_v should be. To cover that, the following expression is developed:

$$k_v = \int -a_v(1 - ((V_{min} - V_r) + 1)^{b_v}) \cdot dt;\ -1 \leq k_v \leq 0 \tag{9}$$

where a_v and b_v are the linear and exponential gains of the function defining the dynamics of k_v. The tuning of a_v and b_v is directly related with the sensitivity of the VEM. Here, a trade-off exists. Higher gain values increase the sensitivity but also cause unnecessary actuation in short-term violations. Low gains instead cause a non-reaction in time of the HP.

The post-actuation zone bounds the moment of the voltage

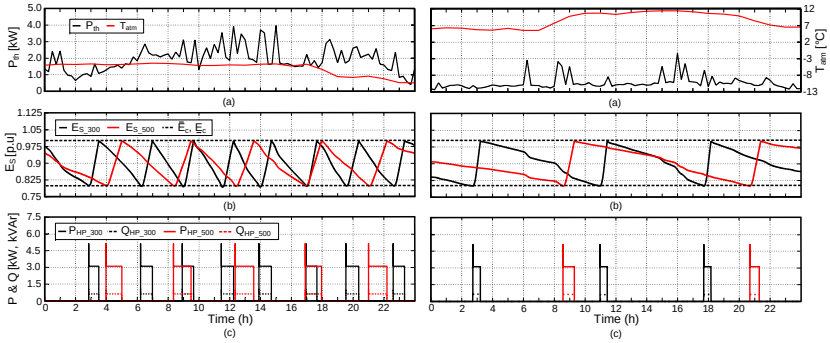

Fig. 2. HP performance in February and May: (a) P_{th} and T_{atm}, (b) E_S and its $\underline{E}_C$ and $\bar{E}_C$ operation limits, (c) P_{HP} and Q_{HP} consumption pattern.

violation clearance and the moment when HP control leaves the VEM. In this zone, even if the voltage has recovered ($V_{min} > V_r$), the return to NOM should be gradually performed in order to give enough time to the voltage to settle. Therefore, the k_v factor is linearly adapted towards the k_l:

$$k_v = \int c_v \cdot dt; \quad -1 \leq k_v \leq 0 \tag{10}$$

where c_v is the linear gain defining how fast the mode shifting is made. Moreover, the undesirable situation of having the start-up current from many HP coinciding should be avoided. This could happen when the operation modes are shifted. Therefore, an inclination of the $\underline{E}_C$ is designed.

$$\underline{E}_C = \int d_v \cdot dt; \; \underline{E}_C^{no} - (\bar{E}_C^{no} - \underline{E}_C^{no}) \cdot 0.2 \leq \underline{E}_C \leq \underline{E}_C^{no} \tag{11}$$

where d_v is the gain defining the speed of this transition.

2) Model Validation: Two HWSTs are considered to validate the introduced HP system model. Even though, the sizes of the HWSTs are different, 300 l and 500 l, the UA assumed in both is the same, 1 W/°C. Having same UA, even if the tank areas are different, means that the heat losses for the same temperature conditions are the same in both HWSTs, due to different insulation characteristics. Since it is supposed that the HWSTs are installed in the household basement T_r is set to 10°C. Under the NOM, the hot water inside the tank is controlled within the thermal range of 60 to 75°C. Based on [23], it can be said that this is equivalent to control the HWST within the energy range of 20.93-26.17 kWh for the 300 l tank and 34.89-43.61 kWh for the 500 l one. This limits in per unit are $\underline{E}_C^{no}$=0.8 p.u. and $\bar{E}_C^{no}$=1 p.u.

The performance of the HP system model is compared in Fig. 2 under different operating conditions. In the left hand illustrations, the HP with different HWSTs is compared under high thermal demand conditions, representative of a cold winter day in February. The figures on the right-hand side instead compare the same but for a typical day in May. Fig. 2.a shows the T_{atm} and the P_{th} for a single household within a 24 h period. Fig. 2.b illustrates the evolution of E_S within this period and Fig. 2.c the active and reactive power (P_{HP}, Q_{HP}) consumption based on how E_S varies. Notice how for the same T_{atm} and P_{th} conditions, the HWST with lower capacity produces more frequent P_{HP} and Q_{HP} consumption. Similarly, differences can be found in the HP performance among different seasons. With a lower P_{th} and a favorable atmospheric conditions, which implies a higher COP, the E_S has much slower variation. As result, the HP stays OFF longer time being reflected in the P_{HP} and Q_{HP} consumption too.

In Fig. 3 an example of the VEM performance for a single HP is depicted. Fig. 3.a illustrates the V_{min} variation for a given time frame. The voltage limit set by the standard EN 50160 for LV grids is $\pm$10%. However, a more conservative value of $\pm$6%, is selected based on practical experiences from DSOs in Denmark. Since the severity of a voltage violation is normally characterized by the sag amplitude and the violation duration, the VEM has to be tuned accordingly taking those in consideration. In this work, the pre-actuation zone is tuned in order to make $\underline{E}_C$ react in about 5 minutes to an undervoltage of 0.935 p.u and in less than 4 seconds to a one of 0.9 p.u. Even if the tuning selected may seem a bit conservative it allows the HPs reacting when it is necessary and not in each moment that a violation occurs. The post-actuation zone

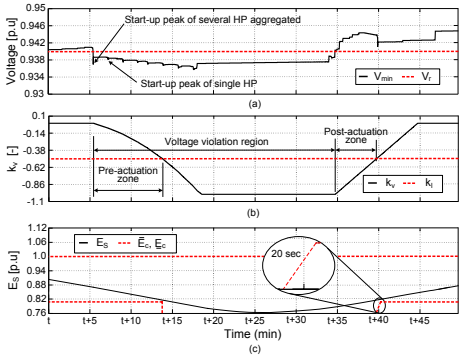

Fig. 3. VEM example: (a) $V_{min}$and V_r, (b) k_v and k_l, (c) E_S, $\underline{E}_C$ and $\bar{E}_C$.

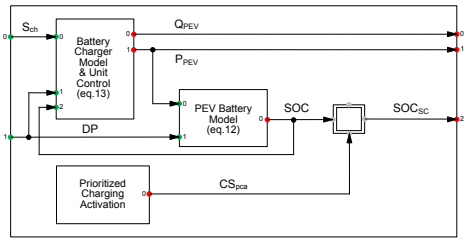

Fig. 4. DIgSILENT model lay-out of the PEV system.

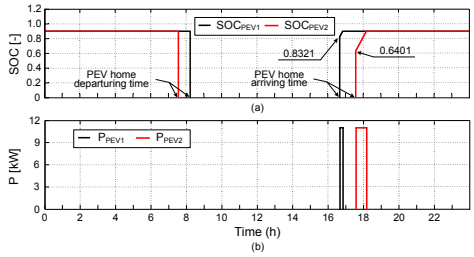

Fig. 5. Performance of two PEVs with different DP: (a) SOC and (b) P_{PEV}.

instead is designed with the purpose of leaving the VEM and returning to NOM in about 5 minutes. The last 20 seconds of this transition refer to the slope designed for $\underline{E}_C$. Table I provides the parameters selected for determining the evolution of k_v in eq.9 and eq.10 and the inclination of $\underline{E}_C$ in eq.11.

TABLE I
VOLTAGE EMERGENCY MODE TUNING

Parameter	k_l	a_v	b_v	c_v	d_v
Value	-0.5	0.00258	100	0.001667	0.01

Under the considered tuning the k_v evolution is shown in Fig. 3.b. The result is depicted in Fig. 3.c. When the HP control senses a severe voltage violation $\underline{E}_C$ is shifted delaying its activation and avoiding a deterioration of the voltage profile.

B. Plug-in Electric Vehicle System

The PEV system model is composed of a battery storage and a domestic charging station at the household level.

1) Model Implementation: Fig. 4 shows the DSL block diagram of the PEV system model. The battery is represented by a Thevenin-based electrical model, neglecting any transient effects. The relation between the terminal voltage and the open circuit voltage is assumed linear. Hence, the existing energy loss due to internal resistance of the battery is reflected as the efficiency η_b. The battery state of charge (SOC) in p.u is:

$$SOC = SOC_0 + \frac{\frac{C_{max}}{3600} \cdot \eta_b \cdot \int P_{PEV} \cdot dt}{SOC_{max}} \qquad (12)$$

where SOC_0 is the initial SOC in p.u and C_{max} and SOC_{max} the maximum battery capacity and the maximum SOC in kWh.

The PEV battery is charged through a domestic charger placed at household level. The non-negligible impact that a concentration of synchronized PEV can originate in an LV network reinforces the need for controlling their charging process. Therefore, based on [24], the traditional feature of the domestic charger is additionally procured with the ability for regulating the charging rate. Therefore, the charging power (P_{PEV}) is allowed to vary from 0 to rated power (P^{rt}_{PEV}) of the charger. P_{PEV} is determined as:

$$P_{PEV} = \eta_c \cdot \int S_{ch} \cdot dt; \quad 0 \leq P_{PEV} \leq P^{rt}_{PEV} \qquad (13)$$

where η_c is the charger efficiency in p.u and S_{ch} is an external variable representing the charging capability of an specific PEV. S_{ch} is calculated and dispatched to the PEV battery charger by a SS control. This is developed in section III.b.

The power consumption pattern from a domestic battery charger is highly influenced by the driving pattern (DP) of its PEV user. In the model, the DP is reflected as the home departure and arrival times (t_{dep}, t_{arr}) and the distance driven in the day (d). The possibility for self-imposing priority in the charging has also been contemplated. This option could be adopted by a PEV user, which is based on his driving requirements and the fact of ignoring for being penalized. In this situation the activation signal (CS_{pca}) would reflect in the SOC sent by the charger to the SS control (SOC_{sc}) -see section III.b-. Moreover, to preserve the battery life the SOC is controlled between 0.2 and 0.9 p.u. Even if it is externally required, the unit control makes sure not to violate these limits.

2) Model Validation: The high energy density and long life time, makes the lithium-ion (Li-ion) batteries an interesting solution to be considered for electric transportation applications. Therefore, a 24 kWh Li-ion battery with a η_b of 0.993 is considered in this case. Looking into the actual infrastructure, a 3-ph/400 V off-board represents a feasible solution for satisfying the user charging requirements. Additionally, the battery charger is procured with the ability for regulating the charging rate within 0 kW and 11 kW. Its $\eta_c$is considered 0.98.

Fig. 5 illustrates the comparison between two users holding the same PEV but performing different DP. Since it is for model validation matters, in this case the PEV charging is not externally influenced. Therefore, they are allowed to charge at their rated power. Fig. 5.a shows the SOC sensed by both chargers when the PEV connects at home. Notice in Fig. 5.b that the active power consumption from the chargers differs in time and quantity, demonstrating the strong relationship between the user DP and the impact in the LV grid.

III. HIERARCHICAL CONTROL OF THE LV GRID

This section describes the hierarchical structure proposed to control the operation of HP and PEV loads in the LV grid. A hierarchical arrangement of the distribution system supervision makes it possible to identify, evaluate and tackle the technical constraints in the LV network in singular manner. This is especially relevant when the voltage drop is the key factor representing the grid constraint. Since, the voltage limit violation is normally a local problem it requires local

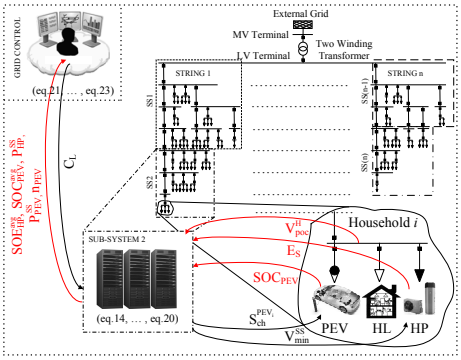

Fig. 6. Hierarchical Control of the LV Grid.

solutions as well. Moreover, since the intermediate layers have the capacity to decide over the controlled assets, less communication infrastructure is required when compared to a fully coordinated control system.

The feasibility of this concept relies on an existing legal agreement between a consumer, holding a flexible load, and the system operator. This agreement allows the flexible unit to be controlled in exchange for ensuring the comfort and power requirements of the consumer and a discount in the energy bill. This strategy could be implemented by DSOs, balance responsible parties (BRP) or aggregators looking for maximizing the LV grid utilization while ensuring the consumer requirements. The approach attempts to respect two important conditions. First, to treat equally the end-consumer no matter to which POC are connected, and second to be in accordance with the actual grid codes (EN 50160). Fig. 6 is an illustration of the proposed control structure. Basically, this structure is composed by three layers, the unit control (UC), the subsystem control (SSC) and the distribution grid control (DGC). As it is represented, a bidirectional information flow exists between the different layers. The DGC has direct communication with the different SSs in order to have a clear overview of the grid condition. Every SSC is responsible for monitoring and operating a group of households which may, or may not, have HP and/or PEV. Finally, the loads report their state to its corresponding SSC.

In terms of flexibility, the PEVs show an advantage in respect to the HPs. Besides of being able to control them ON/OFF, it is possible to vary their charging capacity while they are ON. The HP technology considered instead, either operates at the rated power or it has to be turned OFF. The responsibilities of each component are described below.

A. Unit Control

It refers to the embedded appliance control which maintains the stored energy within the stated limits. In a HP system, the P_{th} of the household has strong influence in its electrical consumption pattern. Therefore, having any external influence makes the user comfort highly vulnerable. As this control approach aims to maintain the comfort unaffected, the HP system acts on its own without being subordinated. The only situation when it adapts its operation is when an under-voltage occurs in its SS. For the PEV load instead, the UC is only responsible for ensuring that the SOC remains within the stated limits because the charging rate is decided by the SSC.

B. Subsystem Control

It is defined as the component, of the control structure, placed at the distribution feeder levels. It monitors a number of households (n_h) and according to its needs acts over the HPs and PEVs under its domain. Its main responsibilities are:

1) Data collection and processing: Assuming that a smart meter is available in each household (H), the SS receives; the voltage at the POC of every household (V^H_{poc}), the SOC of plugged-in PEVs (SOC_{PEV}) and the E_S of the HP systems.

2) Calculation of minimum voltage and set-points: The SS compares the V^H_{poc} data gathered from the households and defines the minimum voltage in the SS (V^{SS}_{min}).

$$V^{SS}_{min} = min(V_h);\ V_h \in [V^{H1}_{poc} ... V^{Hi}_{poc} ... V^{Hn}_{poc}];\ i = 1...n_h \quad (14)$$

where V_h is a vector holding V^H_{poc} data gathered from the different households. V^{SS}_{min} is dispatched to every HP in the SS in order to make them run in VEM when it is required.

3) Prioritize Plugged-in PEVs, calculation and dispatch of S_{ch}: As it was stated in section II.b, the charging power at which a specific PEV is allowed to charge depends on its SOC and the V^{SS}_{min}. The SSC is constantly monitoring the amount of PEVs plugged in the controlled area and their SOC too. The PEVs connected in the SS are sorted, based on the SOCs, in an ascending order and stored in a vector called PEV_{pv}.

$$PEV_{pv} = sort_{min(SOC)}(PEV_V) \quad where$$
$$PEV_V \in [PEV_1 ... PEV_i ... PEV_n];\ i = 1...n_{pev} \quad (15)$$

where PEV_V is a vector holding the n PEVs connected in the SS (n_{pev}). Based on this ranking, PEVs with lower SOC are prioritized in terms of charging capacity with respect to the ones with higher SOC. This is reflected assigning different amplitude values to the S_{ch} variables dispatched to the plugged-in PEVs. The A_p vector holds the pre-defined amplitude values in a descending way.

$$A_p = [(k_p)_1, (k_p - 0.2(i-1))_2, ..., (k_p - 0.2(i-1))_i, ...$$
$$..., (k_p - 0.2(i-1))_n];\ where\ i = 1...n_{pev} \quad (16)$$

where k_p is the gain defining the S_{ch} dynamics. Based on PEV_{pv}, the SSC assigns the A_p values to each PEV and it calculates their S_{ch}. So, the PEV with lowest SOC is assigned with the first value of A_p which makes its S_{ch} to be the highest. S_{ch} for an specific PEV ($S^{PEV_i}_{ch}$) is calculated as:

$$S^{PEV_i}_{ch} = C_L \cdot A_p(i) \cdot x + (x-1);\ x \in [0,1];\ i = 1...n_{pev} \quad (17)$$

where C_L is a limitation variable defined by the DGC in order to influence the PEV charging operation - section III.c-. x is a binary variable defining a voltage violation in the SS.

$$V^{SS}_{min} < V_r \rightarrow x = 0$$
$$V^{SS}_{min} \geq V_r \rightarrow x = 1 \quad (18)$$

The x variable gives an idea to the SSC of the grid

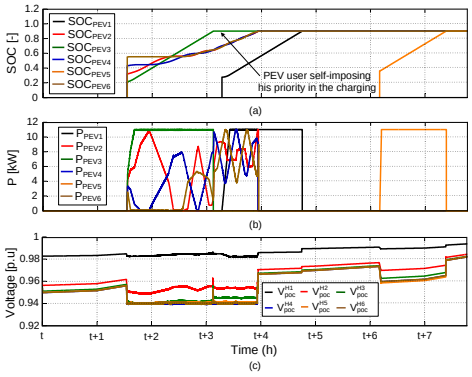

Fig. 7. SSC Performance: (a) SOC, (b) P_{PEV_i} and (c) V^H_{poc}.

status while calculating the different S_{ch} variable. Then, while $V^{SS}_{min} \geq V_r$, the PEVs plugged-in are charged based on their SOC. When the V_r is violated, the SSC makes all the PEVs reduce their P_{PEV} at the same time and in the same proportion. This continues until the V^{SS}_{min} is recovered again.

Fig. 7 is an illustrative example of how the SSC operates. Let us imagine that a specific SSC is in charge of a feeble part of a LV grid. The SSC is constantly aware of the number of PEVs connected in the SS and their SOC. Fig. 7.a shows the SOC of the PEVs when they arrive home. Between the hours $t+1$ and $t+2$ four PEVs arrive and plug-in at the same moment but in different locations and with different SOCs. Fig. 7.b shows the charging rate of each PEV. PEV number 3 and 2 have the lowest SOC, so they are prioritized over 4 and 6. This is reflected in a higher A_p, S_{ch} and charging capacity for those PEVs. As they charge faster, at some point their SOC become higher than the rest, causing a shift on the PEV_{pv} vector. This is not the case for PEV_3, because due to its driving requirements it self-imposes its priority over the rest. From the SSC perspective, this vehicle will hold the first position in PEV_{pv} until it is fully charged. Few minutes past $t+3$ the battery of PEV_3 becomes full which allows the rest of PEVs to be charged at higher capacity. Later on, PEV_1 arrives with a low SOC and plugs-in. As soon as the SSC senses it, the vehicle gets the first position in PEV_{pv}. This makes the PEV_1 to charge at the maximum capacity but subjected to the allowable grid conditions. As a consequence, the rest of the PEVs charging are forced to decrease their charging power capacity. Between hours $t+6$ and $t+7$, PEV_5 arrives and plugs-in. Since the rest of the PEVs, connected in the SS, are already charged PEV_5 is allowed to charge at maximum capacity. As result, the PEV charging is made in the fairest manner and each V^H_{poc} is kept above V_r -see Fig. 7.c-.

4) Delivery of the number of PEVs connected in SS: The DGC is continuously informed, by the SSC, about the n_{PEV}.

5) Calculation and dispatch of the average state of energy (SOE), average SOC and total power consumption from HPs and PEVs: The DGC supervision task requires from each SSC, the average SOE of the HWSTs (SOE^{avg}_{HP}) and the average SOC of the PEVs plugged-in (SOC^{avg}_{PEV}) in the SS:

$$SOE^{avg}_{HP} = \frac{\sum_{i=1}^{n_{hp}} E_{s_i} \cdot k_{ne}}{n_{hp}}; SOC^{avg}_{PEV} = \frac{\sum_{i=1}^{n_{pev}} SOC_{PEV_i}}{n_{pev}} \quad (19)$$

where n_{hp} is the number of HP systems in the SS and k_{ne} is a normalization factor. The aggregated power consumption from the HPs (P^{SS}_{HP}) and the plugged-in PEVs (P^{SS}_{PEV}) are also required:

$$P^{SS}_{HP} = \sum_{i=1}^{n_{hp}} P_{HP_i}; \qquad P^{SS}_{PEV} = \sum_{i=1}^{n_{pev}} P_{PEV_i} \quad (20)$$

C. Distribution Grid Control

The DGC represents the center of the structure and is placed at the secondary substation level. It is responsible for equalizing the SOE of the SSs with the purpose of achieving the whole network equilibrium. The average SOE in a specific SS ($SOE_{SS\#i}$) is defined based on its SOE^{avg}_{HP} and SOC^{avg}_{PEV}.

$$SOE_{SS\#i} = \left(\frac{n_{hp} \cdot SOE^{avg}_{HP} + n_{pev} \cdot SOC^{avg}_{PEV}}{n_{hp} + n_{pev}} \right)_i ; i=1...n_{ss} \quad (21)$$

In practice, the DGC intends to divide the total power transfer capability of the LV grid, among the n SSs (n_{ss}). This is based on the $SOE_{SS\#i}$ and the grid condition. The power transfer capability depends on factors like; the LV grid design and the type, rating and interaction of the different loads. This means that, when the grid reaches its maximum transfer capability point, the only way to increase the power consumption capability of an SS with the lowest SOE is decreasing the capability from the rest. This is performed reducing the PEV charging capability of these SSs, via the C_L variable. Then, the procedure followed by the DGC is:

- Calculate the $SOE_{SS\#i}$ for every SS.
- Define the minimum $SOE_{SS\#i}$ (SOE^{ss}_m) and its SS:

$$SOE^{ss}_m = min(SOE_V);\ SOE_V \in [SOE_{SS\#1}, ..., SOE_{SS\#i}, ..., SOE_{SS\#n}];\ i=1...n_{SS} \quad (22)$$

- Calculate C_L for every SS according to:

$$SOE_{SS\#i} - SOE^{ss}_m \geq \delta \rightarrow C^i_L = (1 - k_c(SOE_{SS\#i} - SOE^{ss}_m))$$
$$SOE_{SS\#i} - SOE^{ss}_m < \delta \rightarrow C^i_L = 1; \quad i=1...n_{SS} \quad (23)$$

  where δ is the SOE difference limit of the compared SSs defined by the operator. k_c is the gain defining the slope of the function representing C_L. Finally, the lower C_L is, the more the PEV charging capability will be limited in the SS.
- Delivery of the corresponding C_L to each SS.

IV. LV Network and Study Cases

The test system selected for the proposed strategy validation is a typical LV network currently operative in Denmark. Through a 630 kVA 10/0.4 kV transformer and an eight string radial network, 166 residential consumers are supplied with electricity. Some strings are equipped with an additional cable that connects them to its adjacent during abnormal service

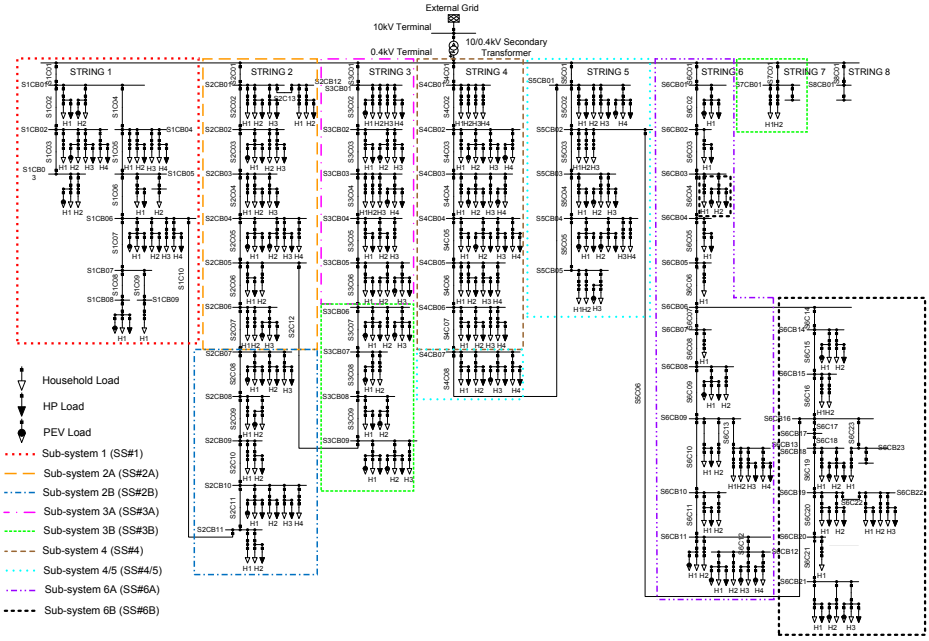

Fig. 8. 0.4 kV LV grid.

conditions. A detailed single-line diagram of the LV network is presented in Fig. 8. The terminology used for referring to the main power carriers is according to the string (S) they belong and the cable (C) number (S#C##). Regarding the cable boxes (CB), their numbering depends on the S and its number (S#CB##). The current household load (HL) and the way the new loads (NL) have been randomly distributed, according Danish TSO estimations, are depicted in this figure.

In order to investigate the impact originated by integration of the NL, a load flow calculation is performed. Four scenarios are simulated; i) the current load in February ($\#_{HL\_Feb}$), ii) the current load on May ($\#_{HL\_May}$), iii) the future load in February ($\#_{HL+NL\_Feb}$) and iiii) the future load on May ($\#_{HL+NL\_May}$). Notice from Fig. 9, the substantial impact originated by HPs and PEVs, and especially on S6. This is especially relevant in the case of February. Therefore, the LV grid is divided in nine SS, where each SS is responsible for a maximum of 12 HPs and 6 PEVs. This consideration is only taken for model construction reasons.

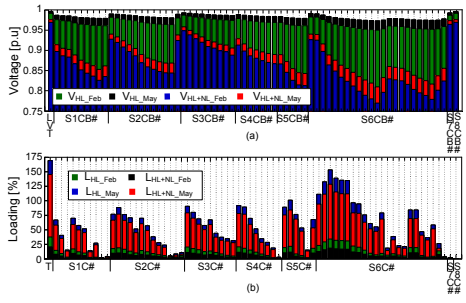

Fig. 9. Power flow results: (a) CB voltage, (b) Line Loading.

Two seasonal scenarios are designed to test the performance of the proposed strategy. On one hand, a cold winter day in February, characterized by the low T_{atm} and the high P_{th} demand. On the other hand, an ordinary day in May, where the T_{atm} is higher, so as the COP, and the P_{th} is lower. Fig. 10.a and Fig. 10.b show the aggregated thermal and electrical demand of the LV network. The P_{th} and DP profiles for each of the users holding a HP and/or PEV are generated according to [25]. t_{dep}, t_{arr} and d are illustrated for every PEV considered in Fig. 10.c and Fig. 10.d.

V. Results and Discussion

Fig. 11 and Fig. 12 summarize the most relevant results obtained, where a comparison between an uncontrolled and controlled network is made. Subfigure a shows aggregated power demand for the HPs, subfigure b represents the aggregated power demand from the PEVs, subfigure c illustrates the total active power supplied by the secondary transformer and subfigure d shows the lowest voltage in the LV network.

In February, the high power demand required by the

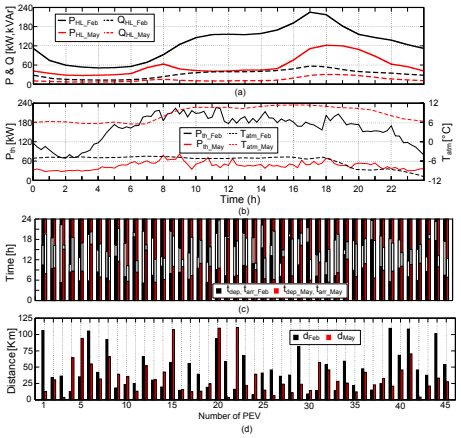

Fig. 10. Study Cases: (a) Aggregated electrical power demand, (b) Aggregated P_{th} and T_{atm}, (c) t_{dep} and t_{arr}, (d) Distance d.

HPs is the first factor to be mentioned. The high P_{th} of the households and the unfavorable atmospheric conditions, which influences COP, induces the HPs to operate more frequently in order to satisfy the thermal requirements of the users. In an uncontrolled scenario, the PEVs tend to plug-in as soon as they arrive home in the late afternoon hours. The combination of these two facts led to a large concentration of power consumption during the peak moment of the day. As result, a large and persistent voltage violation is originated, especially between 16h and 20h. Under the influence of the proposed control strategy different favorable behaviors of the grid operation are achieved. On one hand, the total HP demand is significantly reduced between 17h and 19h coinciding with the severest voltage deviation period. This power reduction is originated by the HPs in the SS where the voltage violation occurred, as they switch to VEM to delay their activation. On the other hand, the PEV charging is completely avoided during this time frame and delayed to moments when the LV grid is less stressed -late evening and early morning-. Consequently, a considerable improvement of the minimum system voltage and a better load distribution along the day is obtained.

One of the advantages of this mechanism over the employment of OLTCs at the secondary transformer level [4], [5], is the local management of the voltage constraints. As previously described, to avoid excessive voltage deviations only the flexible loads of the SS which are affected are directly encouraged to change their natural consumption pattern. This permits not to alter the power supply conditions of those consumers in adjacent feeders keeping their demand unaffected. At the same time, since all the flexible loads within the SS participate evenly, all consumers are fairly treated with reliable electricity supply.

An additional benefit from the implementation of the proposed scheme is the capability to adapt the LV network consumption based on local nodal voltages in real-time. Other hierarchical approaches that employ different optimization techniques for solving the problem in a discrete manner [10]–[13] might find difficulties to capture the uncertain behavior of the users and the system components in the optimization time steps and routines. The continuous tracking of the network status carried out by the proposed mechanism instead ensures reliable system performance.

Finally, considering the prominent resistive characteristics of the LV cables, the control of the active power carried out by the proposed strategy becomes more effective in terms of voltage profile improvement than the control of reactive

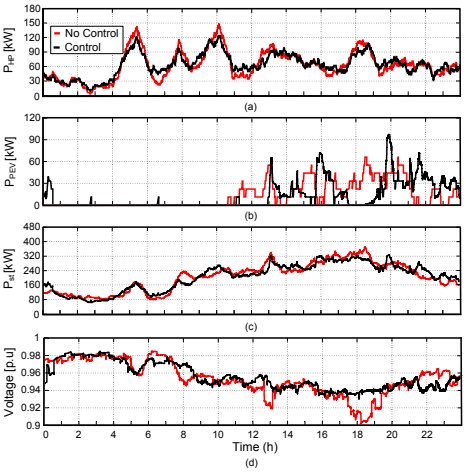

Fig. 11. Results in February: (a) Aggregated P_{HP} demand, (b) Aggregated P_{PEV} demand, (c) Transformer power supply, (d) V_{min} in LV network.

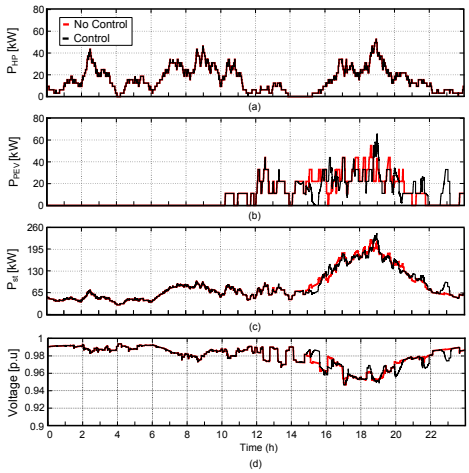

Fig. 12. Results in May: (a) Aggregated P_{HP} demand, (b) Aggregated P_{PEV} demand, (c) Transformer power supply, (d) V_{min} in LV network.

power from DERs [18]. Moreover, the power losses in the LV network are reduced due to the fact that not only the current is reduced as no reactive power control is used but also on the other hand the consumption is postponed to moments where there is less congestion.

In May instead, since the P_{th} of the household is much lower and the fact that better atmospheric conditions implies a higher COP the need for HPs to operate is significantly less. This substantially reduces the total power consumption of these units making the system capacity more available. Since enough capacity exists in the network, the lack of violations allows the HPs to run independently. That is why the uncontrolled and controlled power consumption patterns are overlapped. Regarding the PEVs, even though the network capacity is still enough, the PEV charging is influenced by the GC due to the energy equalization between SSs. Notice that, despite of having a slightly increased peak demand this is not substantially reflected in the voltage profile. Moreover, a more equalized grid behavior and a reasonable PEV charging is obtained without compromising the network power quality.

VI. Conclusion

The electrification of energy sectors like the heating and transportation is expected to increase the HPs and PEVs penetration in LV networks. This is a challenging scenario for the DSOs, since many of these networks are not designed for hosting them in large percentages. This paper introduces a hierarchical supervisory control structure for controlling and coordinating demand of these loads in a distributed manner. This strategy aims to; i) maximize the distribution grid utilization reducing the need for reinforcements, ii) treat the consumers equally no matter their POC and iii) ensure the consumer comfort and power requirements. The control design is validated with a system currently operative in Denmark. The results show that the proposed control structure makes it possible to utilize the flexibility offered by these units. In consequence, a better load distribution makes the voltage levels of the LV network to be maintained within acceptable limits in congested periods.

References

[1] Accelerating Green Energy Towards 2020. The Danish Energy Agreement of Mar. 2012. Ministry of Climate, Energy and Building, 2012.

[2] Smart Grid Strategy. The intelligent energy system of the future. Danish Ministry of Climate, Energy and Building, May 2013.

[3] Smart Grid in Denmark. Danskenergi and Energinet.dk. 2008.

[4] Kadurek, P.; Sarab, M.M.; Cobben, J. F G; Kling, W.L., "Assessment of demand response possibilities by means of voltage control with intelligent MV/LV distribution substation," PES GM, 2012 IEEE , vol., no., pp.1,6, 22-26 July 2012.

[5] Bhattarai, B.P.; Bak-Jensen, B.; Mahat, P.; Pillai, J.R., "Voltage Controlled Dynamic Demand Response," in Proc. 2013 PES ISGT EU Conf.

[6] Marra, F.; Fawzy, Y.T.; Bulo, T.; Blazic, B., "Energy storage options for voltage support in low-voltage grids with high penetration of photovoltaic," ISGT Europe, 2012 3rd IEEE PES International Conf. and Exh. on , vol., no., pp.1,7, 14-17 Oct. 2012.

[7] Yi, J.; Wang, P.; Taylor, P.C.; Davison, P.J.; Lyons, P.F.; Liang, D.; Brown, S.; Roberts, D., "Distribution network voltage control using energy storage and demand side response," ISGT Europe, 2012 3rd IEEE PES Conf. on , vol., no., pp.1,8, 14-17 Oct. 2012.

[8] Richardson, P.; Flynn, D.; Keane, A., "Optimal Charging of Electric Vehicles in Low-Voltage Distribution Systems," PS, IEEE Trans. on , vol.27, no.1, pp.268,279, Feb. 2012.

[9] Wang, Z.; Gu, C.; Li, F.; Bale, P.; Sun, H., "Active Demand Response Using Shared Energy Storage for Household Energy Management," SG, IEEE Trans. on , vol.4, no.4, pp.1888,1897, Dec. 2013.

[10] Schirrer, A.; Konig, O.; Ghaemi, S.; Kupzog, F.; Kozek, M., "Hierarchical application of model-predictive control for efficient integration of active buildings into low voltage grids," MSCPES, 2013 Workshop on , vol., no., pp.1,6, 20-20 May 2013.

[11] Groenbaek, J.; Wallentin, L.; Bessler, S.; Sitter, H., "Use of available power in the LV grid for energy balancing," PowerTech, 2013 IEEE Grenoble , vol., no., pp.1,6, 16-20 June 2013.

[12] Galus, M.D.; Simon Art, G.A., "A hierarchical, distributed PEV charging control in low voltage distribution grids to ensure network security," PES GM, 2012 IEEE , vol., no., pp.1,8, 22-26 July 2012.

[13] Galus, Matthias D.; Waraich, R.A.; Noembrini, F.; Steurs, K.; Georges, G.; Boulouchos, K.; Axhausen, K.W.; Andersson, G., "Integrating Power Systems, Transport Systems and Vehicle Technology for Electric Mobility Impact Assessment and Efficient Control," SG, IEEE Trans. on , vol.3, no.2, pp.934,949, June 2012.

[14] Zhi Chen; Lei Wu; Yong Fu, "Real-Time Price-Based Demand Response Management for Residential Appliances via Stochastic Optimization and Robust Optimization," SG, IEEE Transactions on , vol.3, no.4, pp.1822,1831, Dec. 2012

[15] Moradzadeh, B.; Tomsovic, K., "Two-Stage Residential Energy Management Considering Network Operational Constraints," SG, IEEE Trans. on , vol.4, no.4, pp.2339,2346, Dec. 2013.

[16] Christakou, K.; Tomozei, D.-C.; Le Boudec, J.-Y.; Paolone, M., "GECN: Primary Voltage Control for Active Distribution Networks via Real-Time Demand-Response," SG, IEEE Trans. on , vol.PP, no.99, pp.1,10,0.

[17] W.H. Kersting, "Distribution Systems, Modeling and Analysis" , Third Edition, CRC Press, 2012, ISBN 9781439856222.

[18] Geibel, D.; Degner, T.; Seibel, A.; Bolo, T.; Tschendel, C.; Pfalzgraf, M.; Boldt, K.; Muller, P.; Sutter, F.; Hug, T., "Active, intelligent low voltage networks - Concept, realisation and field test results," CIRED 2013, 22nd International Conference and Exhibition on , vol., no., pp.1,4, 10-13 June 2013

[19] "Stock of heat pumps for heating in all year residence in Denmark", Technical Report, COWI, Nov. 2011.

[20] "Vitocal Air-To-Water Heat pump Technical Guide", Viessmann.2009.

[21] Akmal, M.; Fox, B.; Morrow, D.J.; Littler, T., "Impact of high penetration of heat pumps on low voltage distribution networks," PowerTech, 2011 IEEE Trondheim , vol., no., pp.1,7, 19-23 June 2011.

[22] Masuta,T.; Yokoyama,A.; Tada,Y., "Modeling of a number of Heat Pump Water Heaters as control equipment for load frequency control in power systems," PowerTech 2011 IEEE, vol., no., pp.1,7, 19-23 Jun. 2011.

[23] J.B. Jones and R.E Dugan, "Engineering Thermodynamics" Prentice Hall, 1995, ISBN-10: 0023613327.

[24] Yilmaz, M.; Krein, P.T., "Review of Battery Charger Topologies, Charging Power Levels, and Infrastructure for Plug-In Electric and Hybrid Vehicles," PE, IEEE Trans. on , vol.28, no.5, pp.2151,2169, May 2013.

[25] Diaz de Cerio Mendaza, I.; Pigazo, A.; Bak-Jensen, B.; Zhe Chen, "Generation of domestic hot water, space heating and driving pattern profiles for integration analysis of active loads in low voltage grids," ISGT EUROPE, 2013 4th IEEE/PES , vol., no., pp.1,5, 6-9 Oct. 2013

Iker Diaz de Cerio Mendaza (S'11) received his B.Eng. degree in electrical engineering from the University of the Basque Country, Spain in 2007, its M.Eng. and its M.Sc. degrees in industrial engineering and renewable energy from the University of the Basque Country and University of Zaragoza, Spain in 2009 and 2010 respectively. In 2014, he was entitled with the Ph.D. degree in electrical engineering from Aalborg University, Denmark. From 2010 to 2011, he was with WindVision Ltd, Leuven (Belgium) as a Project Engineer. Lately, he is perusing different research activities as research assistant at the Department of Energy Technology, Aalborg University, Denmark.

His research interest cover demand response and demand side management, the employment of multi-nature energy storage systems for aiding the power system operation, smart grids and active distribution networks.

Ireneusz Grzegorz Szczesny received his B.Sc. and M.Sc. degree from the Technical University of Lodz, Poland, 2013. In the same year, he also received a M.Sc. degree in Power Systems and High Voltage Technology from Aalborg University, Denmark. In 2009, he was with PGE Dystrybucja Lodz, Poland as an electrical control and metrology Specialist. In 2010, he worked as a power generator assistant supervisor at a power plant PGE Belchatow, Poland. Currently, he is with Siemens Wind Power, Denmark as a Grid Connection Engineer. The performance of grid compliance tests on wind turbine prototypes is among its current responsibilities.

His research interests include power systems, electrical machines and network innovation.

Jayakrishnan Radhakrishna Pillai (M'10) received his M.Tech degree in Power Systems from National Institute of Technology, Calicut, India and a M.Sc. degree in Sustainable Energy Systems from the University of Edinburgh, United Kingdom in 2005 and 2007 respectively. He received his Ph.D. degree in Power Systems from Aalborg University in 2011. He currently is an Associate Professor at the Department of Energy Technology, Aalborg University, Denmark.

His research interest includes distribution system analysis, grid integration of electric vehicles and distributed energy resources, smart grids and intelligent energy systems.

Birgitte Bak-Jensen (M'88-SM'12) received her M.Sc. degree in Electrical Engineering in 1986 and a Ph.D. degree in "Modelling of High Voltage Components" in 1992, both degrees from Institute of Energy Technology, Aalborg University, Denmark. From 1986-1988, she was with Electrolux Elmotor A/S, Aalborg, Denmark as an Electrical Design Engineer. She is now an Associate Professor at the Department of Energy Technology, Aalborg University, where she has worked since August 1988.

Her fields of interest are mainly related to power quality and stability in power systems, including integration of dispersed generation and smart grid issues. She has participated in many projects concerning large scale wind power integration and the related balancing issues. During the resent the year the focus has been on operation of small dispersed generation units in the distribution network operated in connected and islanded mode, utilization of electrical vehicles as energy storages and new load such as electric boilers and heat pumps and electrolyzers used for leveling out fluctuations from renewable power units.

Publication J.2

(*Journal Paper*)

Active Control of Demand Response in Low Voltage Grids for Technical and Commercial Aggregation Services

Iker Diaz de Cerio Mendaza, Ireneusz Grzegorz Szczesny, Jayakrishnan R. Pillai and Birgitte Bak-Jensen

The paper is under second review in the
IEEE Transactions on Smart Grids, 2015.